

Exploiting orientation-selective DEER: determining molecular structure in systems containing Cu(II) centres

Alice M. Bowen^{a,b,†}, Michael W. Jones^{a,†}, Janet E. Lovett^{a,c}, Thembanikosi G. Gaule^d, Michael J. McPherson^d, Jonathan R. Dilworth^a, Christiane R. Timmel^{a,*} and Jeffrey R. Harmer^{a,e,*}.

^a Centre for Advanced Electron Spin Resonance, University of Oxford, South Parks Road, Oxford, OX1 3QR, United Kingdom.

^b Institute of Physical and Theoretical Chemistry, Goethe University Frankfurt, Max-von-Laue-Str. 7, 60438, Frankfurt am Main, Germany.

^c SUPA, School of Physics and Astronomy, University of St Andrews, North Haugh, St Andrews, KY16 9SS.

^d Astbury Centre for Structural Molecular Biology, Institute of Molecular and Cellular Biology, Faculty of Biological Sciences, University of Leeds, Leeds LS2 9JT, UK.

^e Centre for Advanced Imaging, University of Queensland, St Lucia, QLD, 4072, Australia

† A.M.B. (ESR measurements and analysis) and M.W.J. (Model system synthesis) contributed equally.

* Corresponding authors; Christiane.timmel@chem.ox.ac.uk and Jeffrey.harmer@cai.uq.edu.au.

Table of Contents

Synthesis ESI.....	3
Synthetic schemes and appropriate references.....	3
Discussion of Scheme ESI 1.....	3
Discussion of Scheme ESI 2.....	4
Discussion of Scheme ESI 3.....	5
Discussion of Scheme ESI 4:.....	6
Discussion of Scheme ESI 5.....	7
Discussion of Scheme ESI 6.....	7
Further Synthetic Supporting Information.....	8
Synthesis and characterisation information.....	8
X-ray diffraction.....	9
Synthetic reaction details.....	11
EPR SI.....	28
Density Functional Theory (DFT) calculations to generate the molecular models for DEER simulations.....	28
Comparison of the DFT analysis to the X-ray structure of 3-phenyl diacid linker.....	30
Construction of model distributions from the DFT data.....	30
DFT determination of the orientation of the <i>g</i> -tensor with respect to the molecular structure.....	32

Copper amine oxidase (AGAO)	33
Nitroxide model systems	37
DEER experimental pulse separations	38
DEER Simulation Parameters	38
Scaling factors and background correction	39
The values of c and k used to fit the simulated DEER data to the experimental traces	40
Further information on the structural models used for analysis.....	41
Geometric model (model 3).....	41
Ball model (model 6).....	41
Simulations for different orientations with both pump and probe pulses exciting the $g_{x/y}$ component of the spectrum	42
Simulations for isotropic excitation and summing traces measured across the spectrum.....	42
SI of the supporting spectra.....	43
References	110

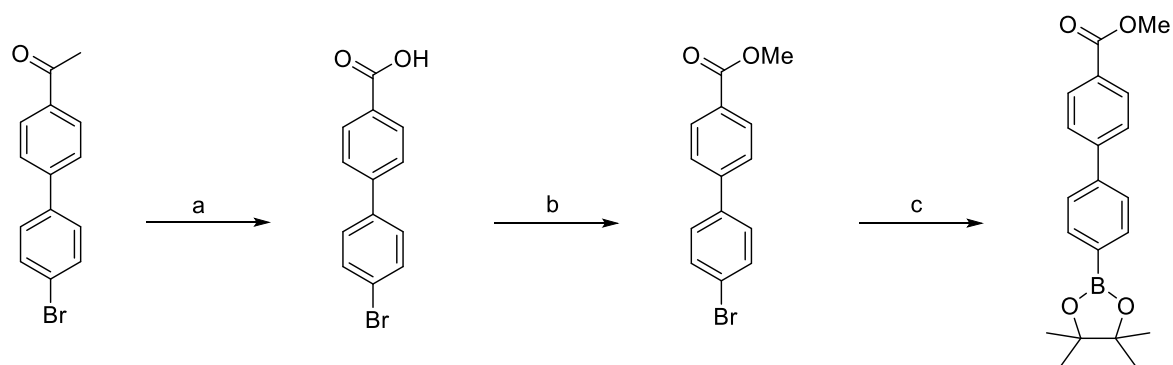
Synthesis ESI

Synthetic schemes and appropriate references.

This is an account of the steps, methods and comments on the synthesis of the eight model compounds and their congeners.

Discussion of Scheme ESI 1.

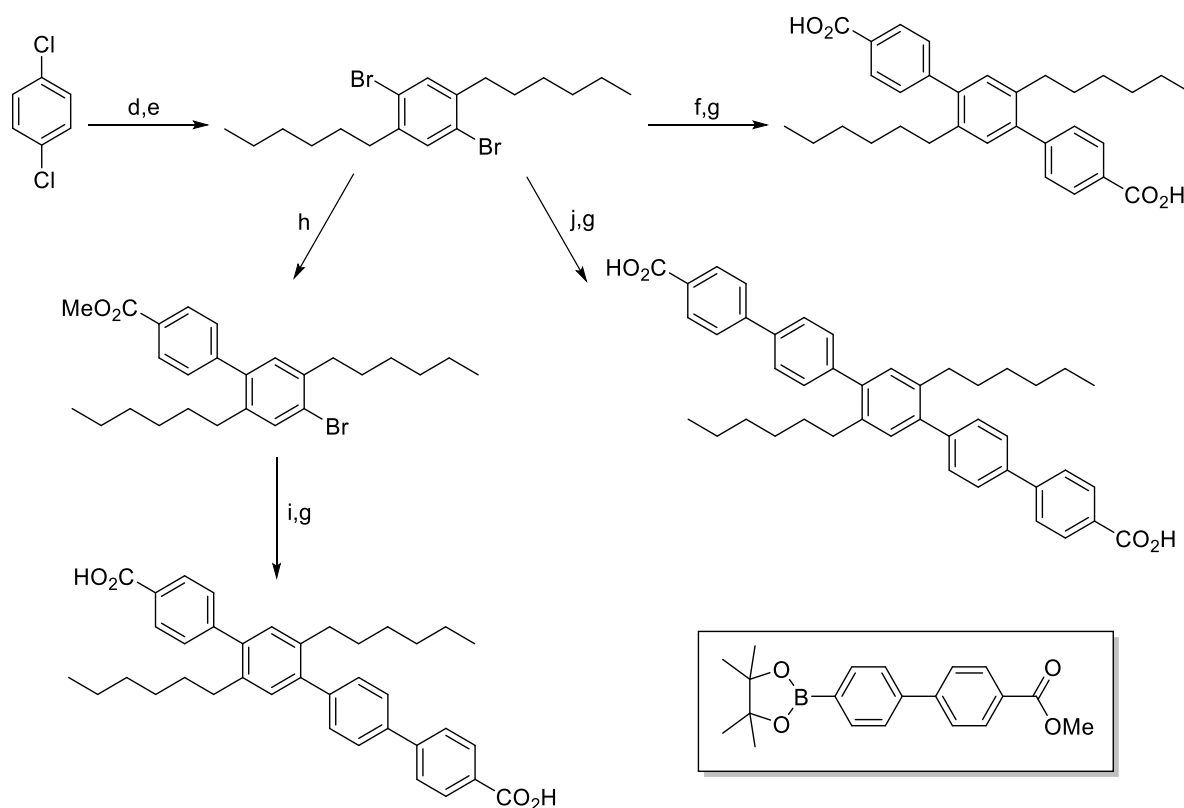
The oxidation of the acetyl motif was achieved using NaOBr generated *in situ* according to the preparation of Byron and co-workers.² The methylation of the carboxylic acid was achieved according to the procedure of D.I. Fletcher *et al.*³ A palladium coupling procedure with bis(pinacolato)diboron afforded the boronate in modest yield. Other methods to prepare the boronate coupling partner were investigated i.e. lithiation using *n*-BuLi and then quenching this with a range of boron sources but these were either found to not work or give unacceptably low yields of the product.



Scheme ESI 1 Reagents/conditions: a Br₂, NaOH, H₂O, dioxane, 35-40°C; b (i) SOCl₂, PhMe, reflux, 1 h (ii) MeOH; c Bis(pinacolato)diboron, PdCl₂(PPh₃)₂, K₂CO₃, THF, reflux, 20 h.

Discussion of Scheme ESI 2.

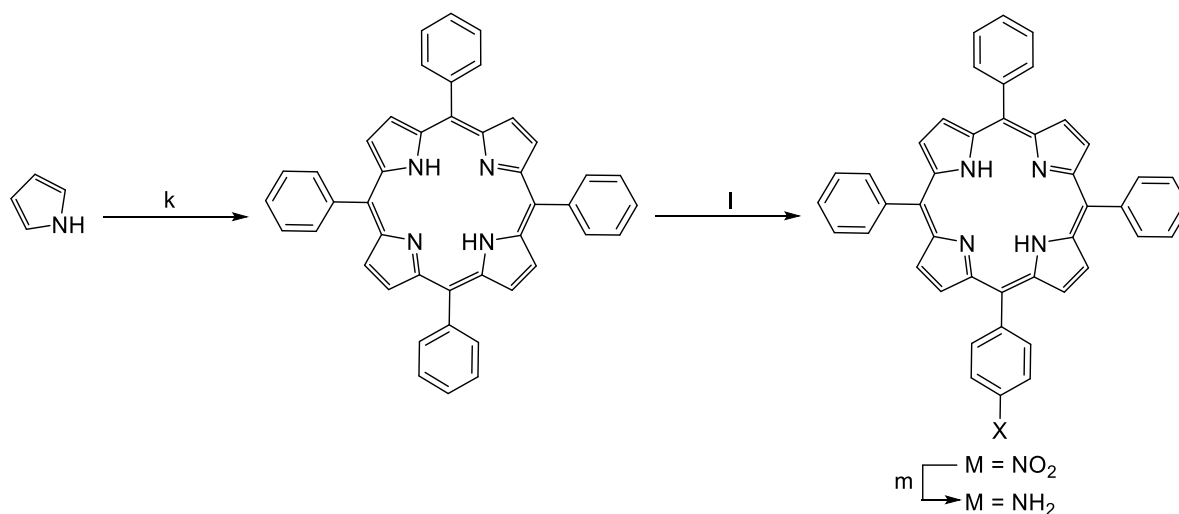
The first two steps (d and e) were according to the protocol of M. Rehahn *et al.*⁴ The Suzuki-Miyaura coupling reaction^{5, 6} was employed successfully for all of the boronate/boronic acid to bromide coupling reactions which proceeded in moderate to high yields. Altering the relative ratio of the boronic acid/boronate to bromide was used to control the amount of mono- or bis-adduct as desired after a not insubstantial amount of column chromatography. The saponification of the esters was performed in a procedure adapted from Jones *et al.*⁷ and was essentially quantitative for each of the diacids.



Scheme ESI 2 Reagents/conditions: d *n*-Hexylbromide, Mg (s), cat. BrCH₂CH₂Br, [Ni(dppp)Cl₂], THF, reflux; e Br₂, cat. I₂ 0°C→RT; f excess 4-(CO₂Me)-phenyl-B(OH)₂, PdCl₂(PPh₃)₂, K₂CO₃, THF, reflux; g LiOH·H₂O, THF, H₂O, reflux; g 1 mol equiv. 4-(CO₂Me)-phenyl-B(OH)₂, PdCl₂(PPh₃)₂, K₂CO₃, THF, reflux; i 1,1'-biphenyl boronate (see inset), PdCl₂(PPh₃)₂, K₂CO₃, THF, reflux; j excess 1,1'-biphenyl boronate (see inset), PdCl₂(PPh₃)₂, K₂CO₃, THF, reflux.

Discussion of Scheme ESI 3.

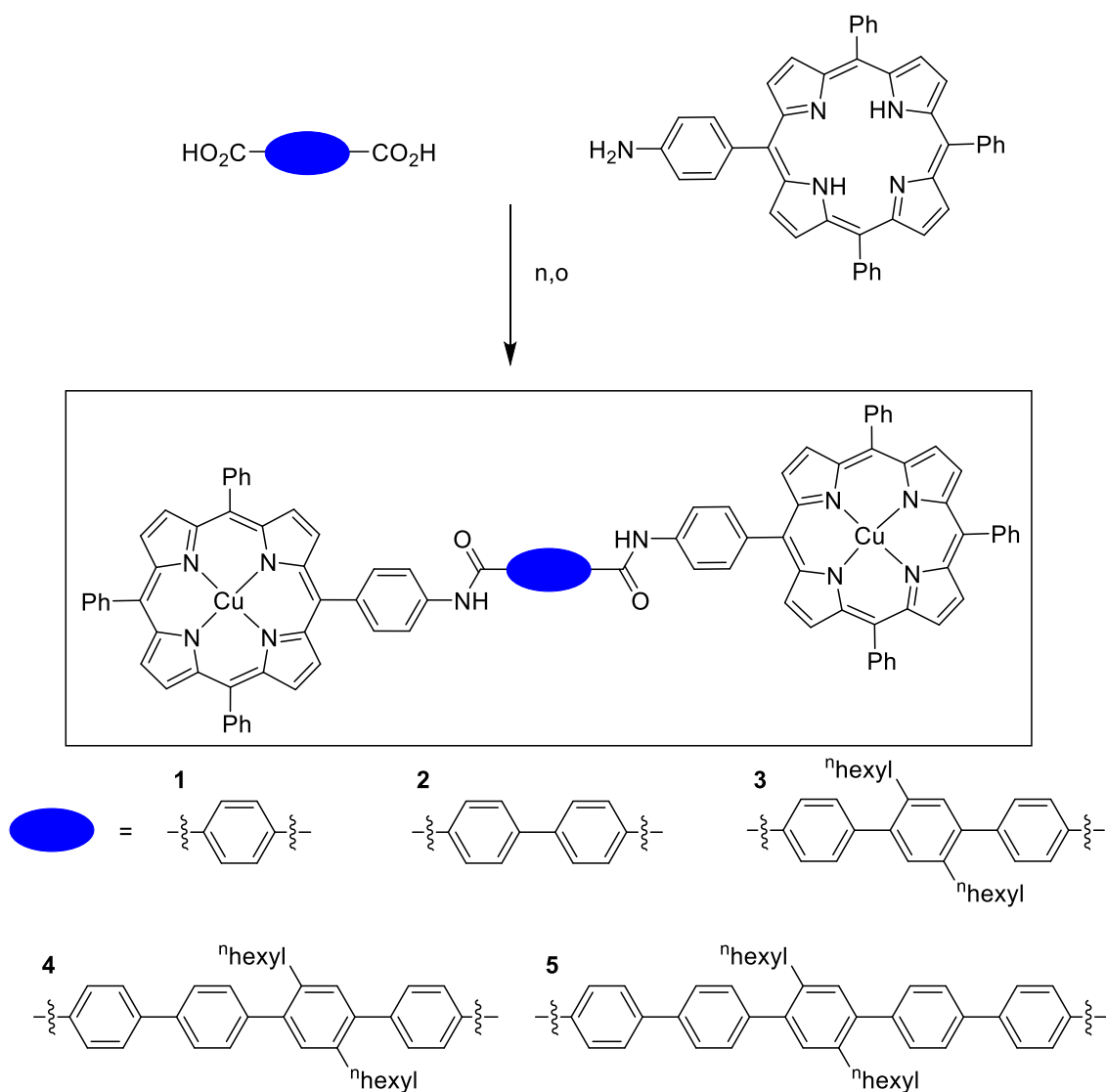
The preparation of the 5-(4-aminophenyl)-10,15,20-triphenylporphyrin was performed according to the literature report of R. Luguya and co-workers,⁸ whereby *meso*-tetraphenylporphyrin (as prepared by the method of A.D. Adler and co-workers⁹) was mono-nitrated selectively on the *para* position of a phenyl ring, and subsequently reduced to the amine using SnCl₂. It was found that to aid purification and expedite the synthesis the crude product from step (I) containing a mixture of mono-nitroTPP and TPP could be treated directly with SnCl₂/HCl. The greater difference in the retention times for the TPP (0.57) and TPPNH₂ (0.32) (both in 1:1 CH₂Cl₂/petroleum ether) meant that column chromatography was much simpler and there was no co-elution of the products.



Scheme ESI 3 Reagents/conditions: k benzaldehyde, propionic acid, reflux, 0.5 h; I (i) NaNO₂, CF₃CO₂H, 5°C, 3 min (ii) H₂O, CH₂Cl₂, NaHCO₃ (aq); m SnCl₂·2H₂O, conc. HCl, 65°C, 2 h (ii) NH₄OH, CH₂Cl₂.

Discussion of Scheme ESI 4:

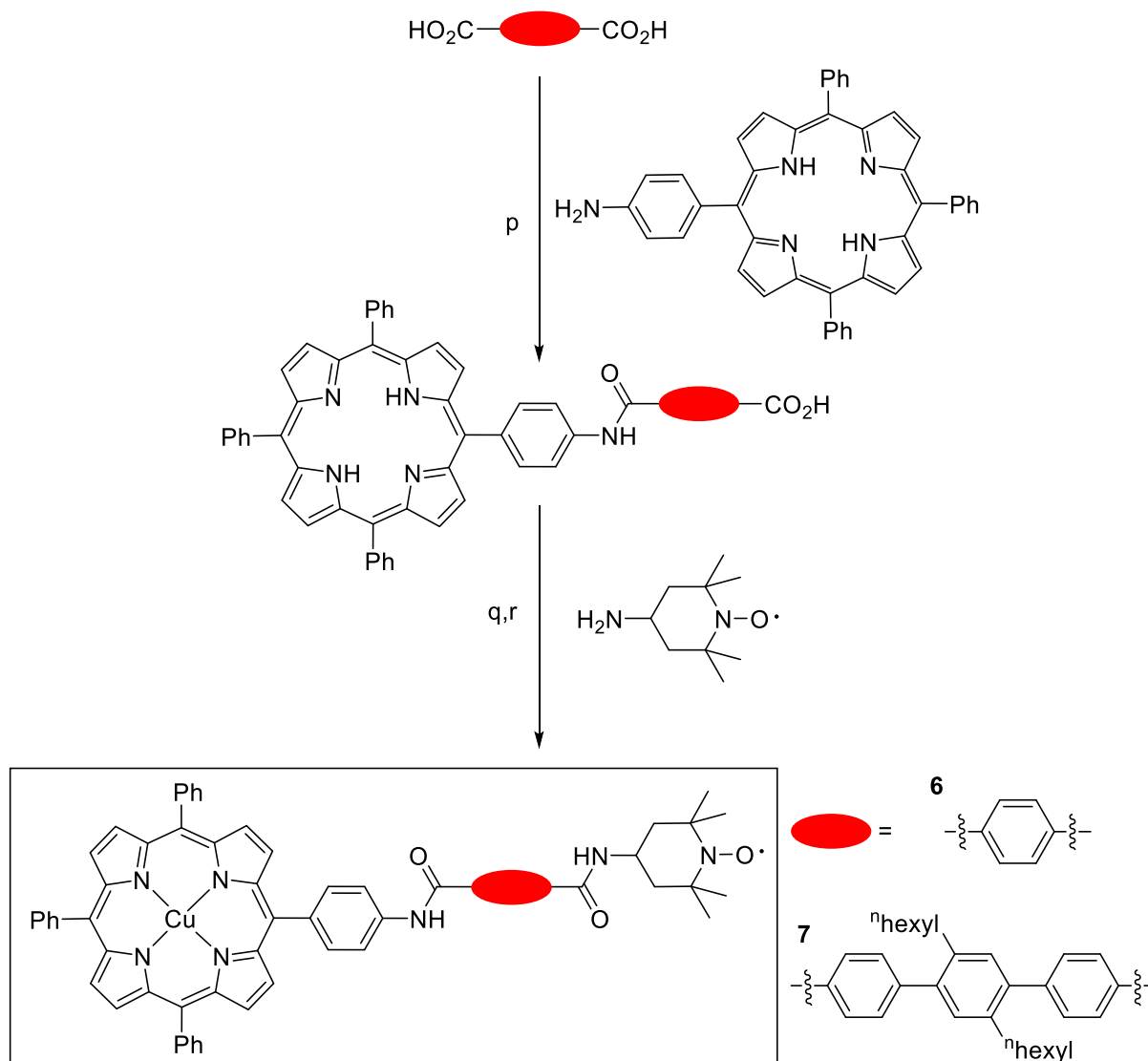
The two smaller compounds, with 1- and 2-phenyl groups as the central spacer, did not suffer from solubility problems, hence simple 4,4'-dicarboxylic acids were either commercially available or prepared without difficulty from available respective congeners. For the compounds containing a central linker with greater than three phenyl rings *n*-hexyl groups were added in the 2- and 5-positions of one central phenyl ring. This also aided purification, as early synthetic attempts were thwarted by the insoluble nature of the polyaromatic compounds. Similar approaches with the addition of aliphatic side-groups to polyaromatic systems have been previously reported, including in the work of Godt and coworkers in their synthesis of model bis(nitroxides) for use in DEER methodology work.¹⁰ BOP (benzotriazol-1- yloxytris(dimethylamino)-phosphonium hexafluorophosphate) coupling with an excess of the TPPNH₂ congener⁸ in all cases afforded the diporphyrin species with phenyl linkers 1-5 in moderate yields after flash chromatography. Metallation of the diporphyrin species was relatively trivial; a methanolic solution of copper(II) acetate was introduced to a stirred solution of diporphyrin in chloroform and the subsequent mixture heated at reflux to afford the model compounds **1-5** cleanly.



Scheme ESI 4 Reagents/conditions: n BOP, DIPEA, DMF, room temp. 4 days; o Cu(OAc)₂·H₂O, CHCl₃, MeOH, reflux 3 h.

Discussion of Scheme ESI 5

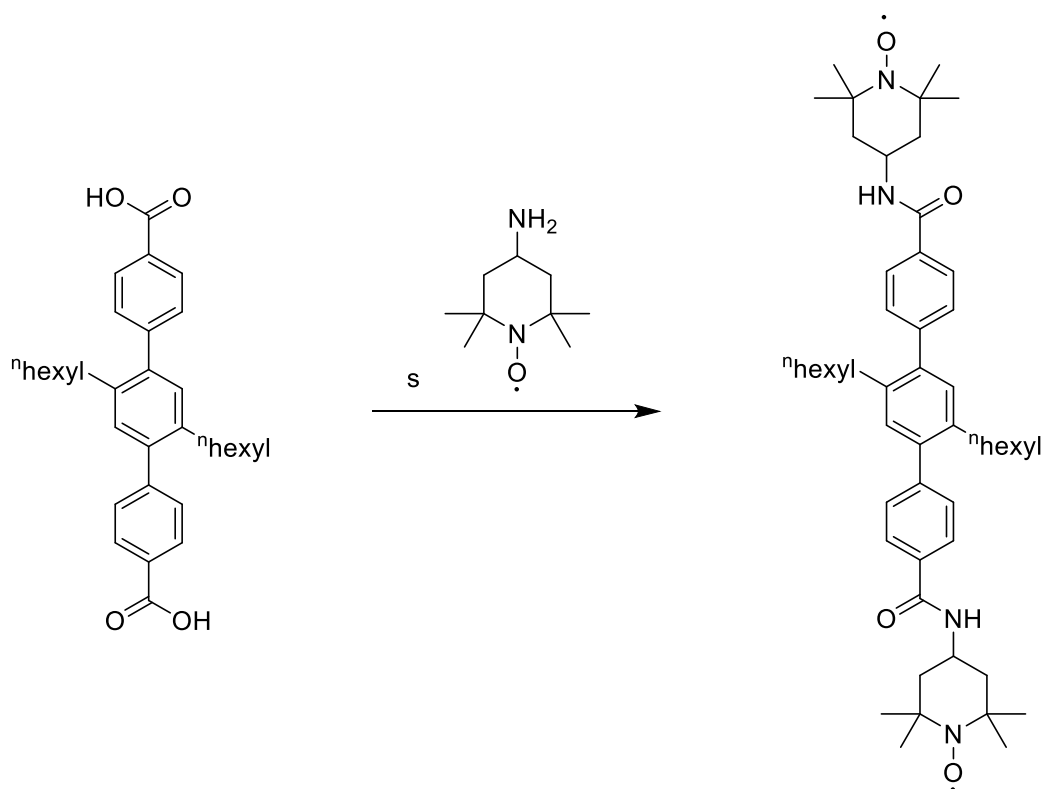
The copper-nitroxide species **6** and **7** were prepared *via* the BOP coupling of one equivalent of TPPNH₂ to the requisite acid, followed by attachment of the TEMPO–NH₂ motif also using a BOP mediated coupling procedure. This order of addition was employed to aid purification processes as the porphyrin derivative is clearly visible (dark purple) on silica gel. Finally, the insertion of metal was achieved in the same way as for the symmetrical dicopper species. The compounds were characterized (where appropriate) by thin layer chromatography and MALDI analysis, UV-vis and IR spectroscopy, ¹H and ¹³C NMR, mass spectrometry and CW-EPR at X-band.



Scheme ESI 5 Reagents/conditions: *p* BOP, DIPEA, DMF, room temp. 2 days; *q* BOP, DIPEA, DMF, room temp. 2 days *r* Cu(OAc)₂·H₂O, CHCl₃, MeOH, reflux 3 h.

Discussion of Scheme ESI 6.

The bis(nitroxide) compound **8** was prepared simply, again by BOP mediated coupling of the TEMPO–NH₂ motif to the 3-phenyl acid.



Scheme ESI 6 Reagents/conditions: s BOP, DIPEA, DMF, room temp, 12h.

Further Synthetic Supporting Information

Synthesis and characterisation information

All reagents and solvents were obtained from commercial sources (SigmaAldrich and Alfa Aesar) and unless otherwise stated, were used as received. Coupling constants, J , are measured to the nearest 0.1 Hz and are presented as observed. ^{13}C NMR spectra were recorded on a Varian Mercury VX300 (300 MHz) spectrometer or a Varian Unity (500 MHz) spectrometer or a Bruker AVX 500 (500 MHz) spectrometer at 298 K and were referenced to the solvent peak. NMR spectra were processed using ACD/Labs software. Mass spectra were recorded by Mr Colin Sparrow at the Chemistry Research Laboratory, University of Oxford, on a Bruker Micromass LCT time-of-flight mass spectrometer by using either positive ion electrospray (ES^+) or chemical ionisation (CI) techniques with methanol or CHCl_3 as the solvent. Accurate masses are reported to four decimal places using tetraoctylammonium bromide (466.5352 Da) as an internal reference. Values are reported as a ratio of mass to charge in Daltons. Electronic absorption spectroscopy (UV/Vis) was performed using a Perkin-Elmer Lambda 19 spectrometer, running UV Winlab software. Spectra were measured using 1.00 cm quartz cuvettes. Thin layer chromatography (TLC): silica gel layered aluminum foil (60 F₂₅₄ Merck, Darmstadt). The resonances (δ values) were measured relative to the signals for CDCl_3 (7.27) and CDCl_3 (77.0), respectively. The assignments of quaternary C, CH, CH_2 and CH_3 were made on the basis of DEPT, HMQC and HMBC spectra. IR spectra were obtained for thin films, or KBR discs on a Bruker Tensor 27 FT-IR spectrophotometer with a Diamond tip. $[\text{Ni}(\text{dppp})\text{Cl}_2] = [1,3\text{-bis}(\text{diphenylphosphino})\text{propane}]\text{-dichloro-nickel(II)}$.

X-ray diffraction

Single crystal X-ray diffraction data was obtained for **3phendiacid**. The crystal was mounted using the oil drop technique, in perfluoropolyether oil at 150(2) K using a Cryostream N₂ open-flow cooling device.¹¹ Diffraction data was collected using graphite monochromated Mo-K α radiation ($\lambda = 0.71073 \text{ \AA}$) on a Nonius Kappa CCD diffractometer. A series of ω -scans were performed in such a way as to collect a complete data set to a maximum resolution of 0.77 \AA . Data reduction including unit cell refinement and inter-frame scaling was carried out using DENZO-SMN/SCALEPACK.¹² Intensity data were processed and corrected for absorption effects by the multi-scan method, based on repeat measurements of identical and Laue equivalent reflections. Structure solution was carried out with direct methods using the programs SIR92¹³ within the CRYSTALS software suite.¹⁴ Coordinates and anisotropic displacement parameters of all non-hydrogen atoms were refined freely except. Hydrogen atoms were generally visible in the difference map and refined with soft restraints prior to inclusion in the final refinement using a riding model. Crystallographic data (excluding structure factors) for all the structures have been deposited with the Cambridge Crystallographic Data Centre (CCDC 1040894). ORTEP depictions of the single crystal X-ray structure are in the Figure ESI 1. Copies of the data can be obtained free of charge from The Cambridge Crystallographic Data Centre *via* www.ccdc.cam.ac.uk/data_request/cif. Tables summarising the X-ray crystallographic data are in the ESI 4.

4'-Bromobiphenyl-4-carboxylic acid,² methyl 4'-bromobiphenyl-4-carboxylate,³ 1,4-dibromo-2,5-dihexyl-benzene⁴ and 5-(4-aminophenyl)-10,15,20-triphenylporphyrin (TPPNH₂)¹⁵ were prepared using literature methods but details of the syntheses used and any notes and adaptations are indicated below.

X-ray table and ORTEP depiction.

Table ESI 4 X-ray crystallographic information for **3phendiacid**.

Crystal identification	3phendiacid
CCDC no.	1040894
Chemical Formula	C ₃₂ H ₃₈ O ₄ ·2DMSO
Formula weight, <i>M</i>	642.92
Temperature, <i>K</i> /°	150
λ /Å	0.71073
Crystal system	Monoclinic
Space group	<i>P</i> 1 21/a 1
<i>a</i> /Å	14.1458(4)
<i>b</i> /Å	7.2193(2)
<i>c</i> /Å	17.4712(4)
α /°	90
β /°	98.5591(13)
γ /°	90
<i>V</i> /Å ³	1764.34(8)
<i>Z</i>	2
<i>D_c</i> /g cm ⁻³	1.210
Absorption coefficient, μ /mm ⁻¹	0.193
<i>F</i> (000)	692
Size /mm	0.06 × 0.20 × 0.26
Crystal description	Colourless plate
θ range collected /°	5.0 ≤ θ ≤ 27.5
Index ranges, <i>hkl</i>	-18 ≤ <i>h</i> ≤ 18, -9 ≤ <i>k</i> ≤ 9, -22 ≤ <i>l</i> ≤ 22
Refl. Measured	7666
Refl. Unique	4019
<i>R</i> _{int}	0.033
Reflections obs., <i>n</i> (<i>I</i> > <i>n</i> σ(<i>I</i>))	2652
Transmission coefficients (min.,	0.96, 0.99
Param. Refined	199
<i>R</i> or <i>R</i> ₁ (2σ)	<i>R</i> = 0.048
<i>wR</i> or <i>R</i> ₂ (2σ)	<i>wR</i> = 0.114
Goodness of fit (GOF)	1.003
Residual electron (min., max.) /eÅ ³	-0.37, 0.49

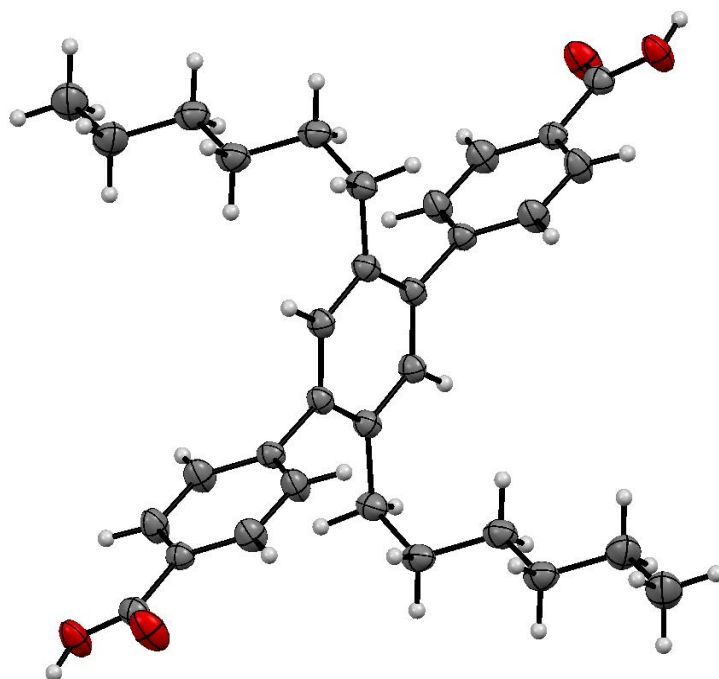
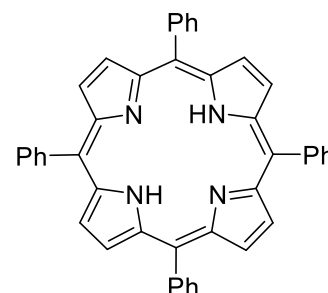


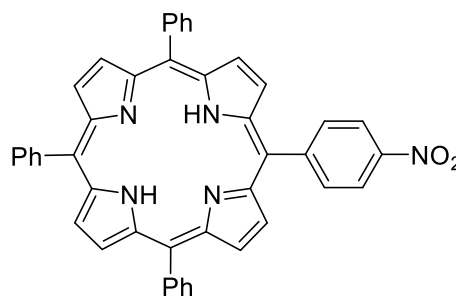
Figure ESI 1: ORTEP depiction of the X-ray crystal structure of **3phendiacid**. Thermal ellipsoids at 50% probability and solvent molecules have been removed for clarity.

Synthetic reaction details

TPP Propionic acid (200 ml) was heated to reflux. Subsequently benzaldehyde (6.10 ml, 60.00 mmol) and pyrrole (4.16 ml, 60.00 mmol) were added and the resultant mixture heated at reflux for 0.5 h. After this time the mixture was cooled to room temperature and the purple solid that precipitated collected by suction filtration. The solids were washed well with ice-cold MeOH and then dried in air to afford the desired product as purple coloured microcrystalline solid (2.178 g, 24 %). *Rf* (1:1 CH₂Cl₂/petroleum ether): 0.69. ¹H NMR (CDCl₃, 300 MHz) δ: 7.77 (12H, m, 12×ArCH), 8.25 (8H, dd, *J* 7.6, 1.8 Hz, 8×pyrrCH), 8.88 (8H, br. s, 8×ArCH), 13.26 (2H, br. s, 2×NH). ¹³C NMR (DMSO-*d*₆, 75.5 MHz) δ: 120.1, 126.6, 127.7, 131.1 (broad), 134.5, 142.2. ES⁺ MS *m/z* 615 (MH⁺, 100%) (M= C₄₄H₃₀N₄)

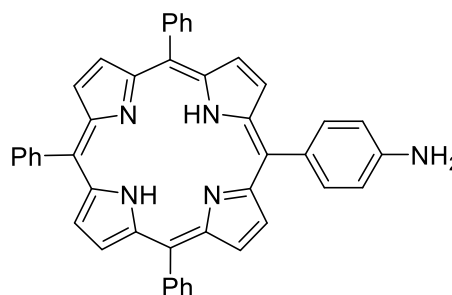


TPPNO₂ According to the procedure of Luguya *et al.*⁸ NaNO₂ (0.400 g, 5.797 mmol) was added in a single solid portion to a stirred green solution of TPP (2.00 g, 3.253 mmol) in TFA (40 ml) at 10°C. The resultant mixture was stirred at 10°C for 3 min before ice-cold H₂O (150 ml) was added, followed by CH₂Cl₂ (150 ml). The layers were separated, then the aqueous phase was extracted with CH₂Cl₂ (5 × 50 ml). The combined organic extracts were washed with sat. NaHCO₃ (aq) (2 × 300 ml), before being dried over anhydrous Na₂SO₄, filtered and concentrated to dryness *in vacuo*. The dark brown-purple product was purified using an elution gradient of CH₂Cl₂-hexanes



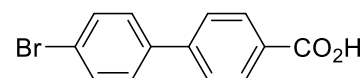
(1:3) to (1:1) ratio to afford, in order of elution, recovered TPP followed by the nitro-adduct (1.01 g, 47 %). (*NB: extended reaction times lead to the formation of the dinitro species in addition to the desired mono-adduct*). *Rf*(1:1 CH₂Cl₂/petroleum ether): 0.57. ¹H NMR (CDCl₃, 300 MHz) δ: 7.80 (9H, m, ArH), 8.24 (6H, dd, *J*7.2, 1.3 Hz, ArH), 8.40 (2H, d, *J*8.7 Hz, ArH), 8.64 (2H, d, *J*8.7 Hz, ArH), 8.76 (2H, d, *J*4.5 Hz, ArH), 8.91 (6H, m, ArH), 14.24 (2H, br. s, 2× pyrrole-NH). ¹³C NMR (CDCl₃, 75.5 MHz) δ: 116.6, 120.7, 121.1, 121.9, 126.76, 126.79, 131.8 (broad), 134.6, 135.1, 141.87, 141.92, 147.7, 149.2. ES⁺ MS *m/z* 660 (MH⁺, 100%) (M = C₄₄H₂₉N₅O₂).

TPPNH₂ According to the procedure of Luguya *et al.*⁸ SnCl₂·2H₂O (4.0 g, 17.728 mmol) was added to a stirred suspension of TPPNO₂ (0.485 g, 0.735 mmol) in conc. HCl (80 ml) at room temperature. The resultant dark green coloured mixture was heated at 65°C for 2 h with stirring. The mixture was then cooled to room temperature, and added to ice-cold H₂O (150 ml) and adjusted cautiously to pH 8 with conc. NH₄OH. The mixture was then filtered through Celite(R) to remove the insoluble particulates, and aid separation. The aqueous layer was extracted with CH₂Cl₂ (5 × 50 ml), before the combined organic extracts were dried over anhydrous Na₂SO₄, filtered and concentrated to dryness *in vacuo*. Purification of the purple-brown coloured product using flash chromatography and CH₂Cl₂ as eluent afforded the desired TPPNH₂ product as a dark purple coloured solid (0.440 g, 95 %). *Rf*(1:1 CH₂Cl₂/petroleum ether): 0.32.

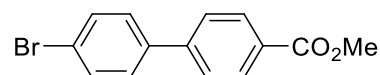


¹H NMR (CDCl₃, 300 MHz) δ: -2.73 (2H, s, 2×pyrrole-NH), 3.98 (2H, s, NH₂), 7.05 (2H, d, *J*8.6 Hz, ArH), 7.76 (9H, m, ArH), 8.03 (2H, d, *J*7.9 Hz, ArH), 8.24 (6H, d, *J*7.3 Hz, ArH), 8.86 (6H, s, ArH), 8.96 (2H, d, *J*4.6 Hz, ArH). ¹³C NMR (CDCl₃, 75.5 MHz) δ: 110.0, 113.4, 119.7, 120.0, 120.9, 126.7, 127.7, 131.1 (broad), 132.4, 134.6, 135.7, 142.22, 142.26, 146.0. ES⁺ MS *m/z* 630 (MH⁺, 100%) (M = C₄₄H₃₁N₅).

4'-Bromo-[1,1'-biphenyl]-4-carboxylic acid According to the procedure of Byron *et al.*² Careful addition of bromine (5.12 ml, 15.982 g, 100 mmol) to a stirred solution of NaOH (14.00 g, 350 mmol) in deionised water (70 ml) at 0°C was used to make NaOBr. The NaOBr solution was then added *via* a dropping funnel over 10 min to a stirred solution of 1-(4'-bromo-[1,1'-biphenyl]-4-yl)ethan-1-one (5.503 g, 20 mmol) in dioxane (50 ml) at 40°C. The resultant mixture was stirred at 40°C for a further 20 min before sodium dithionite (10 g) in water (150 ml) was added, followed by water (150 ml). 2 M HCl (aq) (150 ml) was added to make the mixture acidic as tested by pH paper. The mixture was cooled to 0°C and the solid collected by suction filtration to afford a pale yellow coloured powder (7.022 g). This was recrystallised from hot EtOH to afford 4'-bromo-[1,1'-biphenyl]-4-carboxylic acid as an off-white powder (3.014 g, 54 %). ¹H NMR (DMSO-*d*₆, 300 MHz) δ: 7.67 (4H, s, Ph), 7.77 (2H, d, *J*8.2 Hz, Ph), 8.00 (2H, d, *J*8.2 Hz, Ph), 12.98 (1H, br. s, CO₂H); ¹³C NMR (DMSO-*d*₆, 75.5 MHz) δ: 122.3 (ArCq), 127.2 (ArCH), 129.5 (ArCH), 130.4 (ArCq), 130.5 (ArCH), 132.4 (ArCH), 138.6 (ArCq), 143.4 (ArCq), 167.0 (C=O). ν_{\max} (Diamond ATR) 1662 (C=O), 1596, 1426, 1301, 816, 765 cm⁻¹. ES⁻MS *m/z* 277 (⁸¹BrM-H⁺, 100%), 275 (⁷⁹BrM-H⁺, 90%) (M = C₁₃H₉BrO₂).

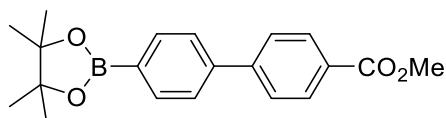


Methyl 4'-bromo-[1,1'-biphenyl]-4-carboxylate The methylation of the carboxylic acid was achieved according to the procedure of D.I. Fletcher *et al.*³ A solution of 4'-



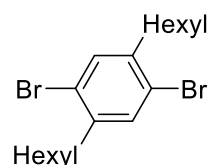
bromo-[1,1'-biphenyl]-4-carboxylic acid (3.00 g, 10.83 mmol) in SOCl₂ (30 ml) was heated at reflux for 1 h. The solvent was then distilled off azeotropically using PhMe (50 ml) before the mixture was concentrated to dryness *in vacuo* to afford pale brown coloured oil. MeOH was added to the oil to afford the desired product as a tan coloured crystalline solid. The solid was recrystallised from hot MeOH to afford the title compound as yellow coloured needles (1.436 g, 46 %). *Rf*(1:3 Et₂O/hexanes): 0.40. ¹H NMR (CDCl₃, 300 MHz) δ: 3.91 (3H, s, CH₃), 7.45 (2H, d, *J* 8.5 Hz, Ph), 7.57 (2H, d, *J* 8.5 Hz, Ph), 7.59 (2H, 8.5 Hz, Ph), 8.07 (2H, d, *J* 8.5 Hz, Ph). ¹³C NMR (CDCl₃, 75.5 MHz) δ: 52.1 (OCH₃), 122.5 (ArCq), 126.8 (ArCH), 128.5 (ArCH), 129.0 (ArCq), 130.2 (ArCH), 132.0 (ArCH), 138.8 (ArCq), 144.3 (ArCq), 166.8 (C=O). ν_{\max} (Diamond ATR) 1715 (C=O), 1436, 1288, 1113 1082, 1000, 954, 823, 767 cm⁻¹. ES⁺-MS *m/z* 315 (⁸¹BrM+Na⁺), 313 (⁷⁹BrM+Na⁺) (M = C₁₄H₁₁BrO₂).

Methyl 4'-(4,4,5,5-tetramethyl-1,3,2-dioxaborolane-2-yl)biphenyl-4-carboxylate A mixture of methyl 4'-bromo-[1,1'-biphenyl]-4-carboxylate (0.500 g, 1.717



mmol), bis(pinacolato)diboron (0.436 g, 1.717 mmol), PdCl₂(PPh₃)₂ (0.025 g, 0.036 mmol), K₂CO₃ (0.949 g, 6.870 mmol) and anhydrous THF (25 ml) was heated at reflux with stirring for 20 h under nitrogen atmosphere. The resultant mixture was then cooled to room temperature, concentrated to dryness *in vacuo*. The residue was dissolved in CH₂Cl₂, filtered through Celite™, and the liquid concentrated to dryness *in vacuo* to afford a mixture of starting material and the desired product. The mixture was purified by flash chromatography using 1:4 Et₂O/petroleum ether to afford the *methyl 4'-(4,4,5,5-tetramethyl-1,3,2-dioxaborolane-2-yl)biphenyl-4-carboxylate* product as colourless needles (0.2166 g, 37%). *Rf*(1:3 Et₂O/hexanes): 0.31. ¹H NMR (CDCl₃, 300 MHz) δ: 1.37 (12H, s, 4×CH₃), 3.94 (3H, s, CO₂CH₃), 7.63 (2H, d, *J* 8.2 Hz, 2×ArCH), 7.68 (2H, d, *J* 8.2 Hz, 2×ArCH), 7.91 (2H, d, *J* 8.2 Hz, 2×ArCH), 8.11 (2H, d, *J* 8.2 Hz, 2×ArCH). ¹³C NMR (CDCl₃, 75.5 MHz) δ: 24.9 (CH₃), 52.1 (CO₂CH₃), 83.9 (Cq), 126.5 (ArCH), 127.1 (ArCH), 129.1 (ArCq), 130.1 (ArCH, ArCq), 135.3 (ArCH), 142.6 (ArCq), 166.9 (C=O); ν_{\max} (KBr)/cm⁻¹ 2976, 1718(C=O), 1611, 1361, 1291, 1272, 1150, 1116, 1093, 864, 829, 773, 739, 654. HRMS (EI/FI⁺) found 338.1693 C₂₀H₂₃BO₄ requires: 338.1689.

Preparation of 1,4-dibromo-2,5-dihexylbenzene According to the procedure of Rehahn *et al.*¹⁶ and analogous to the reaction of Tamao *et al.*¹⁷ 1-Bromohexane (30 ml, 213.73 mmol), Mg(O) (5.196 g, 213.73 mmol) and THF (300 ml) were used to make the organomagnesium compound under strictly anhydrous conditions and under nitrogen atmosphere. The Grignard reagent was prepared first, initiated with 1,2-dibromoethane (3 drops). Initially the mixture was cooled to 0°C in an ice-bath, then allowed to reflux for 0.25 h, and finally by heating at reflux for 1 h. After this time all of the magnesium metal had dissolved and the mixture was homogeneous. The mixture was stirred overnight at room temperature then cooled to 0°C. 1,4-Dichlorobenzene (12.567 g, 85.492 mmol) was added slowly in small solid portions followed by (1,3-bis[diphenylphosphino]propane)dichloronickel(II) (0.232 g, 0.427 mmol). The mixture

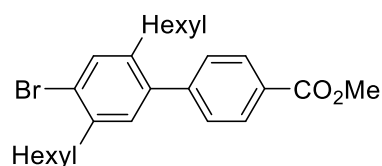


became pale milky green in colour. This mixture was heated at reflux for 32 h then cooled to room temperature. Water (40 ml) was added slowly, followed by 2M HCl (aq) (200 ml) and Et₂O (100 ml). The layers were separated and the aqueous layer extracted with Et₂O (5 × 30 ml). The combined organic extracts were dried over anhydrous Na₂SO₄, filtered and concentrated to dryness *in vacuo* to afford a dark yellow coloured oil. This was purified by flash chromatography using 1:1 Et₂O/petroleum ether as eluent to afford *1,4-di(hexyl)benzene* as a pale yellow coloured oil (20.40g, 97%).

Bromine (27.12 g, 8.7 ml, 169.71 mmol) was added dropwise over 0.5 h to a stirred and ice-cooled mixture of *1,4-di(hexyl)benzene* (20.40 g, 82.785 mmol) and iodine (0.214 g, 0.828 mmol) under rigorous exclusion of light. (*NB: Caution must be taken when adding the bromine as a large volume of fumes are evolved and heat generated*). The subsequent mixture was allowed to slowly warm to room temperature and stirred for 24 h. After this time KOH (aq) (20% *w/v*, 100 ml) was added slowly and the mixture stirred vigorously at 40°C for 1.5 h, then overnight at room temperature during which time the colour of the mixture disappeared. The liquid was then decanted, before more water (100 ml) was added and again decanted to afford an off-white solid. This solid was recrystallised from EtOH to afford *1,4-dibromo-2,5-dihexylbenzene* as a colourless crystalline solid (21.689 g, 65%) *Rf*(1:1 Et₂O/petroleum ether): 0.74. ¹H NMR (CDCl₃, 300 MHz) δ: 0.90 (6H, t, *J* 6.6 Hz, 2×CH₃), 1.34 (12H, m, 6×CH₂), 1.58 (4H, m, 2×CH₂), 2.64 (4H, dd, *J* 8.1, 7.5 Hz, 2×benzylic CH₂), 7.35 (2H, s, ArH). ¹³C NMR (CDCl₃, 75.5 MHz) δ: 14.1 (CH₃), 22.6 (CH₂), 29.0 (CH₂), 29.8 (CH₂), 31.6 (CH₂), 35.5 (CH₂), 123.0 (ArCq), 133.7 (ArCH), 141.3 (ArCq). ν_{\max} (Diamond ATR)/cm⁻¹ 2948, 2925, 2849, 1458, 1417, 1053, 902, 862, 787, 727 cm⁻¹. Calc for C₁₈H₂₈Br₂ C, 53.48; H, 6.98. Found C, 53.13; H, 7.14.

Preparation of methyl 4'-bromo-2',5'-dihexyl biphenyl-4-carboxylate and 3-phenyl dimethyl ester *1,4-Dibromo-2,5-dihexylbenzene* (2.707 g, 6.696 mmol), 4-(methoxycarbonyl)benzene boronic acid (3.000 g, 16.739 mmol), K₂CO₃ (3.686 g, 26.671 mmol) and PdCl₂(PPh₃)₂ (0.200 g) in anhydrous THF (75 ml) were combined at room temperature under inert atmosphere (N₂), and the resultant suspension heated at reflux with stirring for 20 h. The mixture was then cooled to room temperature, and concentrated to dryness *in vacuo*. The residue was taken up in H₂O (200 ml) and CH₂Cl₂ (100 ml), and the layers separated. The aqueous phase was extracted with CH₂Cl₂ (3×40 ml), then the combined organic extracts were dried over anhydrous MgSO₄, filtered and concentrated to dryness *in vacuo*. The mixture was purified by flash chromatography using 1:9 Et₂O/petroleum ether to afford, in order of elution, recovered dibromide (0.973 g, 36% recovery), methyl 4'-bromo-2',5'-dihexyl biphenyl-4-carboxylate (0.804 g) as a colourless oil and dimethyl 2',5'-dihexyl-[1,1':4',1''-terphenyl]-4,4''-dicarboxylate (0.871 g) as a colourless solid.

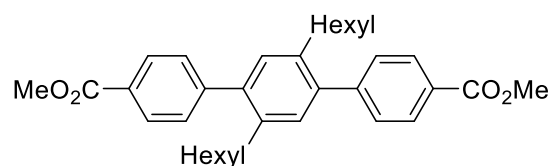
Methyl 4'-bromo-2',5'-dihexyl biphenyl-4-carboxylate *Rf* (1:1 Et₂O/petroleum ether): 0.66. ¹H NMR (CDCl₃, 300 MHz) δ: 0.82 (3H, t, *J* 6.9 Hz, CH₃), 0.87 (3H, t, *J* 6.9 Hz, CH₃), 1.32 (6H, m, 3×CH₂), 1.38 (8H, m, 4×CH₂), 1.61 (2H, m, CH₂), 2.46 (2H, t, *J* 7.8 Hz, CH₂), 2.70, (2H, t, *J* 7.8 Hz, CH₂), 3.95 (3H, s, OCH₃), 7.01 (1H, s, Ph), 7.34 (2H, d, *J* 8.4 Hz, Ph), 7.45 (1H, s, Ph), 8.07 (2H, d, *J* 8.4 Hz, Ph); ¹³C NMR (CDCl₃, 75.5 MHz) δ: 14.0 (CH₃), 14.1 (CH₃), 22.4 (CH₂) 22.6 (CH₂), 29.0 (CH₂), 29.1 (CH₂), 30.0 (CH₂), 31.1 (CH₂), 31.6 (CH₂), 32.4 (CH₂), 35.7 (CH₂), 52.2 (O₂CH₃), 123.8 (ArCq), 129.2 (ArCH), 129.4 (ArCH), 131.2 (ArCH), 133.2 (ArCH), 139.4



(ArCq), 139.6 (ArCq), 139.9 (ArCq), 145.9 (ArCq), 167.0 (C=O); $\nu_{\max}(\text{film})/\text{cm}^{-1}$ 2954, 2927, 2857, 1726(C=O), 1610, 1460, 1435, 1277, 1178, 1113, 1101, 1019, 968, 860, 774, 710. HRMS found 458.1824 $\text{C}_{26}\text{H}_{35}\text{BrO}_2$ requires: 458.1820.

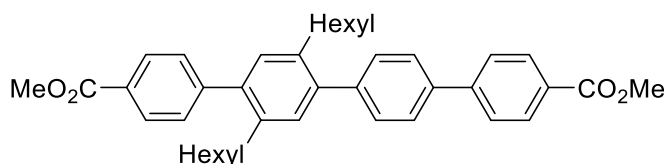
Dimethyl 2',5'-dihexyl-[1,1':4',1''-terphenyl]-4,4''-dicarboxylate

Rf (1:1 Et₂O/petroleum ether): 0.38. ¹H NMR (CDCl₃, 300 MHz) δ : 0.80 (6H, t, *J*7.0 Hz, 2×CH₃), 1.17 (12H, m, 6×CH₂), 1.44 (4H, m, 2×CH₂), 2.55 (4H, dd, *J*7.8, 7.8 Hz, 2×CH₂), 3.96 (6H, s, 2×OCH₃), 7.12 (2H, s, Ph), 7.43 (4H, d, *J*8.4 Hz, Ph), 8.10 (4H, d, *J*8.4 Hz, Ph); ¹³C NMR (CDCl₃, 75.5 MHz) δ : 14.0 (CH₃), 22.5 (CH₂), 29.1 (CH₂), 31.36 (CH₂), 31.44 (CH₂), 32.6 (CH₂), 52.1 (OCH₃), 128.6 (ArCq), 129.3 (ArCH), 129.4 (ArCH), 130.7 (ArCH), 137.5 (ArCq), 140.3 (ArCq), 146.6 (ArCq), 167.1 (C=O); $\nu_{\max}(\text{KBr})/\text{cm}^{-1}$ 2957, 2925, 2857, 1723 (C=O), 1609, 1567, 1437, 1273, 1115, 1102, 1016, 866, 766, 707. HRMS found 514.3089 $\text{C}_{34}\text{H}_{42}\text{O}_4$ requires: 514.3083.



Dimethyl 2',5'-dihexyl-[1,1':4',1''':4''',1''''-quaterphenyl]-4,4''''-dicarboxylate

Methyl 4'-bromo-2',5'-dihexyl biphenyl-4-carboxylate (110 mg, 0.239 mmol), methyl 4'-(4,4,5,5-tetramethyl-1,3,2-dioxaborolane-2-yl)biphenyl-4-carboxylate (85 mg, 0.251 mmol), PdCl₂(PPh₃)₂ (20 mg), K₂CO₃ (132 mg, 0.957 mmol) and anhydrous THF (15 ml) were treated by the general procedure to afford an off-white solid. This was purified by flash chromatography using 1:9 Et₂O/petroleum ether to afford, in order of elution, starting bromide (47.4 mg, 43% recovery) and the *dimethyl 2',5'-dihexyl-[1,1':4',1''':4''',1''''-quaterphenyl]-4,4''''-dicarboxylate* (46 mg, 57%). *Rf* (1:1 Et₂O/petroleum ether): 0.42. ¹H NMR (CDCl₃, 300 MHz) 0.81 (6H, t, *J*7.2 Hz, 2×CH₃), 1.18 (12H, m, 6×CH₂), 1.48 (4H, m, 2×CH₂), 2.59 (4H, m, 2×CH₂), 3.960 (3H, s, OCH₃), 3.964 (3H, s, OCH₃), 7.14 (1H, s, Ph), 7.18 (1H, s, Ph), 7.45 (2H, d, *J*8.4 Hz, Ph), 7.47 (2H, d, *J*8.4 Hz, Ph), 7.70 (2H, d, *J*8.4 Hz, Ph), 7.74 (2H, d, *J*8.4 Hz, Ph), 8.12 (2H, d, *J*8.4 Hz, Ph), 8.15 (2H, d, *J*8.4 Hz, Ph). ¹³C NMR (CDCl₃, 75.5 MHz) 14.00 (CH₃), 14.03 (CH₃), 22.5 (CH₂), 29.2 (CH₂), 31.38 (CH₂), 31.41 (CH₂), 31.46 (CH₂), 31.47 (CH₂), 32.6 (CH₂), 52.1 (OCH₃), 126.91 (ArCH), 126.92 (ArCH), 127.6 (ArCq), 128.5 (ArCq), 128.9 (ArCq), 129.4 (ArCH), 130.1 (ArCH), 130.6 (ArCH), 131.0 (ArCH), 135.4 (ArCq), 137.4 (ArCq), 137.7 (ArCq), 138.4 (ArCq), 139.9 (ArCq), 140.6 (ArCq), 141.7 (ArCq), 145.2 (ArCq), 146.8 (ArCq), 167.0 (C=O), 167.1 (C=O). HRMS-EI/FI Found 590.3385 [$\text{C}_{40}\text{H}_{46}\text{O}_4$] requires 590.3396.

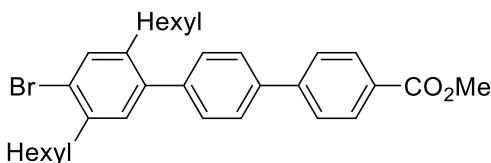


Preparation of methyl 4'-bromo-2',5'-dihexyl triphenyl-4-carboxylate and dimethyl 2',5'-dihexyl-[1,1':4',1''':4''',1''''-quinquephenyl]-4,4''''-dicarboxylate 1,4-Dibromo-2,5-dihexyl-benzene (50.7 mg, 0.126 mmol), methyl 4'-(4,4,5,5-tetramethyl-1,3,2-dioxaborolane-2-yl)biphenyl-4-carboxylate (106.5 mg, 0.264 mmol), K₂CO₃ (69.4 mg, 0.502 mmol) and PdCl₂(PPh₃)₂ (10 mg) in anhydrous THF (15 ml) were combined at room temperature under inert atmosphere (N₂), and the resultant suspension heated at reflux with stirring for 20 h. The mixture was then cooled to room temperature, and concentrated to dryness *in vacuo*. The residue was taken up in H₂O (30 ml) and CH₂Cl₂ (30 ml), and the layers separated. The aqueous phase was extracted with CH₂Cl₂ (3×20 ml), then the combined organic extracts were dried over anhydrous MgSO₄, filtered and

concentrated to dryness *in vacuo*. The mixture was purified by flash chromatography using 1:9 Et₂O/petroleum ether to afford, in order of elution, *methyl 4'-bromo-2',5'-dihexyl triphenyl-4-carboxylate* (18.2 mg) as a colourless solid and *dimethyl 2'',5''-dihexyl-[1,1':4',1'':4'',1''':4''',1''''-quinquephenyl]-4,4''''-dicarboxylate* (49.5 mg, 59%) as a colourless solid.

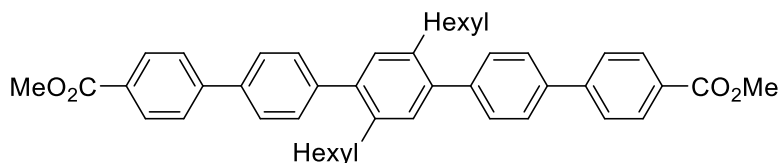
Methyl 4'-bromo-2',5'-dihexyl triphenyl-4-carboxylate *Rf* (1:1 Et₂O/petroleum ether): 0.71.

¹H NMR (CDCl₃, 500 MHz) δ: 0.82 (3H, t, *J* 7.0 Hz, CH₃), 0.90 (3H, t, *J* 7.0 Hz, CH₃), 1.21 (6H, m, 3×CH₂), 1.32 (4H, m, 2×CH₂), 1.40 (2H, m, CH₂), 1.48 (2H, m, CH₂), 1.63 (2H, m, CH₂), 2.55 (2H, dd, *J* 8.0, 7.8 Hz, CH₂), 2.72 (2H, dd, *J* 8.0, 7.8 Hz, CH₂), 3.96 (3H, s, CO₂CH₃), 7.08 (1H, s, ArH), 7.39 (2H, d, *J* 7.7 Hz, ArH), 7.47 (1H, s, ArH), 7.69 (2H, d, *J* 7.7 Hz, ArH), 7.73 (2H, d, *J* 8.7 Hz, ArH), 8.15 (2H, d, *J* 8.2 Hz, ArH). ¹³C NMR (CDCl₃, 125.8 MHz) δ: 14.02 (CH₃), 14.08 (CH₃), 22.4 (CH₂), 22.6 (CH₂), 29.0 (CH₂), 29.1 (CH₂), 30.0 (CH₂), 31.2 (CH₂), 31.4 (CH₂), 31.6 (CH₂), 32.4 (CH₂), 35.7 (CH₂), 52.1 (CO₂CH₃), 123.5 (ArCq), 126.93 (ArCH), 126.94 (ArCH), 128.9 (ArCq), 129.7 (ArCH), 130.2 (ArCH), 131.6 (ArCH), 133.1 (ArCH), 138.5 (ArCq), 139.3 (ArCq), 139.8 (ArCq), 140.3 (ArCq), 141.1 (ArCq), 145.2 (ArCq), 167.0 (CO). ν_{max}(Diamond ATR) 2955, 2926m, 2855, 1722s (C=O), 1608, 1275s, 1109, 831, 773 cm⁻¹. HRMS found 534.1965 C₃₂H₃₉BrO₂ requires: 534.2133.



Dimethyl 2'',5''-dihexyl-[1,1':4',1'':4'',1''':4''',1''''-quinquephenyl]-4,4''''-dicarboxylate *Rf* (1:1 Et₂O/petroleum ether): 0.20

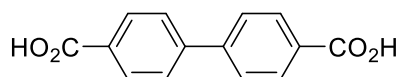
¹H NMR (CDCl₃, 500 MHz) δ: 0.81 (6H, t, *J* 6.8 Hz, 2×CH₃), 1.19 (12H, m, 6×CH₂), 1.53 (4H, m, 2×CH₂), 2.63 (4H, dd, *J* 8.1, 7.8 Hz, 2×CH₂), 3.96 (6H, s, 2×OCH₃), 7.19 (2H, s, Ph), 7.48 (4H, d, *J* 8.4 Hz, Ph), 7.71 (4H, d, *J* 8.4 Hz, Ph), 7.75 (4H, d, *J* 8.7 Hz, Ph), 8.14 (4H, d, *J* 8.7 Hz, Ph); ¹³C NMR (CDCl₃, 75.5 MHz) δ: 14.0 (CH₃), 22.5 (CH₂), 29.2 (CH₂), 31.4 (CH₂), 31.5 (CH₂), 32.6 (CH₂), 52.2 (OCH₃), 126.90 (ArCH), 126.94 (ArCH), 128.9 (ArCq), 129.9 (ArCH), 130.1 (ArCH), 130.9 (ArCH), 137.6 (ArCq), 138.3 (ArCq), 140.3 (ArCq), 141.9 (ArCq), 145.3 (ArCq), 167.0 (CO₂). ν_{max}(KBr)/cm⁻¹ 3427, 2949, 2925, 2850, 1715(C=O), 1607, 1436, 1277, 1194, 1181, 1112, 866, 837, 475. HRMS found 666.3709 C₄₆H₅₀O₄ requires: 666.3608.



General procedure for synthesis of diacids

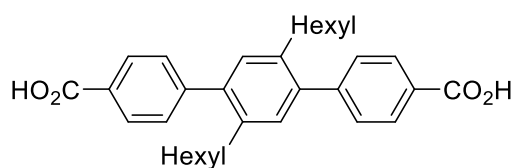
A solution of LiOH·H₂O (8 mol equiv) in H₂O was added to a stirred solution of diester in THF at room temperature. The resultant mixture was heated at reflux with stirring overnight, and then cooled to room temperature. 2M HCl (aq) and EtOAc were added. The layers were separated and the aqueous phase extracted with EtOAc (3×). The combined organic extracts were dried over anhydrous Na₂SO₄, filtered and concentrated to dryness *in vacuo* to afford a colourless powder.

[1,1'-Biphenyl]-4,4'-dicarboxylic acid In a deviation from the general procedure used for all of the other saponifications dimethyl-4,4'-biphenyl dicarboxylate



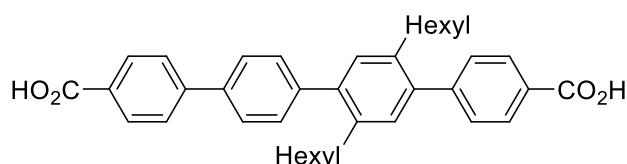
(500 mg, 1.700 mmol), LiOH·H₂O (571 mg, 13.60 mmol), THF (15 ml) and H₂O (10 ml) were heated at 80°C for 14 h with stirring. The mixture was then cooled to room temperature and concentrated to approximately ¼ of the original volume *in vacuo*. 1M HCl (50 ml) was added and the resultant colourless precipitate collected by suction filtration. The solid was washed well with cold H₂O and then Et₂O to afford the [1,1'-biphenyl]-4,4'-dicarboxylic acid as a colourless powder (318 mg, 71%). ¹H NMR (DMSO-*d*₆, 400 MHz) δ: 7.86 (4H, d, *J* 7.8 Hz, ArCH), 8.06 (4H, d, *J* 7.8 Hz, ArCH). ¹³C NMR (DMSO-*d*₆, 100 MHz) δ: 127.1 (ArCH), 130.0 (ArCH), 130.7 (ArCq), 143.0 (ArCq), 167.1 (C=O). ν_{\max} (Diamond ATR): 2830, 1673 (C=O), 1606, 1497, 1293, 880, 757 cm⁻¹. ES⁺-MS *m/z* 241 ((M-H)⁺), 100% (M = C₁₄H₁₀O₄).

2',5'-dihexyl-[1,1':4',1''-terphenyl]-4,4''-dicarboxylic acid
 Dimethyl 2',5'-dihexyl-[1,1':4',1''-terphenyl]-4,4''-dicarboxylate (500 mg, 0.972 mmol), LiOH·H₂O (326 mg, 7.772 mmol), H₂O (10 ml) and THF (10 ml) were



treated by the general procedure to afford the desired 2',5'-dihexyl-[1,1':4',1''-terphenyl]-4,4''-dicarboxylic acid as a colourless powder (467 mg, 99%). Crystals suitable for single crystal X-ray analysis were obtained by the slow evaporation of a concentrated DMSO solution of the 2',5'-dihexyl-[1,1':4',1''-terphenyl]-4,4''-dicarboxylic acid. (Found: C, 79.04; 7.81% C₃₂H₃₈O₄ requires C, 78.98; H, 7.87%); ¹H NMR (DMSO-*d*₆, 500 MHz) δ: 0.70 (6H, m, 2×CH₃), 1.06 (12H, m, 6×CH₂), 1.33 (4H, m, 2×CH₂), 2.46 (4H, m, 2×CH₂), 7.09 (2H, s, 2×ArCH), 7.44 (4H, d, *J* 6.3 Hz, 4×ArCH), 7.98 (4H, d, *J* 6.3 Hz, 4×ArCH), 12.96 (2H, s, 2×CO₂H). ¹³C NMR (DMSO-*d*₆, 125 MHz) δ: 13.8 (CH₃), 21.8 (CH₂), 28.4 (CH₂), 30.6 (CH₂), 30.7 (CH₂), 31.8 (CH₂), 40.4 (CH₂), 129.2 (2×ArCH), 129.4 (ArCq), 130.6 (ArCH), 137.1 (ArCq), 139.9 (ArCq), 145.6 (ArCq), 167.2 (C=O). ν_{\max} (KBr disc): 3432, 2956, 2928, 2857, 1687 (C=O), 1607, 1420, 1315, 1288, 1178, 1044, 904, 805, 773, 708 cm⁻¹. HRMS found 485.2696 C₃₂H₃₇O₄ requires 485.2697.

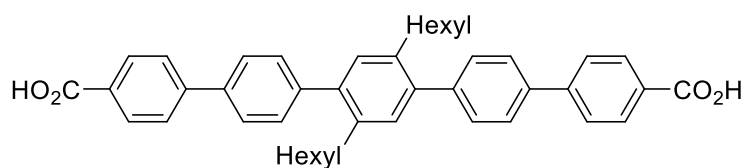
2',5'-Dihexyl-[1,1':4',1''':4''',1''''-quaterphenyl]-4,4''''-dicarboxylic acid
 Dimethyl 2',5'-dihexyl-[1,1':4',1''':4''',1''''-quaterphenyl]-4,4''''-dicarboxylate (30 mg, 0.0508 mmol), LiOH·H₂O (17 mg, 0.406 mmol), THF (5 ml) and H₂O (2 ml) were treated by the general procedure to afford



the 2',5'-dihexyl-[1,1':4',1''':4''',1''''-quaterphenyl]-4,4''''-dicarboxylic acid as a colourless powder (27 mg, 95%). ¹H NMR (DMSO-*d*₆, 500 MHz) δ: 0.74 (3H, t, *J* 7.0 Hz, CH₃), 0.75 (3H, t, *J* 7.0 Hz, CH₃), 1.11 (12H, m, 6×CH₂), 1.40 (4H, m, 2×CH₂), 2.56 (2H, dd, *J* 7.5, 7.5 Hz, CH₂), 2.60 (2H, dd, *J* 7.8, 7.8 Hz, CH₂), 7.14 (1H, s, ArCH), 7.16 (1H, s, ArCH), 7.48 (2H, d, *J* 8.2 Hz, 2×ArCH), 7.49 (2H, d, *J* 8.2 Hz, 2×ArCH), 7.84 (2H, d, *J* 8.2 Hz, 2×ArCH), 7.88 (2H, d, *J* 8.5 Hz, 2×ArCH), 8.03 (2H, d, *J* 8.2 Hz, 2×ArCH), 8.06 (2H, d, *J* 8.2 Hz, 2×ArCH), 12.96 (2H, br. s, 2×OH). ¹³C NMR (DMSO-*d*₆, 125 MHz) δ: 13.84 (CH₃), 13.86 (CH₃), 28.38 (CH₂), 28.42 (CH₂), 30.57 (CH₂), 30.63 (CH₂), 30.69 (CH₂), 30.74 (CH₂), 31.85 (CH₂), 31.88 (CH₂), 126.72 (ArCH), 126.76 (ArCH), 129.23 (ArCH), 129.26 (ArCH), 129.29 (ArCq), 129.65 (ArCq), 129.71 (ArCH), 130.0 (ArCH), 130.5 (ArCH), 130.8 (ArCH), 137.0 (ArCq), 137.2 (ArCq), 137.5 (ArCq), 139.6 (ArCq), 140.2 (ArCq), 141.1 (ArCq), 143.9 (ArCq), 145.8 (ArCq), 167.14 (C=O), 167.21 (C=O). ν_{\max} (Diamond ATR): 2955, 2926,

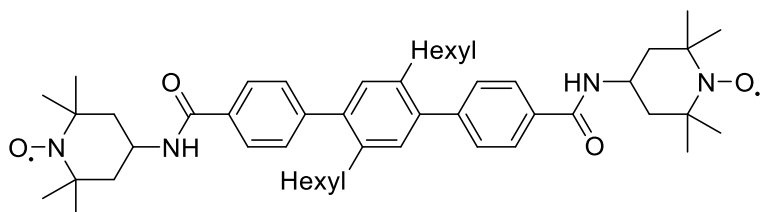
2854, 1680(C=O), 1607, 1423, 1280, 1178, 945, 775 cm⁻¹. HRMS-ES⁻ Found 561.3007 [C₃₈H₄₂O₄-H⁺]⁻ requires 561.3010.

2'',5''-Dihexyl-
[1,1':4',1'':4'',1''':4''',1''''-quinquephenyl]-4,4''''-
dicarboxylic acid Dimethyl
 2'',5''-dihexyl-



[1,1':4',1'':4'',1''':4''',1''''-quinquephenyl]-4,4''''-dicarboxylate (37.8 mg, 0.0567 mmol), LiOH·H₂O (19.0 mg, 0.4535 mmol), THF (10 ml) and H₂O (10 ml) were treated by the general procedure to afford *2'',5''-dihexyl-[1,1':4',1'':4'',1''':4''',1''''-quinquephenyl]-4,4''''-dicarboxylic acid* as a colourless powder (35.0 mg, 97%). Crystals suitable for single crystal X-ray analysis were obtained by the slow evaporation of a concentrated DMSO solution of the *2'',5''-dihexyl-[1,1':4',1'':4'',1''':4''',1''''-quinquephenyl]-4,4''''-dicarboxylic acid*. ¹H NMR (DMSO-*d*₆, 300 MHz) δ: 0.73 (6H, t, *J* 6.8 Hz, 2×CH₃), 1.11 (12H, m, 6×CH₂), 1.42 (4H, p, *J* 6.6 Hz, 2×CH₂), 2.59 (4H, dd, *J* 7.7, 7.3 Hz, 2×CH₂), 7.15 (2H, s, Ph), 7.47 (4H, d, *J* 8.3 Hz, Ph), 7.82 (4H, d, *J* 8.3 Hz, Ph), 7.87 (4H, d, *J* 8.5 Hz, Ph), 8.05 (4H, d, *J* 8.5 Hz, Ph). ¹³C NMR (DMSO-*d*₆, 75.5 MHz) δ: 13.9 (CH₃), 21.9 (CH₂), 30.7 (CH₂), 30.8 (CH₂), 31.9 (CH₂), 126.73 (ArCH), 126.77 (ArCH), 129.6 (ArCq), 129.7 (ArCH), 130.1 (ArCH), 130.7 (ArCq), 137.1 (ArCq), 137.5 (ArCq), 139.9 (ArCq), 141.2 (ArCq), 143.9 (ArCq), 167.2 (CO₂). ν_{max}(KBr)/cm⁻¹ 3441, 2954, 2926, 2856, 2665, 2542, 1686(C=O), 1607, 1423, 1294, 1179, 1106, 1005, 837, 776. MS-ES⁻ *m/z* 637 ([M-H⁺]⁻, 100%), 318 (59), 273 (67), 213 (70). HRMS found 637.3329 C₄₄H₄₅O₄ requires: 637.3323.

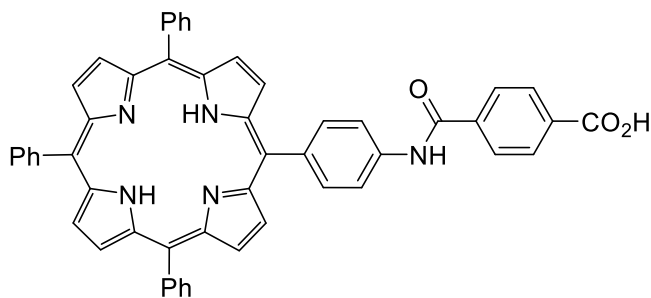
3-Phenyl bisnitroxide
(Compound 8) 2',5'-Dihexyl-
 [1,1':4',1'':4'',1''':4''',1''''-quinquephenyl]-4,4''''-
 dicarboxylic acid (100.0 mg,
 0.205 mmol), 4-amino-TEMPO
 (106 mg, 0.616 mmol), BOP
 (0.364 mg, 0.822 mmol),



DIPEA (0.213 ml, 1.644 mmol) and anhydrous DMF (5 ml) were combined at room temperature under atmosphere of nitrogen. The resultant mixture was stirred at room temperature for 12 h, after which tlc analysis indicated the reaction was complete. The mixture was concentrated to dryness *in vacuo* to afford a solid. The solid was purified by flash chromatography on silica using 1:1 EtOAc/petroleum ether as eluent to afford the title compound as a pale pink coloured solid (127.0 mg, 78%) EPR parameters at X-Band CW g: [2.0087 2.0063 2.0036] Nucs: 'N' A: [21.9117 21.5106 88.7862] lwpp: [0 0.2235]; ν_{max}(Diamond ATR) 3400 (NH), 2926, 1655 (C=O), 1506, 1484, 1461, 1299, 1219, 844 cm⁻¹ HRMS found 792.5530 C₅₀H₇₂N₄O₂²⁻ requires 792.5548.

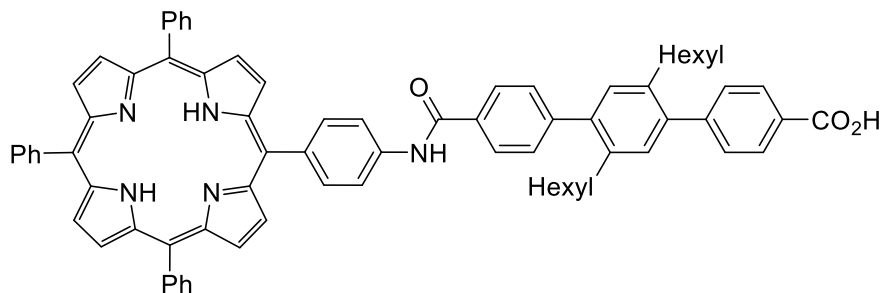
4-((4-(10,15,20-Triphenylporphyrin-5-yl)phenyl)carbamoyl)benzoic acid

Terephthalic acid (39.6 mg, 0.2389 mmol), TPPNH₂ (150 mg, 0.2389 mmol), BOP (115.9 mg, 0.2620 mmol), DIPEA (0.170 ml, 0.9528 mmol) and DMF (5 ml) were combined at room temperature under atmosphere of nitrogen. The resultant mixture was



stirred at room temperature for 12 h, after which tlc analysis indicated the reaction was complete. The mixture was concentrated to dryness *in vacuo* to afford a solid. The solid was purified by flash chromatography on silica using firstly EtOAc/CHCl₃ (1:4) which afforded trace amounts of the bisadduct, followed by EtOAc/MeOH/CH₂Cl₂ (1:1:3) which afforded the mono-adduct *4-((4-(10,15,20-triphenylporphyrin-5-yl)phenyl)carbamoyl)benzoic acid* as a purple coloured solid (74.3 mg, 40%) ¹H NMR (CDCl₃, 500 MHz) δ: -2.90 (2H, br. s, 2×pyrrNH), 7.85 (9H, m, ArH), 7.99 (2H, d, *J*8.5 Hz, ArH), 8.04 (2H, d, *J*8.2 Hz, ArH), 8.16 (5H, q_{AB}, *J*8.5 Hz, ArH), 8.23 (7H, m, ArH), 8.28 (3H, d, *J*8.5 Hz, ArH), 8.84 (6H, m, ArH), 8.93 (4H, br. d, ArH), 10.82 (1H, br. s, CO₂H). ¹³C NMR (CDCl₃, 125.8 MHz) δ: 118.7, 120.0, 127.0, 128.1, 128.9, 129.3, 129.4, 134.2, 136.7, 136.5, 139.1, 141.21, 141.24, 165.5, 165.7. ν_{max}(Diamond ATR) 3665, 3595, 3317, 1721, 1658, 1630 (C=O), 1593 (C=O), 1522, 1400, 1005, 966, 819 (s) cm⁻¹. λ_{max}(DMSO)/nm 678 (820), 647 (1690), 591 (1650), 551 (2990), 515 (5170), 420 (120900). ESI-FTMS *m/z* 776.2660 C₅₂H₃₄N₅O₃ requires 776.2667

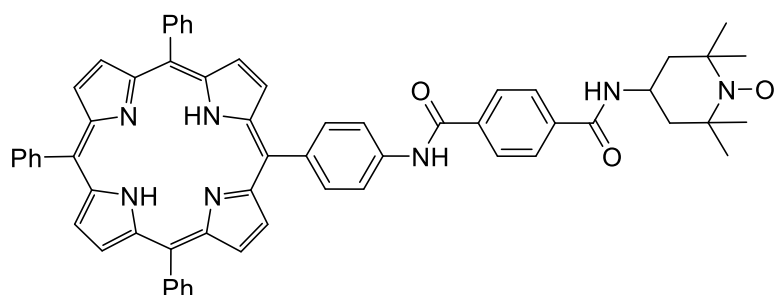
2',5'-Dihexyl-4''-((4-(10,15,20-triphenylporphyrin-5-



yl)phenyl)carbamoyl)-[1,1':4',1''-terphenyl]-4-carboxylic acid 2',5'-Dihexyl-[1,1':4',1''-terphenyl]-4,4''-dicarboxylic acid (100.0 mg, 0.2055 mmol), TPPNH₂ (129.4 mg, 0.2055 mmol), BOP (90.9 mg, 0.2055 mmol), DIPEA (0.15 ml, 0.8220 mmol) and DMF (15 ml) were combined at room temperature under atmosphere of nitrogen. The resultant mixture was stirred at room temperature for 14 h. The mixture was concentrated to dryness *in vacuo* to afford a solid. The solid was taken up in H₂O (50 ml) and CHCl₃ (50 ml) and the layers separated. The organic layer was washed with H₂O (4×15 ml) before then organic extract was dried over anhydrous Na₂SO₄, filtered and concentrated to dryness *in vacuo*. The crude solid was purified by flash chromatography on silica using firstly EtOAc/CHCl₃ (1:4) which afforded the bisadduct (95.6 mg), followed by EtOAc/MeOH/CHCl₃ (1:1:3) which afforded first recovered TPPNH₂ (32.3 mg) and then the desired mono-adduct *2',5'-dihexyl-4''-((4-(10,15,20-triphenylporphyrin-5-yl)phenyl)carbamoyl)-[1,1':4',1''-terphenyl]-4-carboxylic acid* as a purple coloured solid (69.4 mg, 31%) *R_f*(1:1 EtOAc/CHCl₃): 0.49. ¹H NMR (CDCl₃, 500 MHz) δ: -2.75 (2H, br. s, 2×pyrrNH), 0.85 (3H, t, *J*6.6 Hz, CH₃), 0.88 (3H, t, *J*6.6 Hz, CH₃), 1.24 (6H, m, 3×CH₂), 1.53 (4H, m, 2×CH₂), 2.62 (2H, m, ArCH₂), 2.65 (2H, m, ArCH₂), 7.20 (1H, s, ArCH), 7.22

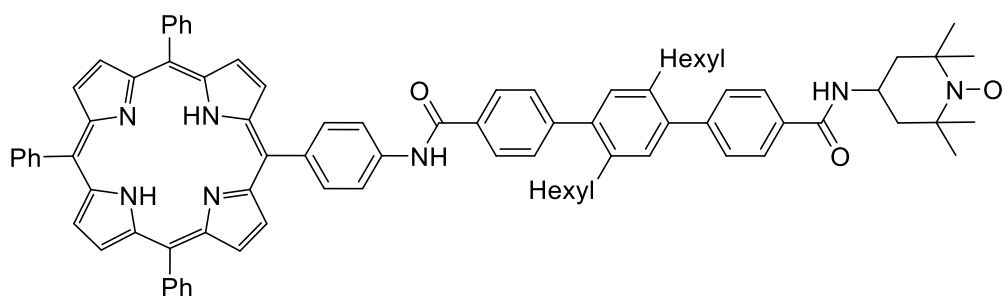
(1H, s, ArCH), 7.64 (4H, d, *J* 8.0 Hz, ArCH), 7.78 (17H, m, ArCH), 8.12 (4H, d, *J* 8.0 Hz, ArCH), 8.16 (4H, d, *J* 8.0 Hz, ArCH), 8.25 (17H, m, ArCH), 8.87 (8H, s, ArCH), 8.92 (4H, d, *J* 4.5 Hz, pyrrole), 8.95 (4H, d, *J* 4.5 Hz, pyrrole), plus the acid peak at 10.85 (1H, br. s, CO₂H). ¹³C NMR (CDCl₃, 125.8 MHz) δ: 14.0 (CH₃), 14.1 (CH₃), 22.49 (CH₂), 22.52 (CH₂), 28.3 (CH₂), 29.12 (CH₂), 29.23 (CH₂), 31.40 (CH₂), 31.48 (CH₂), 31.54 (CH₂), 32.62 (CH₂), 32.67 (CH₂), 118.4, 119.4, 120.2, 126.7, 126.8, 127.7, 129.4, 129.5, 129.9, 130.0, 130.8, 130.9, 133.4, 134.6, 135.3, 137.65, 137.67, 137.72, 137.9, 138.5, 140.23, 140.28, 142.2, 145.9, 147.5, 165.9, 169.6. *m/z* 1098.5308 C₇₆H₆₈N₅O₃ requires 1098.5317. λ_{max}(CHCl₃)/nm (ε/dm³mol⁻¹cm⁻¹), 645 (3300), 589 (4300), 551 (6900), 516 (14000), 419 (356500).

1-Phenyl porphyrin nitroxide
4-((4-(10,15,20-Triphenylporphyrin-5-



yl)phenyl)carbamoyl)benzoic acid (50.0 mg, 0.0643 mmol), TEMPO-NH₂ (22.0 mg, 0.1286 mmol), BOP (42.6 mg, 0.0964 mmol), DIPEA (0.090 ml, 0.5142 mmol) and DMF (2.5 ml) were treated by the general procedure. The crude adduct was purified by flash chromatography on silica using 1:4 EtOAc/CHCl₃ to afford the product as a purple coloured solid (35.0 mg, 59 %). *Rf*(2:3 EtOAc/CHCl₃) 0.38. EPR parameters at X-Band CW g: [2.0084 2.0065 2.0035] Nucs: 'N' A: [21.3973 21 88.2998] lwpp: [0.1144 0.2000] *m/z* (MALDI-TOF LD⁺) found 929.4091 C₆₁H₅₁N₇O₃ requires 929.4059. λ_{max}(CHCl₃)/nm 647 (10870), 591 (12320), 550 (7610), 516 (12080), 419 (22680).

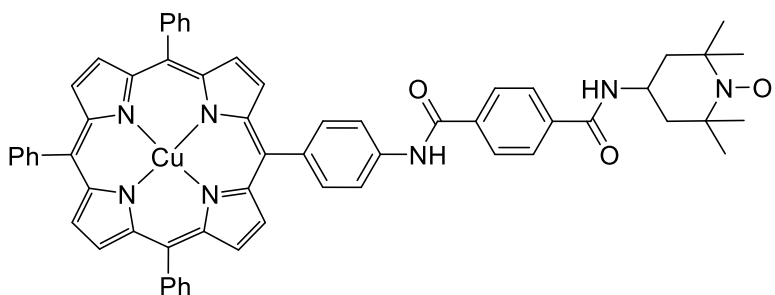
3-Phenyl porphyrin nitroxide
2',5'-Dihexyl-4''-((4-(10,15,20-



triphenylporphyrin-5-yl)phenyl)carbamoyl)-[1,1':4',1''-terphenyl]-4-carboxylic acid (20.0 mg, 0.1821 mmol), TEMPO-NH₂ (12.5 mg, 0.7283 mmol), BOP (9.7 mg, 0.2185 mmol), DIPEA (0.026 ml, 1.457 mmol) and DMF (6 ml) were treated by the general procedure to afford after flash chromatography on silica using 1:1 EtOAc/CHCl₃ the title product as a purple coloured solid (19.3 mg, 85 %). *Rf*(1:1 EtOAc/CHCl₃: 0.78. EPR parameters at X-Band CW g: [2.0081 2.0058 2.0046] Nucs: 'N' A: [21.0000 22.7274 89.9919] lwpp: [0.1000 0.2406] MALDI-TOF LD⁺ Found 1251.6709 C₈₅H₈₅N₇O₃ requires 1251.6708. λ_{max}(CHCl₃)/ 646 (1500), 590 (2000), 552 (3200), 516 (6500), 419 (166400).

Cu-1-Phenyl porphyrin nitroxide (Compound 6)

1-Phenyl porphyrin nitroxide (12.2 mg, 0.0131 mmol), Cu(OAc)₂·H₂O (6.5 mg, 0.0326 mmol), CHCl₃ (3 ml) and MeOH (1 ml) were heated at reflux for 4 h and

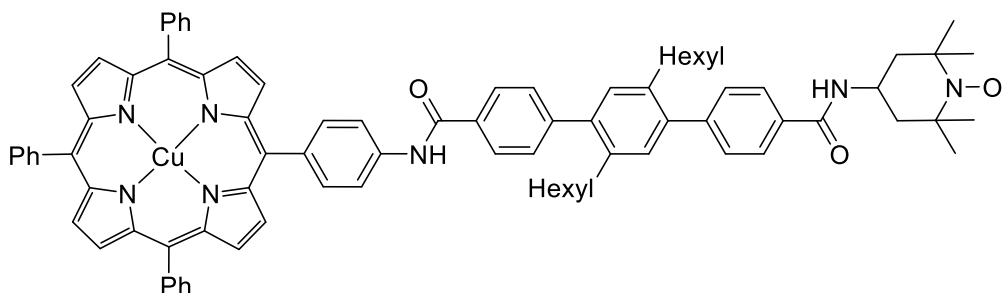


then cooled to room temperature. The mixture was then concentrated to dryness *in vacuo*, before the residue was dissolved in CHCl₃ (30 ml) and H₂O (20 ml). The pink organic layer was washed with H₂O (3×10 ml), then dried over anhydrous Na₂SO₄, filtered and concentrated to dryness *in vacuo* to afford the desired product as a pink-purple coloured solid (12.8 mg, 98%). *Rf*(2:3 EtOAc/CHCl₃) 0.45. EPR parameters at X-Band CW Copper: g: [2.056 2.056 2.205] Nucs: 'N' A: [80 80 593] Hstrain: [221 173 238] Nitroxide: g: [2.01 2.01 2.09] Nucs: 'N' A: [20 20 100] Hstrain: [40 40 40] *m/z* (MALDI-TOF LD⁺) found 990.3198 C₆₁H₄₉CuN₇O₃ requires 990.3198. λ_{max}(CHCl₃)/nm 540 (16,870), 416 (394,500).

Cu-3-phenyl nitroxide (Compound 7)
3-Phenyl porphyrin nitroxide

(10.3 mg,

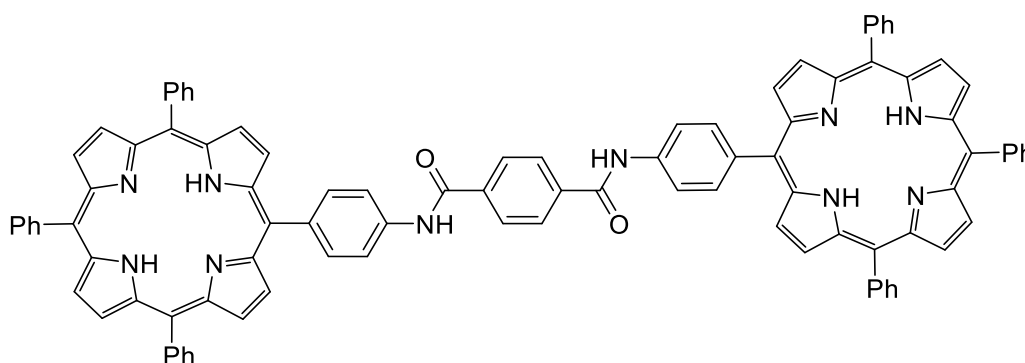
0.0082 mmol), Cu(OAc)₂·H₂O (8.0 mg, 0.0401 mmol), CHCl₃ (5 ml), MeOH (2 ml) were heated at reflux for 1 h with stirring, during which the mixture became pink in colour. The mixture was diluted with CHCl₃ (20 ml) and H₂O (15 ml). The layers were separated and the pink organic layer was washed with H₂O (4×15 ml) before the organic fraction was dried over anhydrous Na₂SO₄, filtered and concentrated to dryness *in vacuo*. This afforded the title compound as a pink-purple coloured solid (9.0 mg, 83 %). *Rf* (1:1 EtOAc/CHCl₃): 0.78. EPR parameters at X-Band CW Copper: g: [2.056 2.056 2.205] Nucs: 'N' A: [80 80 593] Hstrain: [221 173 238] Nitroxide: g: [2.01 2.01 2.09] Nucs: 'N' A: [20 20 100] Hstrain: [40 40 40] λ_{max}(CHCl₃)/nm 540 (12600), 416 (267200). *m/z* (MALDI-TOF LD⁺) 1334.5629 C₈₅H₈₂CuN₇O₃ + Na⁺ requires 1334.5667.



General procedure for synthesis of diporphyrin species

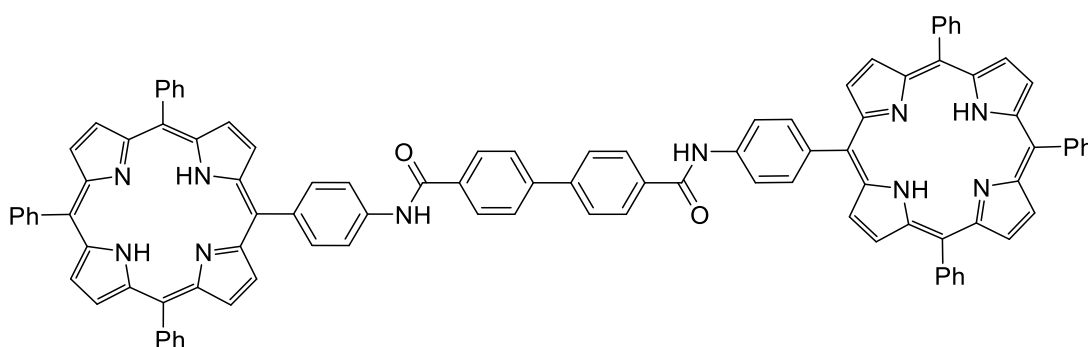
BOP (2.6 mol equiv) was added to a stirred solution of diacid (1 mol equiv), TPPNH₂ (2.2 mol equiv), DIPEA (8 mol equiv) in anhydrous DMF at room temperature under nitrogen atmosphere. The resultant mixture was stirred at room temperature for 4 days, during which time a spot of higher R_f was found by tlc analysis (2:3 EtOAc/CHCl₃). The mixture was then concentrated under reduced pressure, before taken up in CHCl₃ and sat. NaCl (aq). The CHCl₃ layer was washed with sat. NaCl (aq) (5×) then the CHCl₃ layer was dried over anhydrous Na₂SO₄, filtered and concentrated to dryness *in vacuo* to afford a purple solid.

1-Phenyl diporphyrin



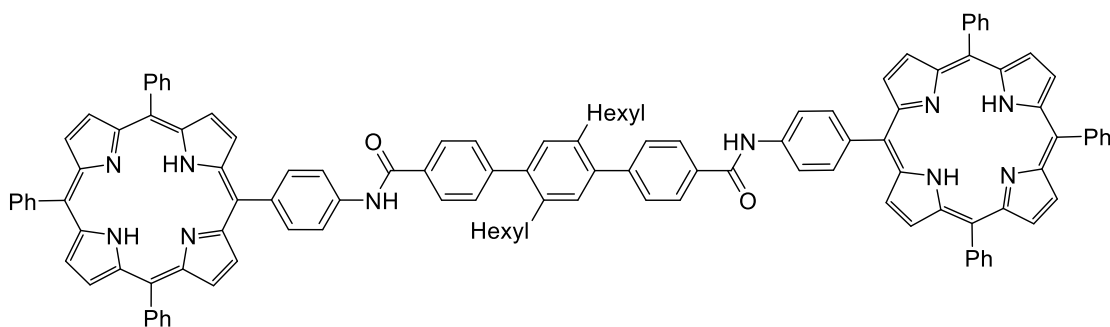
Terephthalic acid (25 mg, 0.150 mmol), TPPNH₂ (194 mg, 0.308 mmol), BOP (173 mg, 0.391 mmol), DIPEA (0.16 ml, 1.203 mmol) in anhydrous DMF (5 ml) was treated according to the general procedure to afford a purple solid. This was purified using 1:2 Et₂O/CH₂Cl₂ to afford the desired 1-phenyl diporphyrin (68.9 mg, 33%). ¹H NMR (CDCl₃, 500 MHz) δ: -2.89 (4H, br. s, 4×pyrrNH), 7.56 (8H, br. d, ArH), 7.86 (6H, br. s, ArH), 7.96 (5H, m, ArH), 8.24 (10H, m, ArH), 8.89 (8H, m, ArH). λ_{max}(CHCl₃)/nm (ε/dm³mol⁻¹cm⁻¹), 646 (8000), 590 (10,400), 551 (16,400), 516 (33,500), 420 (810,900). *m/z* (MALDI-TOF LD⁺) 1390.53 C₉₆H₆₄N₁₀O₂ requires 1390.27.

2-Phenyl diporphyrin



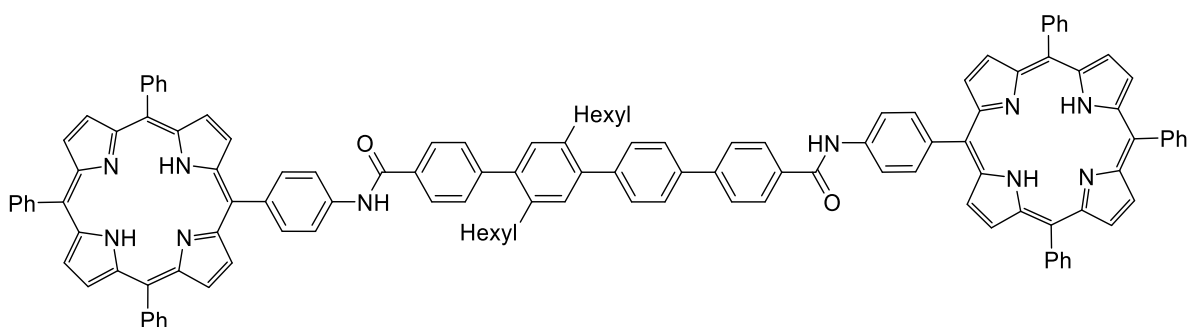
[1,1'-Biphenyl]-4,4'-dicarboxylic acid (20.0 mg, 0.0826 mmol), TPPNH₂ (109.2 mg, 0.174 mmol), BOP (91.3 mg, 0.206 mmol), DIPEA (0.12 ml, 0.661 mmol) in anhydrous DMF (2.5 ml) was treated according to the general procedure to afford a purple solid. This was purified using 1:1 Et₂O/CH₂Cl₂ to afford the desired 2-phenyl diporphyrin (78.3 mg, 65%). ¹H NMR (CDCl₃, 500 MHz) δ: -2.90 (4H, br. s, 4×pyrrNH), 7.55 (6H, m, ArH), 7.86 (10H, m, ArH), 8.24 (8H, br. s, ArH), 8.85 (6H, m, ArH). λ_{max}(CHCl₃)/nm (ε/dm³mol⁻¹cm⁻¹), 645 (10,100), 590 (13,000), 550 (20,400), 516 (40,200), 420 (896,000). *m/z* (MALDI-TOF LD⁺) 1466.56 C₁₀₂H₆₈N₁₀O₂ requires 1466.53.

3-Phenyl diporphyrin



2',5'-Dihexyl-[1,1':4',1'':4,4''-dihexyl-terphenyl]-4,4''-dicarboxylic acid (50 mg, 0.103 mmol), TPPNH₂ (133 mg, 0.211 mmol), BOP (118 mg, 0.267 mmol), DIPEA (0.15 ml, 0.822 mmol) in anhydrous DMF (2.5 ml) were treated by the general procedure to afford a purple solid. This was purified by flash chromatography using 1:1 Et₂O/CHCl₃ to afford, in order of elution, the desired 3-phenyl diporphyrin (41 mg, 23 %) as a dark purple coloured solid and recovered TPPNH₂ (59 mg, 44% recovery). *R_f* (1:1 EtOAc/CHCl₃): 0.64. ¹H NMR (CDCl₃, 500 MHz) δ: -2.73 (4H, br. s, 4×pyrr NH), 0.90 (6H, t, *J*7.0 Hz, 2×CH₃), 1.29 (12H, m, 6×CH₂), 1.58 (4H, m, 2×CH₂), 2.69 (4H, dd, *J*8.0, 8.0 Hz, 2×ArCH₂), 7.26 (2H, s, ArCH), 7.64 (4H, d, *J*8.0 Hz, ArCH), 7.78 (17H, m, ArCH), 8.12 (4H, d, *J*8.0 Hz, ArCH), 8.16 (4H, d, *J*8.0 Hz, ArCH), 8.25 (17H, m, ArCH), 8.87 (8H, s, ArCH), 8.92 (4H, d, *J*4.5 Hz, pyrrole), 8.95 (4H, d, *J*4.5 Hz, pyrrole); ¹³C NMR (CDCl₃, 125.8 MHz) δ: 14.1 (CH₃), 22.6 (CH₂), 29.2 (CH₂), 31.48 (CH₂), 31.56 (CH₂), 32.7 (CH₂), 118.4 (ArCH), 119.4 (ArCq), 120.2 (ArCq); 126.7 (ArCH), 127.0 (ArCH), 127.7 (ArCH), 129.9 (ArCH), 130.9 (ArCH), 131.3 (broad, ArCH), 133.4 (ArCq), 134.6 (ArCH), 135.3 (ArCH), 137.7 (ArCq), 138.5 (ArCq), 140.2 (ArCq), 142.2 (ArCq), 145.9 (ArCq), 165.9 (C=O); ν_{max}(KBr)/cm⁻¹ 3430, 3317, 3026, 2956, 2924, 2854, 1681(C=O), 1606, 1558, 1509, 1473, 1350, 1312, 1272, 1099, 966, 800, 730, 701. λ_{max}(CHCl₃)/nm (ε/dm³mol⁻¹cm⁻¹), 646 (9000), 590 (11,300), 551 (18,000), 516 (36,600), 419 (838,000). *m/z* (MALDI-TOF LD⁺) 1710.59 C₁₂₀H₉₆N₁₀O₂ requires 1710.78.

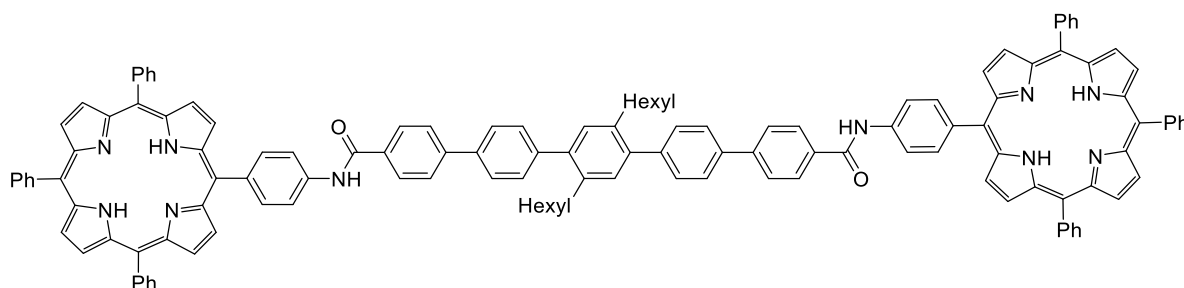
4-Phenyl diporphyrin



2',5'-Dihexyl-[1,1':4',1'':4,4''-dihexyl-quaterphenyl]-4,4''-dicarboxylic acid (30.0 mg, 0.0533 mmol), TPPNH₂ (73.9 mg, 0.1173 mmol), BOP (61.3 mg, 0.1386 mmol), DIPEA (0.076 ml, 0.4265 mmol) in anhydrous DMF (5 ml) was treated according to the general procedure to afford a purple solid. This was purified using 1:1 Et₂O/CH₂Cl₂ to afford, in order of elution, the desired 4-phenyl diporphyrin (41.2 mg, 43%) and recovered TPPNH₂. The 4-phenyl diporphyrin was further purified by elution using CHCl₃ to remove trace amounts of several porphyrin species that were unable to be isolated or characterised. ¹H NMR (CDCl₃, 400 MHz) δ: -2.73 (2H, br. s, 4×pyrrNH), 0.87 (3H, t, *J*7.0 Hz, CH₃), 0.90 (3H, t, *J*

7.0 Hz, CH₃), 1.28 (12H, m, 6×CH₂), 1.56 (4H, m, 2×CH₂), 2.69 (4H, m, 2×ArCH₂), 7.25 (1H, s, ArCH), 7.28 (1H, s, ArCH), 7.56 (2H, d, *J*8.0 Hz, ArCH), 7.64 (2H, d, *J*8.0 Hz, ArCH), 7.79 (20H, m, ArCH), 7.92 (2H, d, *J*8.0 Hz, ArCH), 8.11 (4H, app. dd, *J*8.3, 2.5 Hz, ArCH), 8.15 (2H, d, *J*8.0 Hz, ArCH), 8.18 (2H, d, *J*8.0 Hz, ArCH), 8.25 (17H, m, ArCH), 8.90 (15H, m, ArCH). ¹³C NMR (CDCl₃, 100 MHz) δ: 14.1 (2×CH₃), 22.53 (CH₂), 22.56 (CH₂), 29.23 (CH₂), 22.28 (CH₂), 31.47 (CH₂), 31.50 (CH₂), 31.55 (CH₂), 31.60 (CH₂), 32.71 (CH₂), 32.75 (CH₂), 118.4 (ArCH), 119.4 (ArCq), 120.2 (ArCq), 126.7 (ArCH), 126.98 (ArCH), 127.03 (ArCH), 127.6 (ArCH), 127.75 (ArCH), 127.81 (ArCH), 129.99 (ArCH), 130.01 (ArCH), 130.8 (ArCH), 131.1 (ArCH), 133.4 (ArCq), 133.7 (ArCq), 133.9 (ArCq), 134.6 (ArCH), 135.3 (ArCH), 137.6 (ArCq), 137.77 (ArCq), 137.79 (ArCq), 137.87 (ArCq), 138.3 (ArCq), 138.5 (ArCq), 139.6 (ArCq), 139.9 (ArCq), 140.8 (ArCq), 142.2 (ArCq), 145.7 (ArCq), 146.1 (ArCq), 165.7 (C=O), 165.9 (C=O). λ_{max}(CHCl₃)/nm (ε/dm³mol⁻¹cm⁻¹), 646 (7700), 591 (6800), 550 (4700), 516 (18,100), 419 (489,000). *m/z* (MALDI-TOF LD⁺) 1786.32 C₁₂₆H₁₀₀N₁₀O₂ requires 1786.81.

5-Phenyl diporphyrin

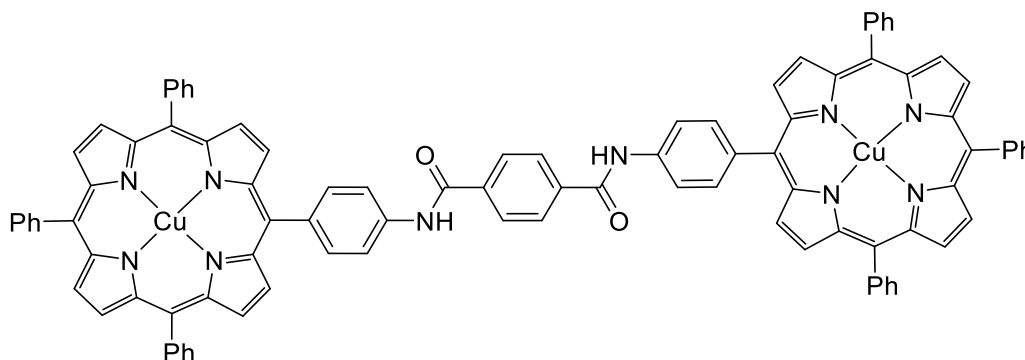


2'',5''-Dihexyl-[1,1':4',1'':4'',1''':4''',1''''-quinquephenyl]-4,4''''-dicarboxylic acid (15.5 mg, 0.0243 mmol), TPPNH₂ (33.6 mg, 0.0534 mmol), BOP (27.9 mg, 0.0631 mmol), DIPEA (0.034 ml, 0.194 mmol) in anhydrous DMF (2 ml) was treated according to the general procedure to afford a purple solid. This was purified using 1:9 Et₂O/CH₂Cl₂ to afford, in order of elution, the desired 5-phenyl diporphyrin (29.9 mg, 66%) and recovered TPPNH₂. ¹H NMR (CDCl₃, 500 MHz) δ: -2.73 (4H, br. s, 4×pyrrNH), 0.89 (6H, t, *J*6.6 Hz, 2×CH₃), 1.27 (12H, m, 6×CH₂), 1.57 (4H, m, 2×CH₂), 2.68 (4H, m, 2×ArCH₂), 7.24 (2H, s, ArCH), 7.56 (4H, d, *J*8.0 Hz, ArCH), 7.78 (22H, m, ArCH), 7.94 (4H, d, *J*8.0 Hz, ArCH), 8.10 (4H, d, *J*8.0 Hz, ArCH), 8.16 (4H, d, *J*8.0 Hz, ArCH), 8.25 (16H, m, ArCH), 8.86 (8H, br. s, ArCH), 8.89 (4H, d, *J*4.7 Hz, pyrrCH), 8.94 (4H, d, *J*4.7 Hz, pyrrCH). ¹³C NMR (CDCl₃, 125.8 MHz) δ: 14.1 (CH₃), 22.5 (CH₂), 29.2 (CH₂), 31.48 (CH₂), 31.55 (CH₂), 32.7 (CH₂), 118.4 (ArCH), 119.4 (ArCq), 120.2 (ArCq), 126.7 (ArCH), 126.9 (ArCH), 127.1 (ArCq), 127.5 (ArCH), 127.7 (ArCq), 127.8 (ArCH), 130.01 (ArCq), 130.03 (ArCH), 130.2 (ArCq), 131.0 (ArCH), 131.4 (ArCq), 133.6 (ArCq), 134.6 (ArCH), 135.3 (ArCH), 137.70 (ArCq), 137.73 (ArCq), 138.2 (ArCq), 138.5 (ArCq), 140.2 (ArCq), 140.5 (ArCq), 142.0 (ArCq), 142.2 (ArCq), 144.6 (ArCq), 165.7 (C=O). λ_{max}(CHCl₃)/nm (ε/dm³mol⁻¹cm⁻¹), 645 (5800), 590 (10,000), 551 (14,700), 516 (25,100), 419 (575,000). *m/z* (MALDI-TOF LD⁺) 1862.85 C₁₃₂H₁₀₄N₁₀O₂ requires 1862.52.

General procedure for synthesis of dicopper compounds 1-5.

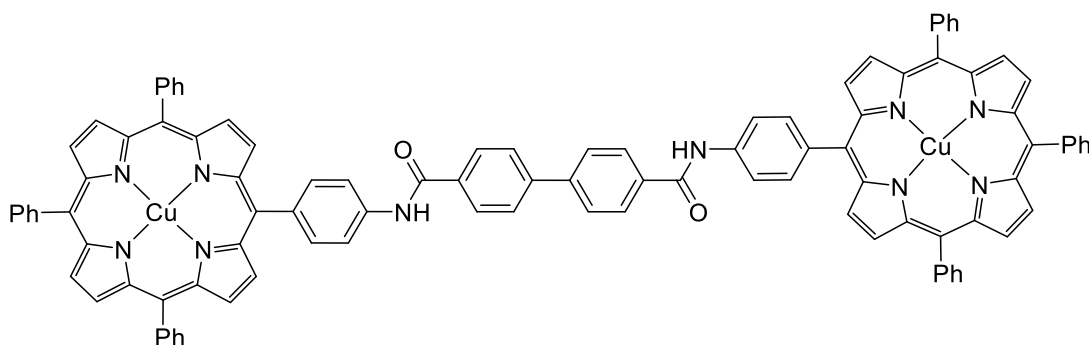
Cu(OAc)₂·H₂O (8 mol equiv) in MeOH was added to a stirred solution of diporphyrin in CHCl₃ at room temperature. The resultant mixture was heated at reflux for 3 h and then cooled to room temperature and stirred at room temperature for 12 h. The mixture was then concentrated to dryness *in vacuo* to generate a dark red/purple solid. This residue was taken up in CHCl₃ and washed with H₂O (3×). The organic phase was dried over anhydrous Na₂SO₄, filtered and concentrated to dryness *in vacuo* to afford the desired dicopper product as a pink/purple solid.

1-Phenyldiporphyrin dicopper (Compound 1)



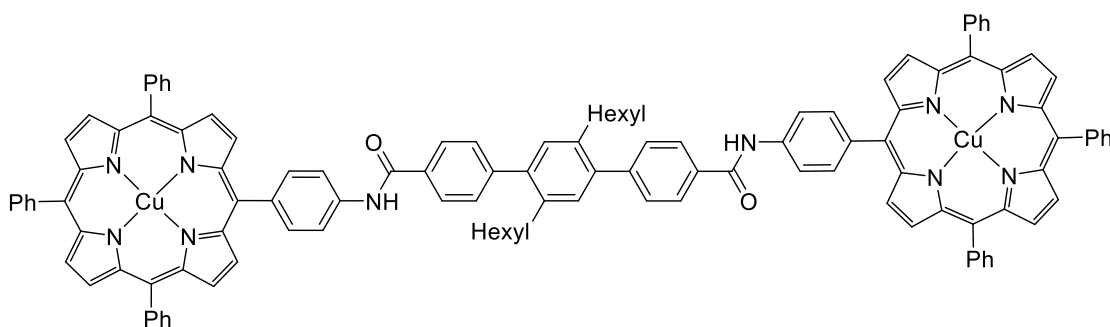
1-Phenyl diporphyrin (11.0 mg, 7.92 μmol), Cu(OAc)₂·H₂O (10.0 mg, 50.09 μmol), CHCl₃ (5 ml) and MeOH (2.5 ml) were treated by the general procedure to afford the title compound **1** as a pink/purple solid (9.0 mg, 75%). EPR parameters at X-Band CW g: [2.05 2.05 2.19] Nucs: 'N' A: [87 87 600] Hstrain: [250 250 250] $\lambda_{\text{max}}(\text{CHCl}_3)/\text{nm}$ 539 ($\epsilon/\text{dm}^3\text{mol}^{-1}\text{cm}^{-1}$ 2600), 417 (70,200), 400sh (7000), 298 (3400); m/z (MALDI-TOF LD⁺) 1514.36 C₉₆H₆₀Cu₂N₁₀O₂ requires 1514.28.

2-Phenyldiporphyrin dicopper (Compound 2)



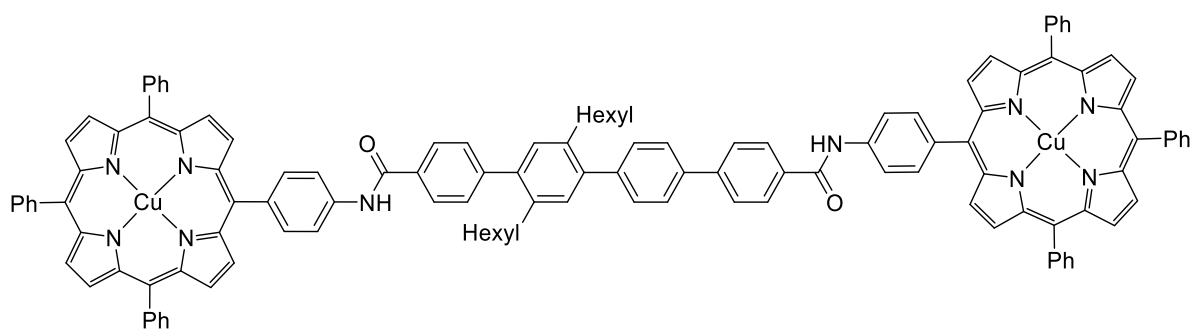
2-Phenyl diporphyrin (12.4 mg, 8.46 μmol), $\text{Cu}(\text{OAc})_2 \cdot \text{H}_2\text{O}$ (9.6 mg, 48.08 μmol), CHCl_3 (15 ml) and MeOH (8 ml) were treated by the general procedure to afford the title compound **2** as a pink/purple solid (11.8 mg, 88%). EPR parameters at X-Band CW g: [2.05 2.05 2.19] Nucs: 'N' A: [87 87 600] Hstrain: [250 250 250] $\lambda_{\text{max}}(\text{CHCl}_3)/\text{nm}$ 539 (16,200), 416 (332,900), 397sh (29,700), 307 (25,400); m/z (MALDI-TOF LD⁺) 1589.39 $\text{C}_{102}\text{H}_{64}\text{Cu}_2\text{N}_{10}\text{O}_2$ requires 1589.12.

3-Phenyldiporphyrin dicopper (Compound 3)



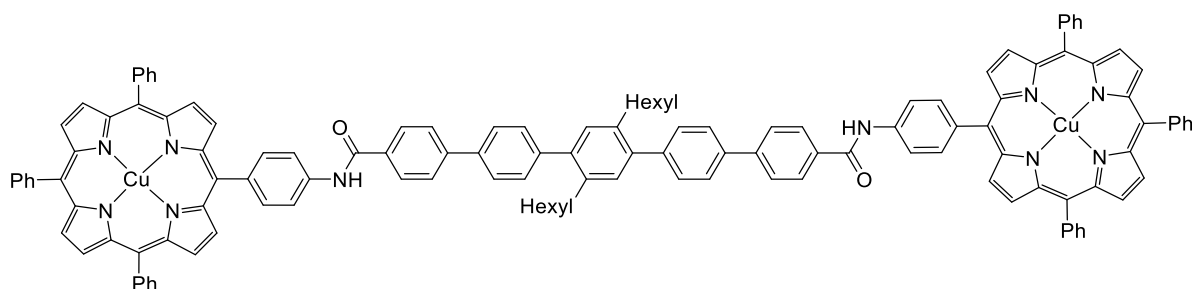
$\text{Cu}(\text{OAc})_2 \cdot \text{H}_2\text{O}$ (14 mg, 70.1 μmol) in MeOH (5 ml) was added to a stirred solution of 3-phenyl diporphyrin (29 mg, 17.0 μmol) in CHCl_3 (10 ml) at room temperature were treated by the general procedure. The residue was taken up in CHCl_3 (15 ml) and washed with H_2O (3×10 ml). The organic phase was dried over anhydrous Na_2SO_4 , filtered and concentrated to dryness *in vacuo* to afford the desired dicopper product **3** as a pink/purple solid (22 mg, 71 %). EPR parameters at X-Band CW g: [2.05 2.05 2.19] Nucs: 'N' A: [87 87 600] Hstrain: [250 250 250] $\nu_{\text{max}}(\text{KBr})/\text{cm}^{-1}$ 3431, 2952, 2924, 2853, 1675(C=O), 1599, 1004, 799, 753, 701. $\lambda_{\text{max}}(\text{CHCl}_3)/\text{nm}$ ($\epsilon/\text{dm}^3\text{mol}^{-1}\text{cm}^{-1}$) 3700, 417 (105,600), 400sh (7000), 296 (5800); m/z (MALDI-TOF LD⁺) 1833.45 $\text{C}_{120}\text{H}_{92}\text{Cu}_2\text{N}_{10}\text{O}_2 + \text{H}^+$ requires 1833.61.

4-Phenyldiporphyrin dicopper (Compound 4)



4-Phenyl diporphyrin (10.3 mg, 5.77 μmol), $\text{Cu}(\text{OAc})_2 \cdot \text{H}_2\text{O}$ (9.0 mg, 45.08 μmol), CHCl_3 (7.5 ml) and MeOH (4 ml) were treated by the general procedure to afford the title compound **4** as a pink/purple solid (8.5 mg, 77%). EPR parameters at X-Band CW g: [2.05 2.05 2.19] Nucs: 'N' A: [87 87 600] Hstrain: [250 250 250] $\lambda_{\text{max}}(\text{CHCl}_3)/\text{nm}$ 539 ($\epsilon/\text{dm}^3\text{mol}^{-1}\text{cm}^{-1}$ 2200), 416 (49,700), 400 (4200), 298(6500). m/z (MALDI-TOF LD⁺) 1910.64 $\text{C}_{126}\text{H}_{96}\text{Cu}_2\text{N}_{10}\text{O}_2$ requires 1910.21.

5-Phenyldiporphyrin dicopper (Compound 5)



5-Phenyl diporphyrin (7.2 mg, 3.87 μmol), $\text{Cu}(\text{OAc})_2 \cdot \text{H}_2\text{O}$ (4.5 mg, 22.54 μmol), CHCl_3 (6 ml) and MeOH (3 ml) were treated by the general procedure to afford the title compound **5** as a pink/purple solid (6.8 mg, 89%). EPR parameters at X-Band CW g: [2.05 2.05 2.19] Nucs: 'N' A: [87 87 600] Hstrain: [250 250 250] $\lambda_{\text{max}}(\text{CHCl}_3)/\text{nm}$ 539 ($\epsilon/\text{dm}^3\text{mol}^{-1}\text{cm}^{-1}$ 2100), 416 (48,800), 399sh (4100), 308 (5100); m/z (MALDI-TOF LD⁺) 1984.67 $\text{C}_{132}\text{H}_{100}\text{Cu}_2\text{N}_{10}\text{O}_2$ requires 1984.80.

EPR SI

Density Functional Theory (DFT) calculations to generate the molecular models for DEER simulations

The allowed sizes of the dihedral angles formed between two chemical moieties are determined by a combination of electrostatic and steric forces. For two adjacent phenyl rings, the most sterically favourable dihedral angle would be 90° , however when two phenyl rings lie in the same plane, an extended conjugated π -electron system can be formed which is energetically favourable. These two opposing factors lead to a broad distribution of bond angles being observed, in order to model the size of this distribution for each type of bond within the molecule Density Functional Theory (DFT) calculations were made using the software package ADF. [SCM, *Amsterdam Density Functional (ADF)*, <http://www.scm.com/>].¹⁸ In order to reduce the computational demands, a fragment analysis was performed; where the structures were broken up into smaller composite fragments (see Figure ESI 2a). For each of the bonds labelled A to G a linear transit over 180° in 10° steps was calculated using a BLYP functional (Becke-Lee-Yang-Parr), with a TZP basis set (triple-zeta polarization). The energy profile produced from these linear transits is plotted in Figure ESI 2b. The value of $k_B T$ at the freezing point of a 1:1:1 volumetric mixture of chloroform, toluene and THF, measured to be 134.15 K, is 0.11547 eV. It was assumed that all angles occurring at an energy within the value of $k_B T$ from the angle of lowest energy are equally accessible at the freezing point of the solvent mix and thus will occur with equal probability in the frozen sample. Therefore, the maximum possible angles accessible for each type of bond were found (see inset Figure ESI 2b).

It should be noted that the six member nitroxide ring was implemented in the calculations in its lower energy chair configuration and that this configuration was assumed to be dominant and therefore used in all calculations.

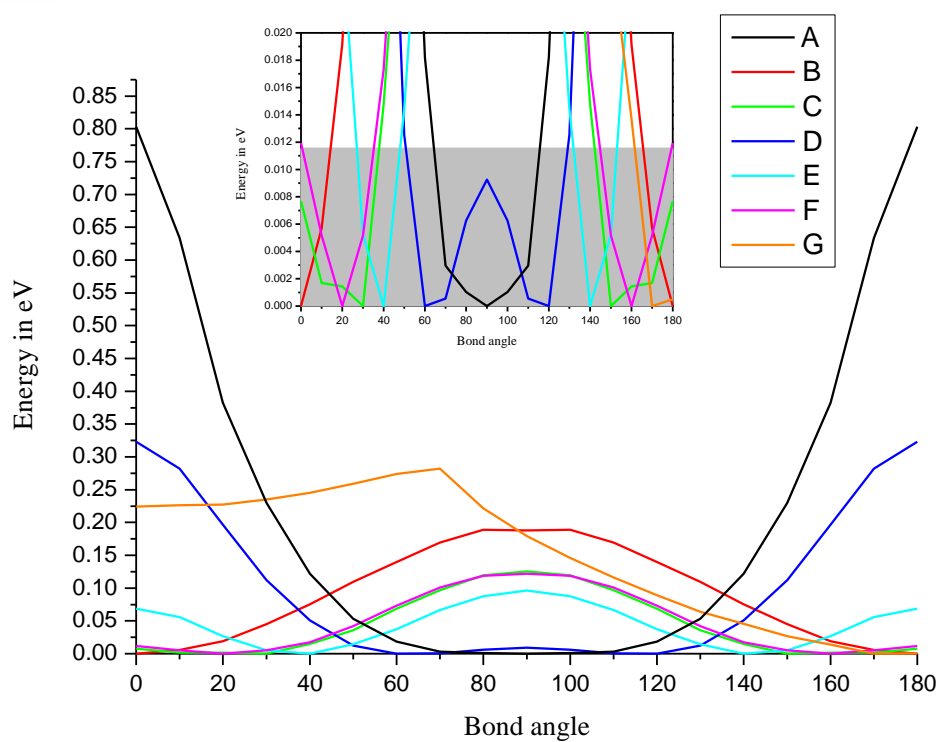
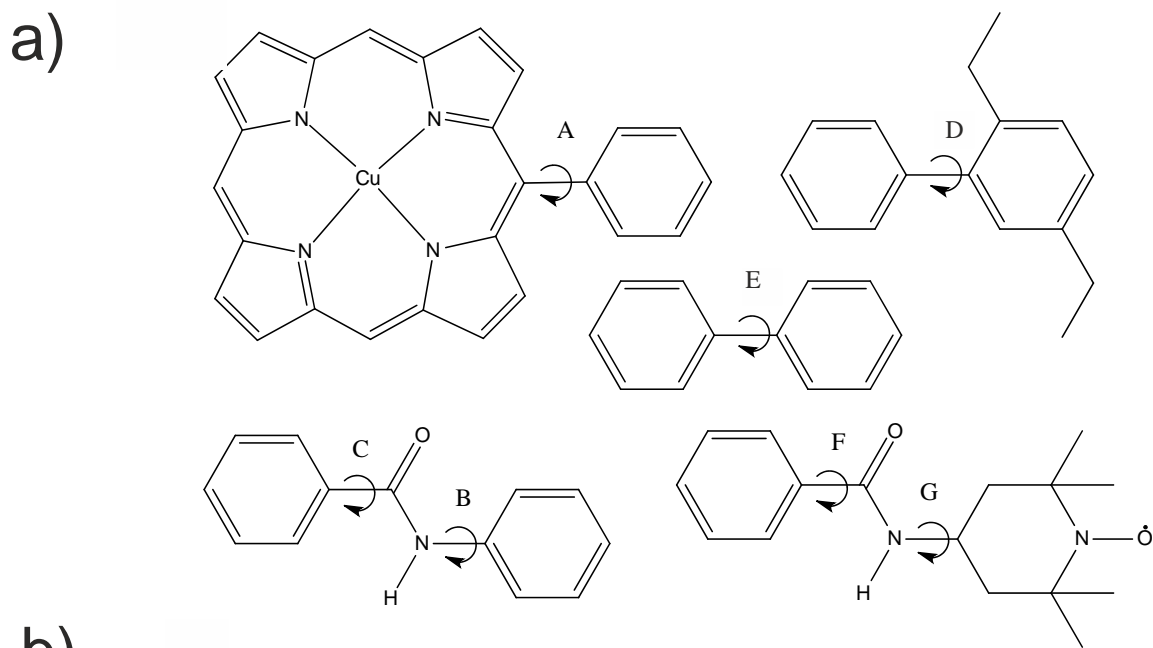


Figure ESI 2 Rotation about dihedral bonds. **a)** Fragments used in the DFT analysis with the bonds used for linear transits of 0° – 180° in 10° steps marked A–G. **b)** Results from DFT analysis calculated, with the BLYP GGA functional and a TZP basis set. The fragment with the copper porphyrin also used the zeroth-order regular approximation (ZORA) to correct the calculated energy, in order to account for relativistic effects. The inset depicts an enlargement of the main plot. The area marked in grey shows thermally accessible angles within the value of $k_B T$ at the freezing point of the solvent mixture. It should be noted that the curves for angles C and F are almost coincident, since these both represent the same type of bond rotation.

Comparison of the DFT analysis to the X-ray structure of 3-phenyl diacid linker

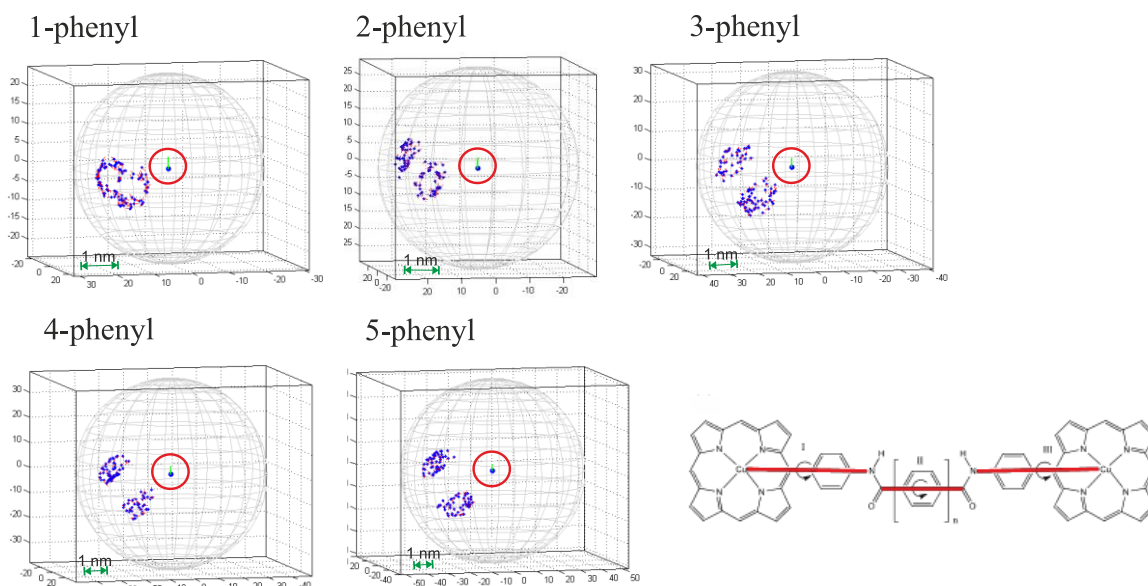
The torsional angle between two phenyl rings in the X-ray structure of the linker was found to be 82.8°. This agrees well with the DFT calculations (bond type D, see Figure ESI 2), since this value, although not the minimum energy angle calculated for this bond rotation (60°) occurs at an energy value that is accessible at the freezing point of the solution (50°-130°). The variation is most likely a result of the fact that the DFT calculation uses a truncated structure and also calculates for the structure *in vacuo*, thus omitting any crystal packing effects. The angle from one phenyl ring to the carboxylic acid is 12.6°. It is assumed that this angle should be similar to the minimum energy angle between the phenyl ring and the amide linker (bond types C and F, see Figure ESI 2), found to be between 20° to 30°. In this case, the DFT is also in fairly good agreement with the crystal structure and the deviation can be assigned to the differences in the bond type and the exclusion of the large copper porphyrin moieties from the crystal structure molecule.

Construction of model distributions from the DFT data

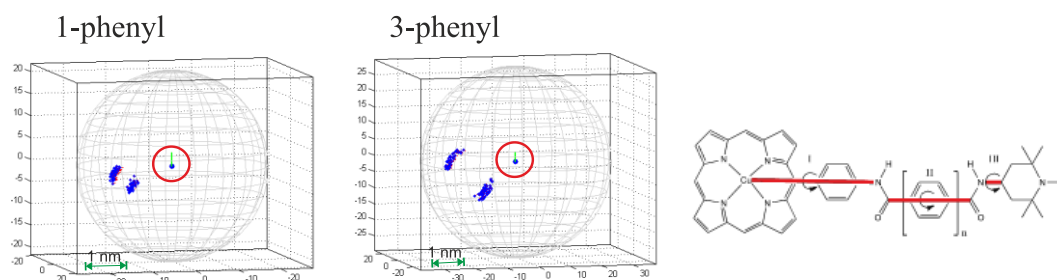
The full structures of the molecules studied can be simplified as 3 rods, each containing two or more different torsional angles about which rotations can occur (Figure ESI 3). The assumption is made that the amide linkage remains planar such that rotation about the Nitrogen-Carbonyl bond is minimal; this is valid due to the large degree of delocalization of the lone pair electrons of the nitrogen into the π -system of the carbonyl.

In order to construct models of the full molecular structure, an angle was selected at random from the allowed angles for each bond type and the angles for the bonds present within each rod were summed to produce three angles of rotation, one for each of the three rods. The full structure was next rotated by the angles described above about the three defined rotation rods, to produce the relative orientation of the two Cu(II) centers for use in the DEER simulation. This was repeated to generate 1,000 random input structures for modelling the DEER spectra using a Monte-Carlo-like protocol.

Cu-Cu Systems



Cu-NO[•] Systems



NO[•]-NO[•] System

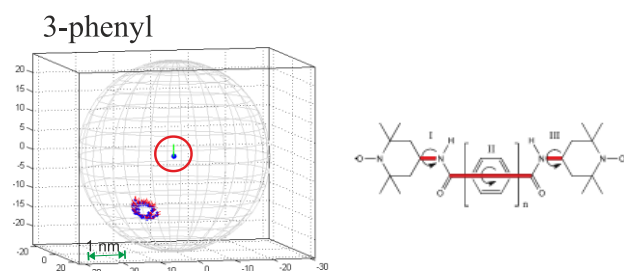


Figure ESI 3 Plots of the distribution of the two centres with respect to one another in the DFT models. One centre is held static (centre 1), this is plotted in a red ring, and the other centre (centre 2) is plotted as a distribution of positions with respect to centre 1. All of the axes are given in Å. Simplified structures of the three types of molecule investigated, with the rigid rods used for rotation marked in red and labelled I, II and III are also shown. For the Cu(II)-Cu(II) molecules $n=1-5$ (compounds **1-5**), for the Cu(II)-NO[•] molecules $n=1,3$ (compounds **6** and **7**) and for the NO[•]-NO[•] molecule $n=3$ (compound **8**).

DFT determination of the orientation of the g -tensor with respect to the molecular structure

When attempting to model and interpret orientationally selective spectra, it is vital to know the orientation of the g -matrix with respect to the molecular frame. Copper in an approximately planar environment is well-known for having an axial g -matrix, which can be assumed to lie perpendicular to the plane in which the equatorial ligands are bound. DFT calculations were used to corroborate this for the copper porphyrin fragment (see Figure ESI 4). The calculation of magnetic resonance parameters using the internal magnetic resonance calculation unit in ADF showed an axial g -tensor with principal g -values of $g_x = 2.0352$, $g_y = 2.0362$, $g_z = 2.1049$; aligned with the g_z axis perpendicular to the plane of the porphyrin ring.

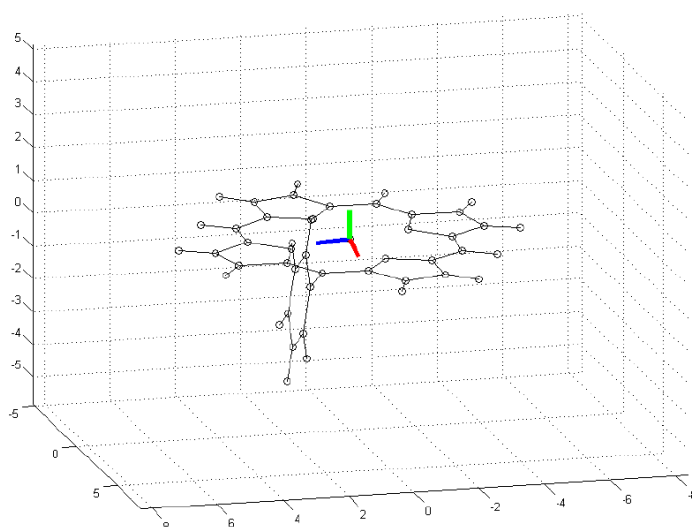


Figure ESI 4 Diagram showing the orientation of the g -matrix on the porphyrin structure; green is the z -axis, blue the x -axis and red the y -axis. The calculated g -values are; $g_x = 2.0352$, $g_y = 2.0362$, $g_z = 2.1049$.

Copper amine oxidase (GAO)

The goodness of fit, for a simulated trace to the experimental data was characterised by the least-squares residual (LSR) between the experimental data (D) and the simulated data (S):

$$LSR = \sum_{i=1}^n (D_i - S_i)^2.$$

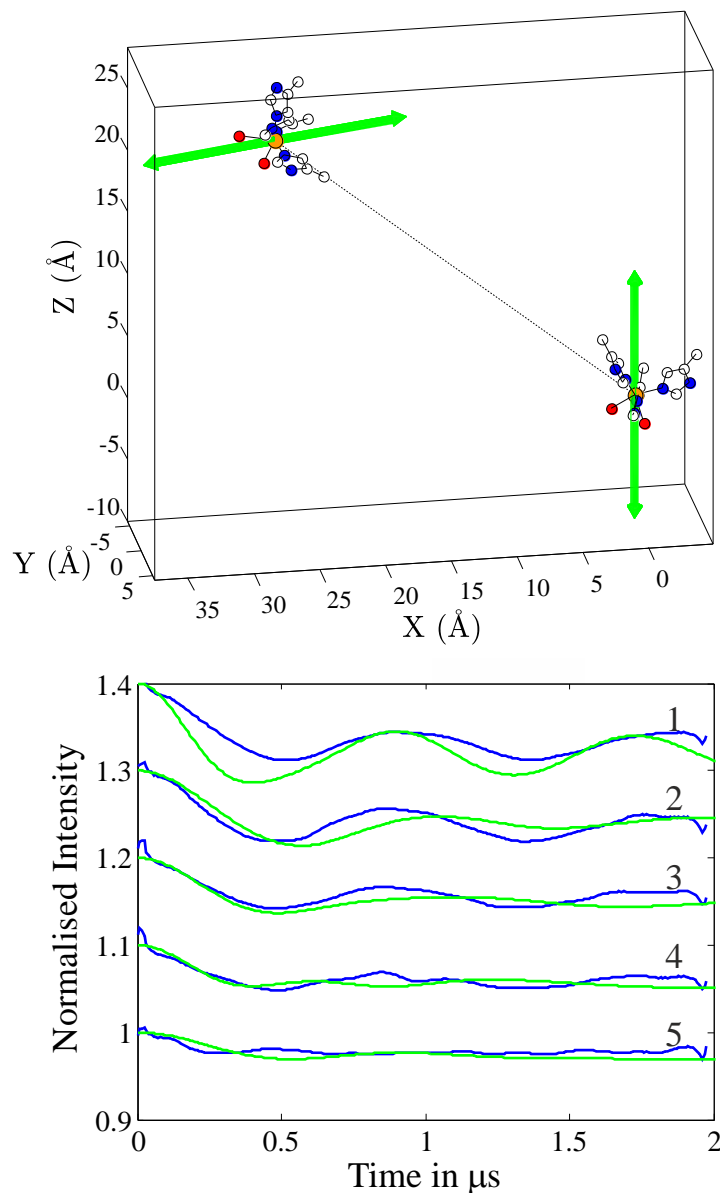


Figure ESI 5 Top: green arrows demonstrating the relative orientations of the g_z vector of both centres plotted relative to a molecular frame for the g_z orientation perpendicular to the plane of the three ligating nitrogen. Bottom: comparison of simulated DEER traces for this g_z orientation (plotted in green) to the experimental form factors computed by removing the background $B(t)$ (blue lines). The numbers to the right of each trace correspond to the key for the different experimental fields illustrated in Figure 2 of the main text.

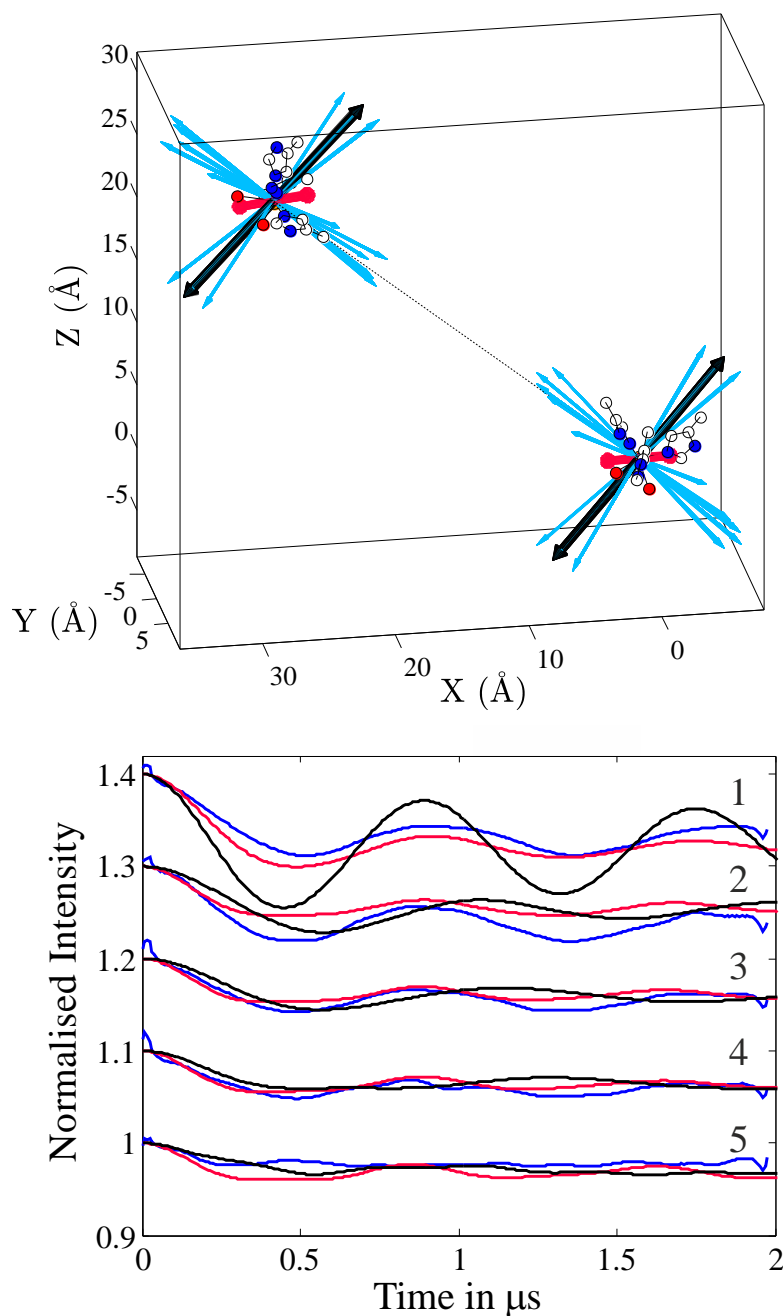


Figure ESI 6 X-band DEER data from the Copper Amine Oxidase (AGAO) homodimer from *A. globiformis*. Top: Arrows representing the orientation of the 10 g -vectors for both centres relative to a molecular frame for the 10 worst fitting DEER traces. The worst fitting orientation is depicted by a black arrow and the 10th worst fit by a red arrow. Due to the symmetry of the g -tensor it is not possible to define an absolute direction for the vector and thus the orientations are shown as double headed arrows projecting through the central copper ions. Bottom: the 10th worst (red) and worst (black) fitting DEER traces along with the experimental form factors (blue) computed by removal of the background $B(t)$. The numbers to the right of each trace identify the DEER positions within the EPR spectrum in Figure 2 of the main text.

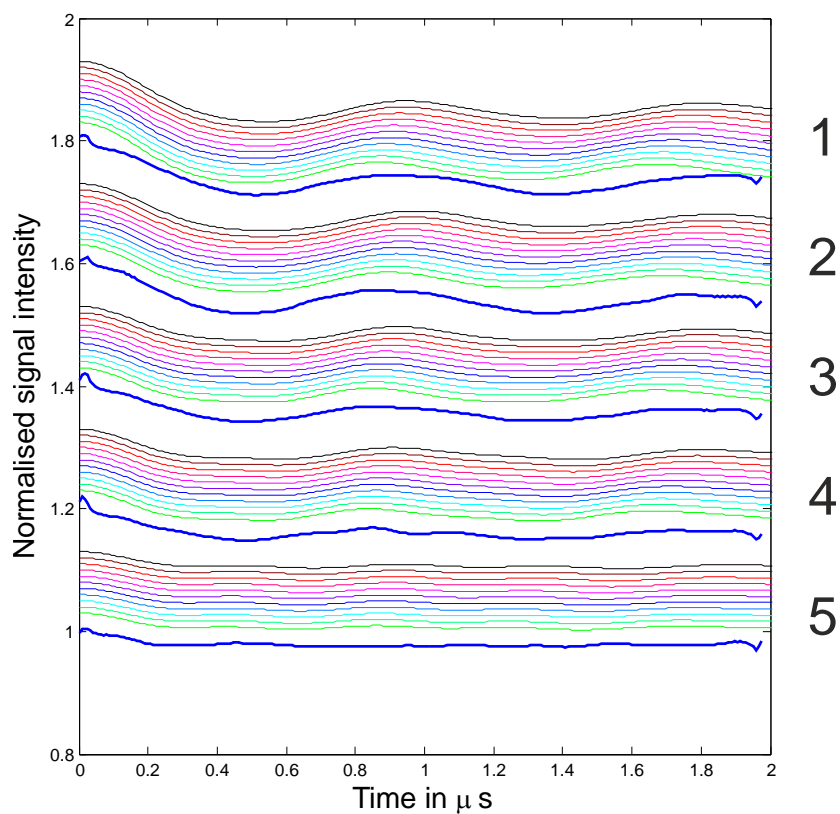


Figure ESI 7 Varying the distance in the AGAO simulation from 3.592 nm (first green trace) to 3.692 nm (final black trace). A distance of 3.642 nm was found to be optimal. The experimental data traces are shown as thick blue lines and the simulations are offset from one another for clarity. The numbers to the right of each trace correspond to the key for the different experimental fields illustrated in Figure 2 of the main text.

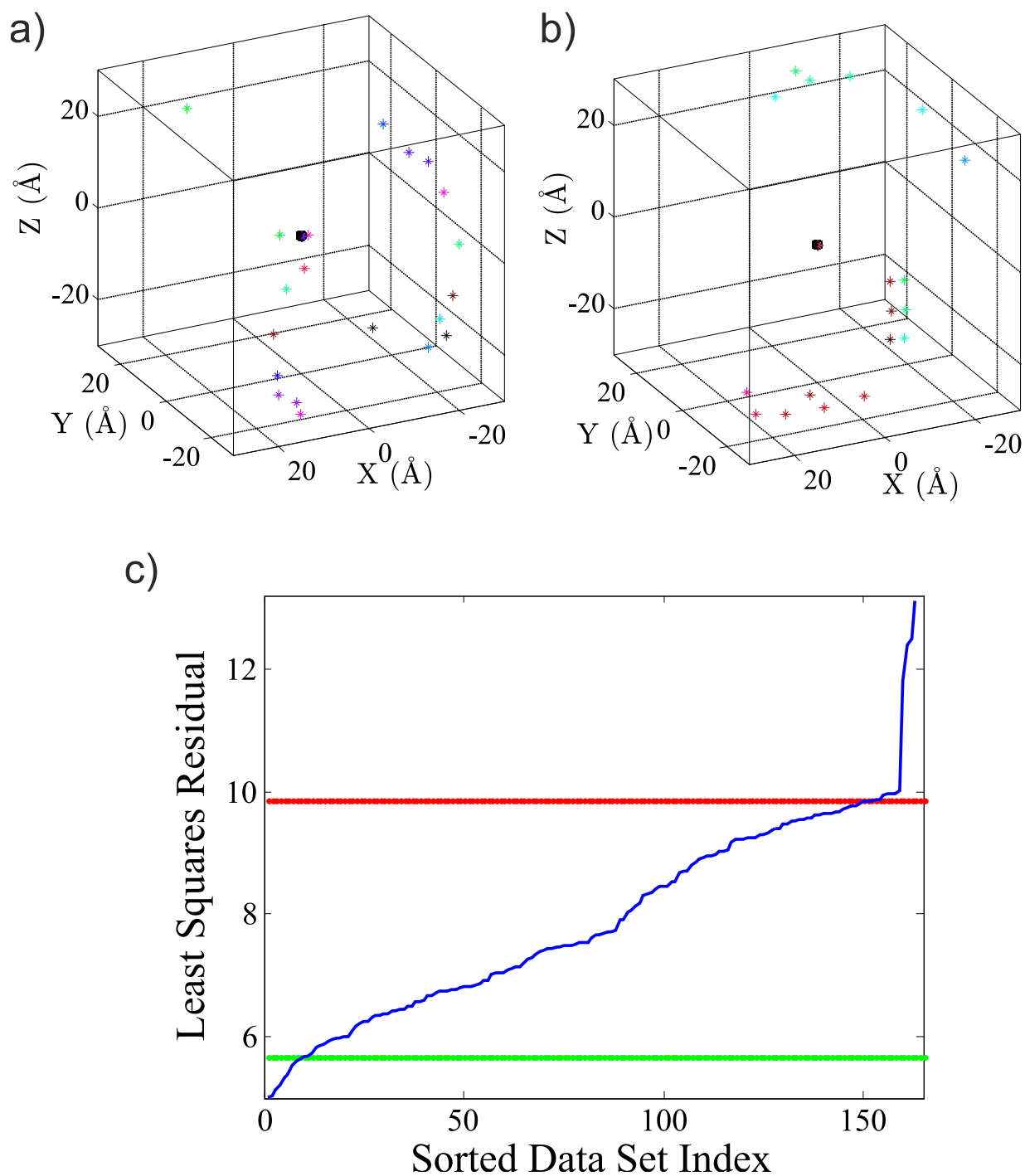


Figure ESI 8 The relative positions in space of centre 1 (black circle) and centre 2 (coloured crosses) for a) the 10 best fitting orientations and b) the 10 worst fitting orientations with their symmetrical equivalents, providing 20 coloured crosses in total. Corresponding DEER traces for the best and worst fits within each set are shown in Figure 3 of the main paper and Figure ESI 6 of the ESI, respectively. In this representation of the data sets rather than plotting the relative positions of vector \mathbf{g}_z for each of the centres in a fixed molecular frame (as in Figure 3 and Figure ESI 6), we instead fix the g -matrix (\mathbf{g}_z vector) of the first centre, and plot the relative position of the \mathbf{g}_z of centre 2 in this frame. In this representation the centre 1 \mathbf{g}_z axis is $[0\ 0\ 1]$ and is shown starting from the point $(0, 0, 0)$. c) The total least-squares residual values summed from the five orientation-selective DEER traces and their simulation, for each structural orientation trialled (161 in total). Symmetrically identical orientations have been removed for simplification. The green line shows the cut off value for the 10 best fitting data sets and the red line shows the cut off value for the 10 worst fitting data sets.

Nitroxide model systems

To verify the validity of the DFT calculations, the method was initially tested using a $\text{NO}\cdot\text{-NO}\cdot$ 3-phenyl model system. It was assumed that flexibility of the nitroxide moieties in this molecule was sufficient such that the result from this molecule could be analysed using DeerAnalysis,¹ and the results of this analysis compared to those from the DFT modelling. Comparison of the Tikhonov regularization fits and those generated directly from the DFT model to the experimental data shows good agreement in both cases and the average distances in both cases are the same. There is some variation in the widths of the distance distributions for the experiments recorded at 80 MHz and -108 MHz offsets which is probably due to a small degree of orientation selection in the experimental data. The distance distribution for the DFT derived structures is narrower than both of the Tikhonov derived distributions, however the fit of the simulated data to the experimental data is good for both the experimental traces validating the DFT model.

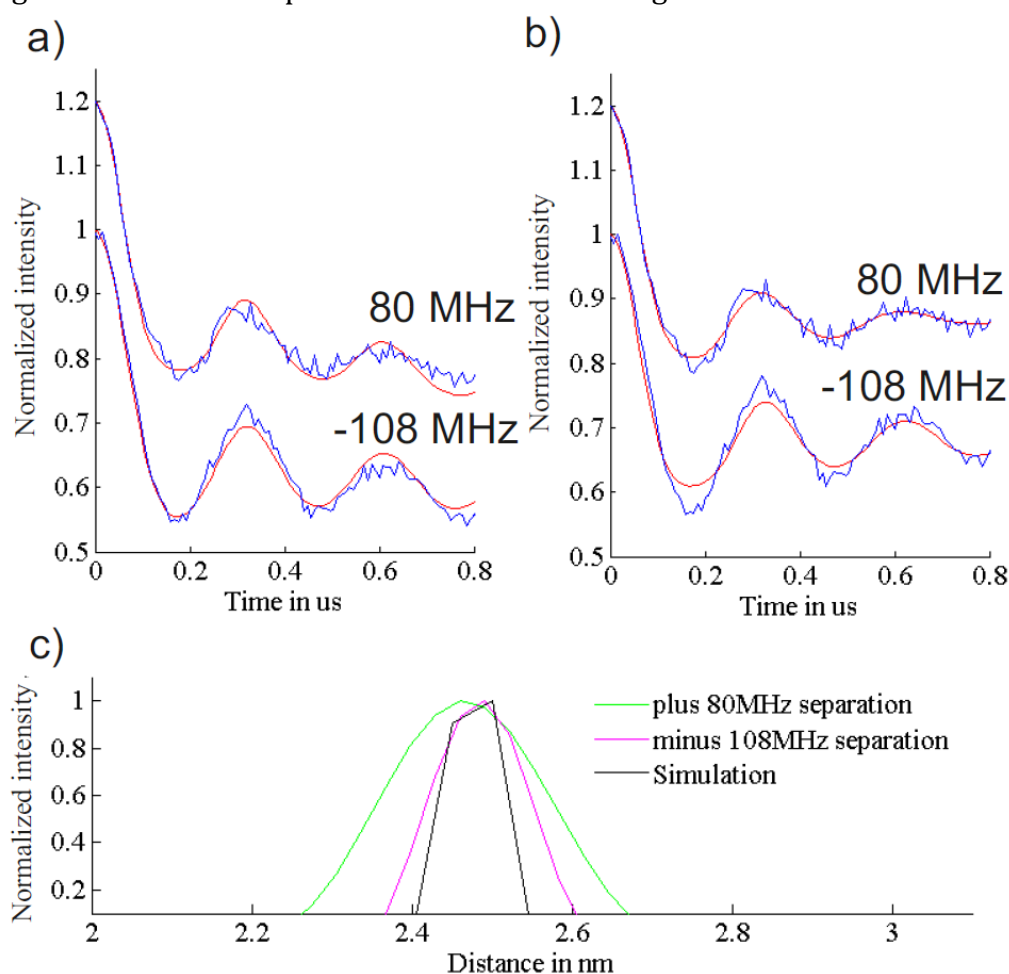


Figure ESI 9 Results for the 3-phenyl bisnitroxide ($\text{NO}\cdot\text{-NO}\cdot$) system, compound **8**. **a)** Raw experimental DEER traces with no background correction (blue) plotted with DEER traces simulated using the orientationally selective DEER simulation program that have been multiplied by a homogenous background correction and a modulation depth correction (red). **b)** Background corrected experimental DEER traces (blue) with Tikhonov regularization fits from DeerAnalysis (red). The experimental data has been background corrected to allow the Tikhonov fitting. **c)** Distance distribution derived from the 1,000 structures formed from the DFT calculations and used as input for the orientation-selective DEER simulations, in (a) (black curve). Also, the distance distributions extracted by Tikhonov regularization in DeerAnalysis from the experimental (magenta [-108 MHz] and green [+80 MHz] curves).

DEER experimental pulse separations

NO-NO model system (compound 8)					
Pulse separation (MHz)	80		-108		
Detection Frequency (GHz)	9.8261		9.6383		
Pump Frequency (GHz)	9.7461		9.7461		
Magnetic Field (mT)	346.38		346.38		
Cu(II)-NO model systems (compounds 6 and 7)					
Pulse separation (MHz)	274.2				
Detection Frequency (GHz)	9.63470				
Pump Frequency (GHz)	9.36047				
Magnetic Field (mT)	332.87				
Cu(II)-Cu(II) model systems (compounds 1 to 5)					
Identifier	Upper traces		Lower traces		
Pulse separation (MHz)	200		200		
Detection Frequency (GHz)	9.53 (9.60)		9.53 (9.60)		
Pump Frequency (GHz)	9.33 (9.40)		9.33 (9.40)		
Magnetic Field (mT)	323.5 (325.9)		316.5 (318.9)		
AGAO					
Identifier	1	2	3	4	5
Pulse separation (MHz)	100	100	100	100	100
Detection Frequency (GHz)	9.446	9.446	9.446	9.446	9.446
Pump Frequency (GHz)	9.346	9.346	9.346	9.346	9.346
Magnetic Field (mT)	323.3	315.0	312.0	310.0	300.0

Values in brackets for the Cu(II)-Cu(II) systems (compounds **1** to **5**) were used for the 4-phenyl system (compound **4**), the values not in brackets were used for all of the other Cu(II)-Cu(II) systems.

DEER Simulation Parameters

Fitting parameters extracted from X-band CW EPR spectra using EasySpin¹⁹ for the Cu(II)–Cu(II) 3-phenyl model system (compound **3**).

Parameter	x-component	y-component	z-component
<i>g</i> -values	2.05	2.05	2.19
A-values (Cu) [MHz]	87	87	600
H strain (line broadening) [MHz]	250	250	250

Fitting parameters extracted from CW EPR spectra using EasySpin¹⁹ for the copper and nitroxide portions of the Cu–NO• 3-phenyl model system (compound **7**). The same nitroxide parameters were also used found to fit the NO•–NO• 3-phenyl model system (compound **8**). Although the hyperfine splitting's for the nitroxide are listed in the table below, they are not used as part of the orientation-selective DEER simulations as the nitroxide centre is assumed to be isotopically excited by the DEER mw pulses.

<i>Copper Parameters</i>			
Parameter	x-component	y-component	z-component
<i>g</i> -values	2.056	2.056	2.205
A-values (Cu) [MHz]	80	80	593
H strain (line broadening) [MHz]	221	173	238
<i>Nitroxide Parameters</i>			
Parameter	x-component	y-component	z-component
<i>g</i> -values	2.01	2.01	2.009
A-values (N) [MHz]	20	20	100
H strain (line broadening) [MHz]	40	40	40

Scaling factors and background correction

Experimental DEER traces consist of an oscillating form factor, $F(t)$, resulting from the intra-molecular contribution and the inter-molecular or background contribution $B(t)$:

$$D(t) = F(t)B(t) \quad \text{Eq.A}$$

The form of this background correction is that of a homogenous three dimensional distribution of spins:

$$B(t) = \exp\left(-kt^{\frac{d}{3}}\right) \quad \text{Eq.B}$$

Where the dimensionality, $d = 3$ and k quantifies the density of spins.

The output $S(t)$ of the simulations (Eq. D), contains both a modulated part $\Delta_{\text{sim}}f(t)$ (corresponding to orientations where one spin center is excited by the pump pulse and the other by the detection pulses) and an unmodulated part $1 - \Delta_{\text{sim}}$ (corresponding to orientations where one center is excited by the detection pulses but the other not by the pump pulse). However no consideration is taken in the simulation program of the degree of labeling in the system, and the exact pulse excitation profile is difficult to model exactly. Both these factors affect the modulation depth. Therefore it is necessary to correct the simulated modulation depth by a constant scaling factor, c , in order to form $F(t)$.

$$F(t) = 1 - c(1 - S(t)) \quad \text{Eq.C}$$

The output of the simulation is

$$S(t) = 1 - \Delta_{\text{sim}}(1 - f(t)) \quad \text{Eq.D}$$

where $f(t)$ is the reduced form factor and Δ_{sim} is the simulated modulation depth. Substitution of Eq.D into Eq.E yields

$$F(t) = 1 - \Delta(1 - f(t)) = 1 - c\Delta_{\text{sim}}(1 - f(t)) \quad \text{Eq. E}$$

where $\Delta = c\Delta_{\text{sim}}$ gives the modulation depth of the experimental trace (as stated in Eq. 2 of the main text).

The modulation depth scaling factor, c , and k are found empirically by fitting the simulation to the experimental data, such that:

$$D(t) = [1 - c\Delta_{\text{sim}}(1 - f(t))]\exp(-kt) \quad \text{Eq.F}$$

The values of c and k used to fit the simulated DEER data to the experimental traces

Table ESI 1. The scaling factors necessary in order to fit the data for the NO•–NO• system (compound **8**). The parameters correspond to those in Eq.F. The same c value is used in each case, since this is a system-dependent parameter. c takes into account the labelling efficiency of the system and also the pulse efficiencies.

Pulse separation	c	k
80 MHz	0.7	0.045
–108 MHz	0.7	0.02

Table ESI 2. The scaling factors necessary in order to fit the data for the Cu–NO• system (compounds **6** and **7**). The parameters correspond to those in Eq.F. The same c value is used in each case as this is a system-dependent parameter.

Model System	c	k
Cu–NO•1-phenyl (compound 6)	0.9	0.4
Cu–NO•3-phenyl (compound 7)	1.0	0.72

Table ESI 3. The scaling factors used in the simulation of the Cu(II)–Cu(II) systems (compounds **1** to **5**). The parameters correspond to those in Eq.F. The same c value is used in each case, since this is a system-dependent parameter.

Model system	Field of experiment (mT)	c	k
Cu(II)–Cu(II) 1-phenyl (compound 1)	316.5	0.12	0.075
	323.5	0.12	0.1
Cu(II)–Cu(II) 2-phenyl (compound 2)	316.5	0.26	0.07
	323.5	0.26	0.09
Cu(II)–Cu(II) 3-phenyl (compound 3)	316.5	0.9	0.15
	323.5	0.9	0.2
Cu(II)–Cu(II) 4-phenyl (compound 4)	316.5 (318.9)	0.13	0.12
	323.5 (325.9)	0.13	0.17
Cu(II)–Cu(II) 5-phenyl (compound 5)	316.5	0.16	0.05
	323.5	0.16	0.07

Further information on the structural models used for analysis

Geometric model (model 3)

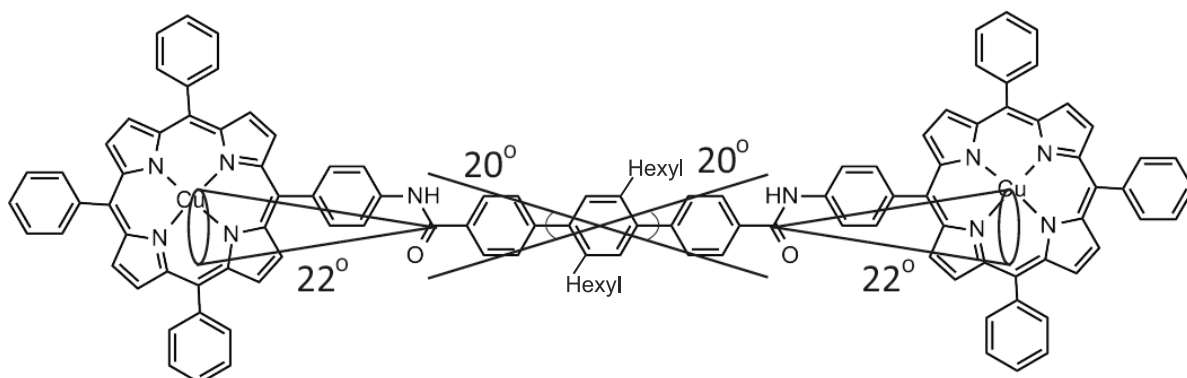


Figure ESI 10: Shown is the bending angles, of 20° and cones of 22°, about which free rotation was allowed, used to generate the geometric based model 4 for compound 3.

Ball model (model 6)

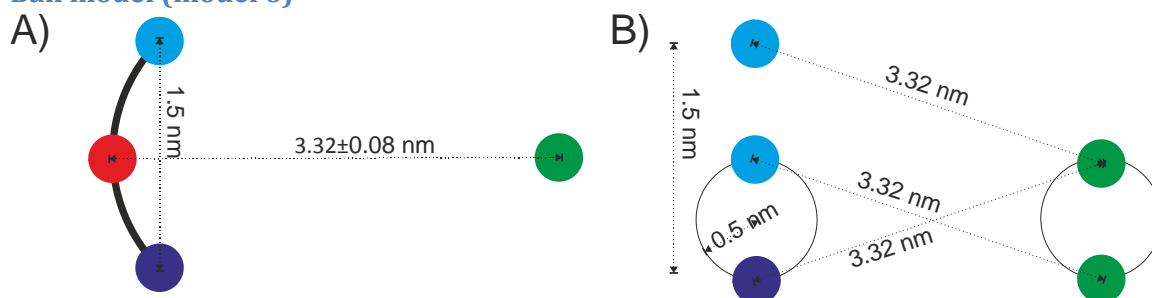


Figure ESI 11 A) Model 6 for the 3-phenyl system (molecule 3). Schematic diagram for the distribution of centre 2, where the red circle is the equilibrium position for this centre and the dark and light blue circles show the maximum and minimum of the distribution with respect to centre 1, the green circle. B) In order to make spherical distributions with the same radius for both centres such that the maximum and minimum positions of the distribution calculated from the DFT results are contained within these two spheres a radius of 0.5 nm is required.

Simulations for different orientations with both pump and probe pulses exciting the $g_{x/y}$ component of the spectrum

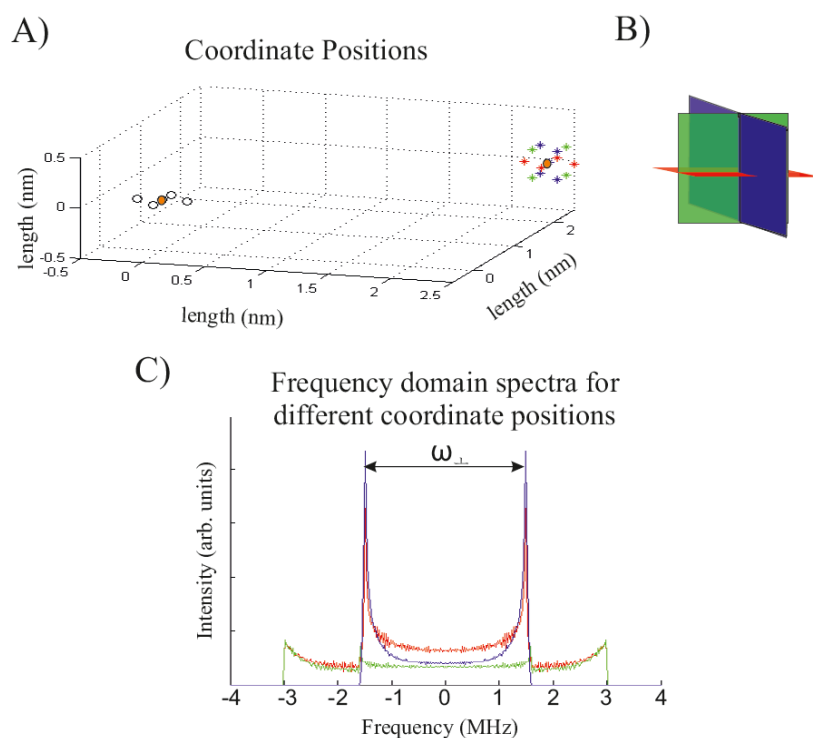


Figure ESI 12 **A)** Three possible orientations of two copper centres (shown as orange circles), ligated by four nitrogens (shown as white circles or coloured stars) with respect to one another. This is a model for a copper porphyrin. The axes are in nm. **B)** An expansion of the three intersecting planes of the porphyrin nitrogens depicted as stars in A). The three simulations in C) each correspond to one of these orientations. **C)** The dipolar spectrum calculated for the interaction between the centres in different orientations using the pump and probe corresponding to the magenta excitation positions of Figure 6a in the main text. The noise on this spectrum is a result of the use of a limited set of discrete angles for the orientation of the molecule with respect to the external magnetic field, **B**₀.

Simulations for isotropic excitation and summing traces measured across the spectrum

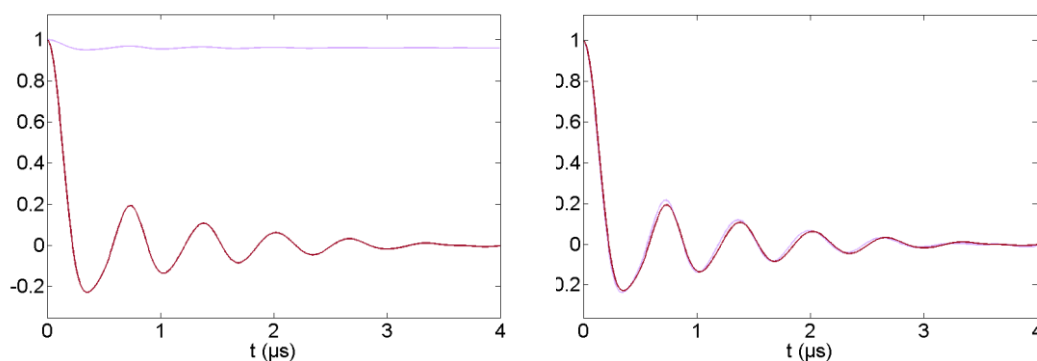
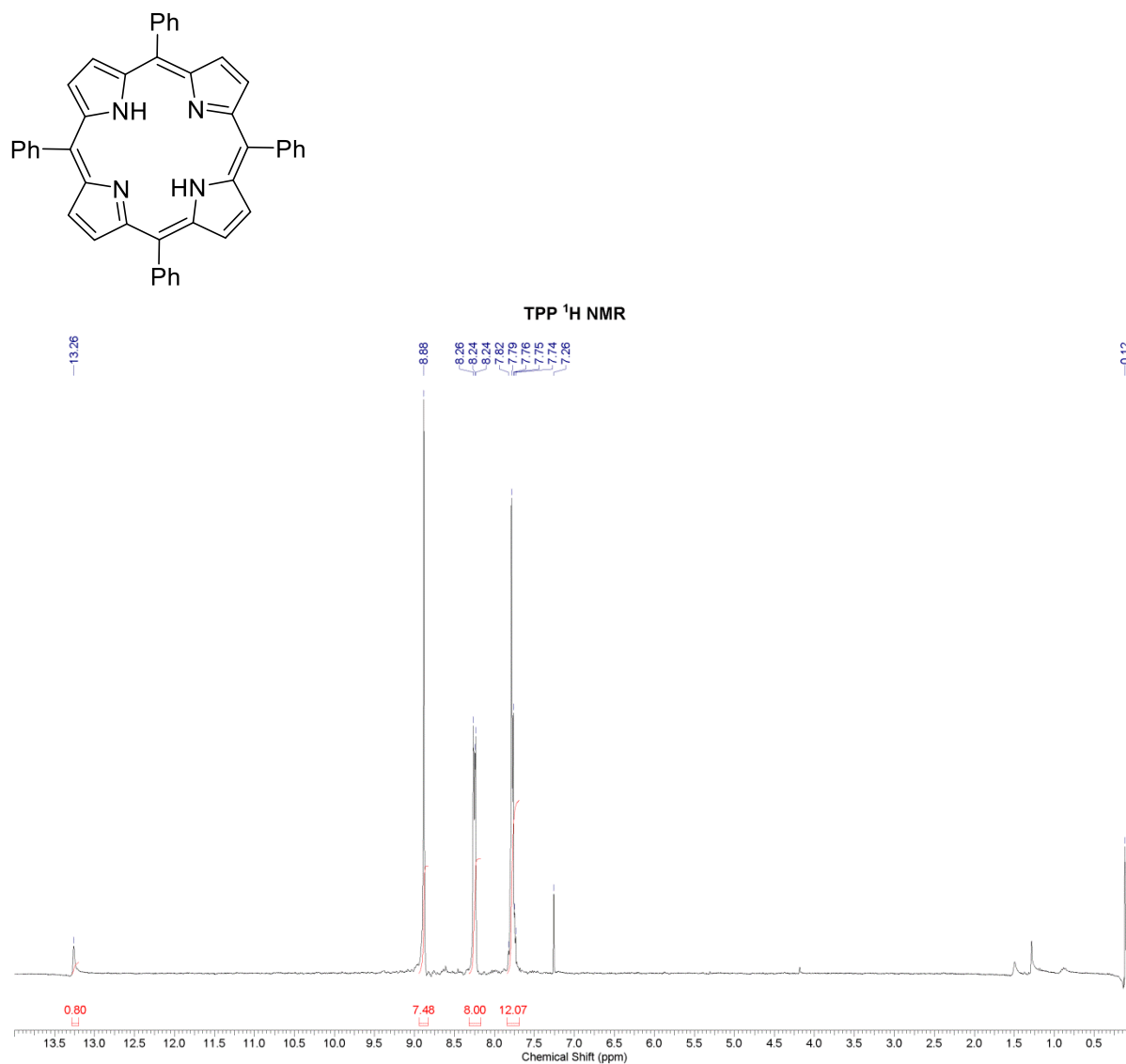


Figure ESI 13 DEER traces from the DFT derived model of compound **3** for isotropic excitation of both centres by both pulses (red) and the sum of 8 traces with $\Delta\nu = 100$ MHz at fields evenly positioned across the copper EPR spectrum (maroon). Although the modulation depths of the two traces are significantly different (left figure), the agreement between the shapes of the two sets of traces when the modulation depths are scaled to the same value is very good (right figure).

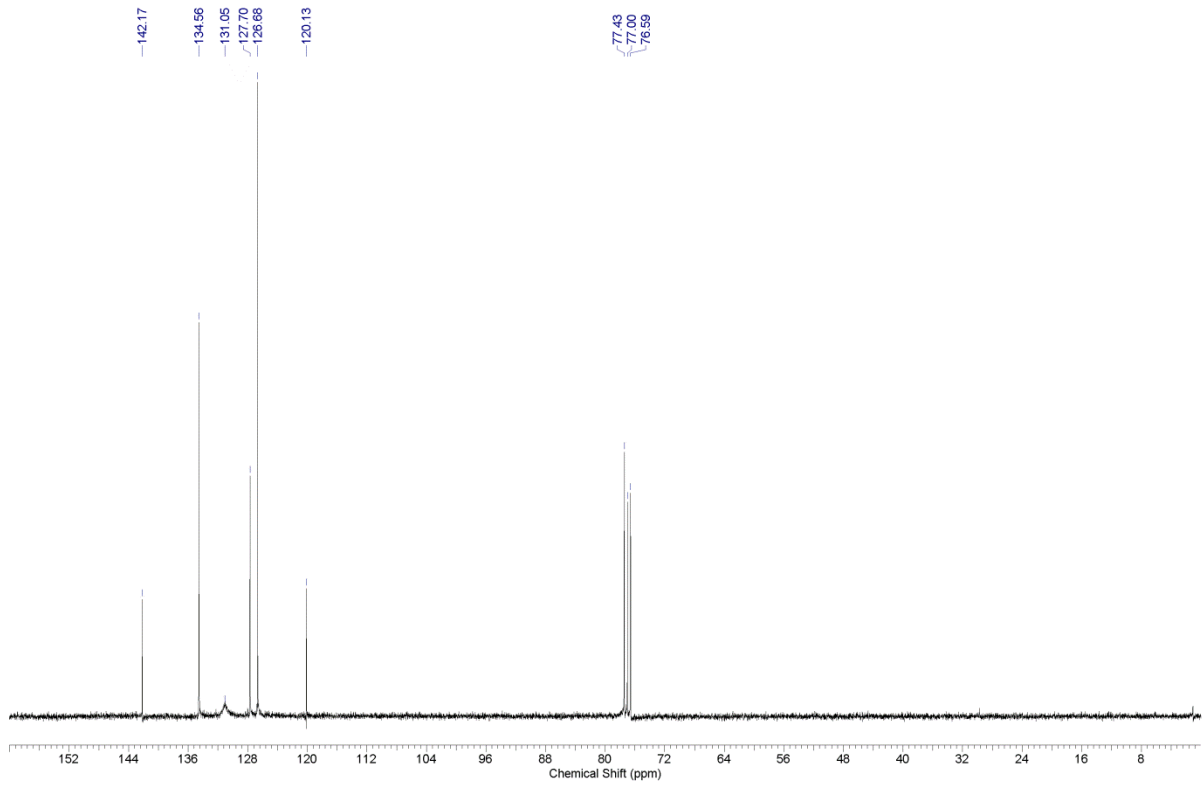
SI of the supporting spectra.

Characterisation data for compounds

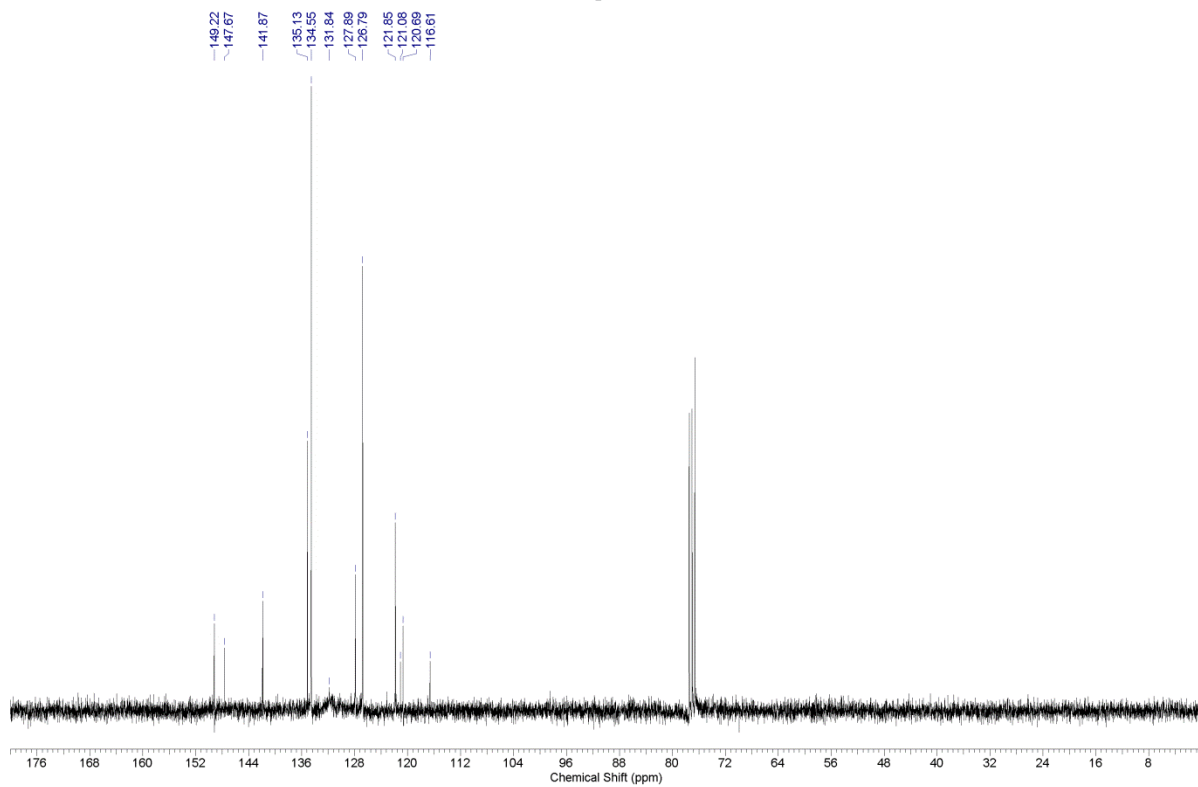
Attached are the relevant ^1H , ^{13}C NMR and CW-EPR spectra and the MALDI traces for a selection of the compounds synthesised.

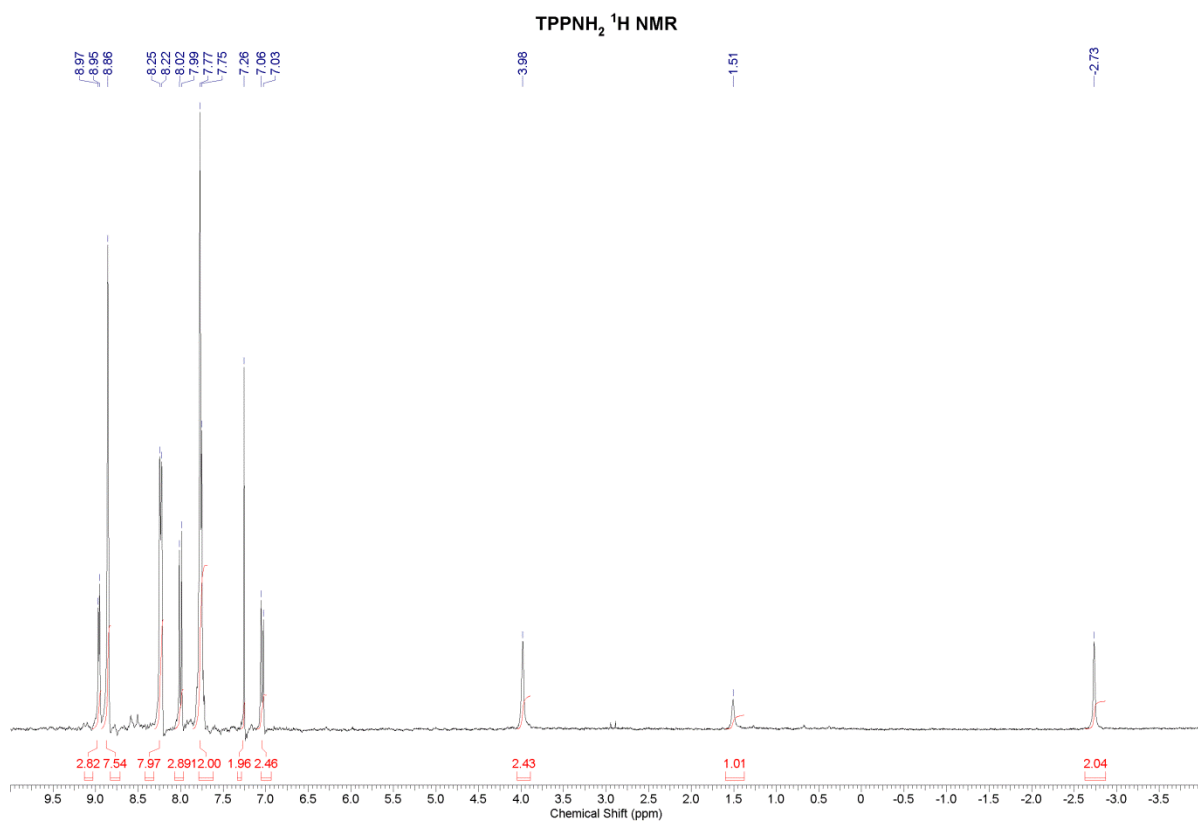
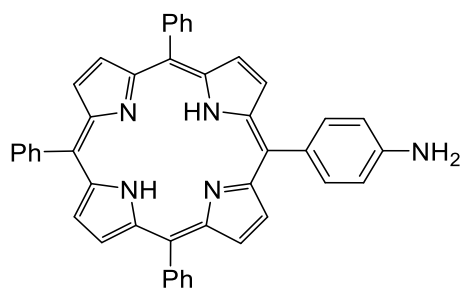


TPP ¹³C NMR

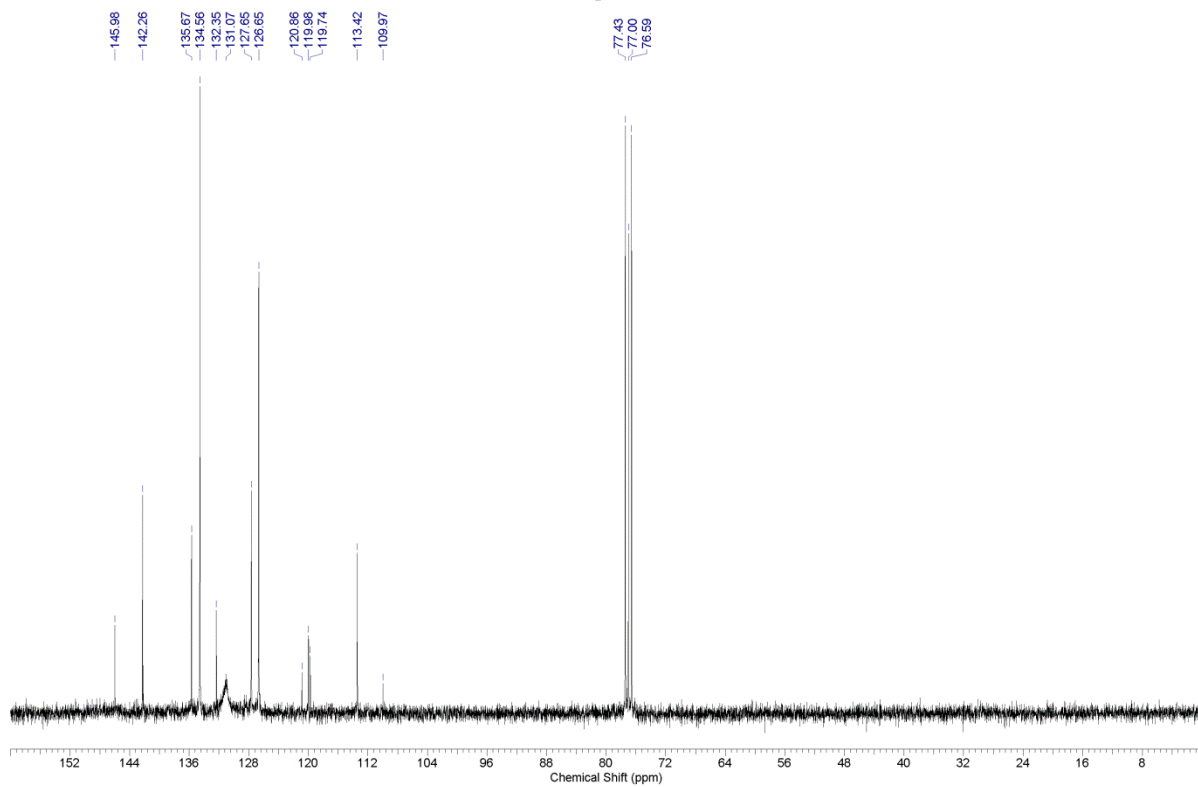


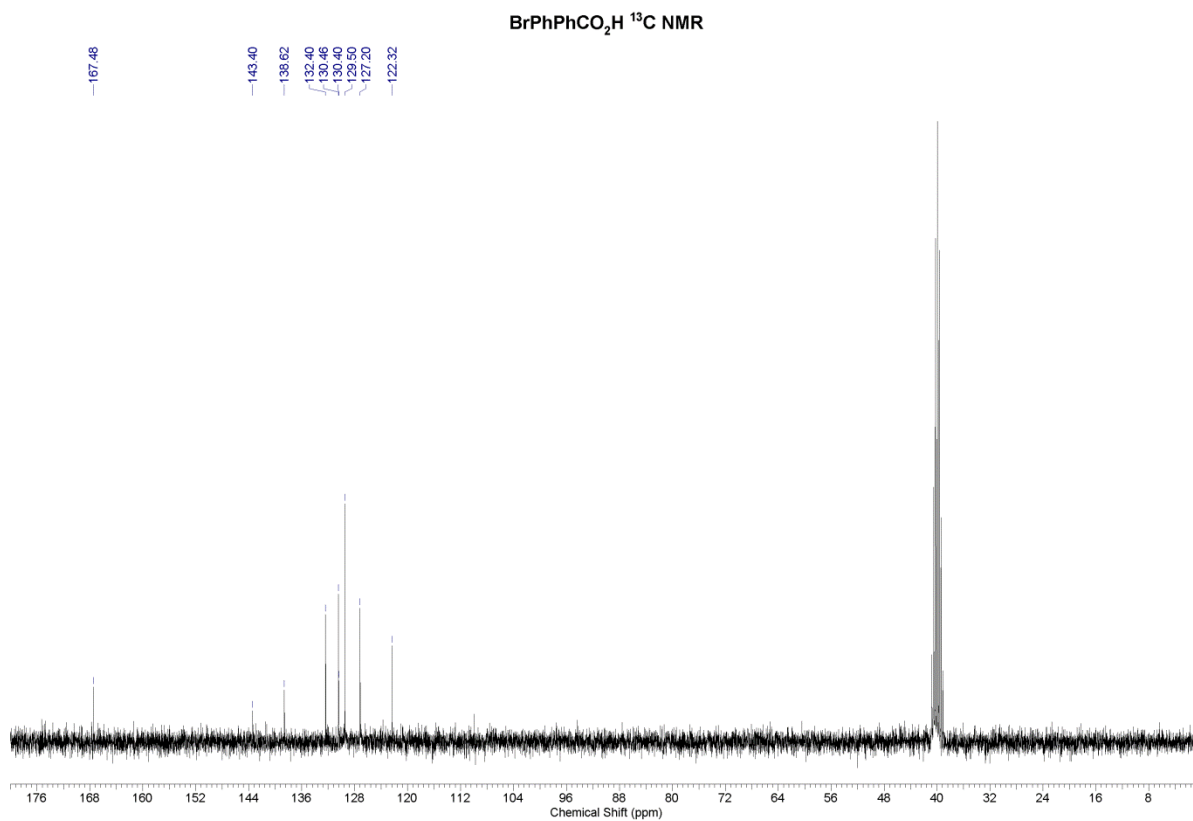
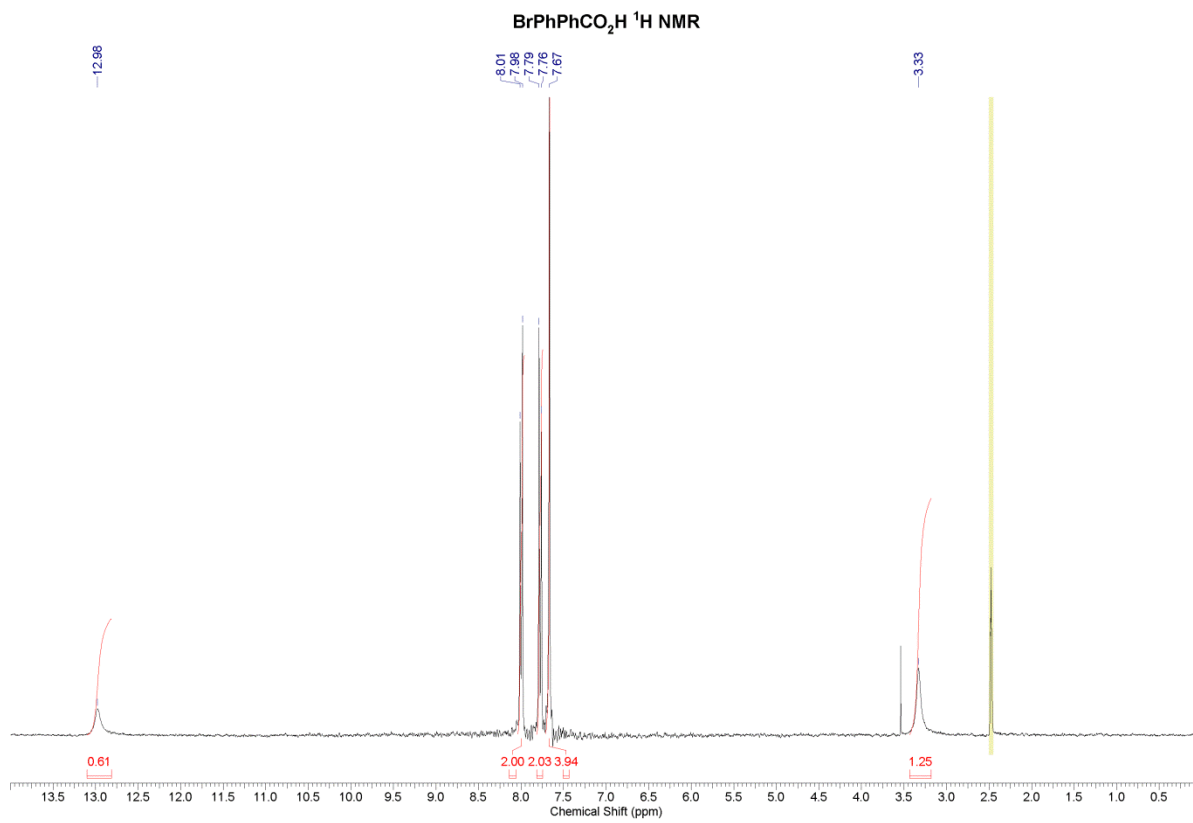
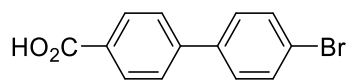
TPPNO₂ ¹³C NMR

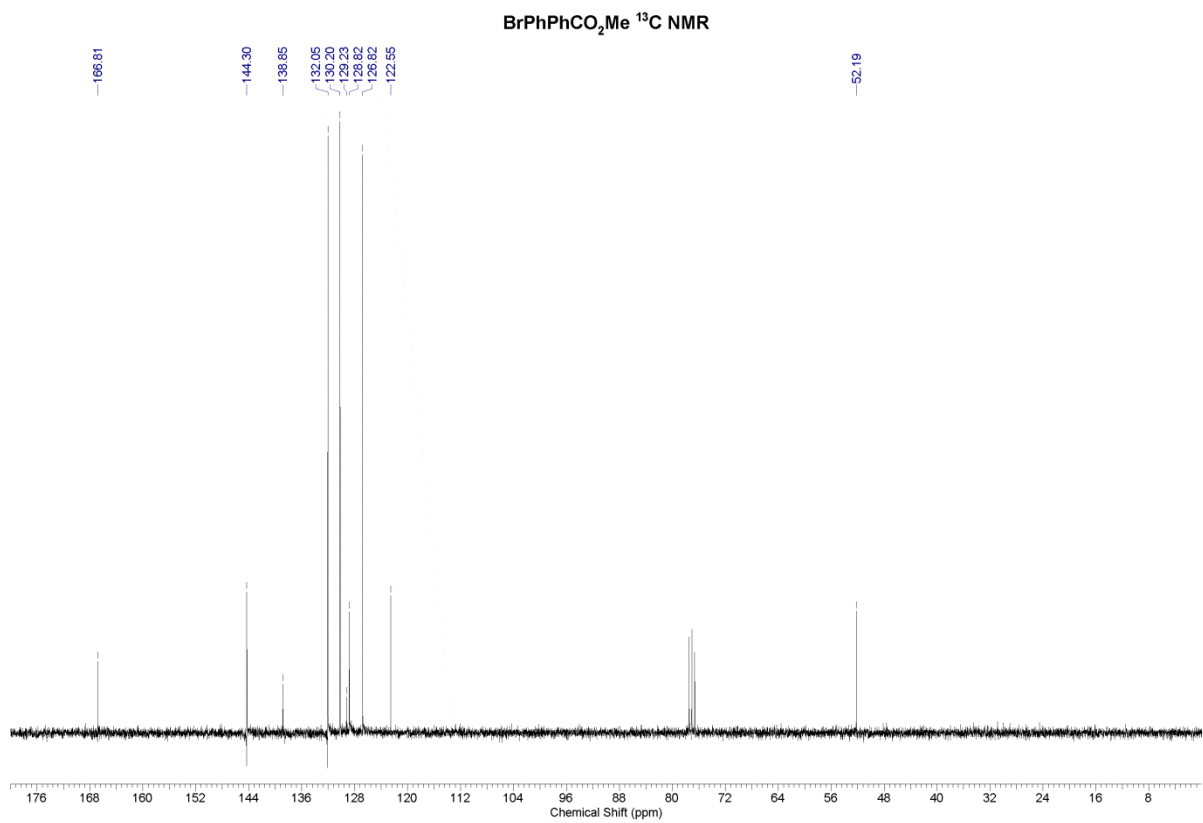
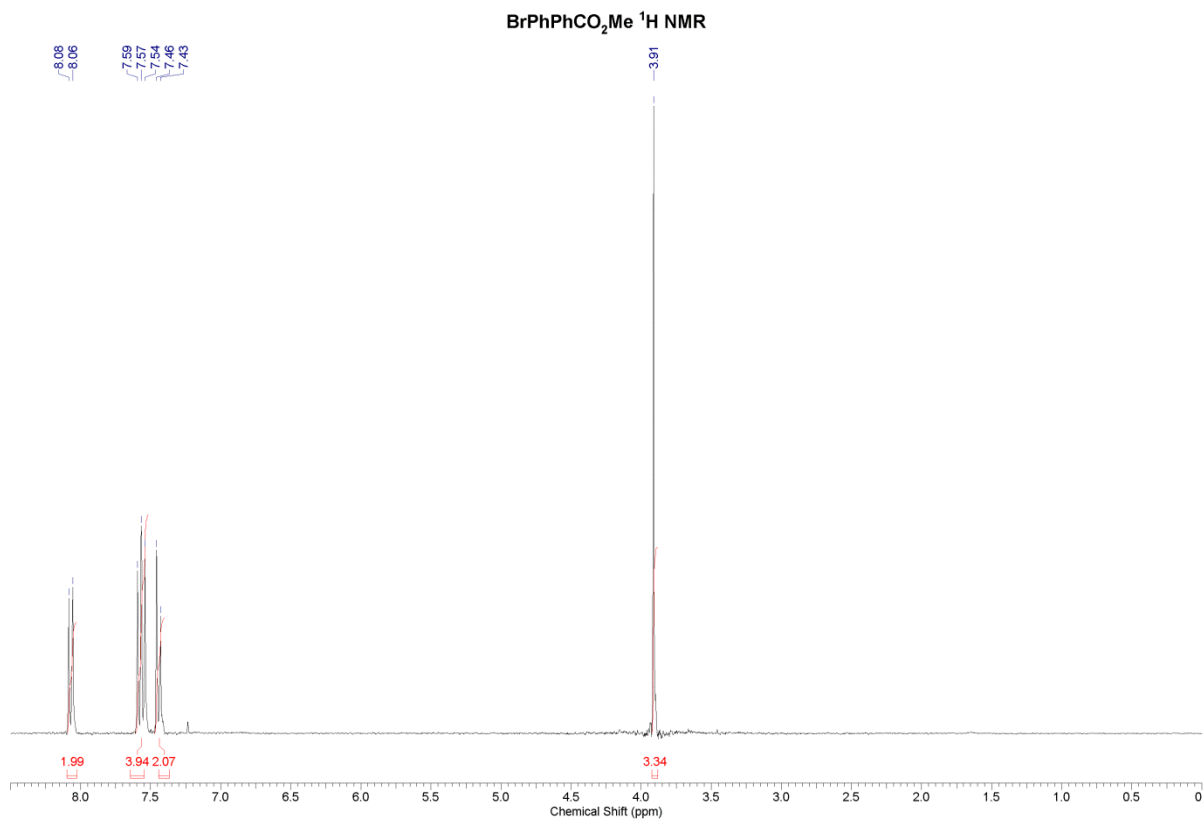
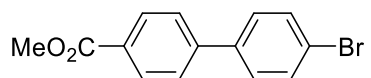


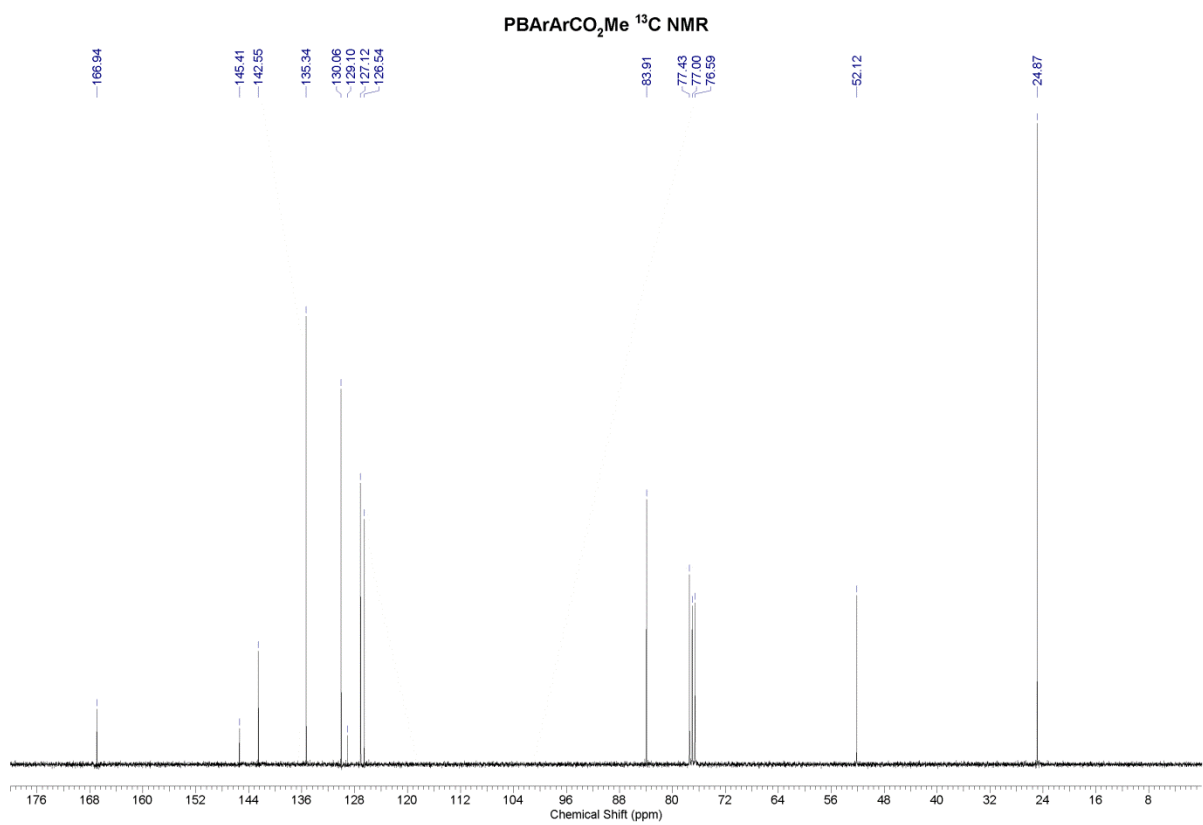
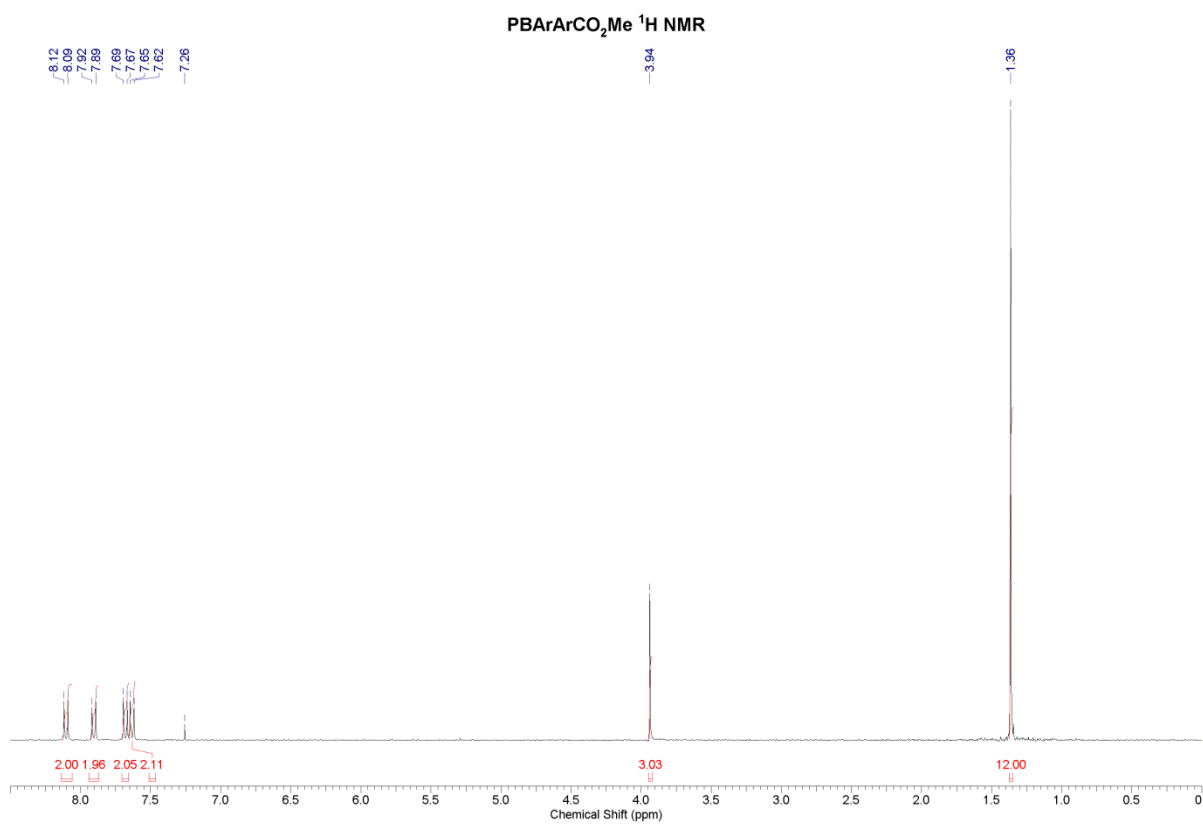
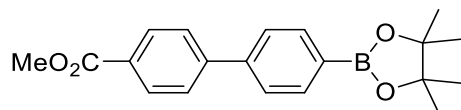


TPPNH₂ ¹³C NMR









FI MSS 05931 [C20 H23 B O4]

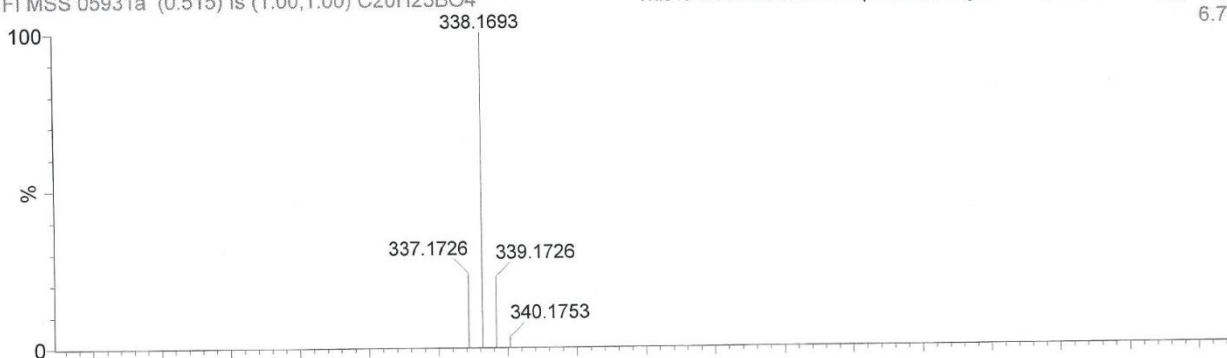
FI MSS 05931a (0.515) Is (1.00,1.00) C20H23BO4

Probe EI/FI

This is the theoretical isotope model of your compound.

07-Apr-2009 12:15:52

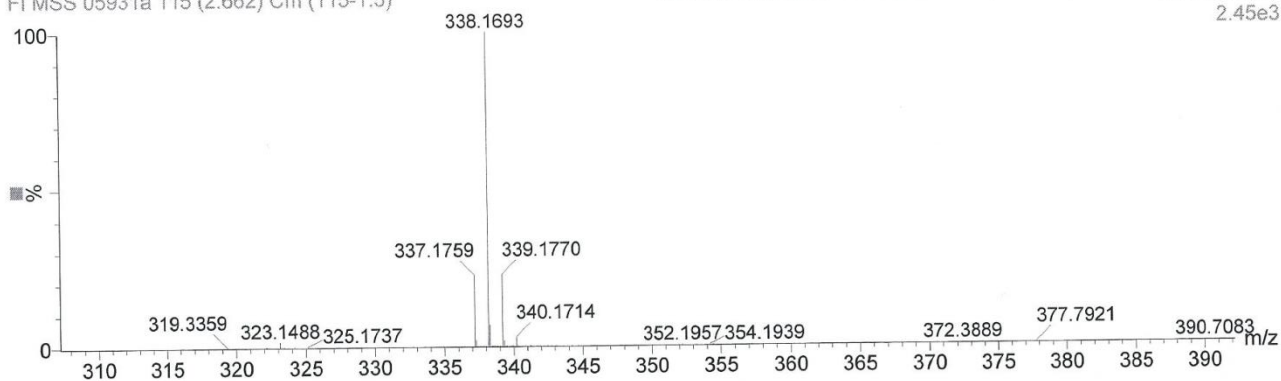
TOF MS FI+
6.70e12

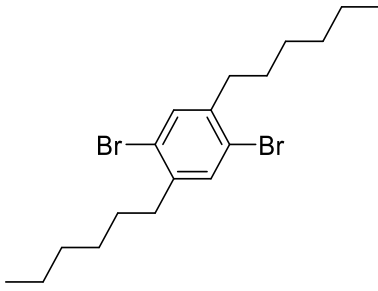


FI MSS 05931a 115 (2.662) Cm (115-1:5)

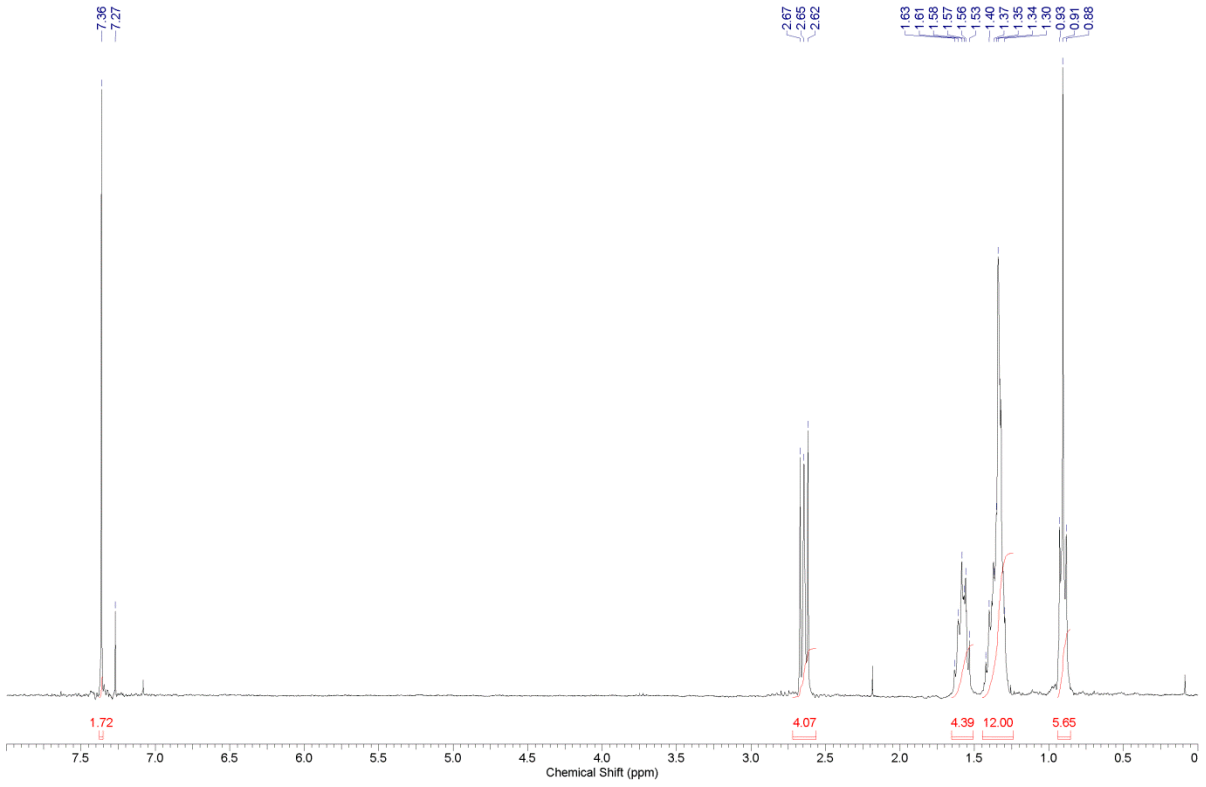
This is the measured mass spectrum of your sample.

TOF MS FI+
2.45e3

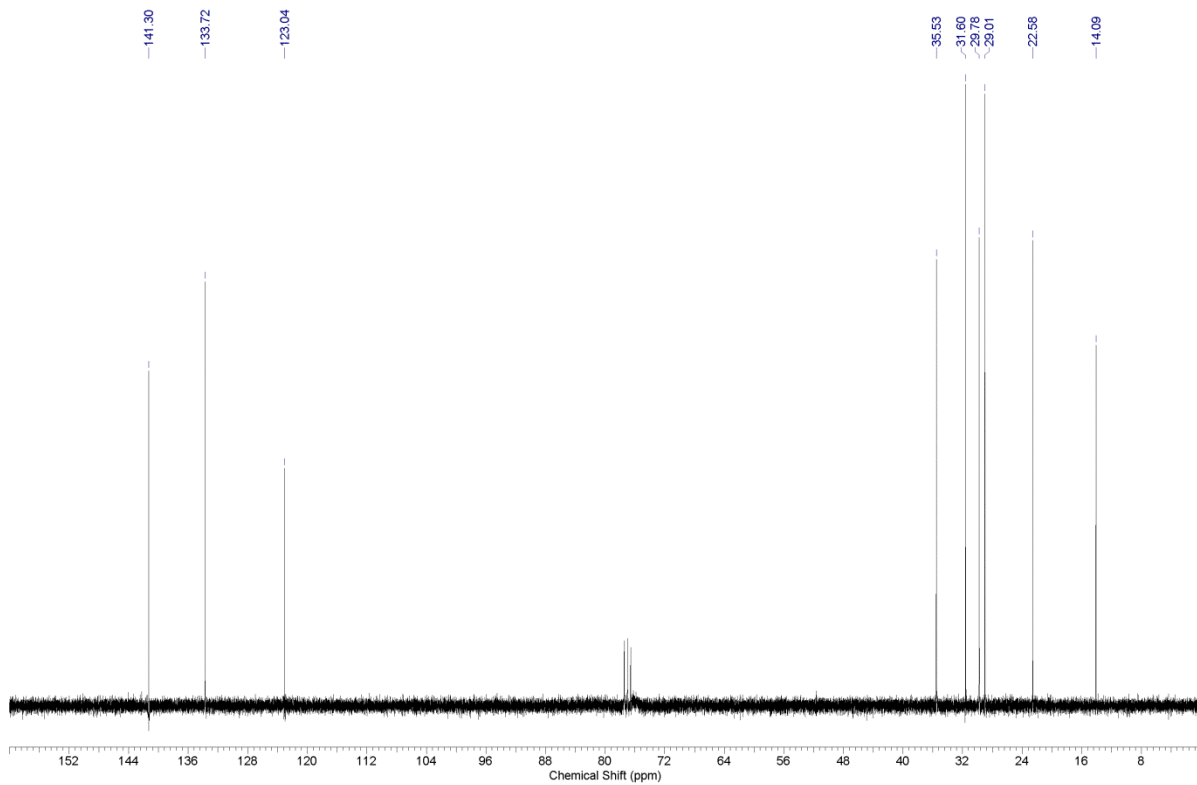


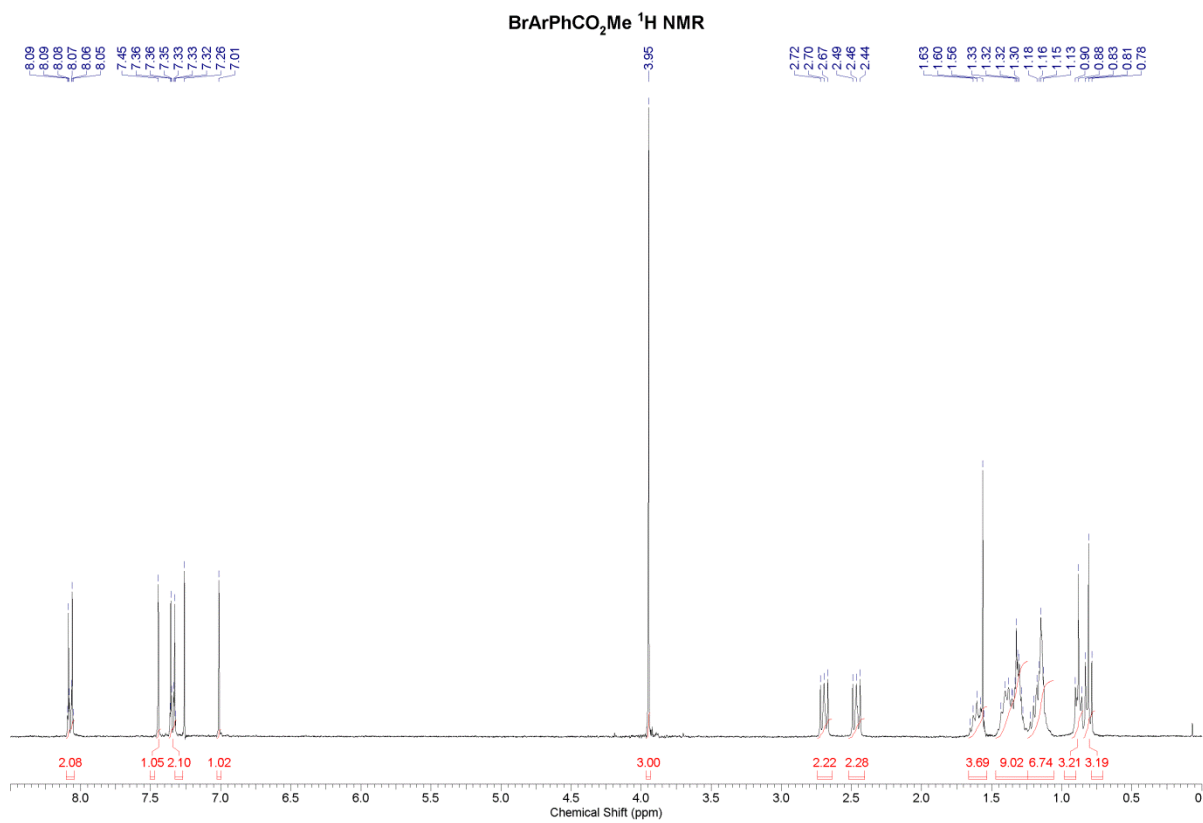
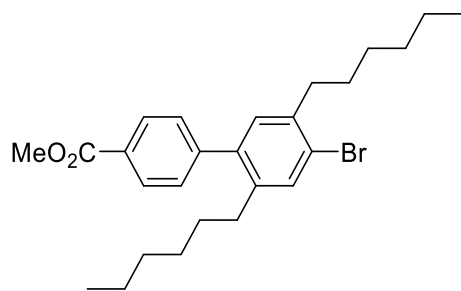


dibromo dihexyl benzene ^1H NMR

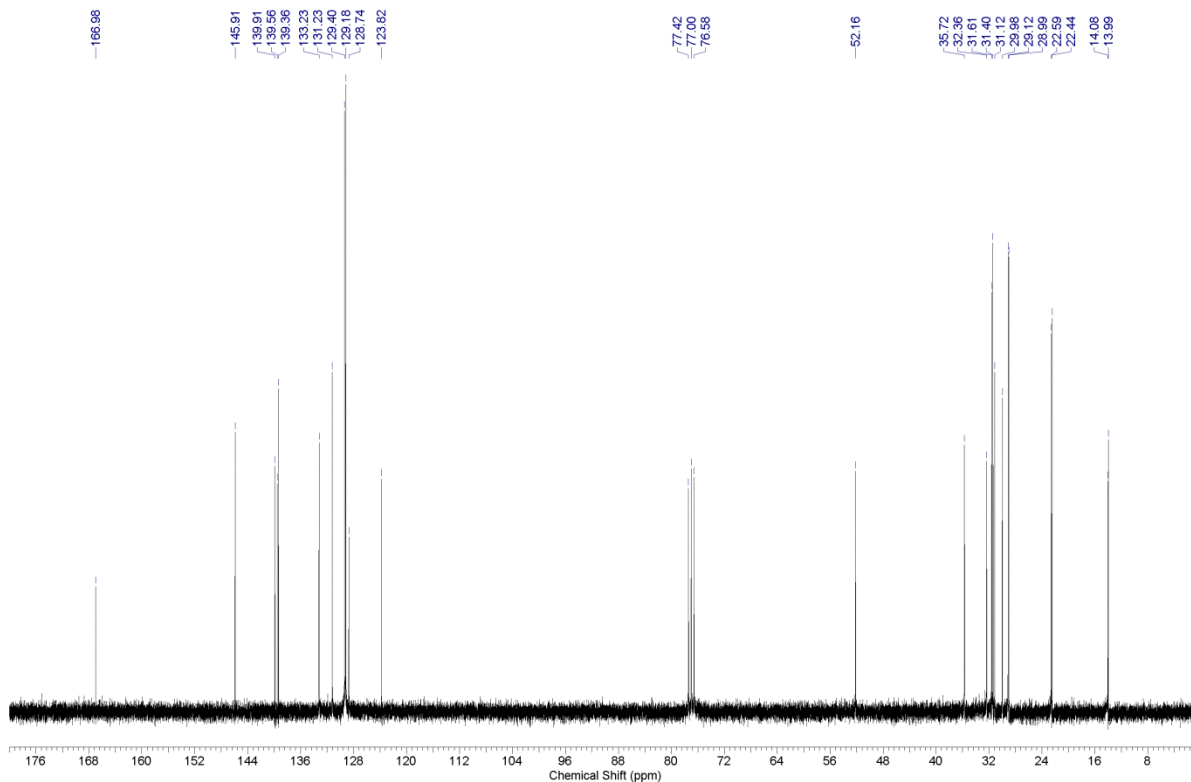


dibromodihexyl ¹³C NMR





BrArPhCO₂Me ¹³C NMR



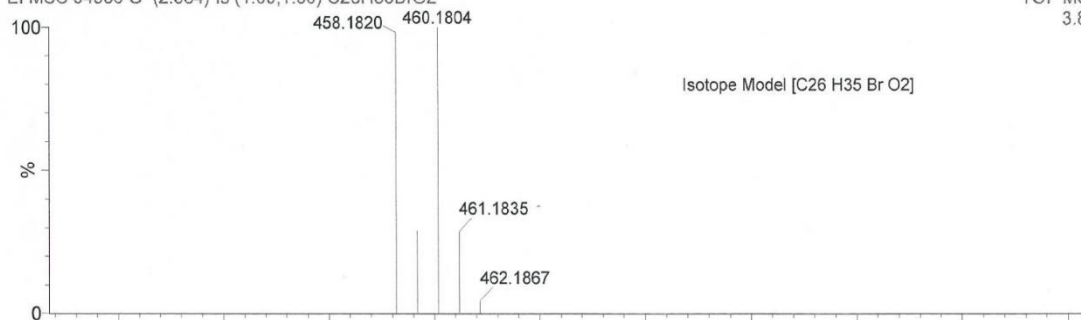
EI MSS 04956 [C₂₆H₃₅BrO₂]

Probe EI/CI

10:45:37 02-Sep-2008

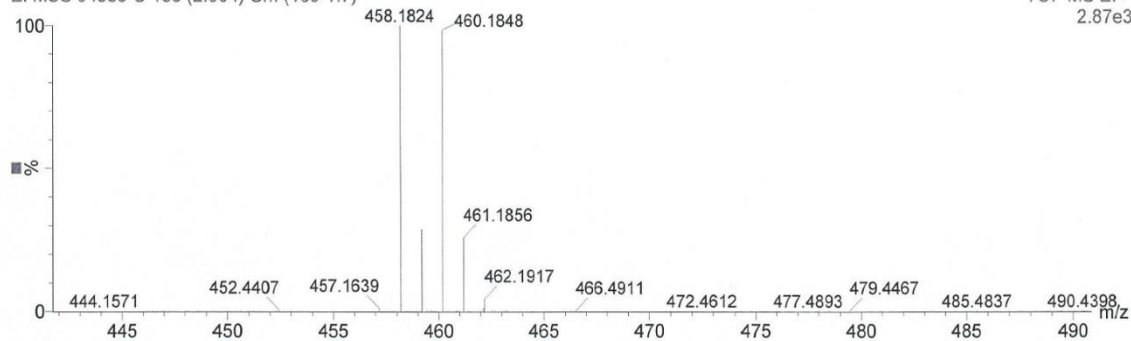
EI MSS 04956 O (2.534) Is (1.00,1.00) C₂₆H₃₅BrO₂

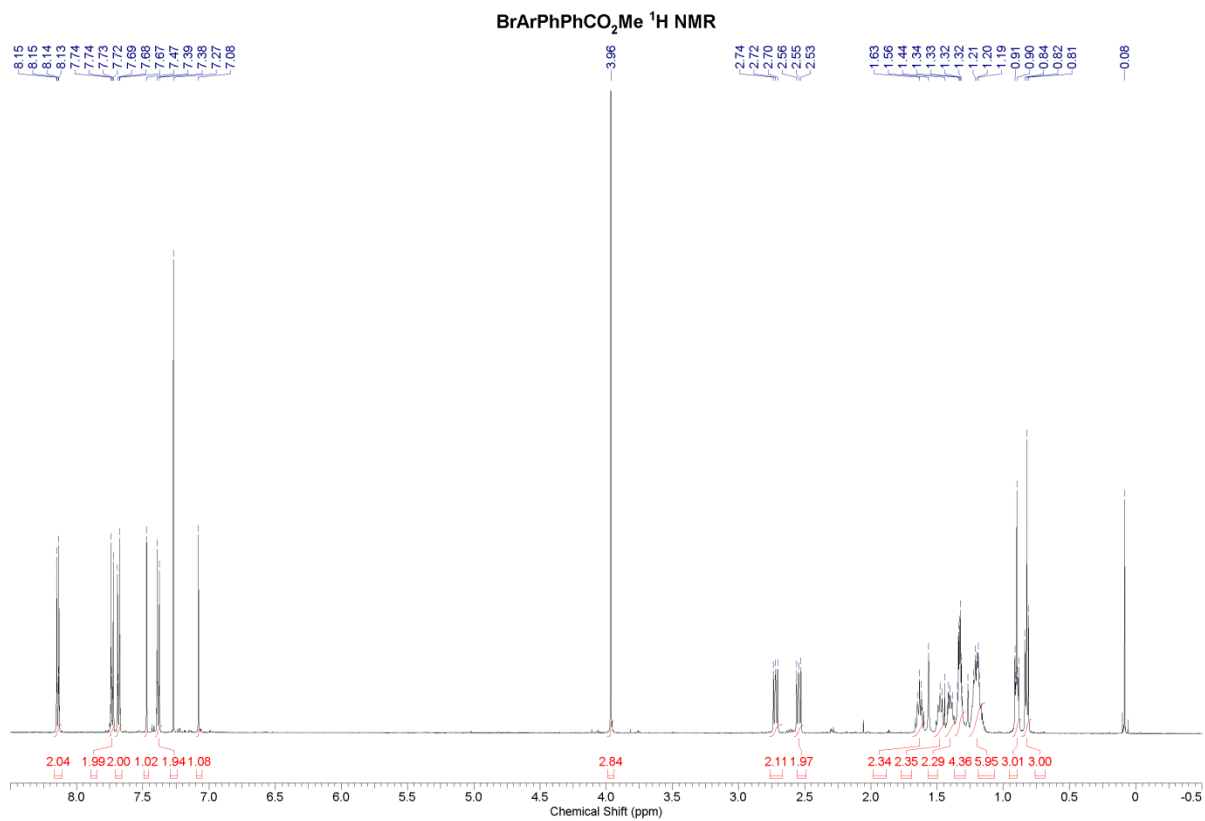
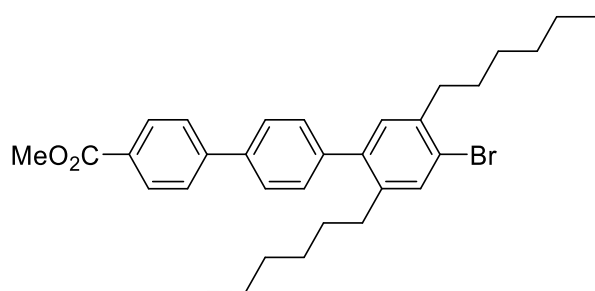
TOF MS EI+
3.83e12



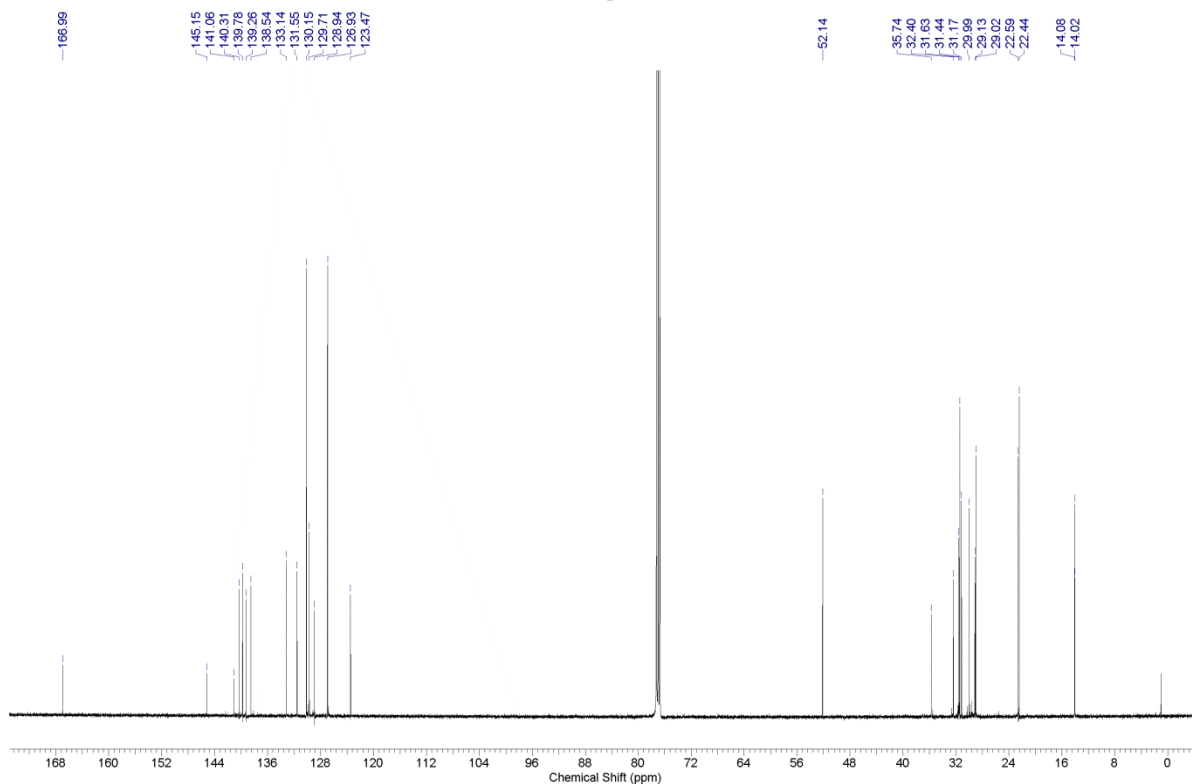
EI MSS 04956 O 155 (2.584) Cm (155-1:7)

TOF MS EI+
2.87e3





BrArPhPhCO₂Me ¹³C NMR



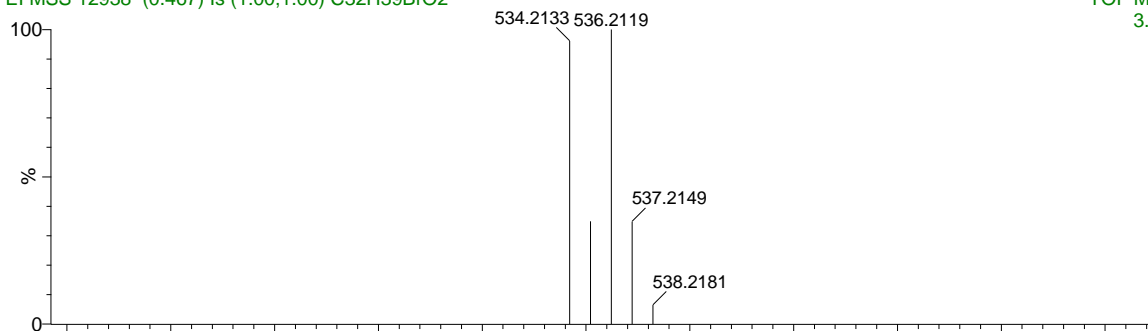
EI MSS 12938 [C32 H39 Br O]

Probe EI/CI

29-Jul-2013 07:58:59

EI MSS 12938 (0.467) Is (1.00,1.00) C32H39BrO2

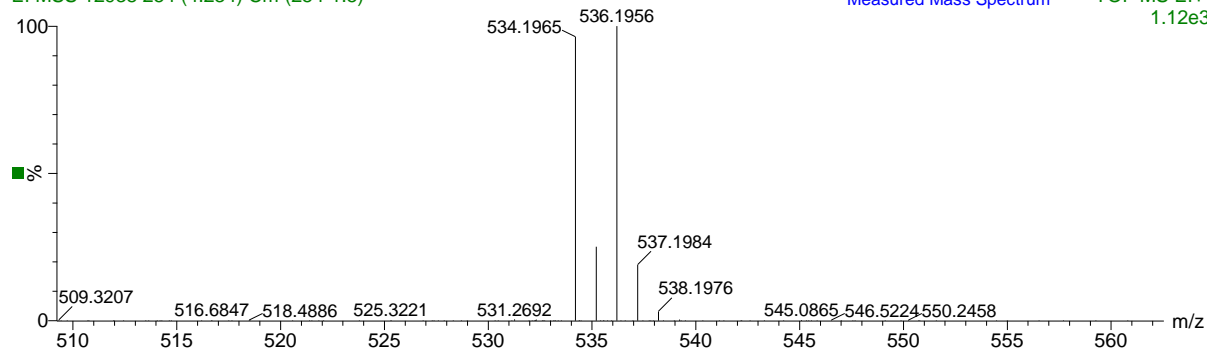
TOF MS EI+
3.66e12

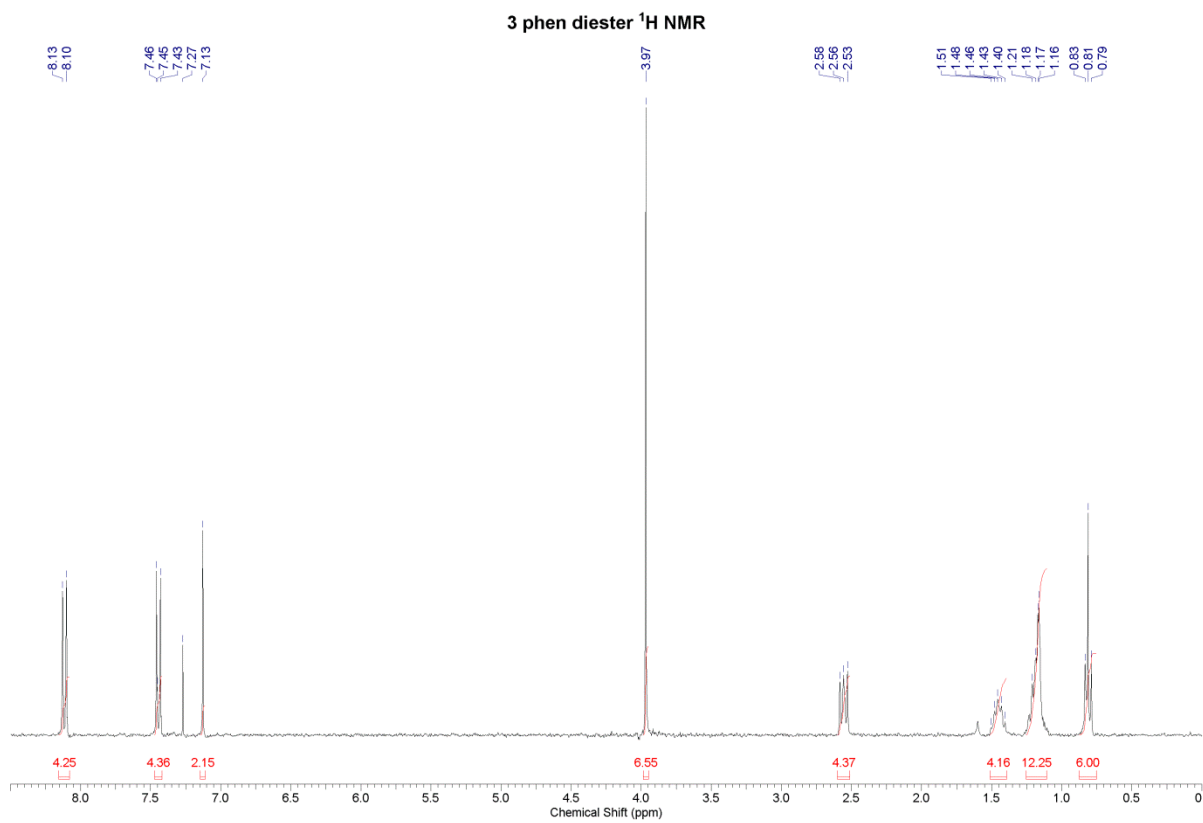
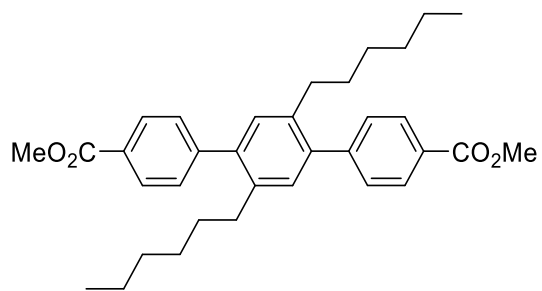


EI MSS 12938 254 (4.234) Cm (254-1:5)

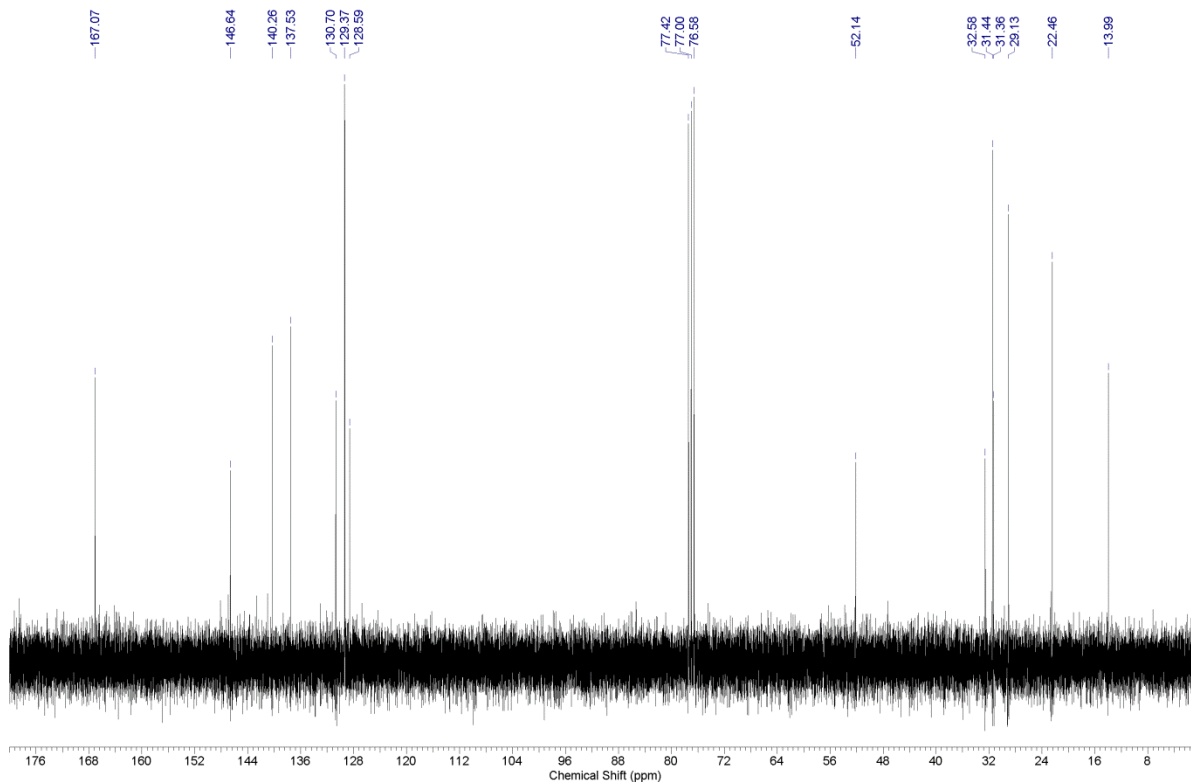
Measured Mass Spectrum

TOF MS EI+
1.12e3





3 phenyl diester ¹³C NMR



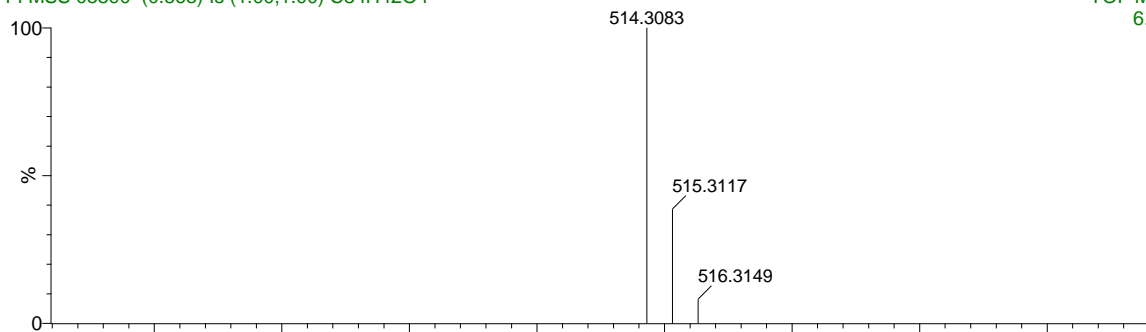
FI MSS 05890 [C34 H42 O4]

Probe EI/FI

27-Mar-2009 13:32:54

FI MSS 05890 (0.563) Is (1.00,1.00) C34H42O4

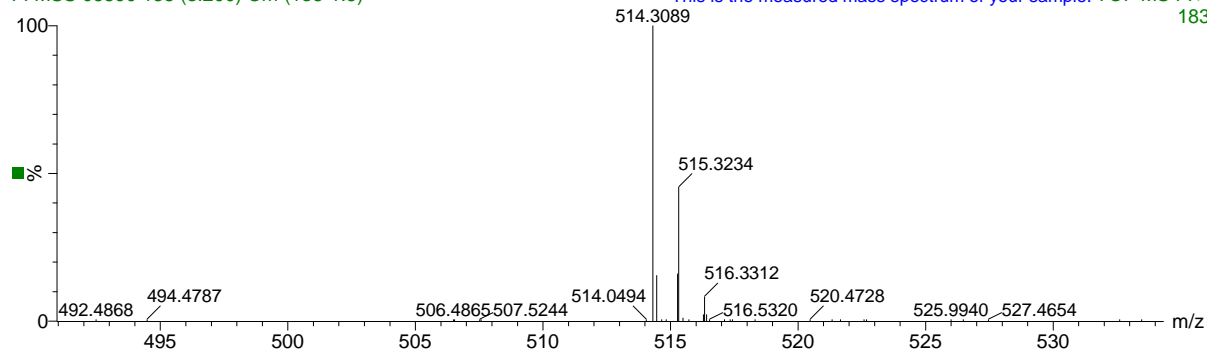
TOF MS FI+
6.76e12

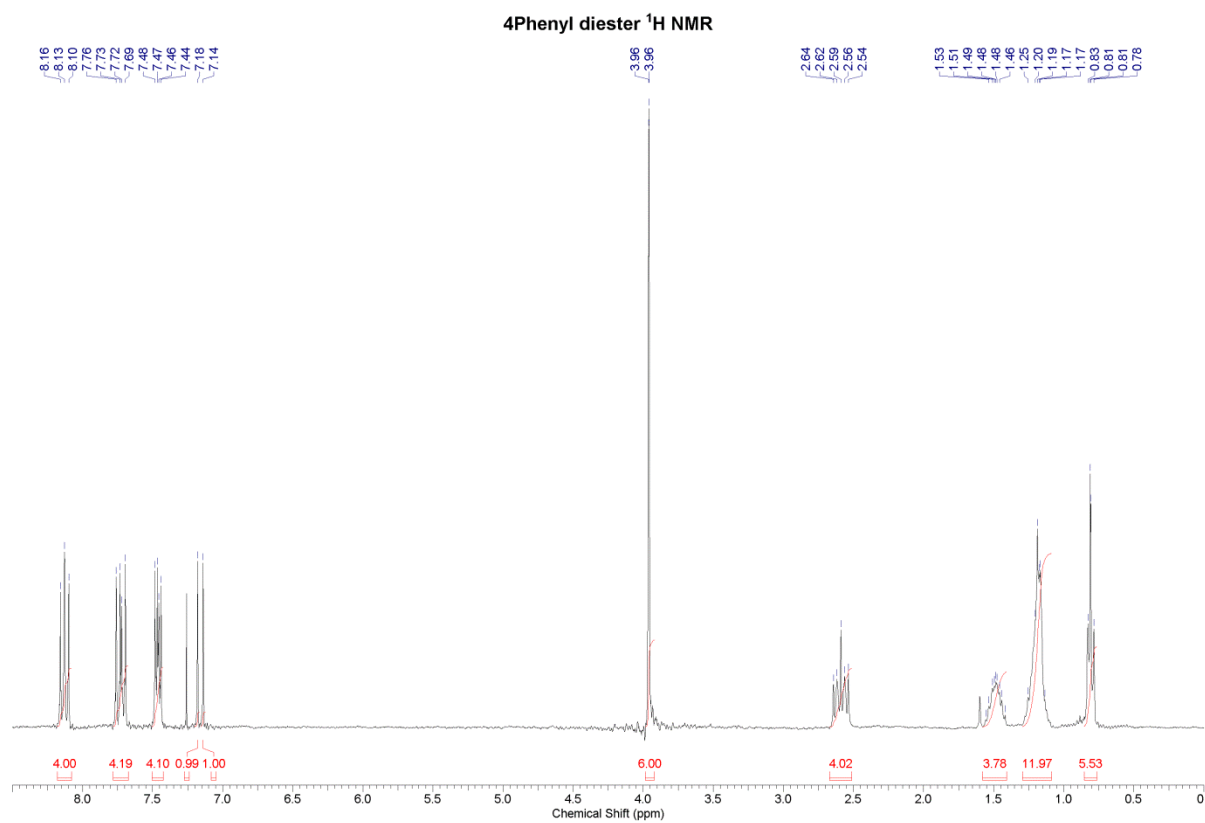
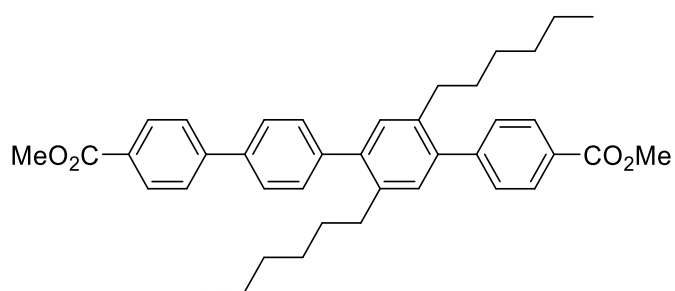


FI MSS 05890 138 (3.200) Cm (138-1:5)

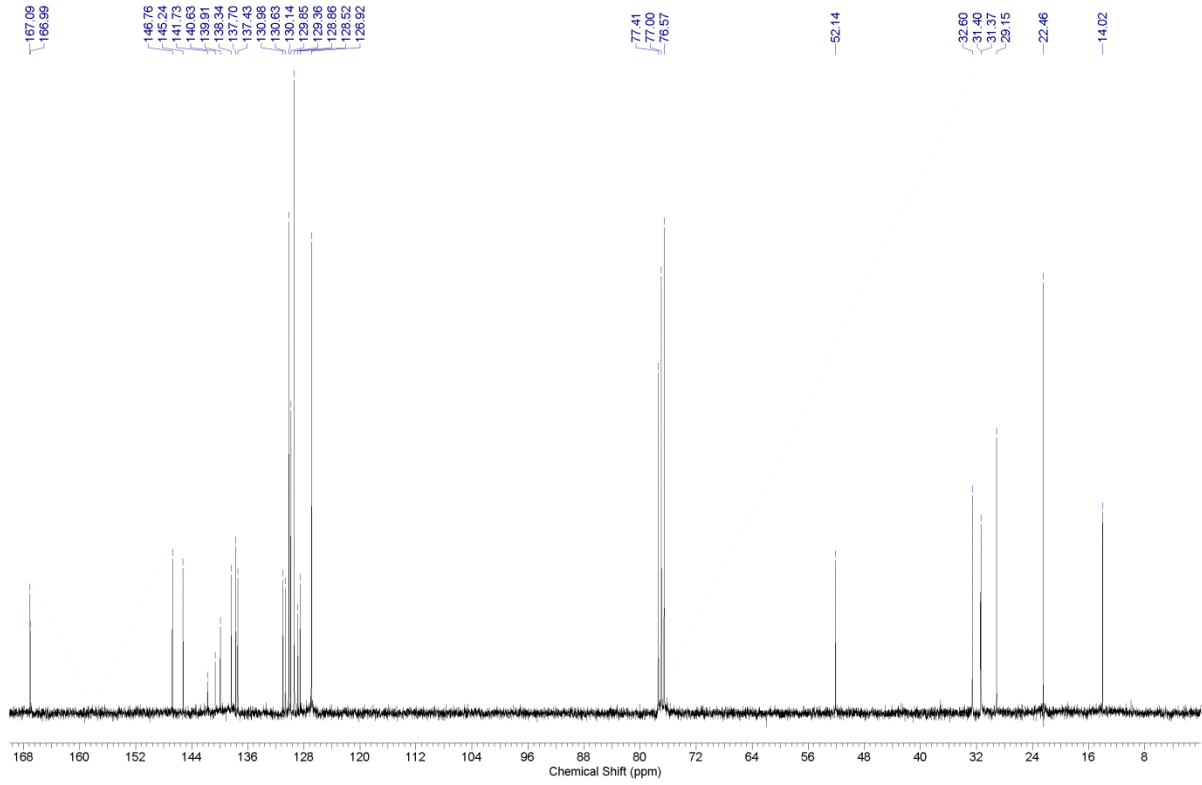
This is the measured mass spectrum of your sample. TOF MS FI+

183





4phenyl diester ¹³C NMR



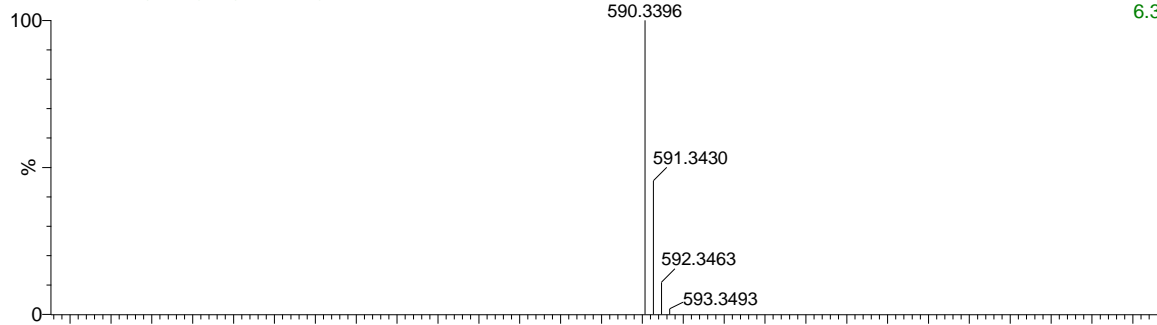
EI MSS 13040 [C40 H46 O4]

EI MSS 13040 (0.451) Is (1.00,1.00) C40H46O4

Probe EI/CI

03-Sep-2013 11:24:43

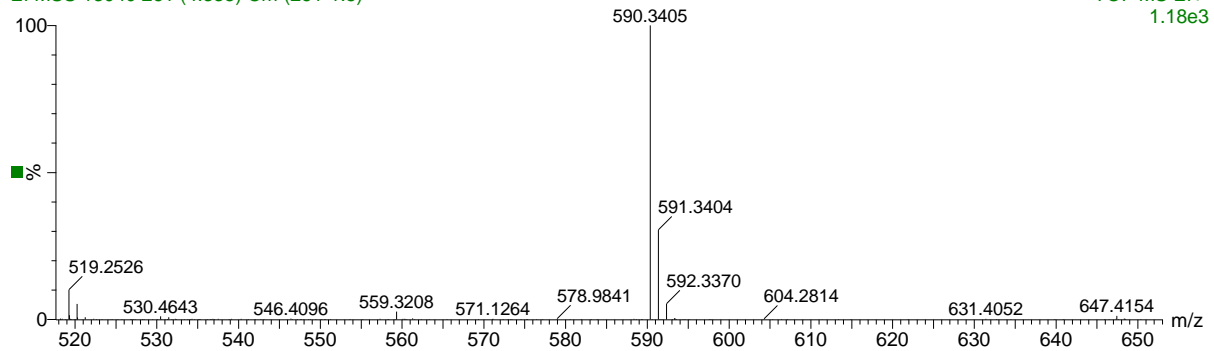
TOF MS EI+
6.32e12

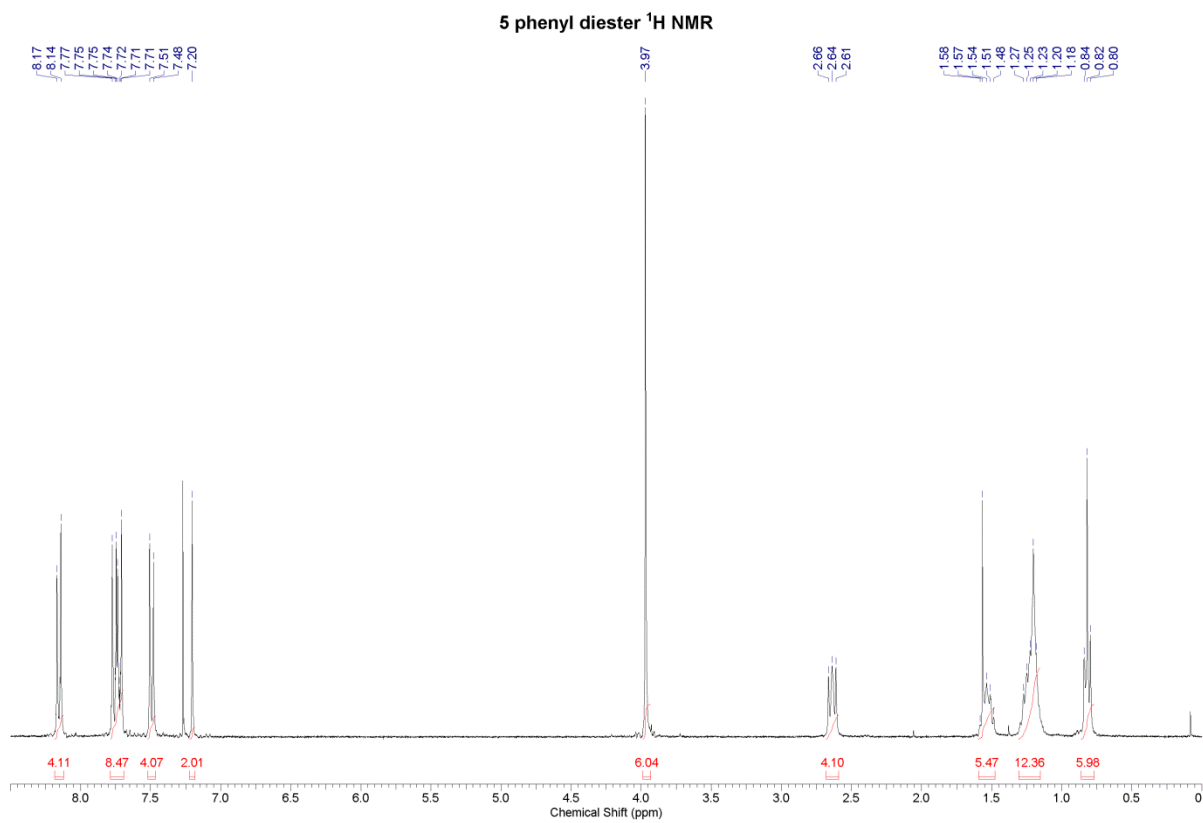
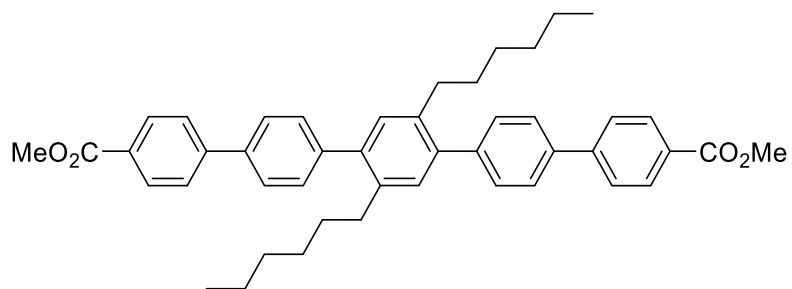


EI MSS 13040 261 (4.335) Cm (261-1:5)

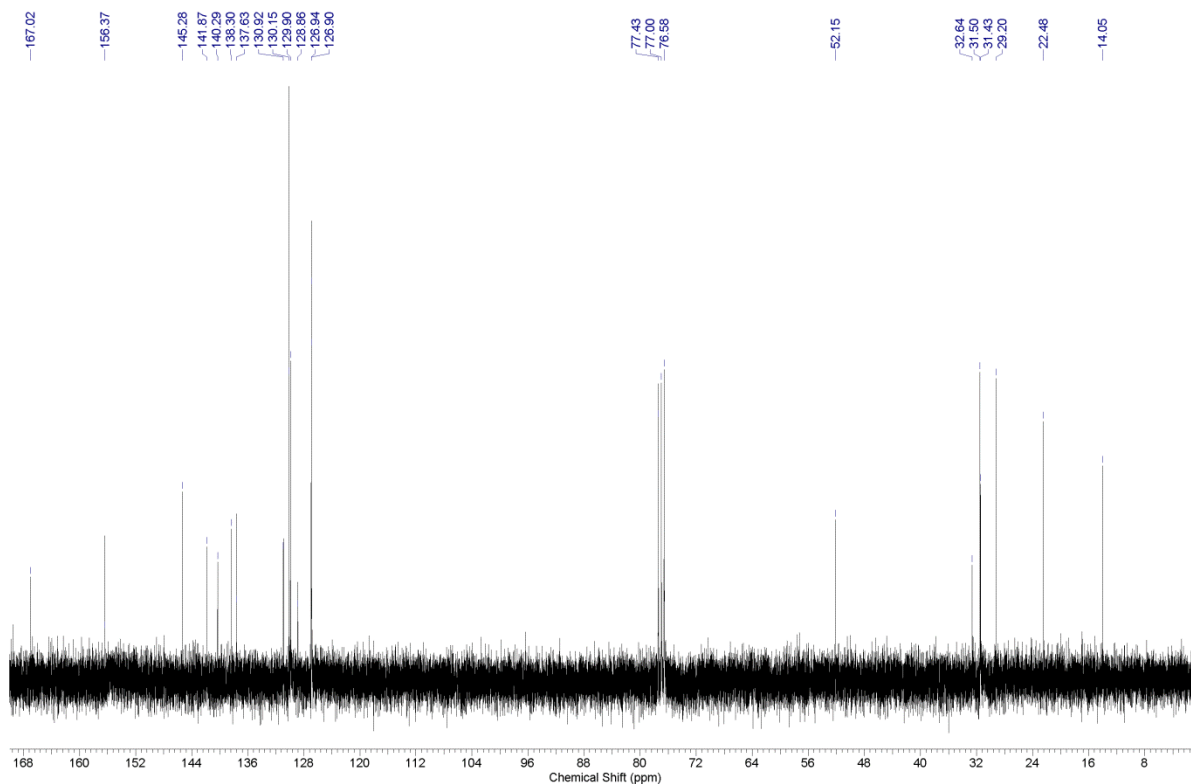
Measured Mass Spectrum

TOF MS EI+
1.18e3





5 phenyl diester ¹³C NMR



EI MSS 05785 [C46 H50 O4]

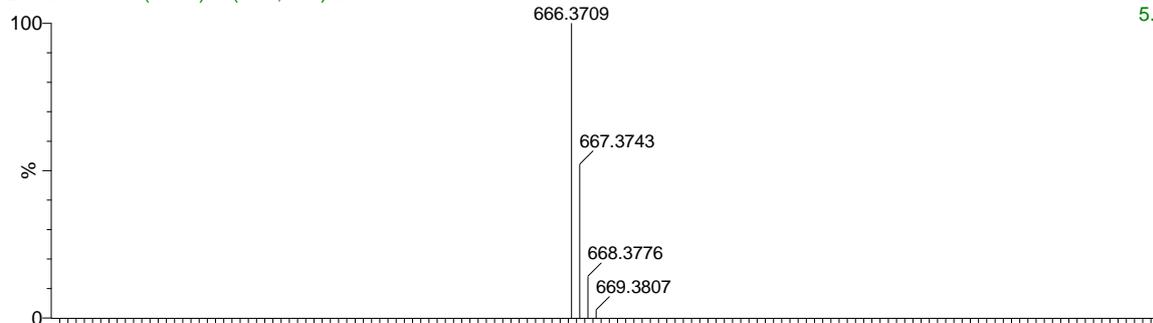
EI MSS 05785 (0.517) Is (1.00,1.00) C46H50O4

Probe EI/CI

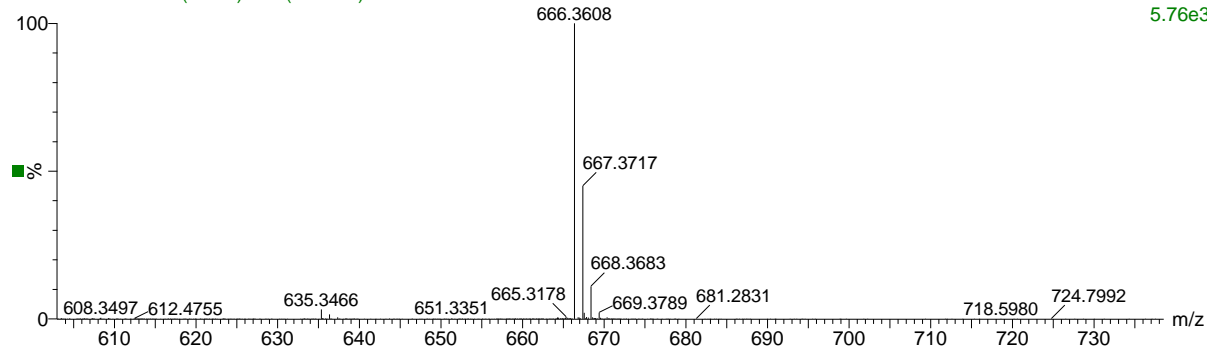
This is the theoretical isotope model of your compound.

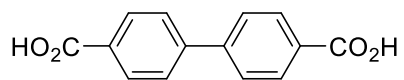
13-Mar-2009 10:38:37

TOF MS EI+
5.91e12

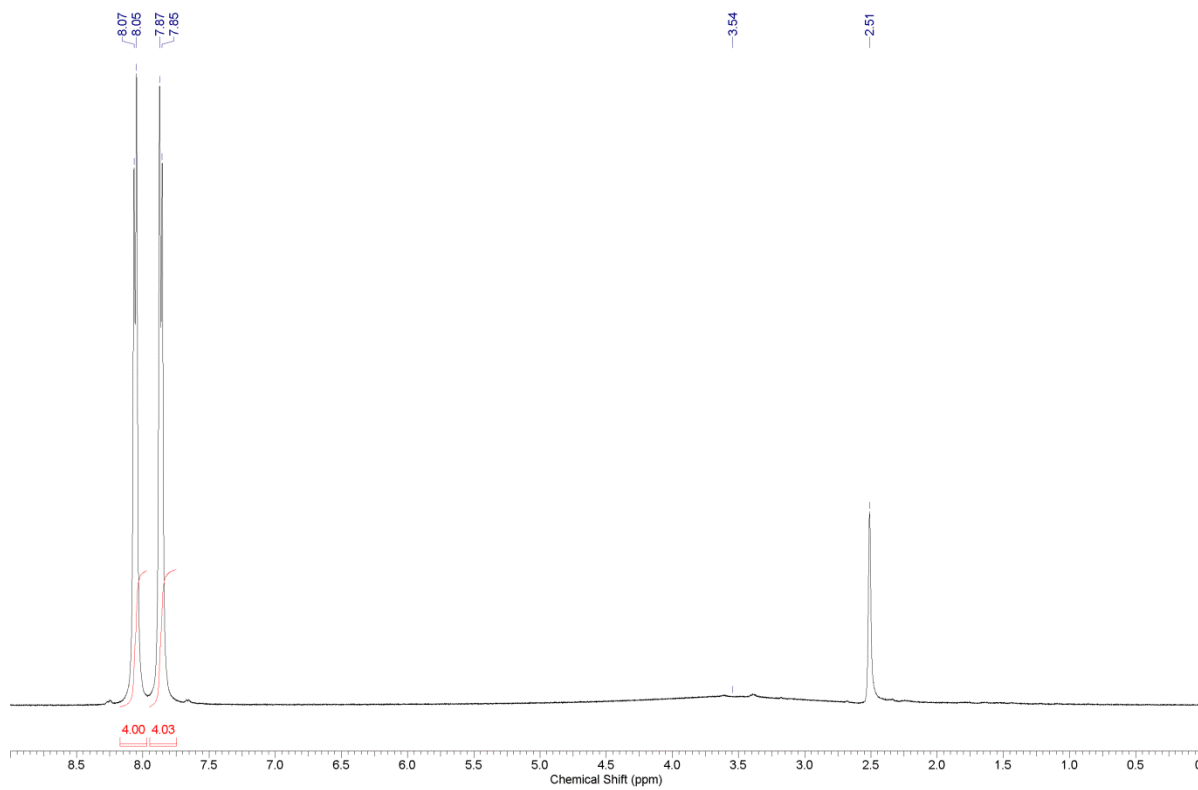


EI MSS 05785 272 (4.535) Cm (272-1:5)

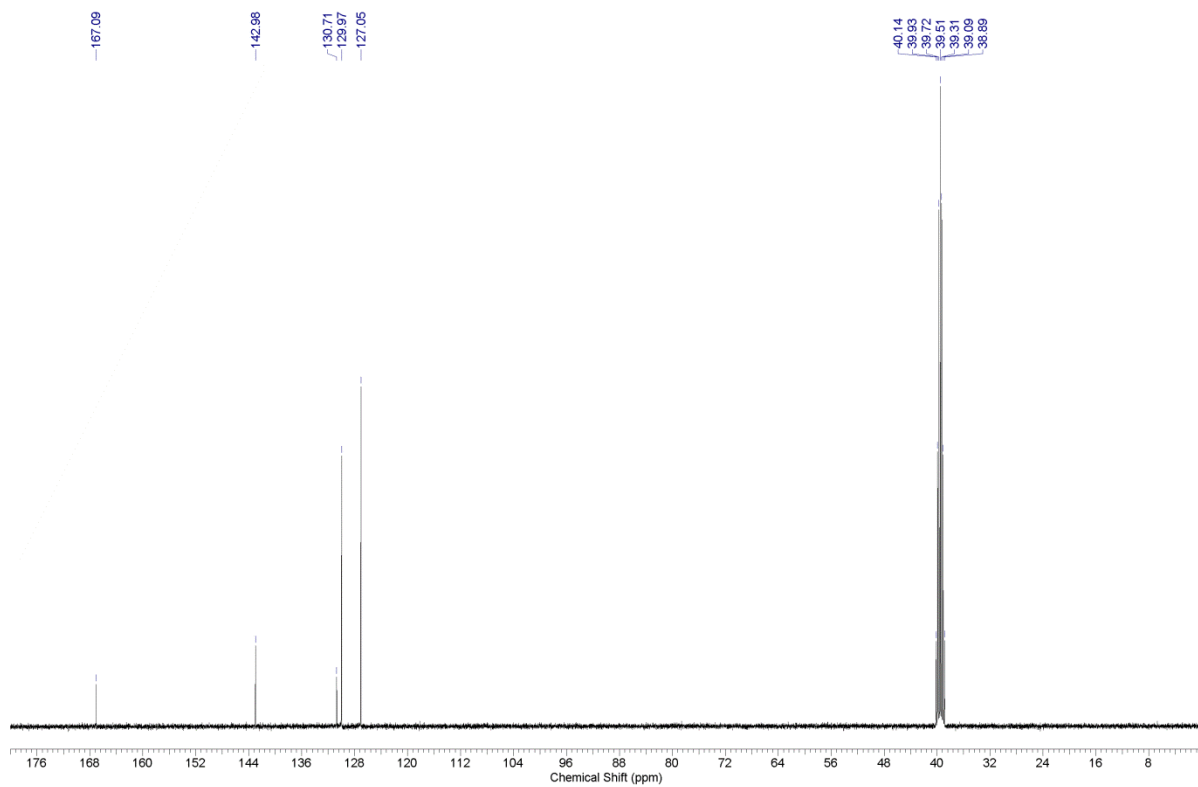


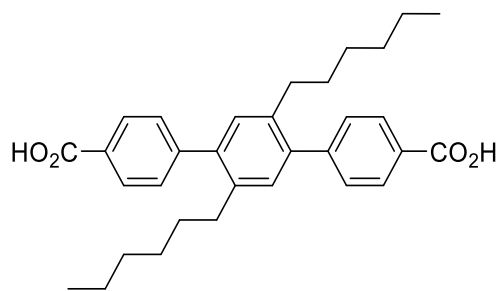


2 phen diacid ¹H NMR

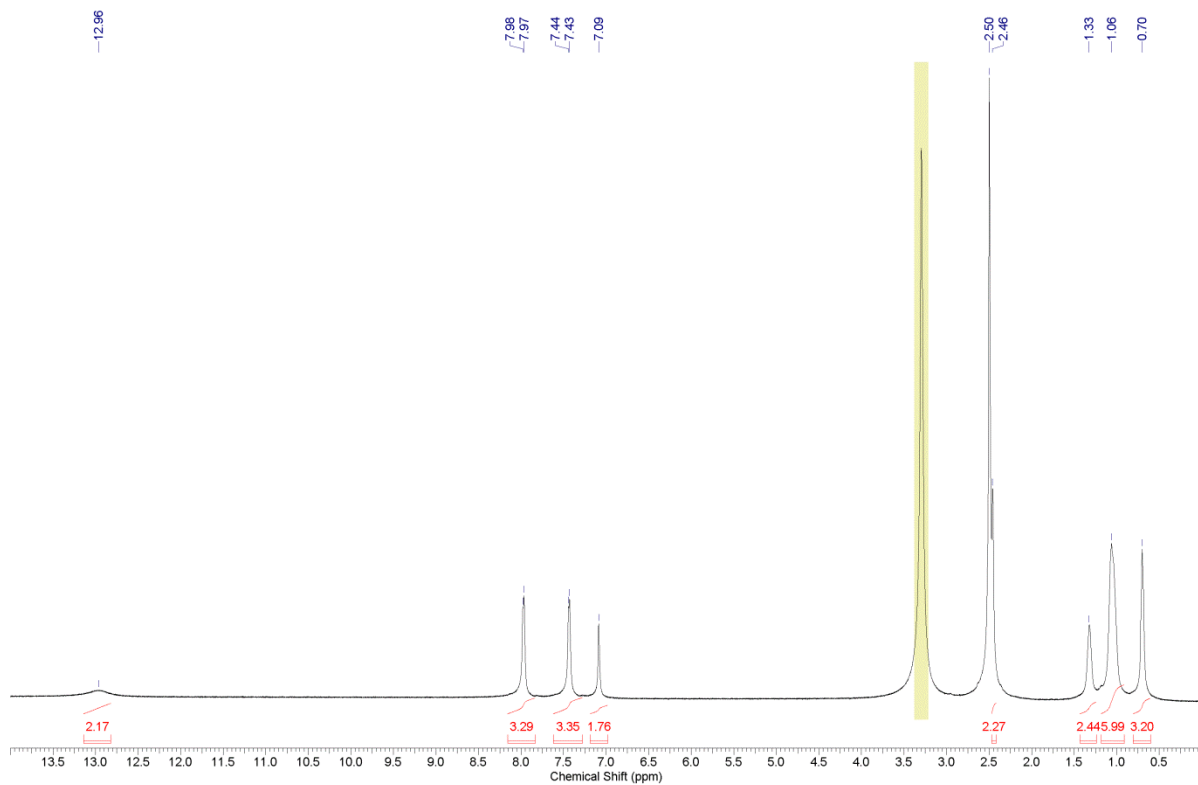


2 phen diacid ¹³C NMR

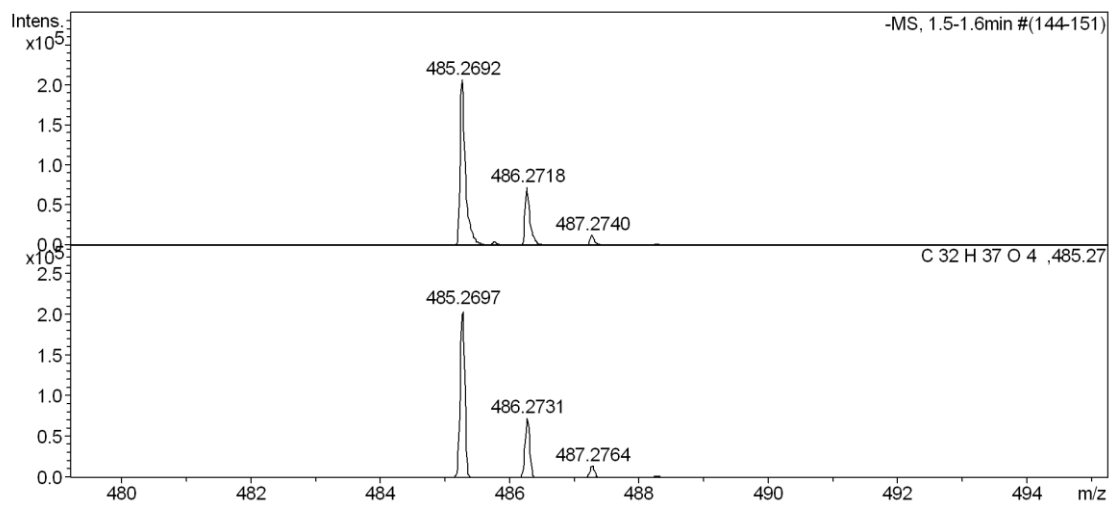
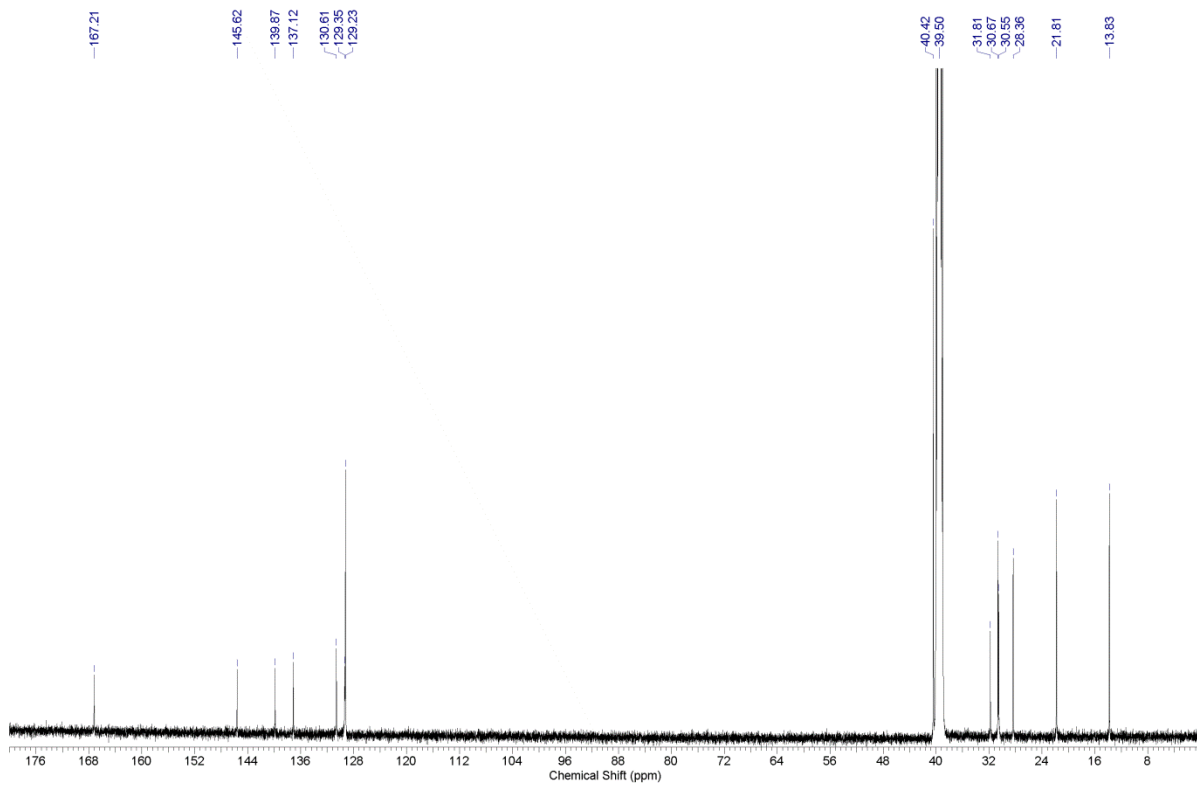


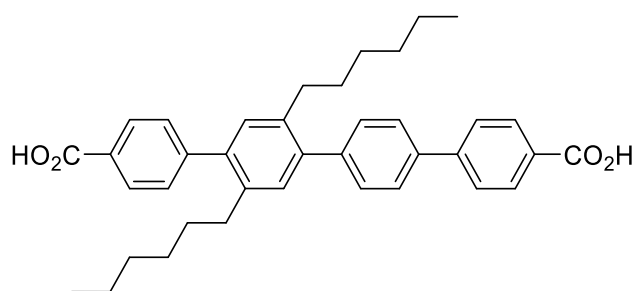


3 Phenyl diacid ¹H NMR

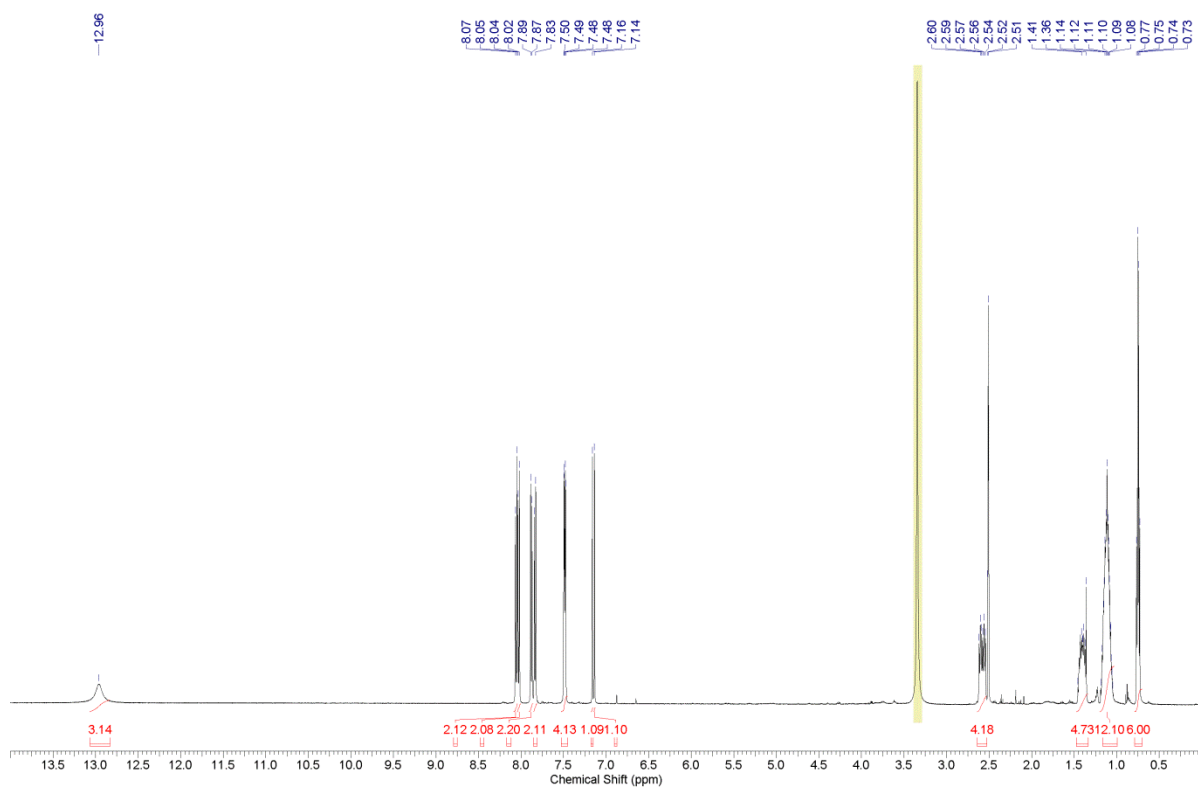


3 Phenyl diacid ¹³C NMR

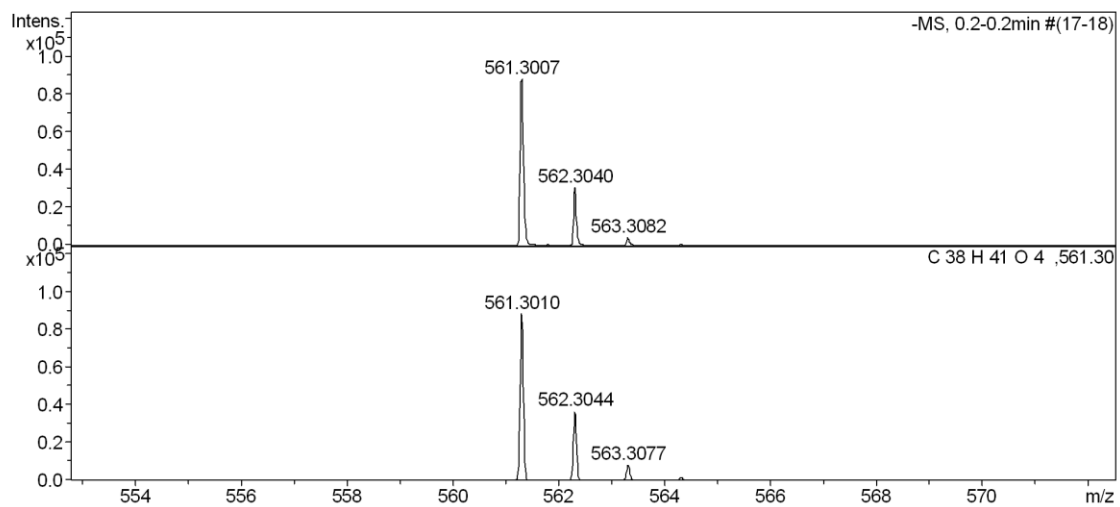
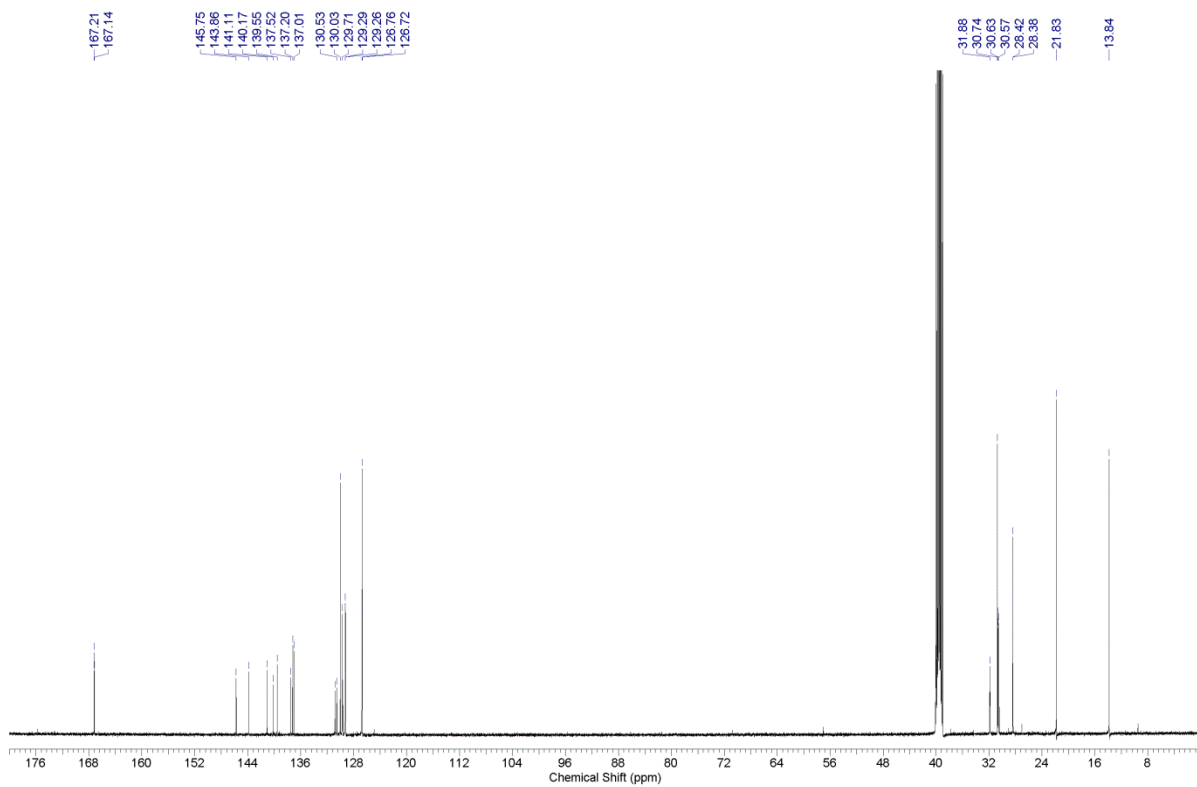


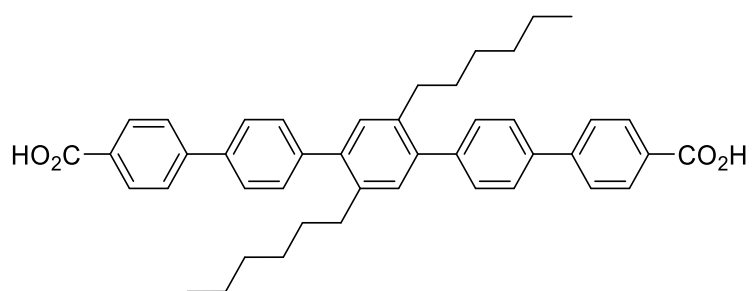


4 Phenyl diacid ¹H NMR

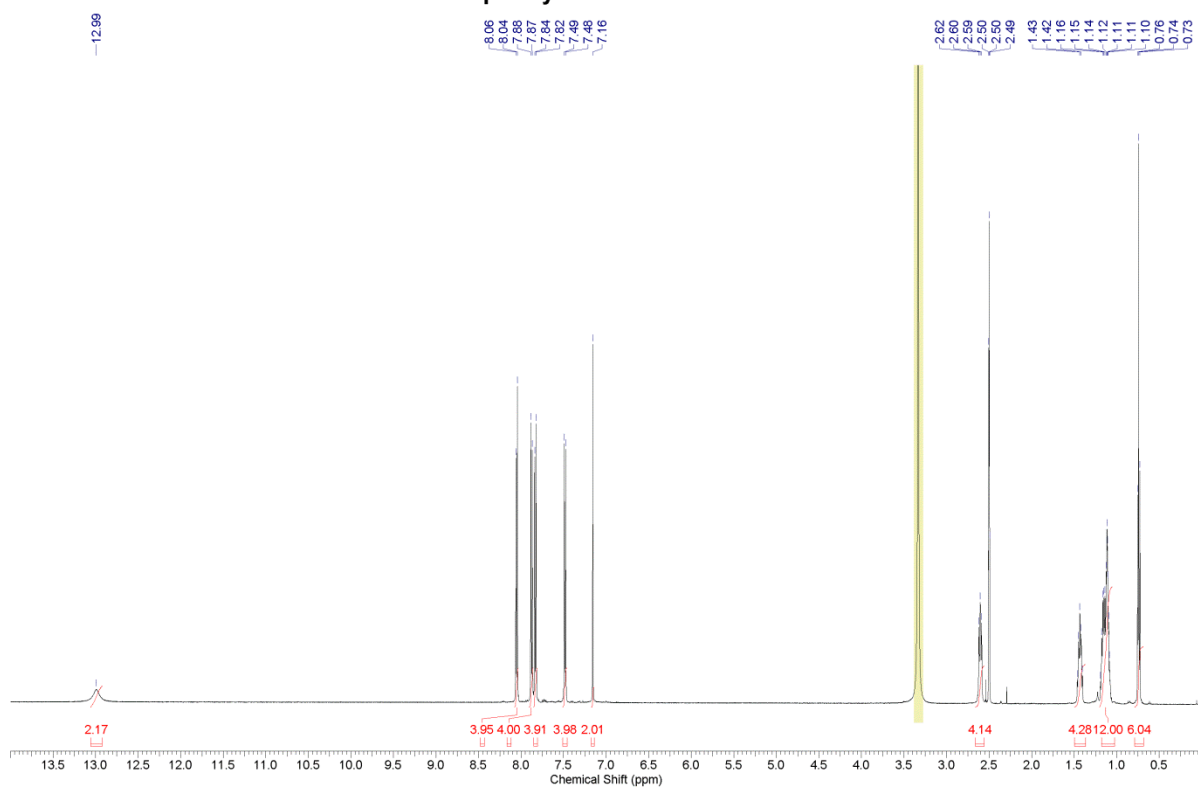


4 Phenyl diacid ¹³C NMR

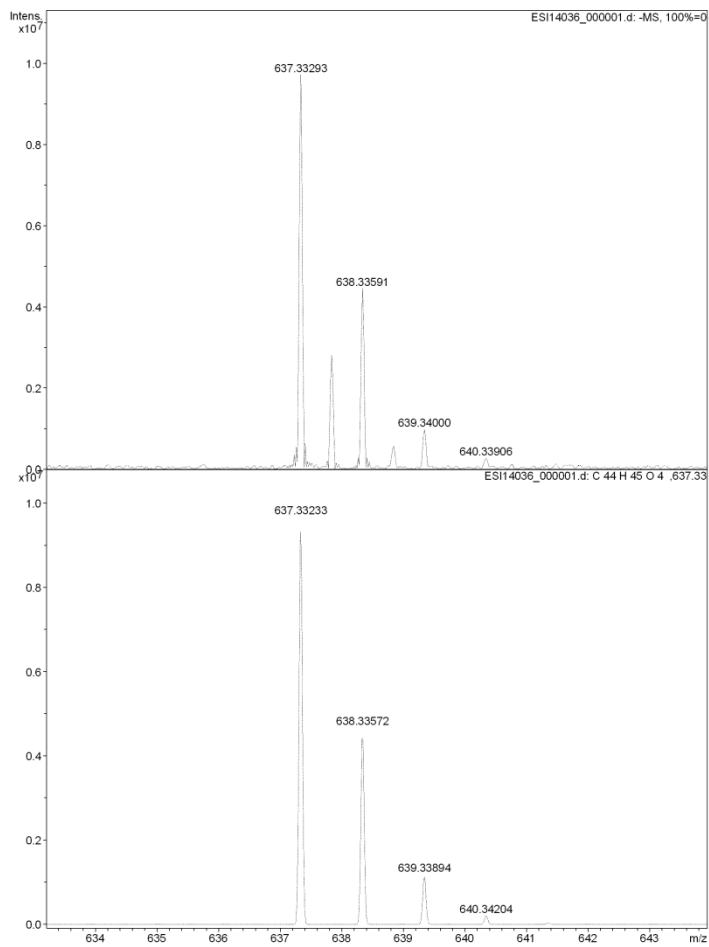
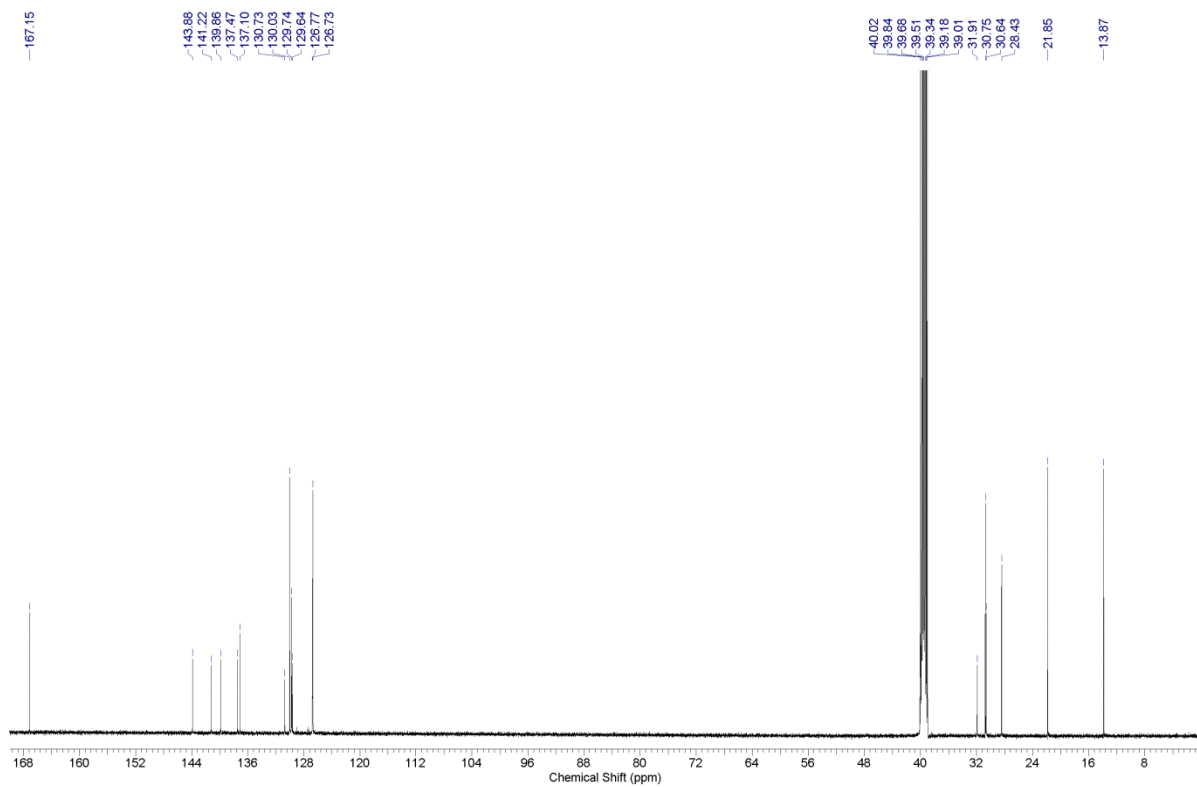


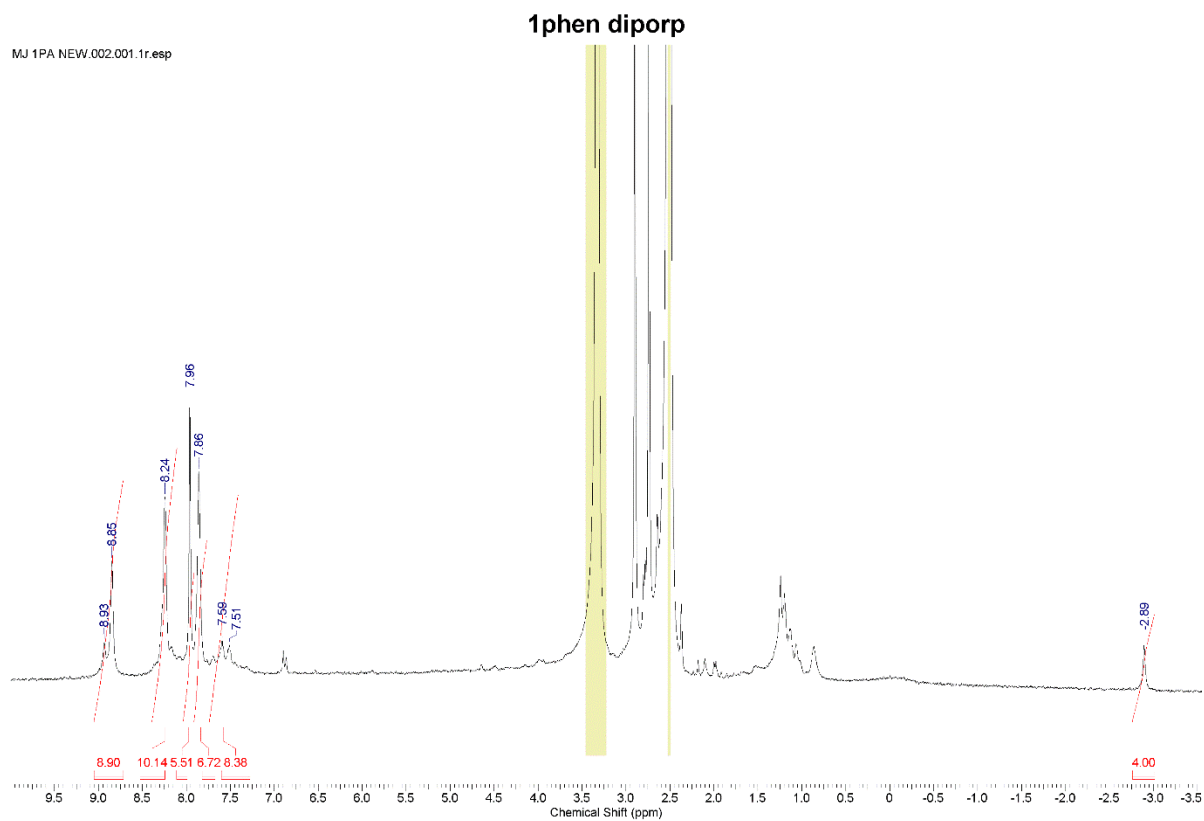
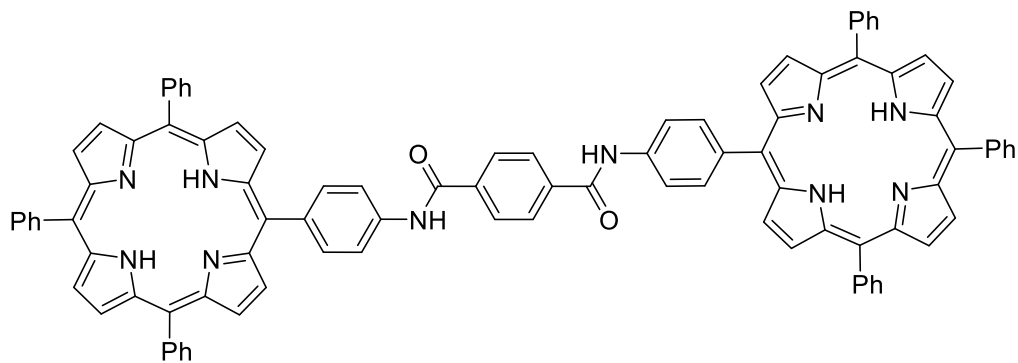


5phenyl diacid 1H NMR



5 phenyl diacid ¹³C NMR





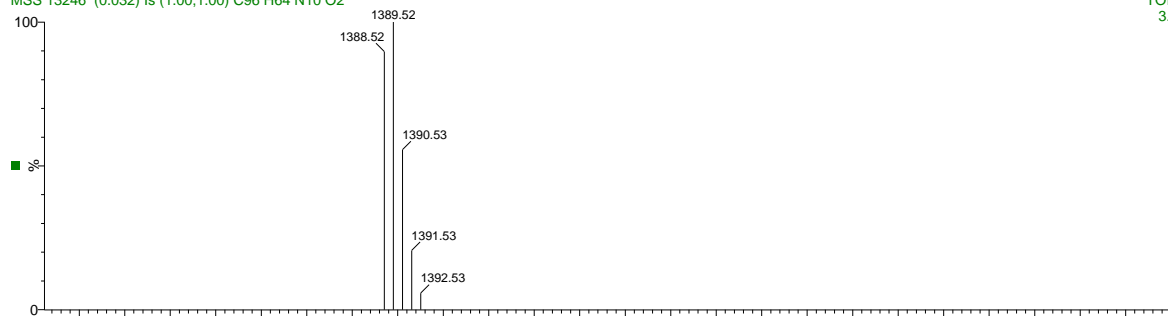
MSS 13246 [C96 H64 N10 O2]

MALDI

18-Nov-2013 10:54:02

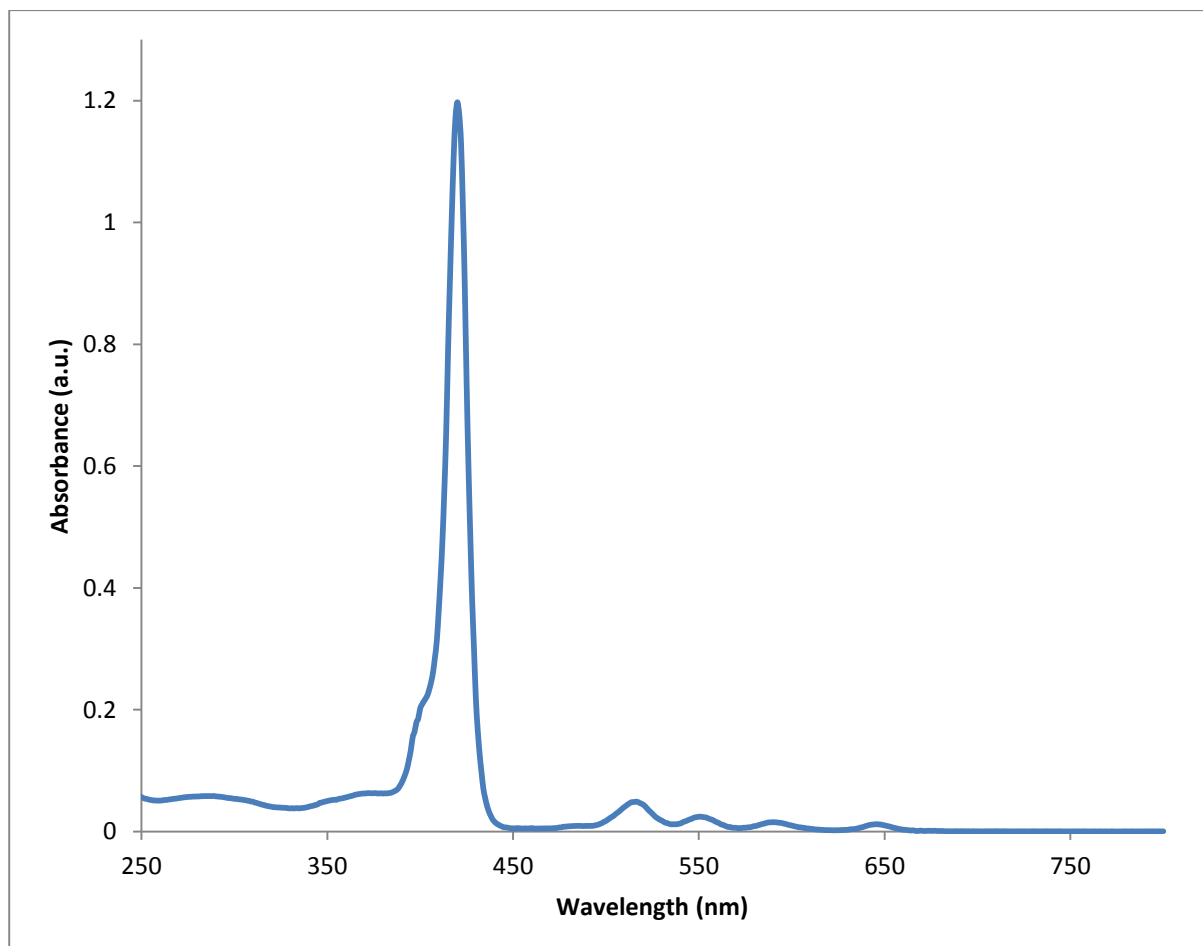
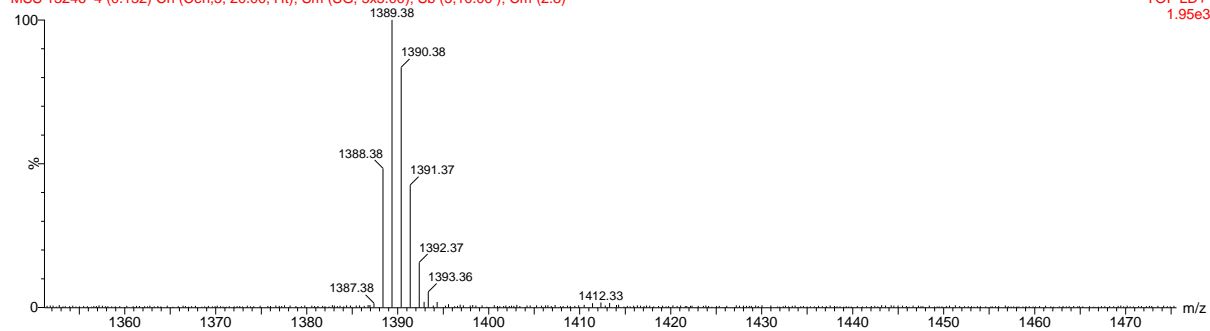
MSS 13246 (0.032) Is (1.00,1.00) C96 H64 N10 O2

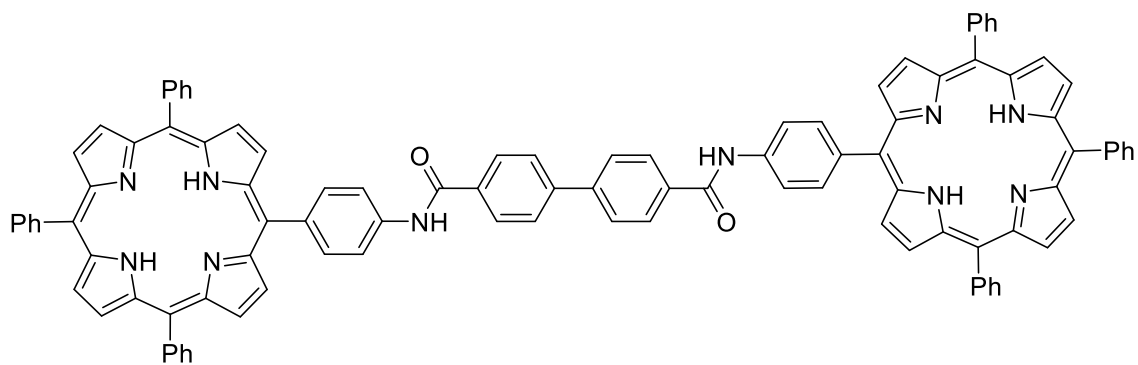
TOF LD+
3.66e12



MSS 13246 4 (0.132) Cn (Cen,5, 20.00, Ht); Sm (SG, 5x5.00); Sb (5,10.00); Cm (2:8)

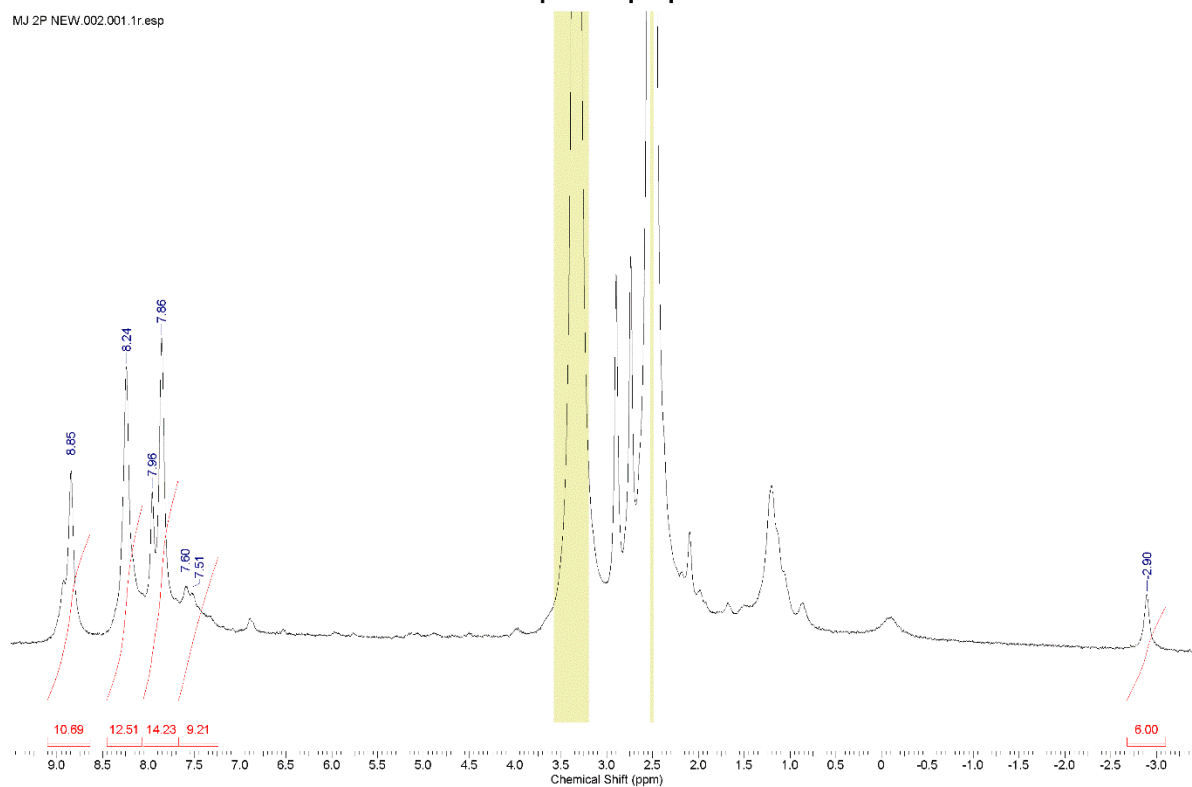
TOF LD+
1.95e3





MJ 2P NEW.002.001.1r.esp

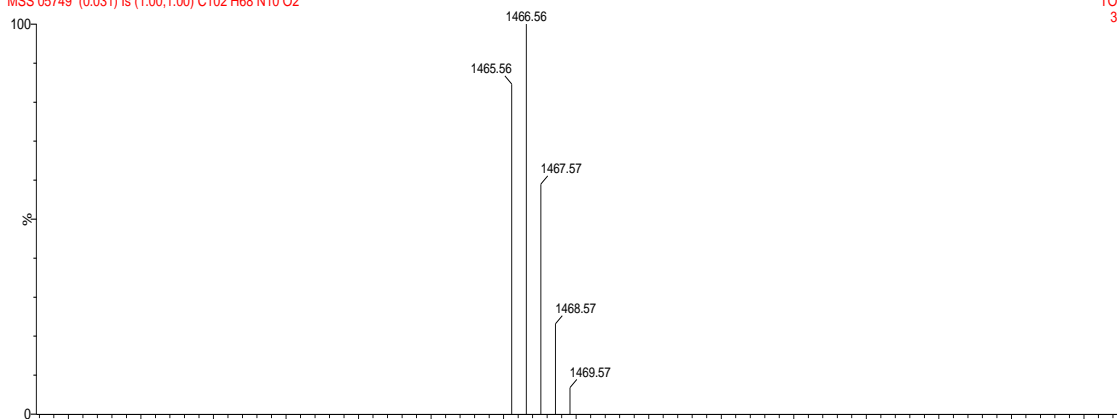
2phen diporp



MSS 05749 [C102 H68 N10 O2]

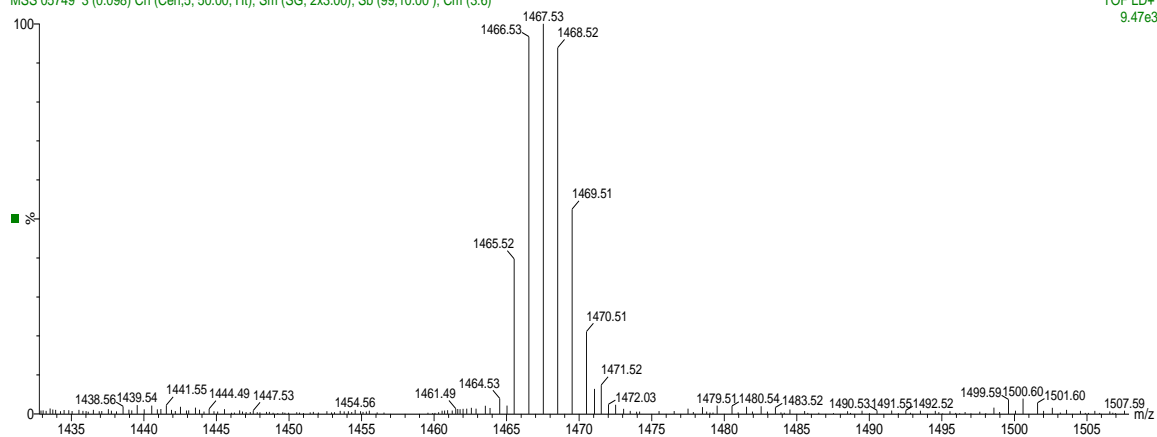
MSS 05749 (0.031) Is (1.00,1.00) C102 H68 N10 O2

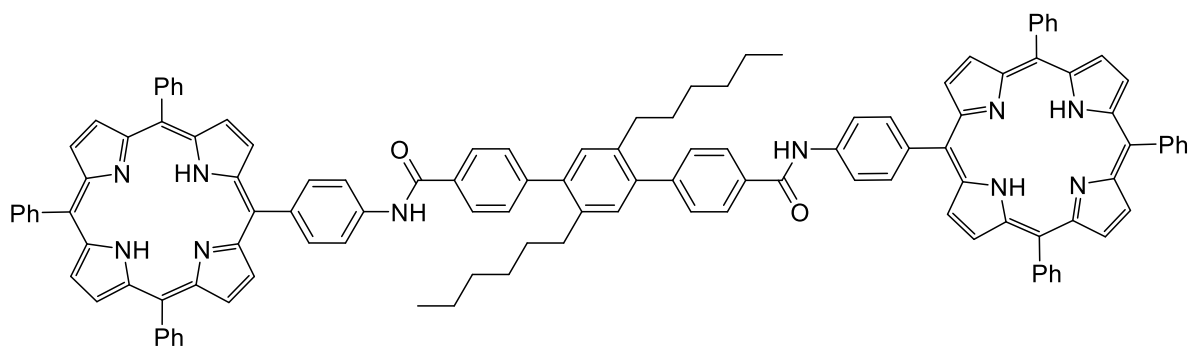
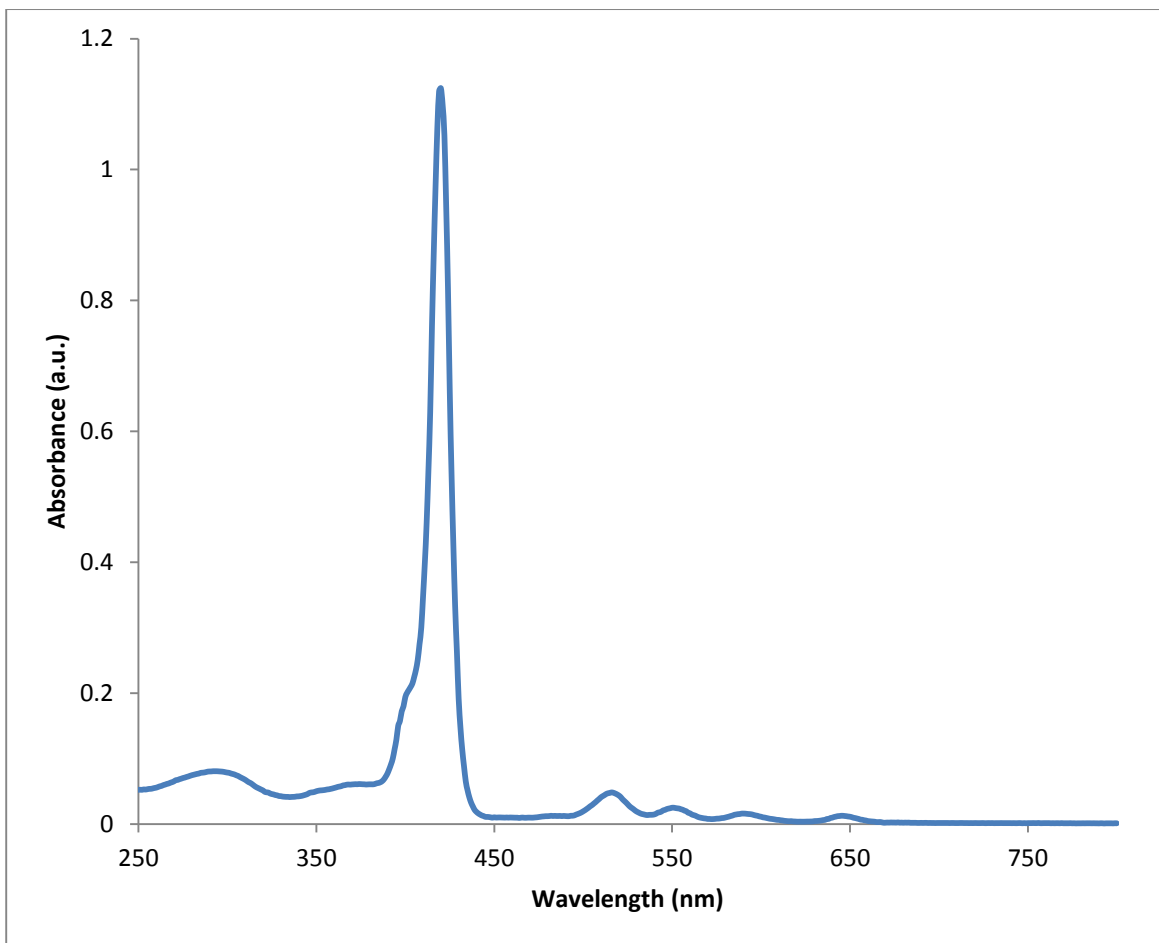
TOF LD+
3.63e12



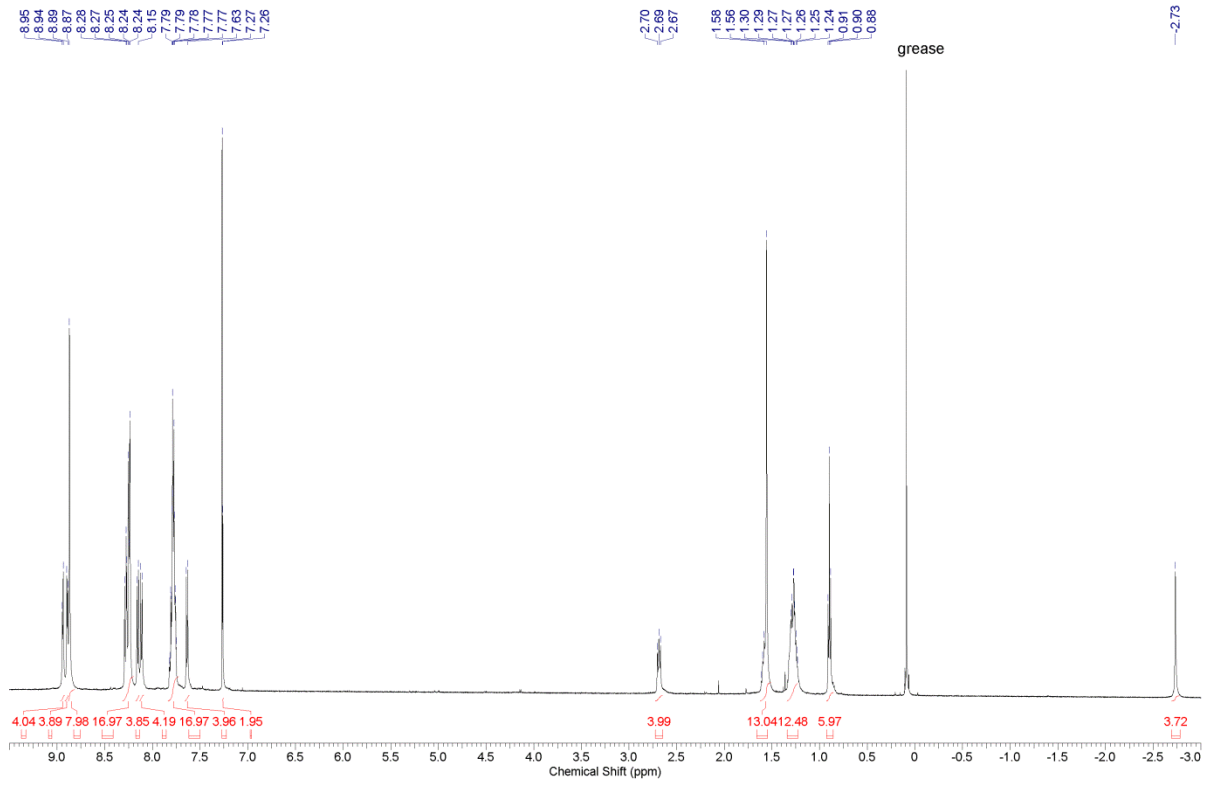
MSS 05749 3 (0.098) Cn (Cen,5, 50.00, Ht); Sm (SG, 2x3.00); Sb (99,10.00); Cm (3:6)

TOF LD+
9.47e3

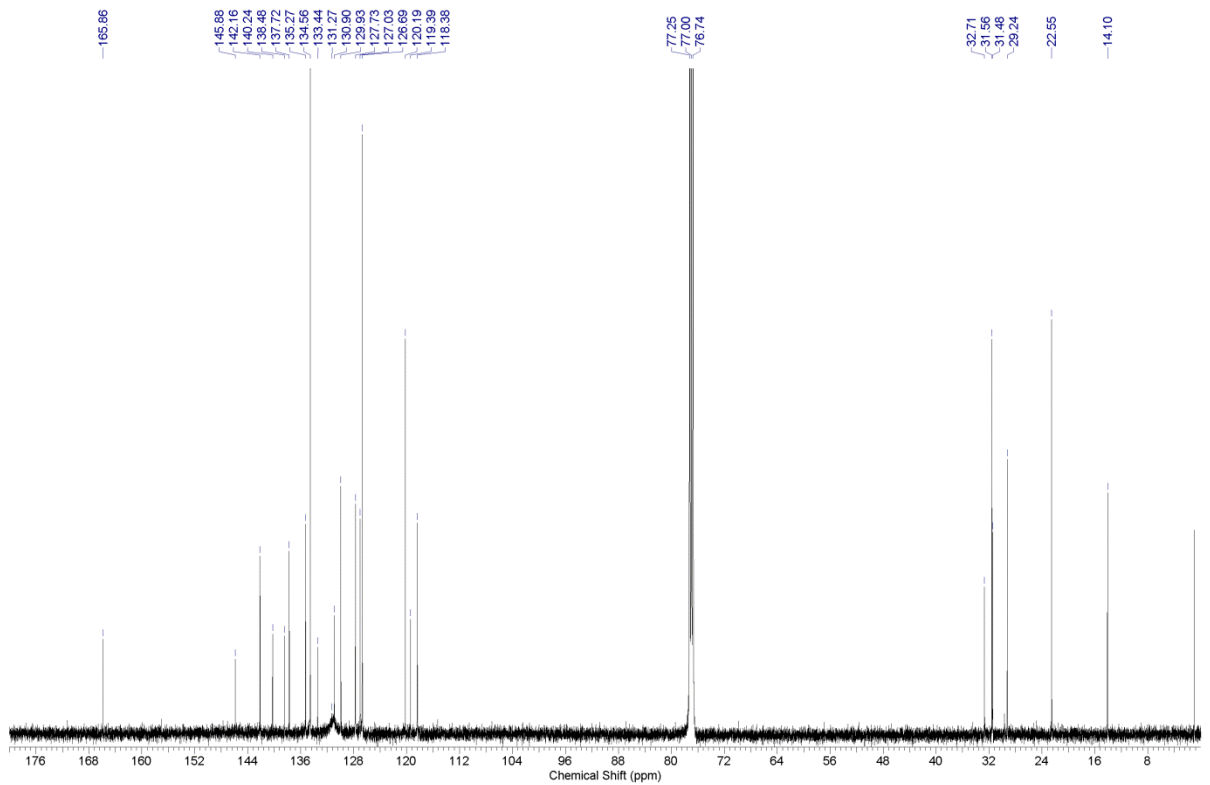


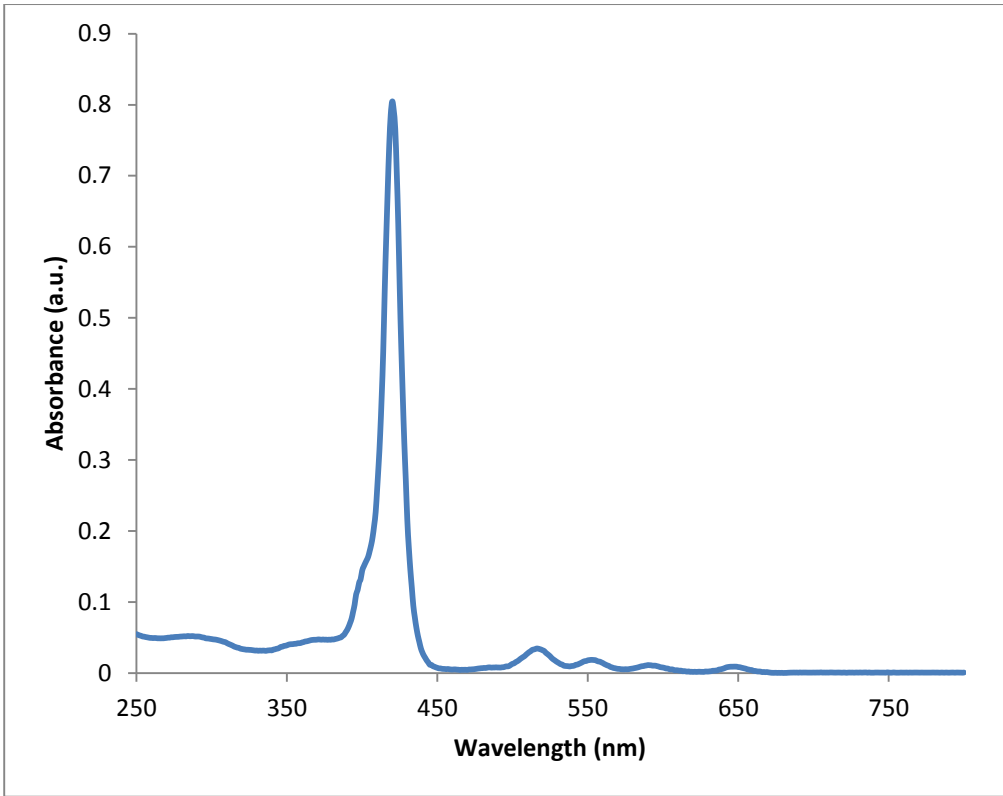


3phen diporphyrin ¹H NMR



3 phen diporphyrin ¹³C NMR





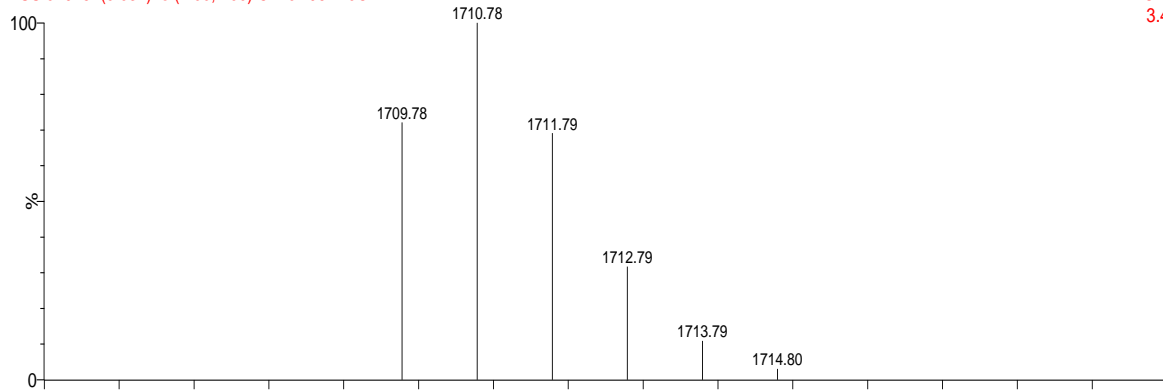
MSS 04945 [C120 H96 N10 O2]

MSS 04945 (0.031) Is (1.00,1.00) C120H96N10O2

MALDI

04-Sep-2008 08:54:25

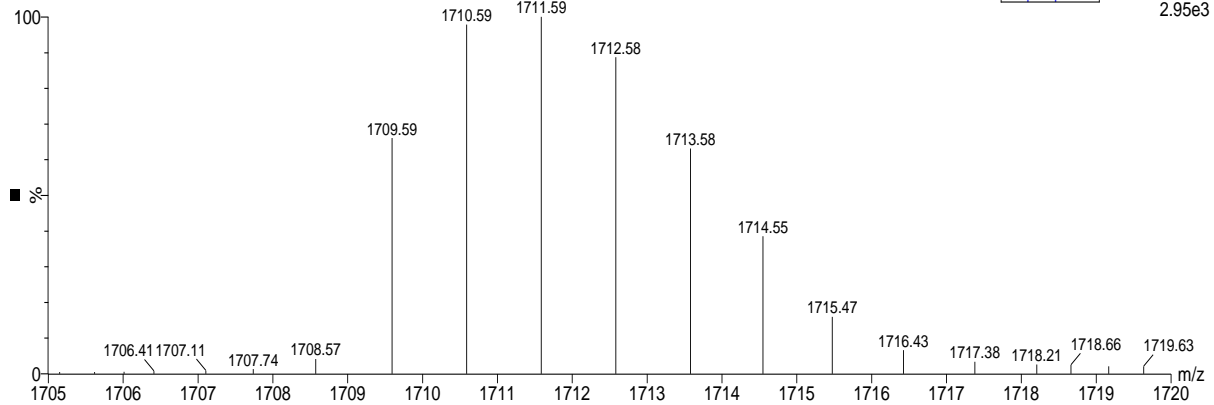
TOF LD+
3.48e12

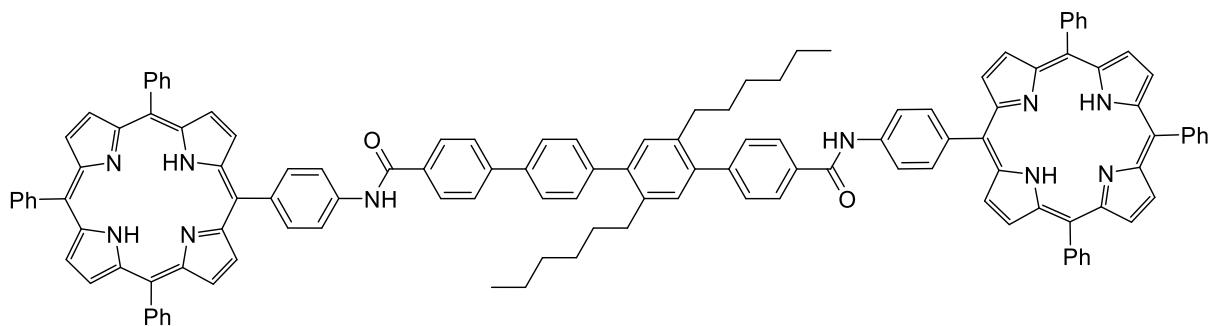


MSS 04945 4 (0.131) Cn (Cen,5, 50.00, Ht); Sm (SG, 2x5.00); Sb (99,1.00); Cm (3:5)

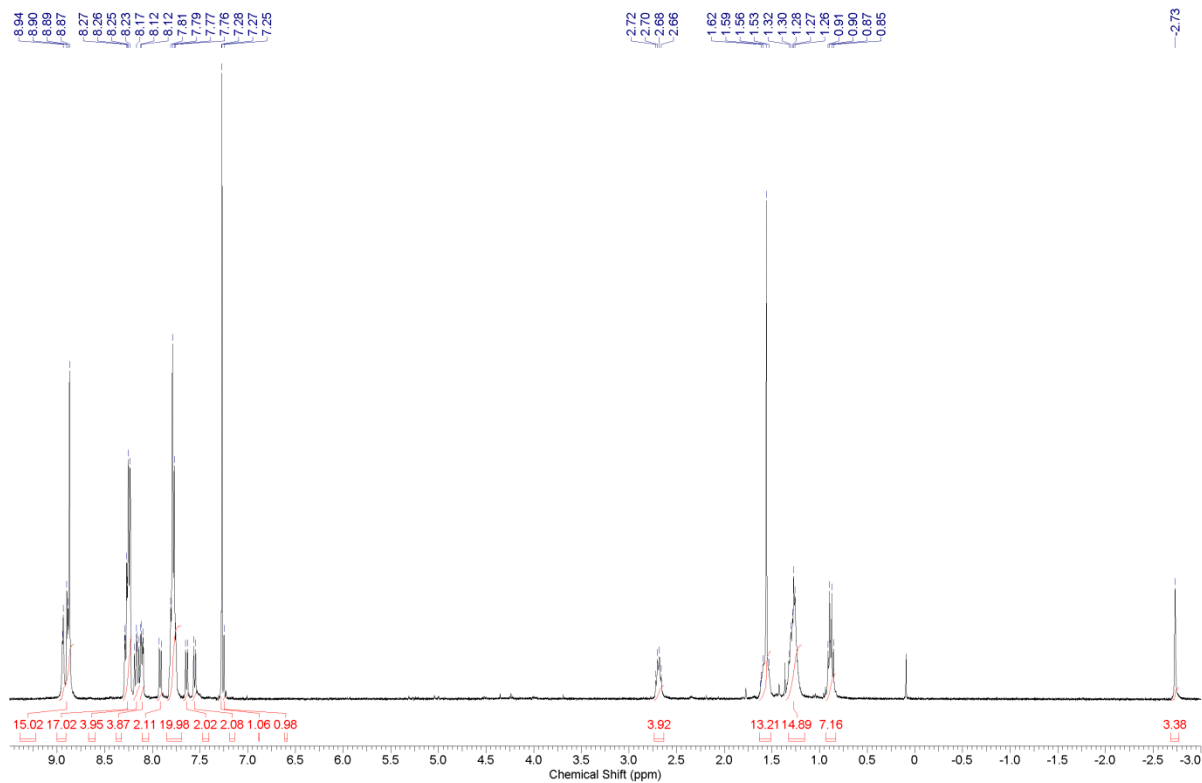
Sample Spectrum

TOF LD+
2.95e3

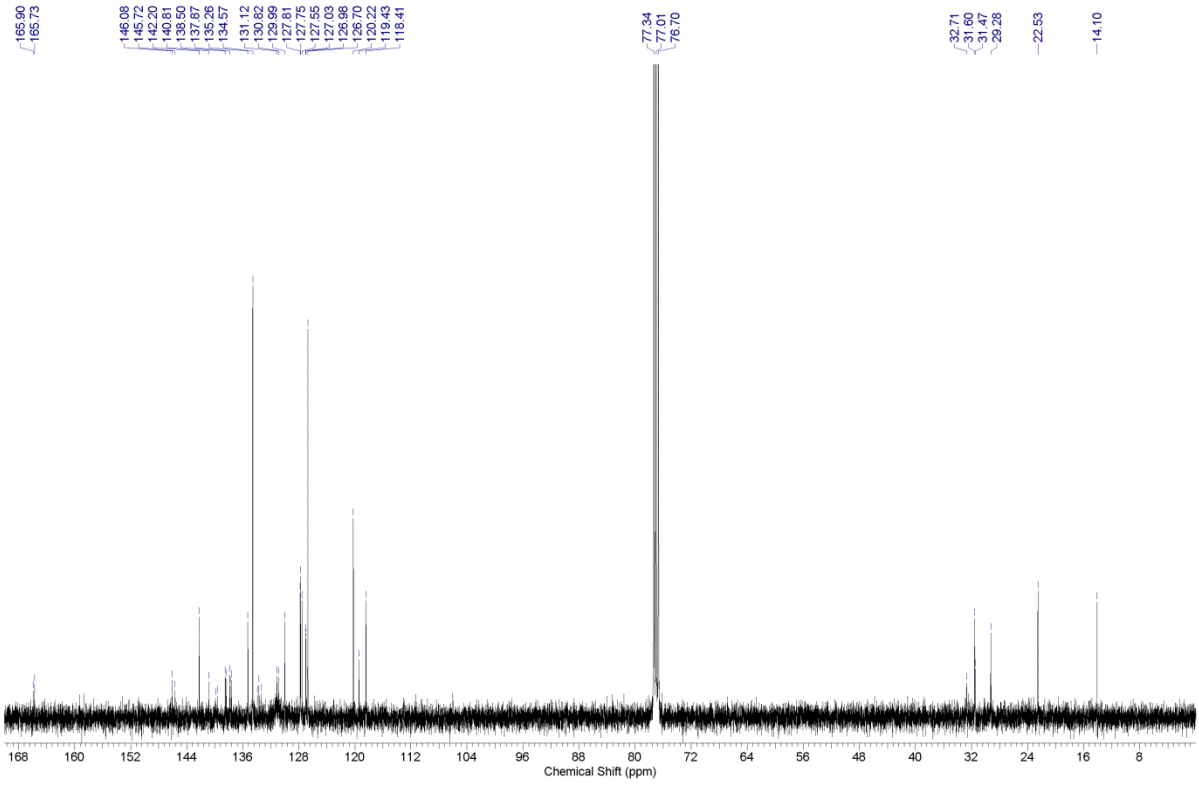




4 phenyl diporphyrin ¹H NMR



4 phenyl diporphyrin ¹³C NMR

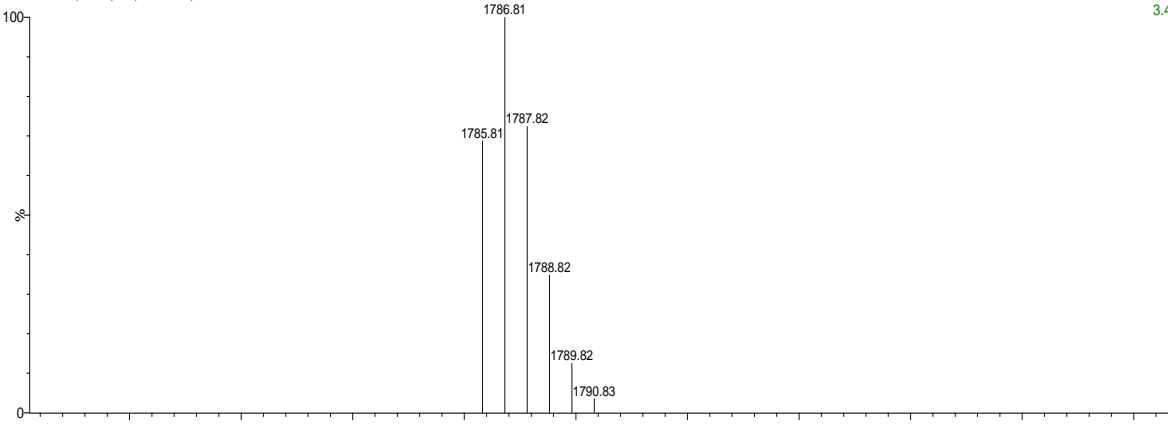


MSS 05644 [C126 H100 N10 O2]

MSS 05644 (0.031) ls (1.00,1.00) C126 H100 N10 O2

TOF LD+

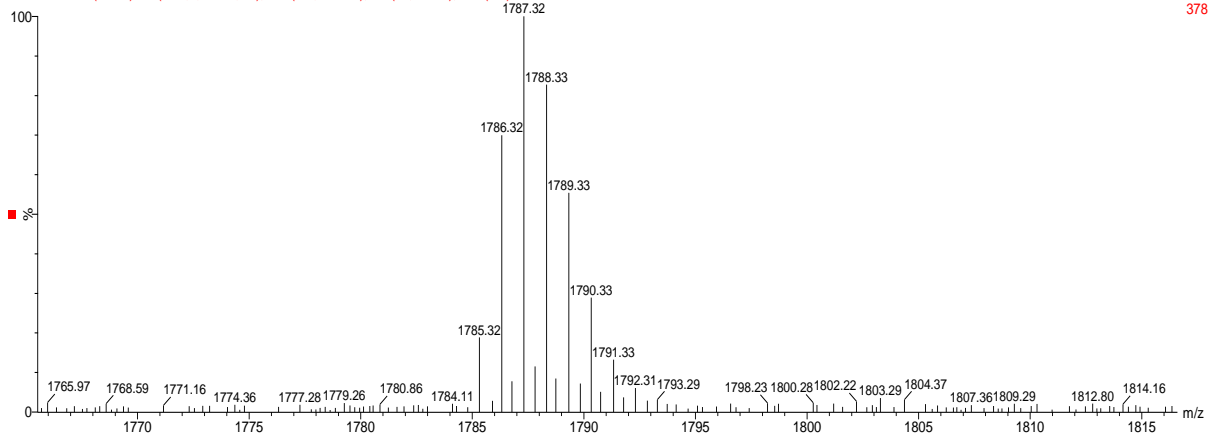
3.41e12

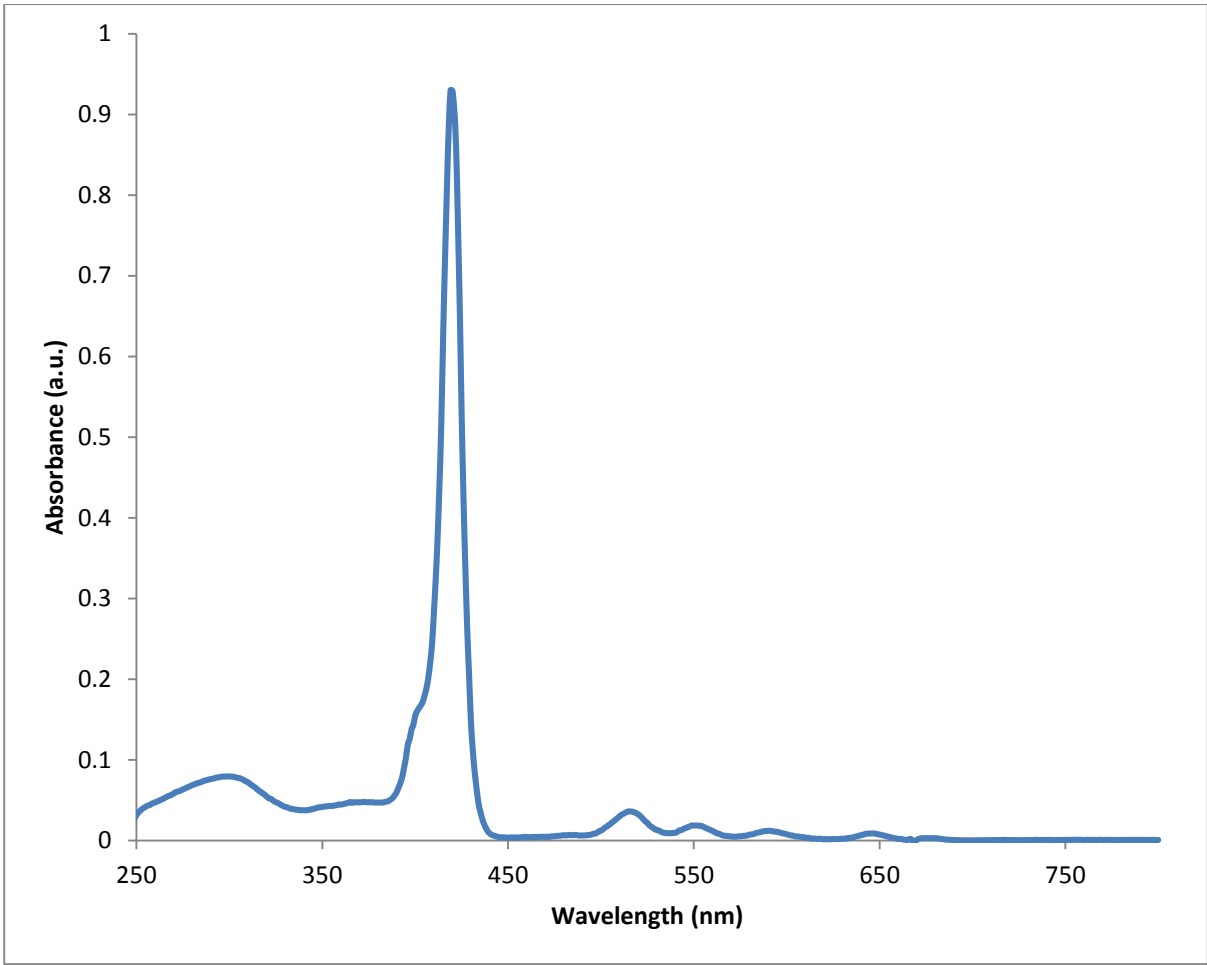


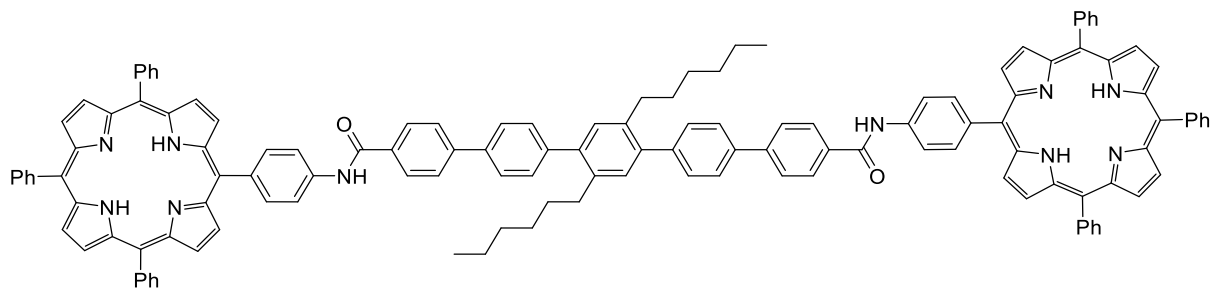
MSS 05644 4 (0.131) Cn (Cen,5, 50.00, Ht); Sm (SG, 2x3.00); Sb (99,10.00); Cm (3:4)

TOF LD+

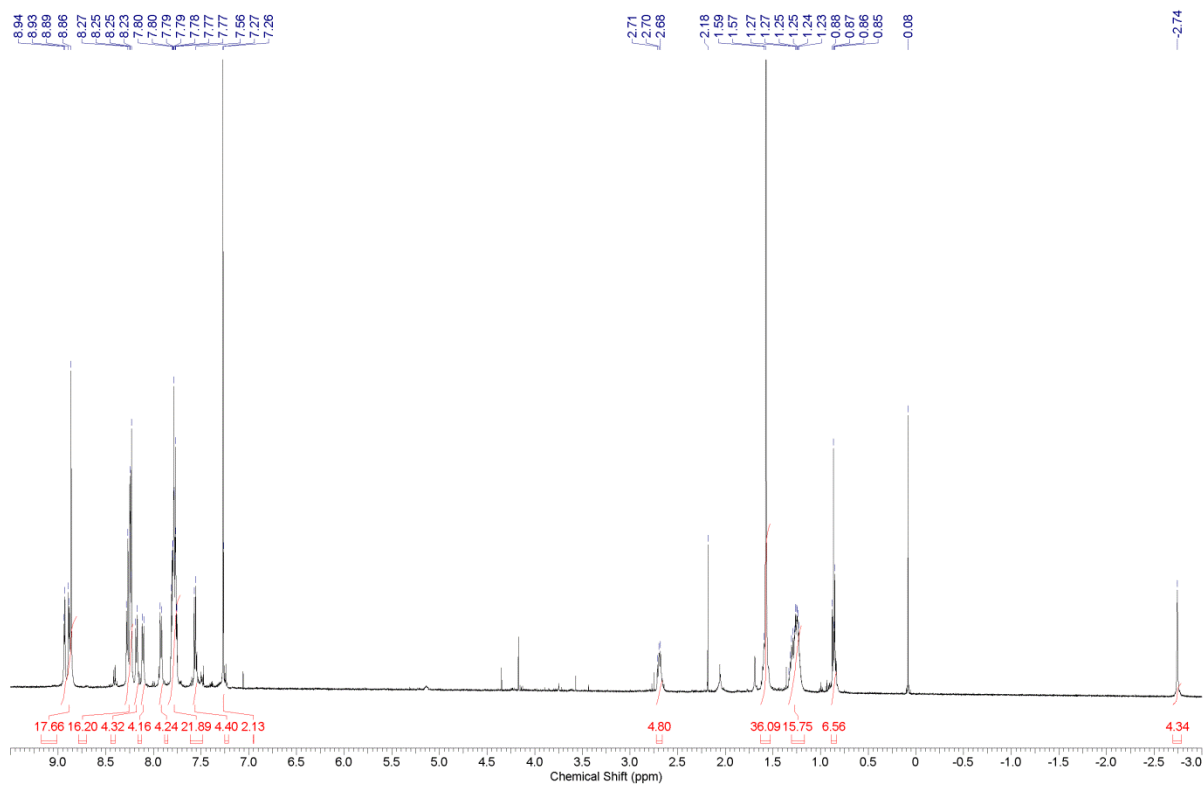
378



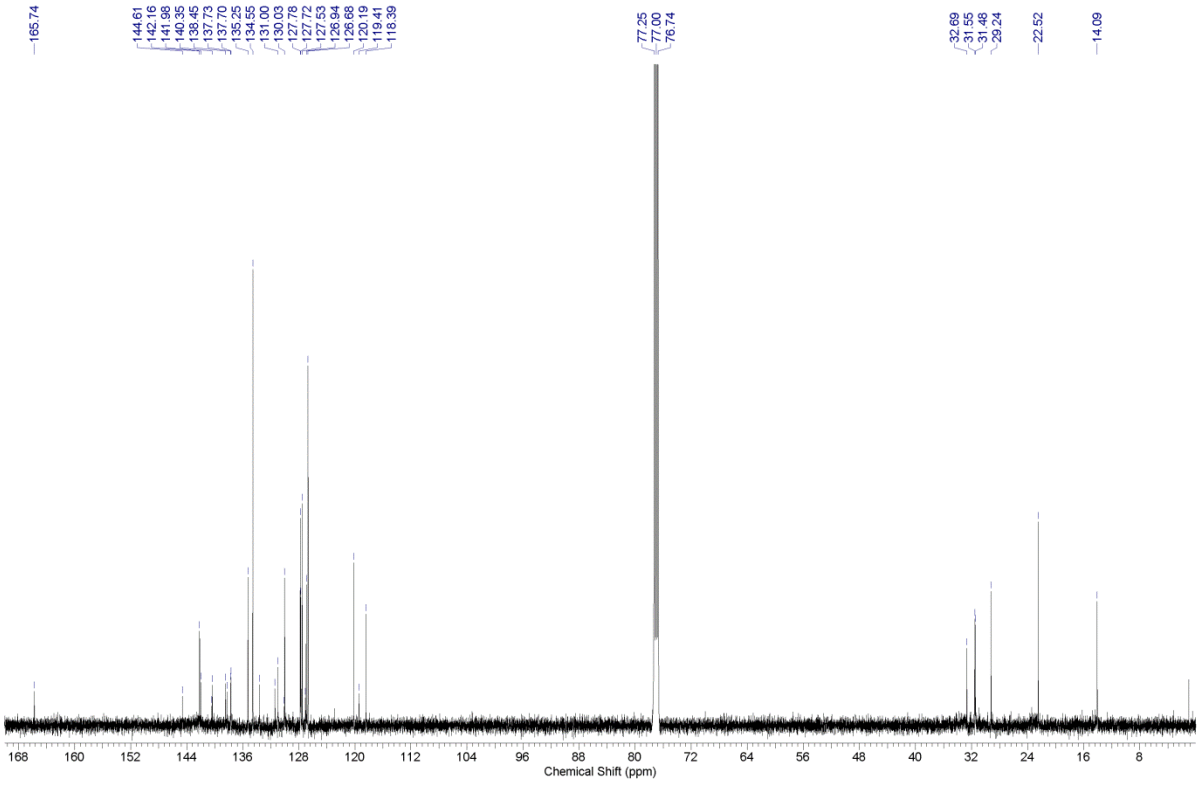




5 phenyl diporphyrin ^1H NMR



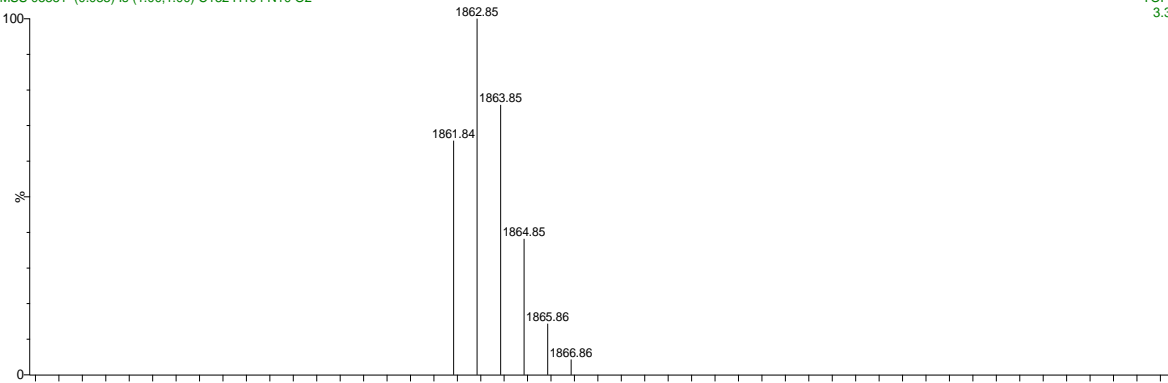
5 phenyl diporphyrin ¹³C NMR



MSS 05351 [C132 H104 N10 O2]

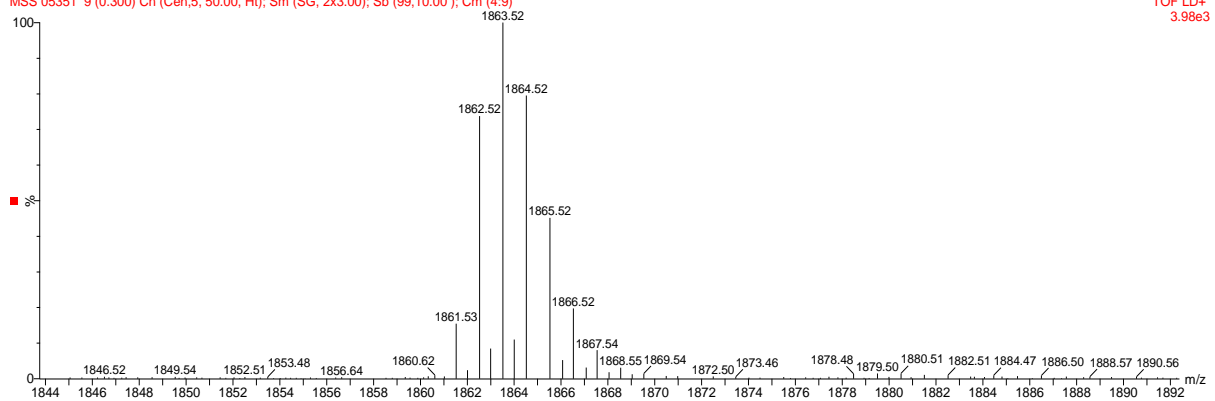
MSS 05351 (0.033) Is (1.00,1.00) C132 H104 N10 O2

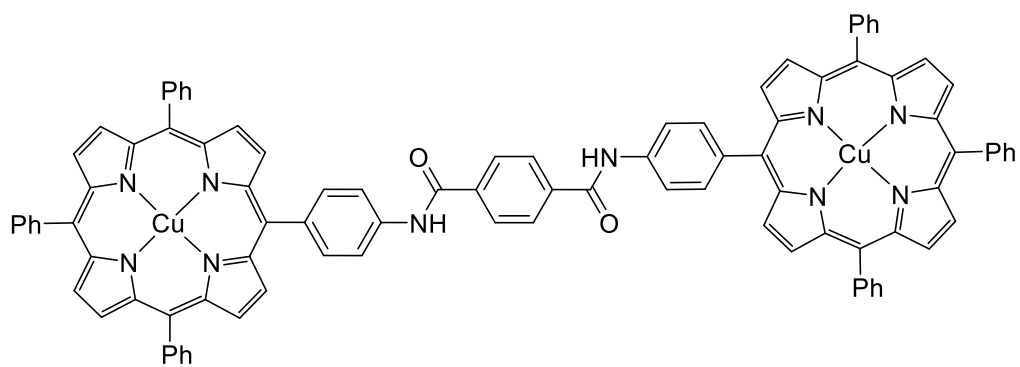
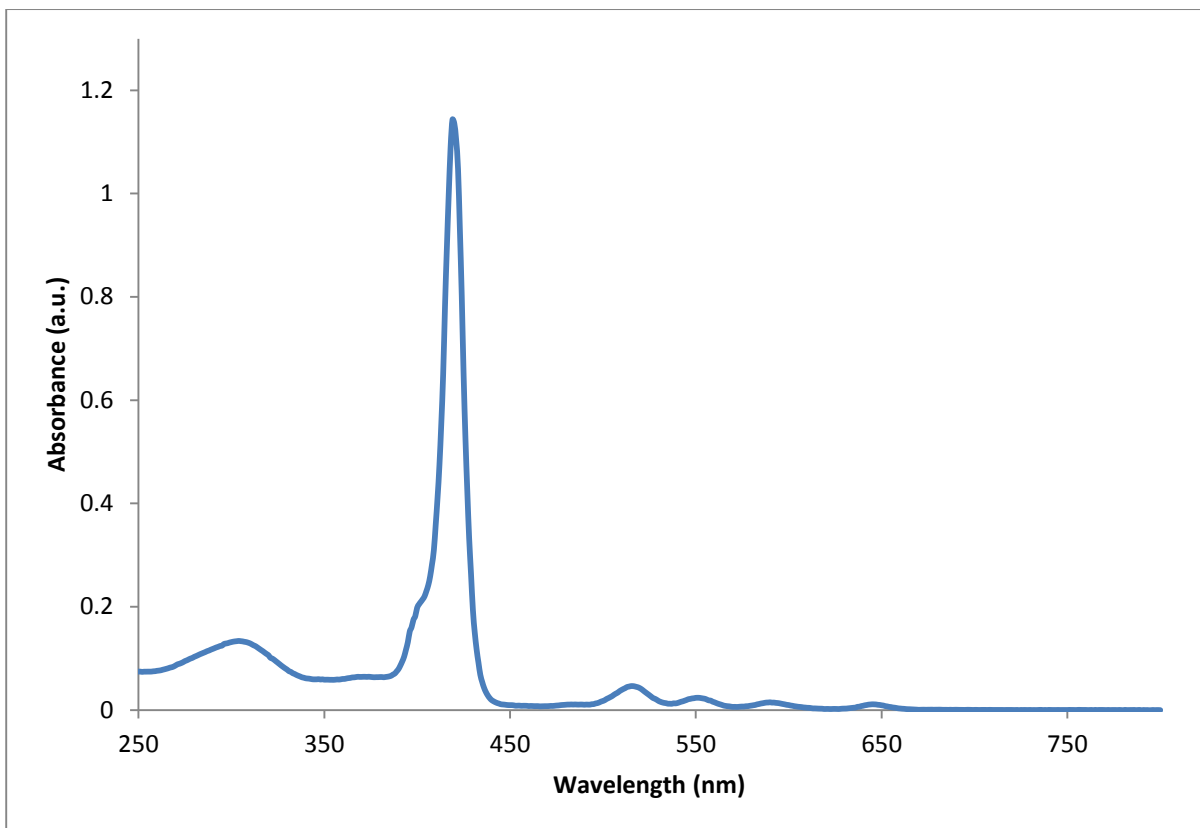
TOF LD+
3.34e12



MSS 05351 9 (0.300) Cn (Cen.5, 50.00, Ht); Sm (SG, 2x3.00); Sb (99,10.00); Cm (4:9)

TOF LD+
3.98e3

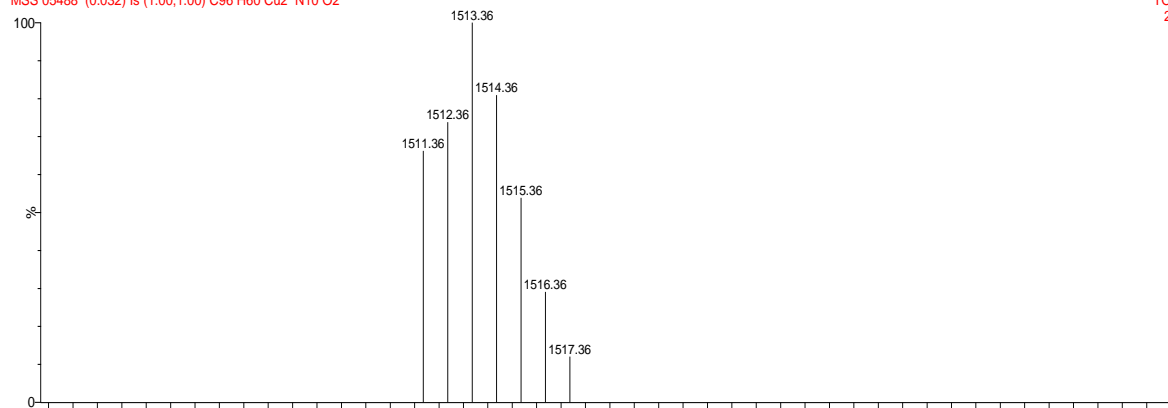




MSS 05488 [C96 H60 Cu2 N10 O2]

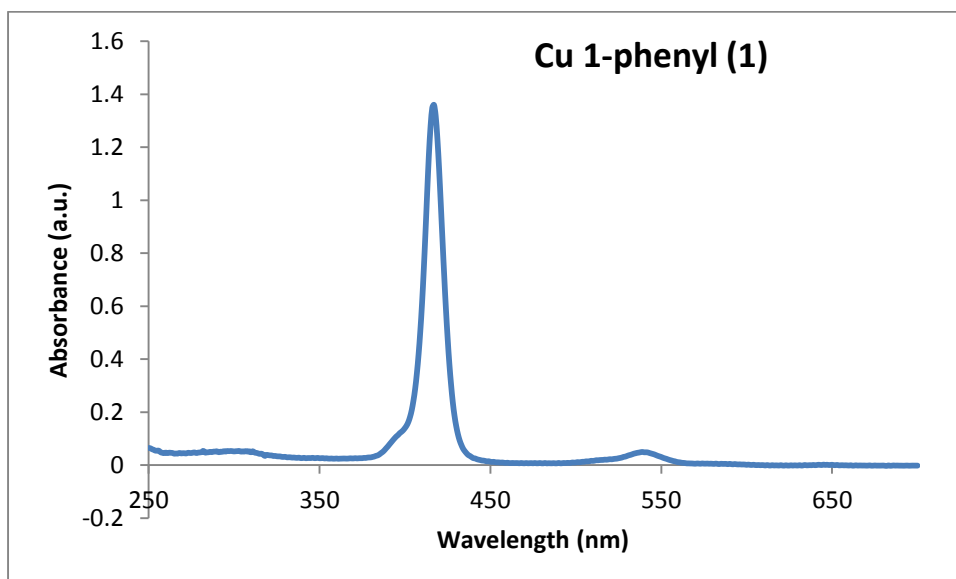
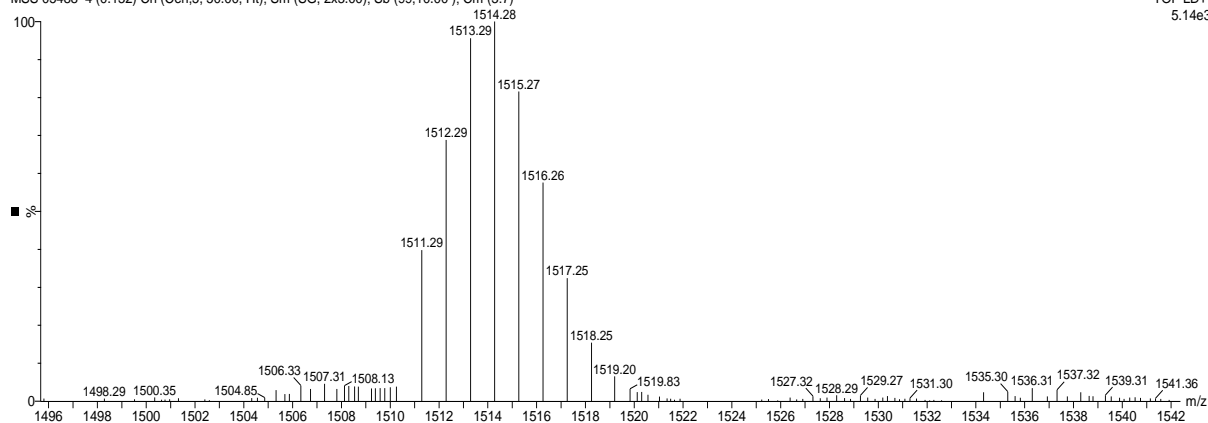
MSS 05488 (0.032) Is (1.00,1.00) C96 H60 Cu2 N10 O2

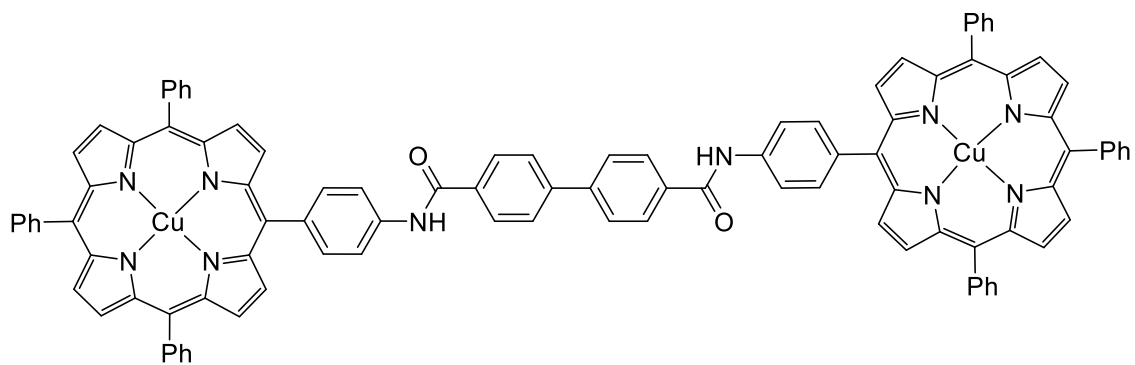
TOF LD+
2.38e12



MSS 05488 4 (0.132) Cn (Cen,5, 50.00, Ht); Sm (SG, 2x3.00); Sb (99,10.00); Cm (3:7)

TOF LD+
5.14e3

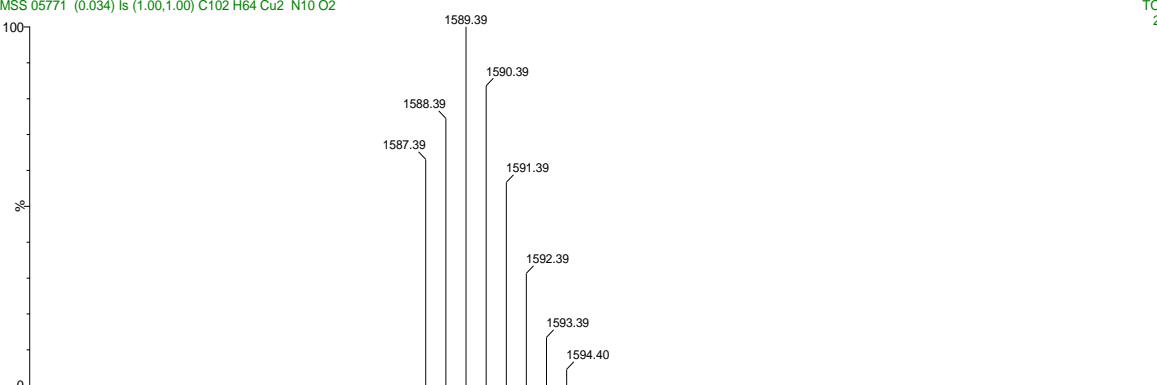




MSS 05771 [C102 H64 Cu2 N10 O2]

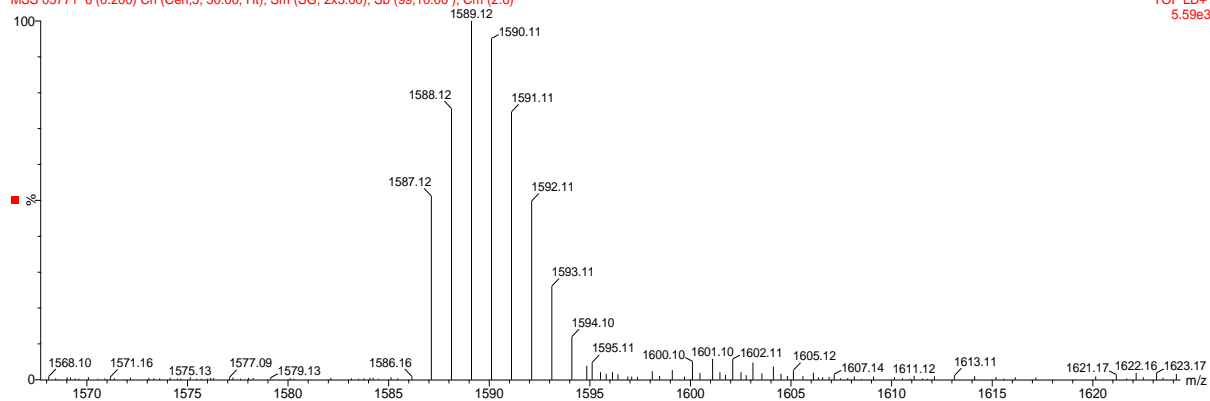
MSS 05771 (0.034) Is (1.00,1.00) C102 H64 Cu2 N10 O2

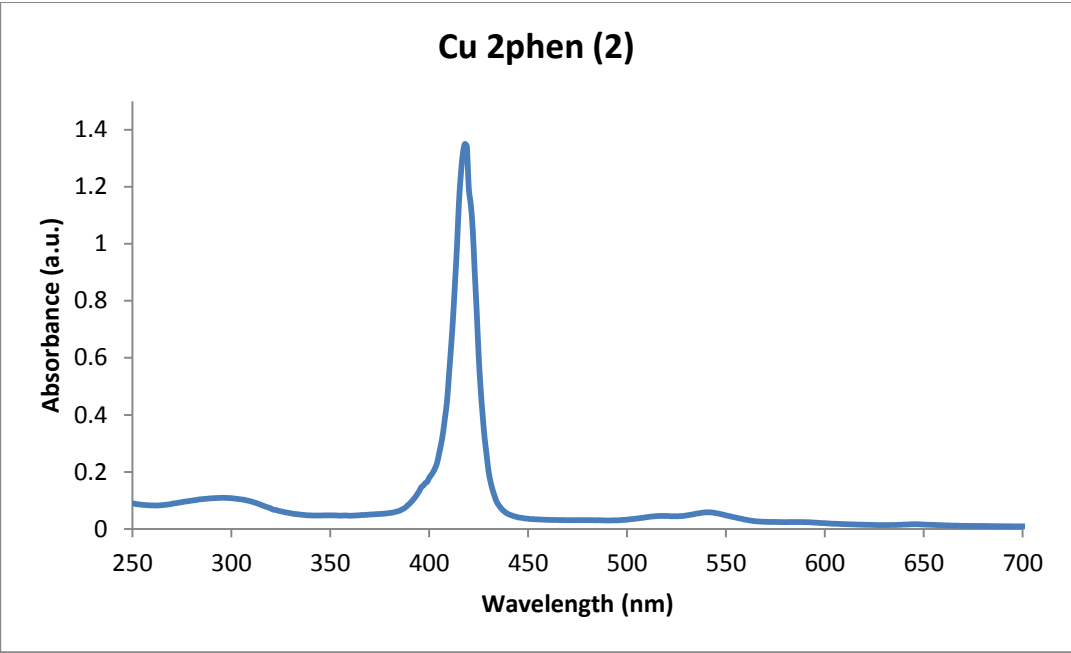
TOF LD+
2.34e12

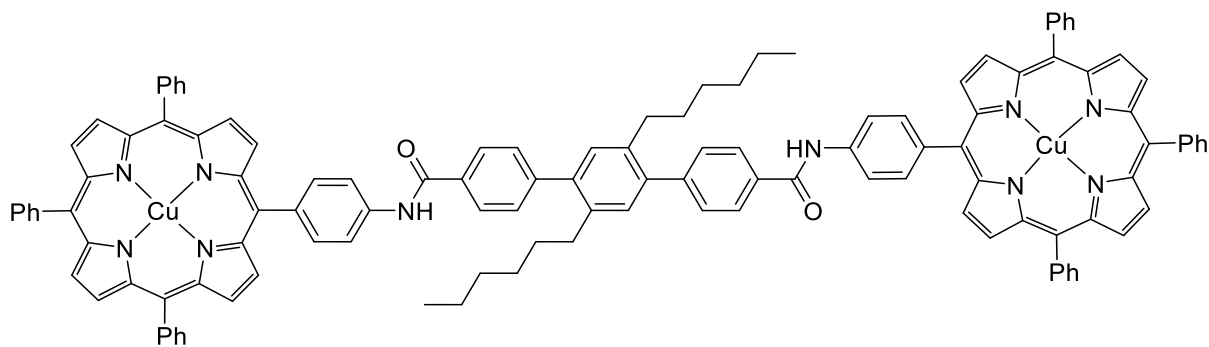


MSS 05771 6 (0.200) Cn (Cen,5, 50.00, Ht); Sm (SG, 2x3.00); Sb (99,10.00); Cm (2:6)

TOF LD+
5.59e3







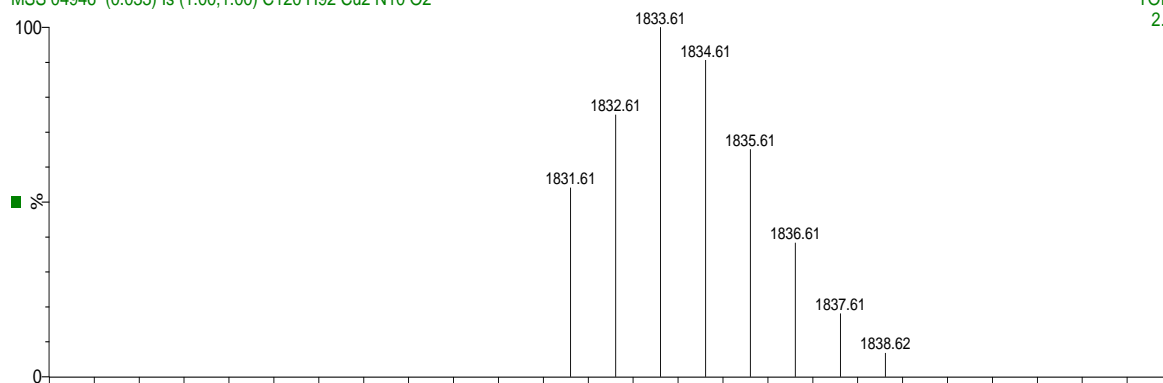
MSS 04946 [C120 H92 Cu2 N10 O2]

MALDI

04-Sep-2008 08:58:05

MSS 04946 (0.033) Is (1.00,1.00) C120 H92 Cu2 N10 O2

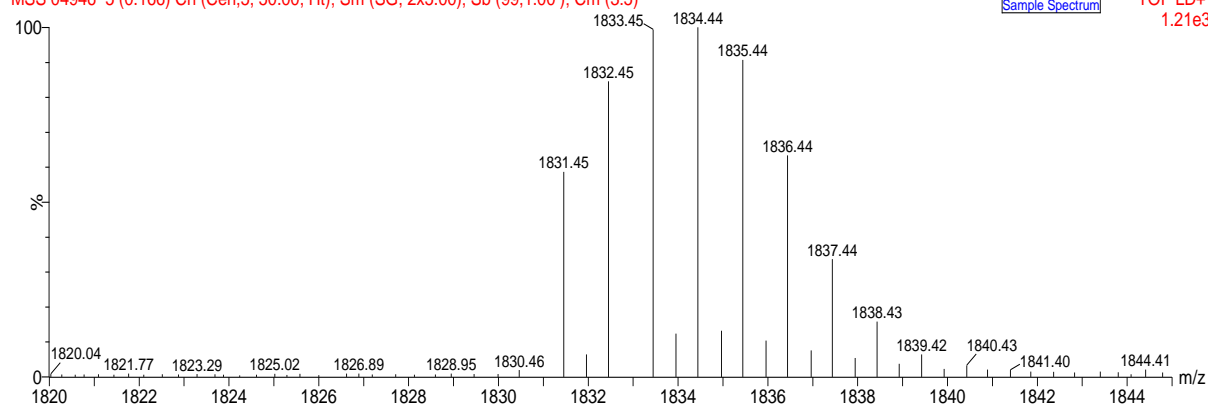
TOF LD+
2.22e12

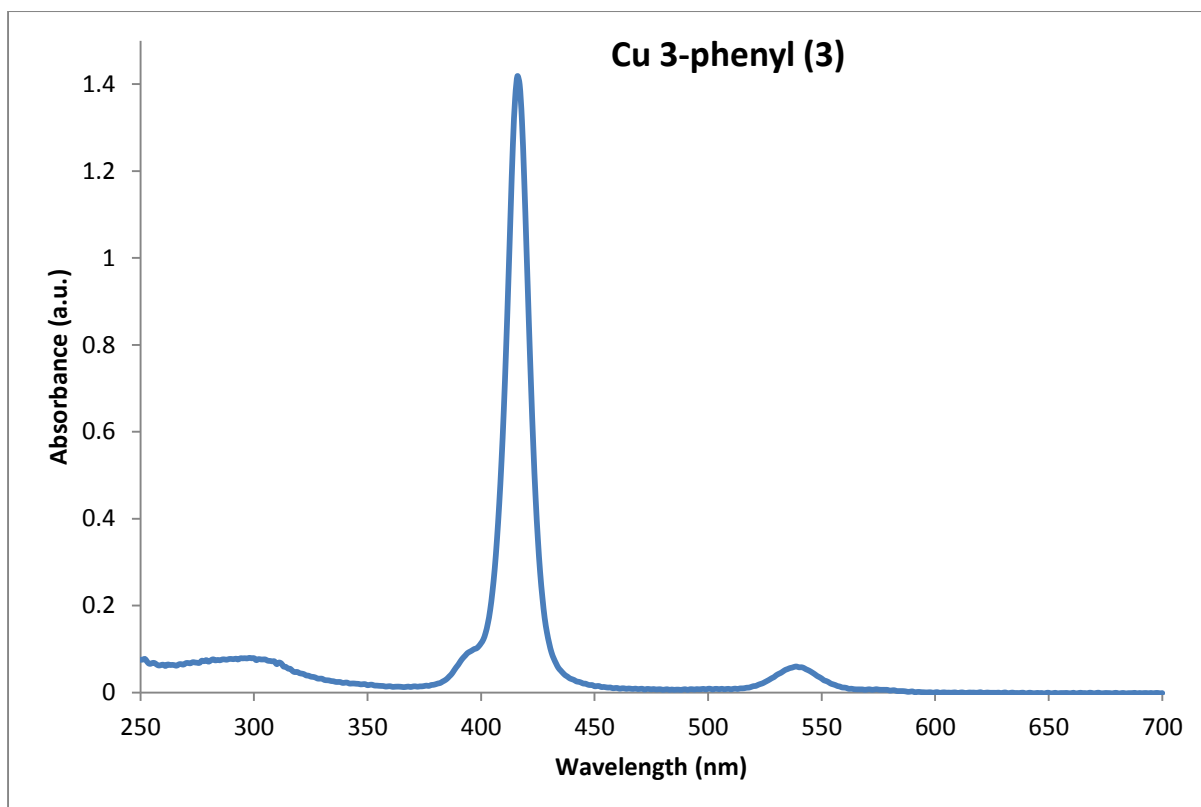


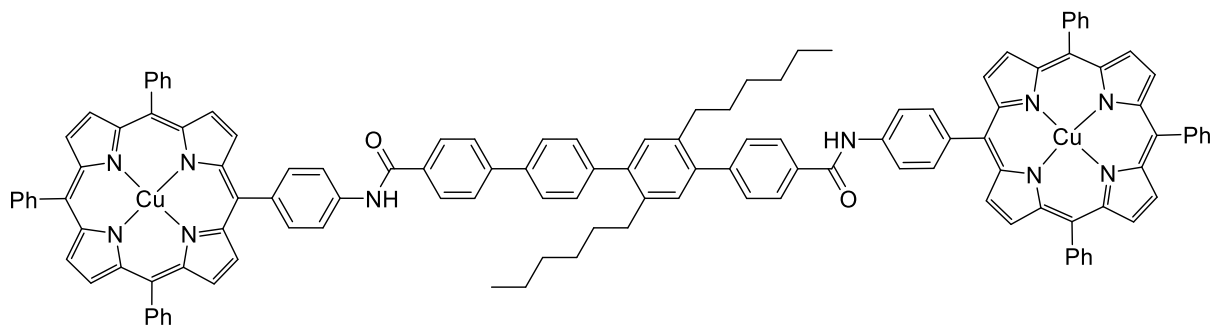
MSS 04946 5 (0.166) Cn (Cen,5, 50.00, Ht); Sm (SG, 2x5.00); Sb (99,1.00); Cm (3:5)

Sample Spectrum

TOF LD+
1.21e3



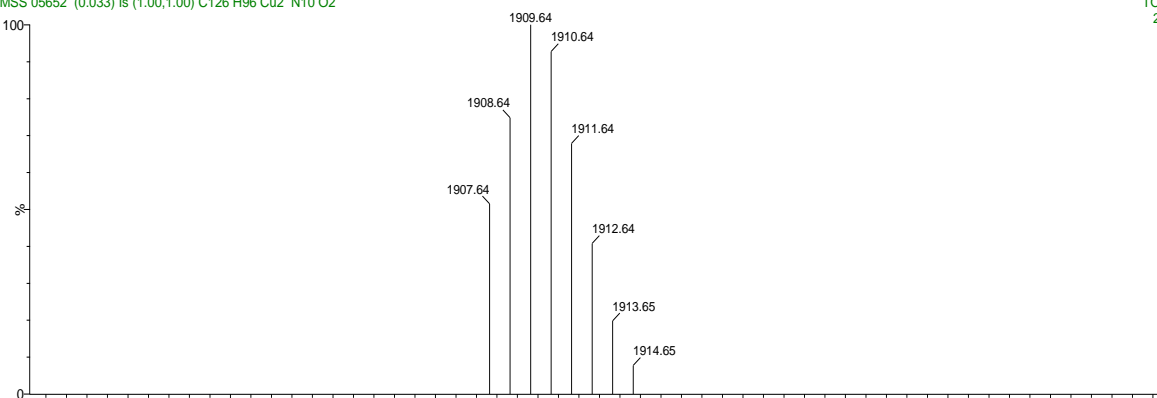




MSS 05652 [C126 H96 Cu2 N10 O2]

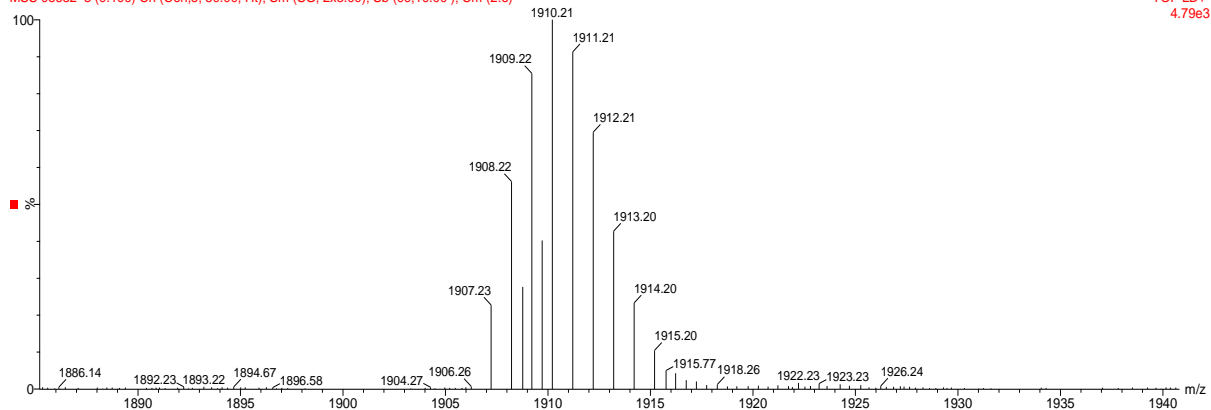
MSS 05652 (0.033) Is (1.00,1.00) C126 H96 Cu2 N10 O2

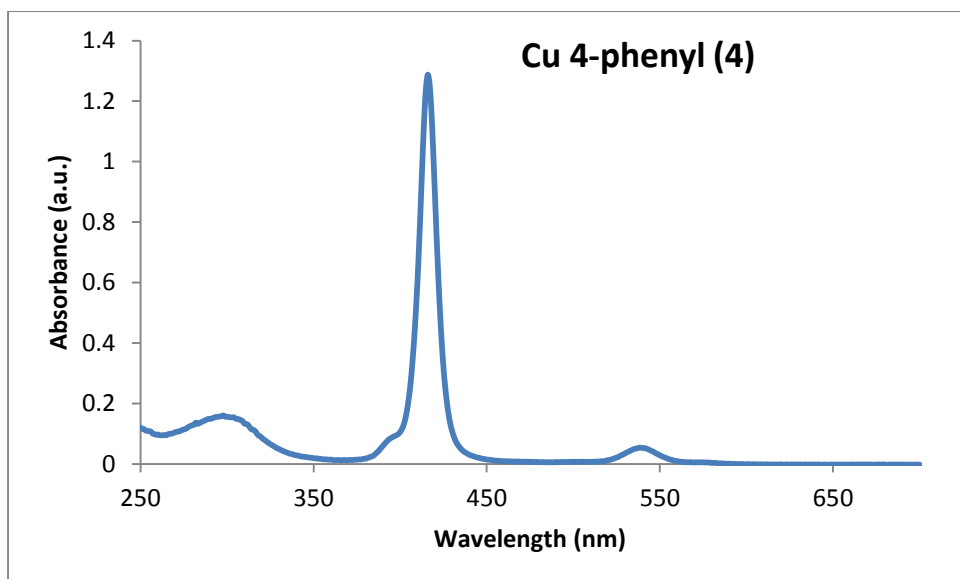
TOF LD+
2.18e12

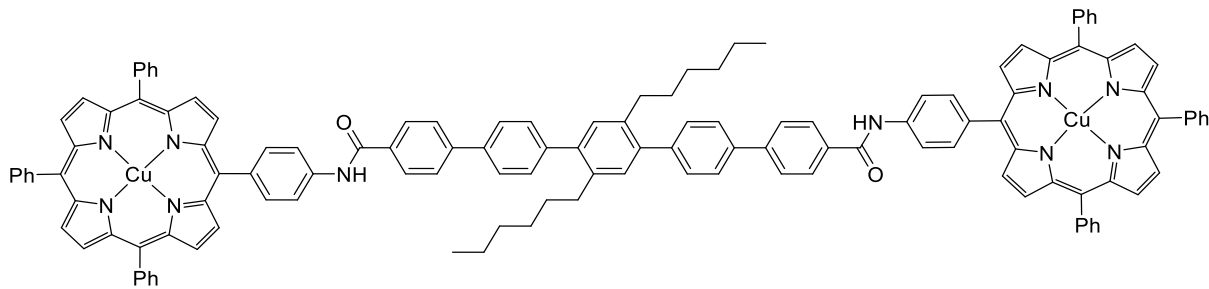


MSS 05652 3 (0.100) Cn (Cen,5, 50.00, Ht); Sm (SG, 2x3.00); Sb (99,10.00); Cm (2:6)

TOF LD+
4.79e3



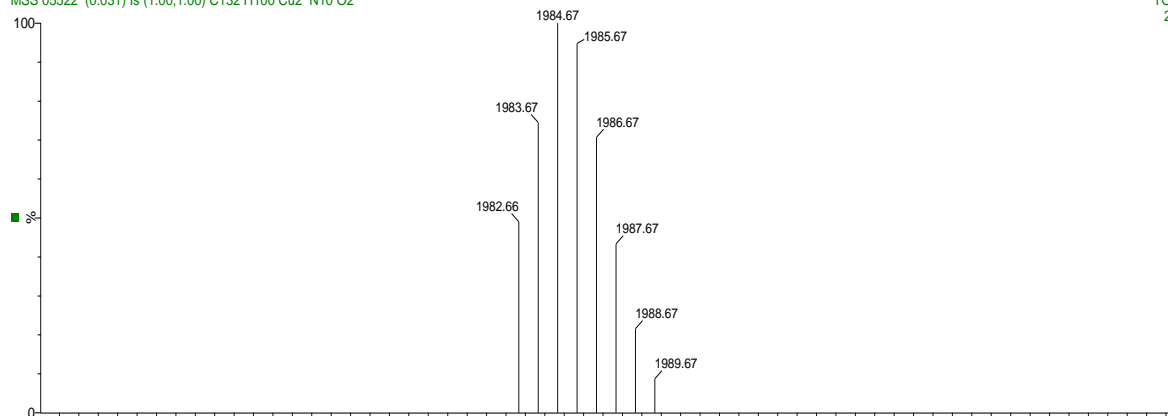




MSS 05522 [C132 H100 Cu2 N10 O2]

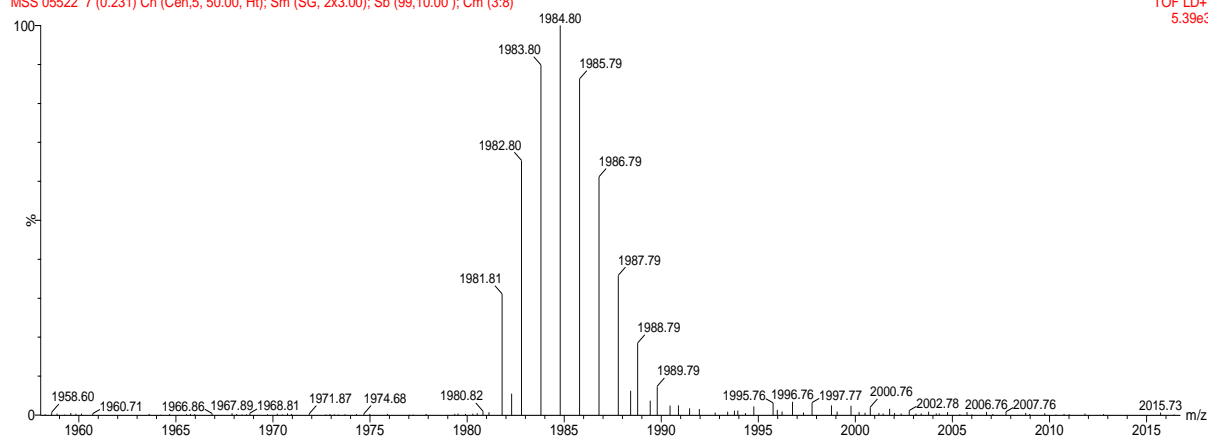
MSS 05522 (0.031) Is (1.00,1.00) C132 H100 Cu2 N10 O2

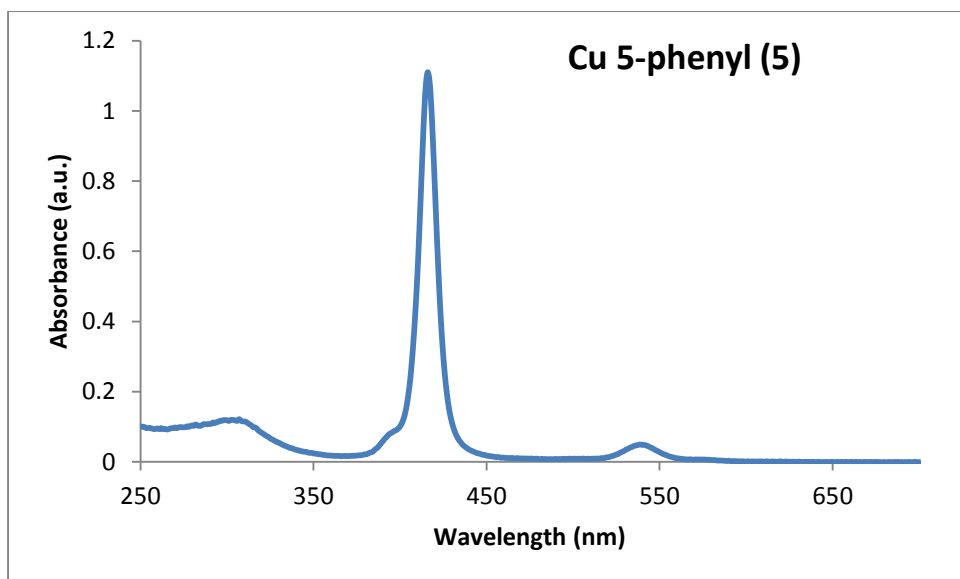
TOF LD+
2.15e12

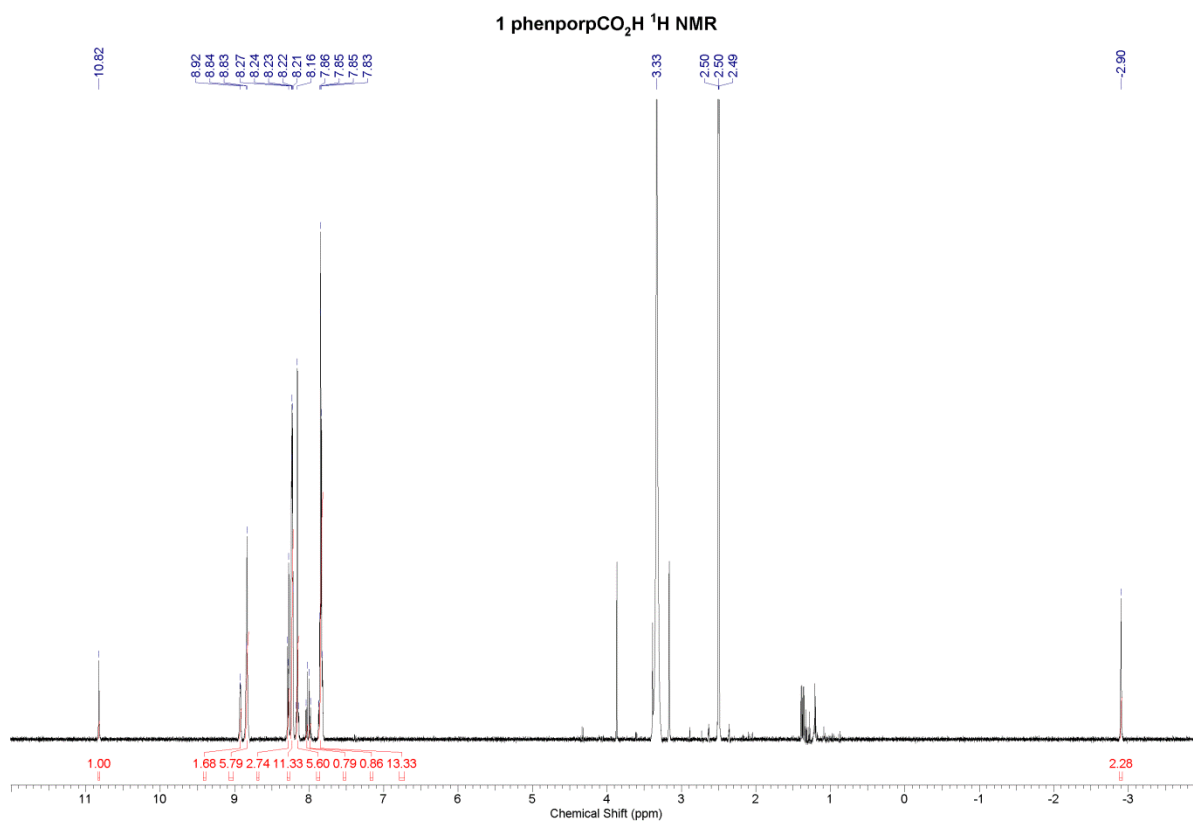
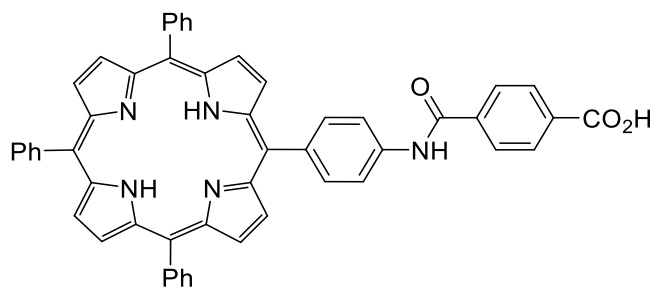


MSS 05522 7 (0.231) Cn (Cen,5, 50.00, Ht); Sm (SG, 2x3.00); Sb (99,10.00); Cm (3:8)

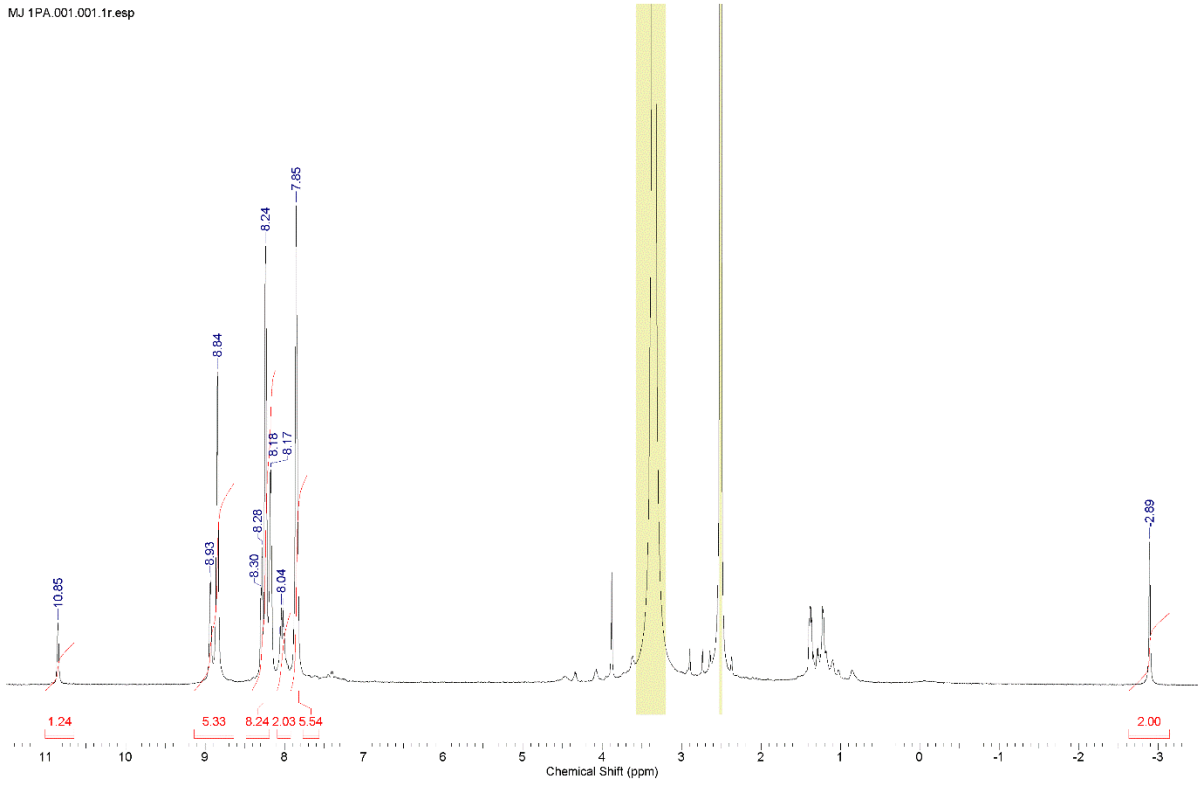
TOF LD+
5.39e3



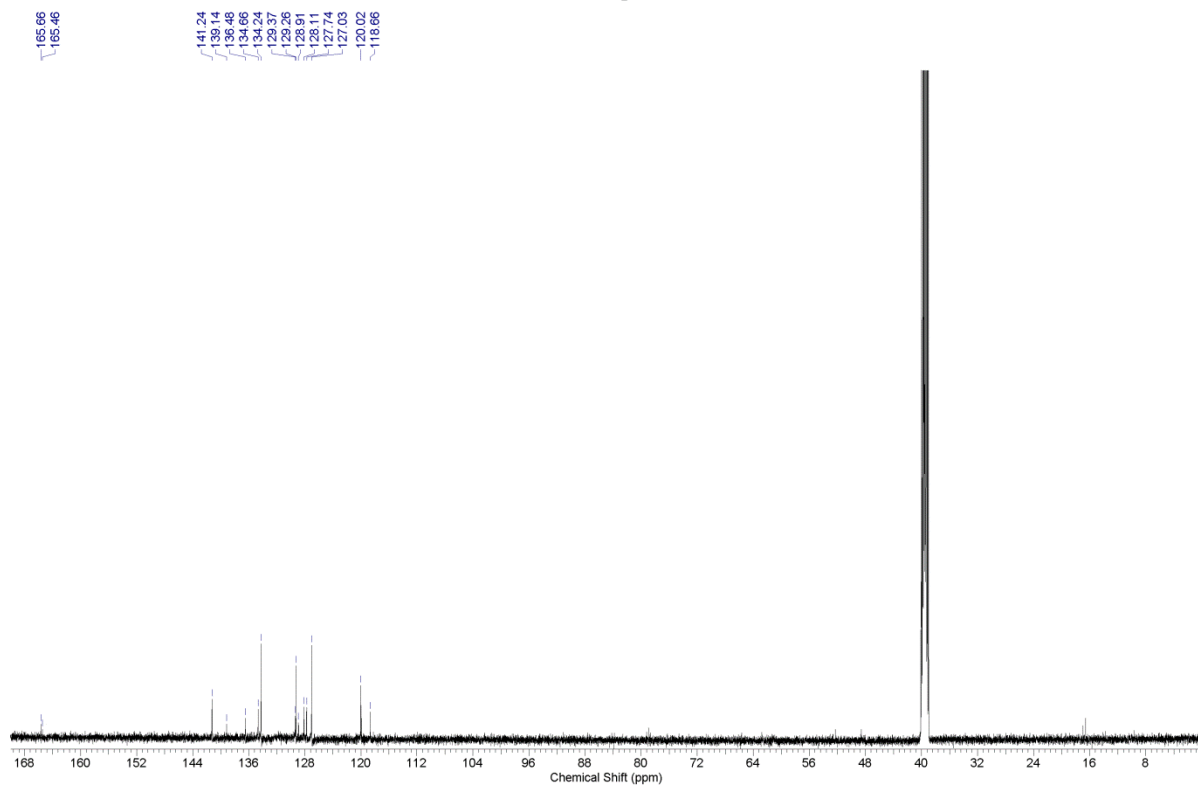


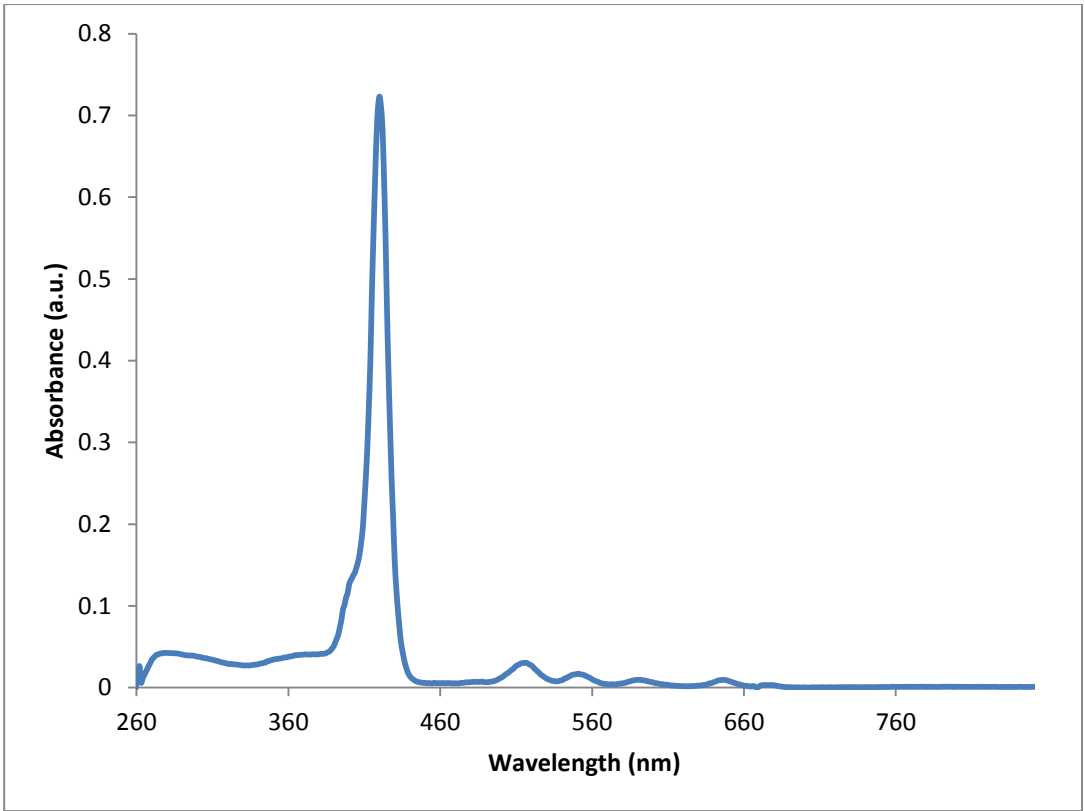


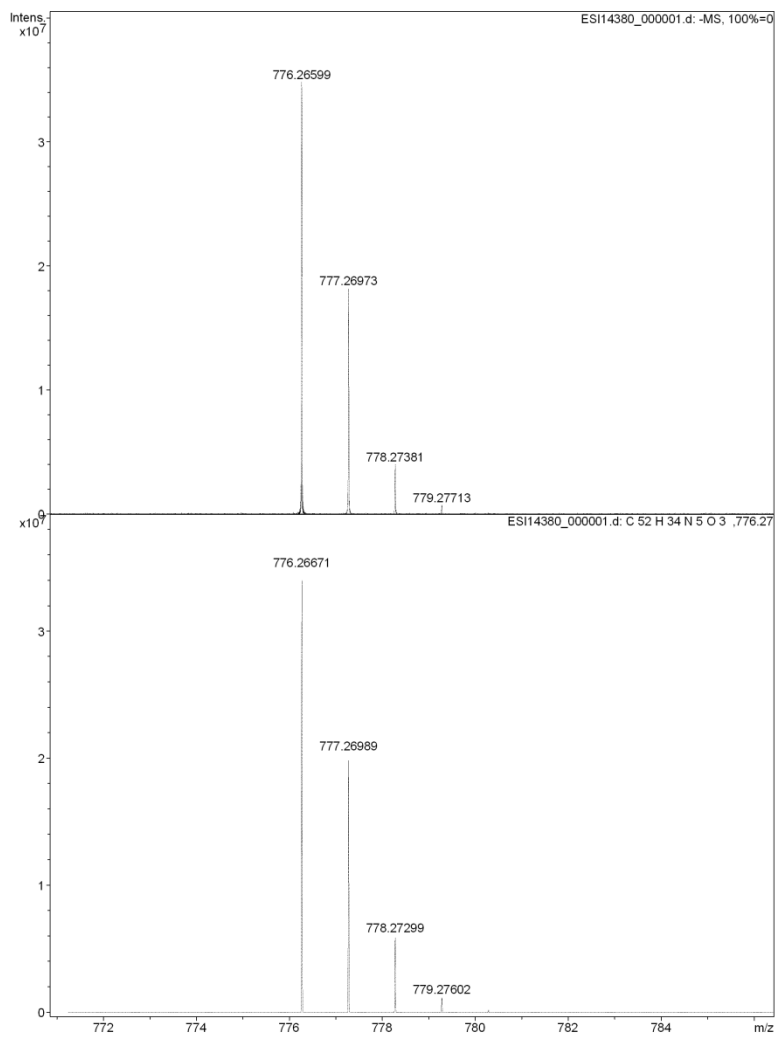
1phen acid

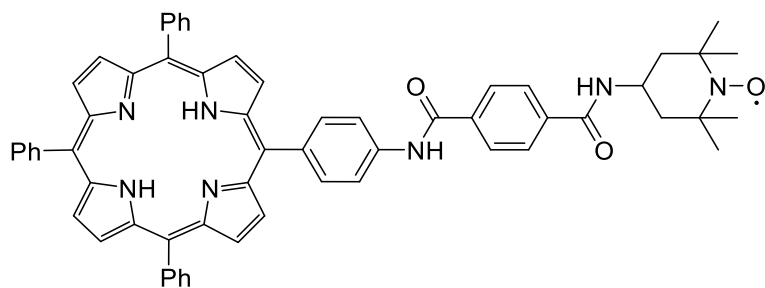


1 phenporpCO₂H ¹³C NMR

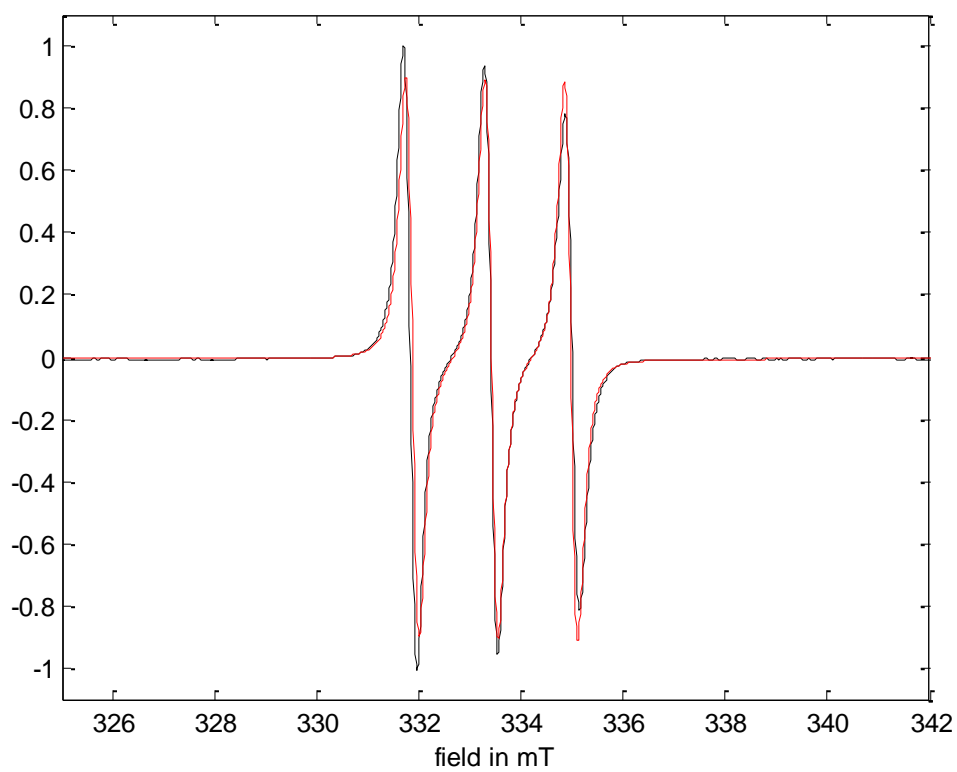


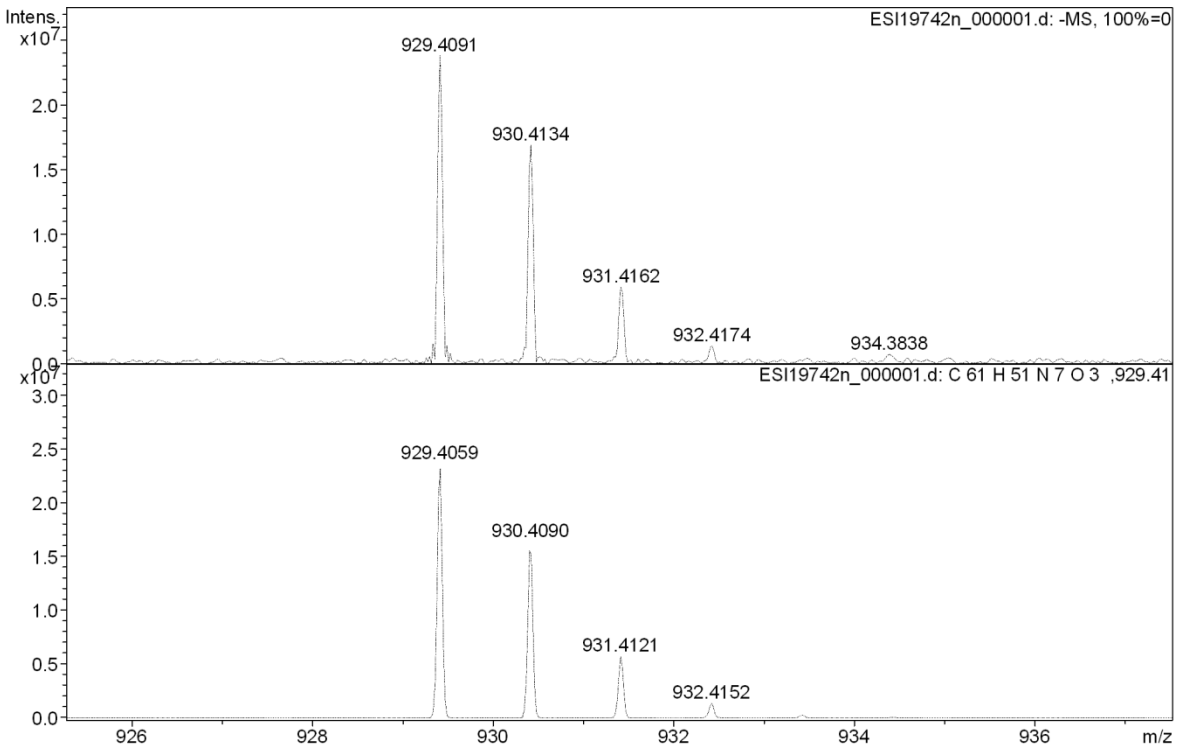
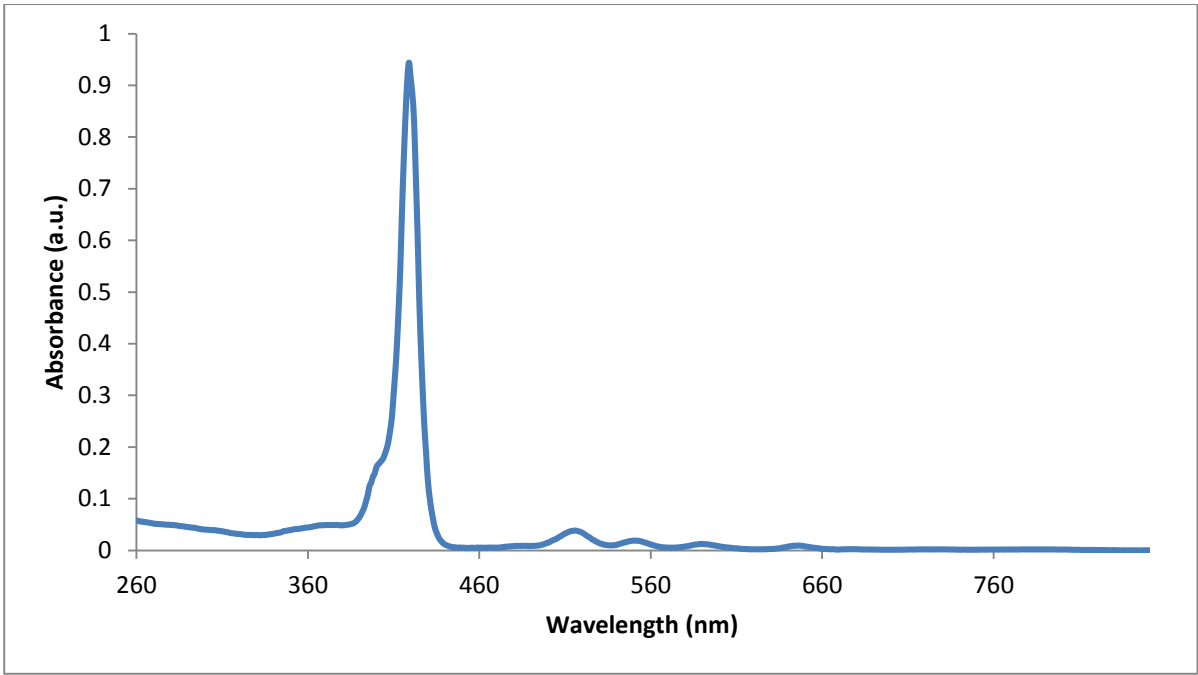


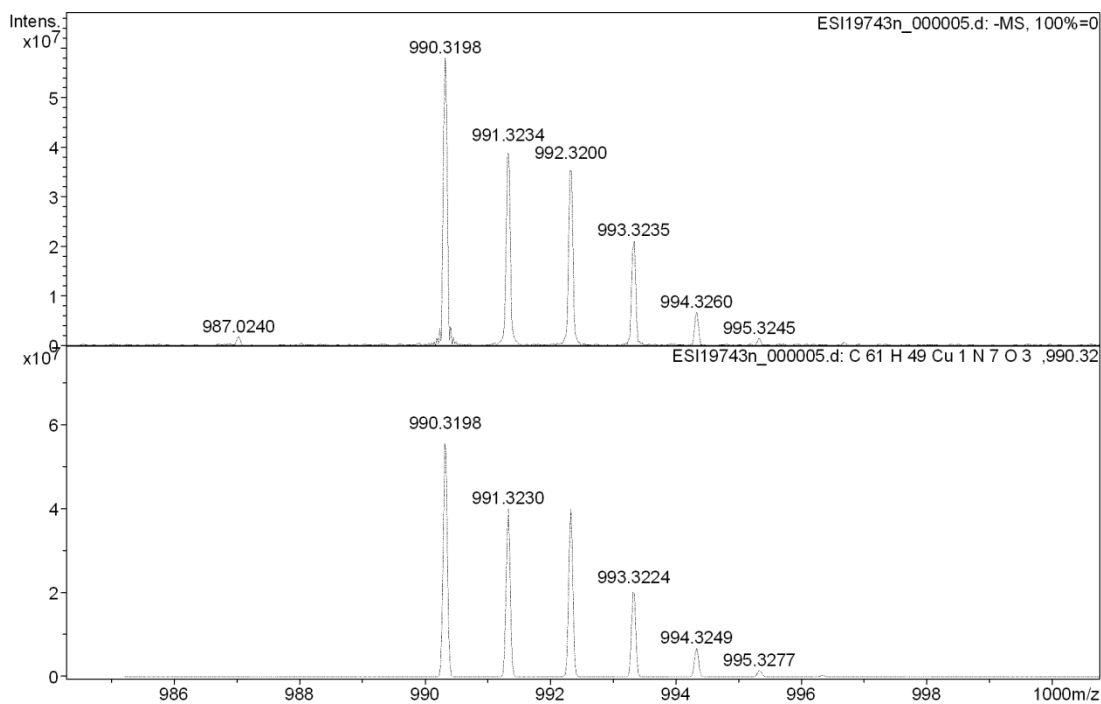
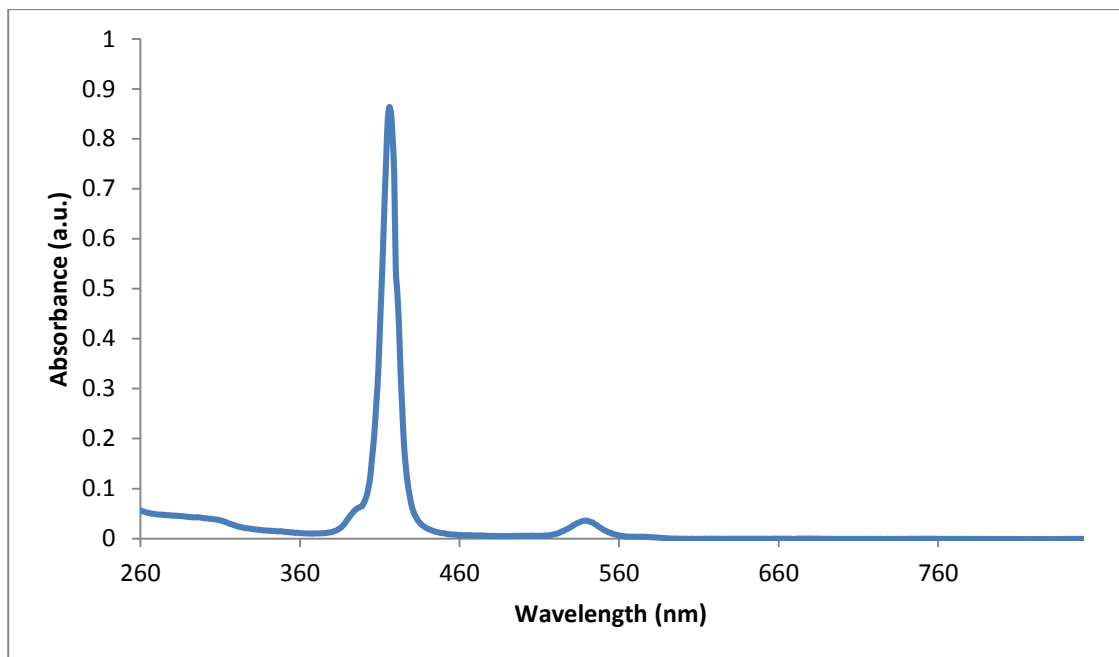
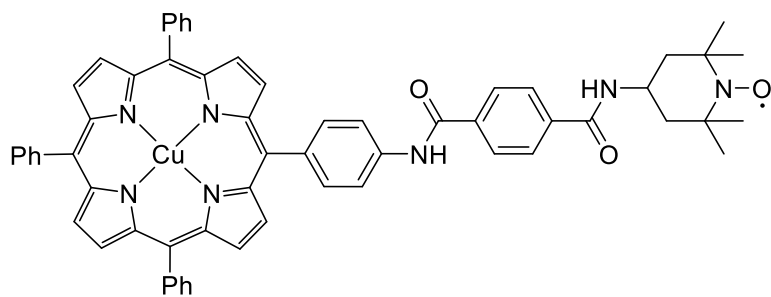


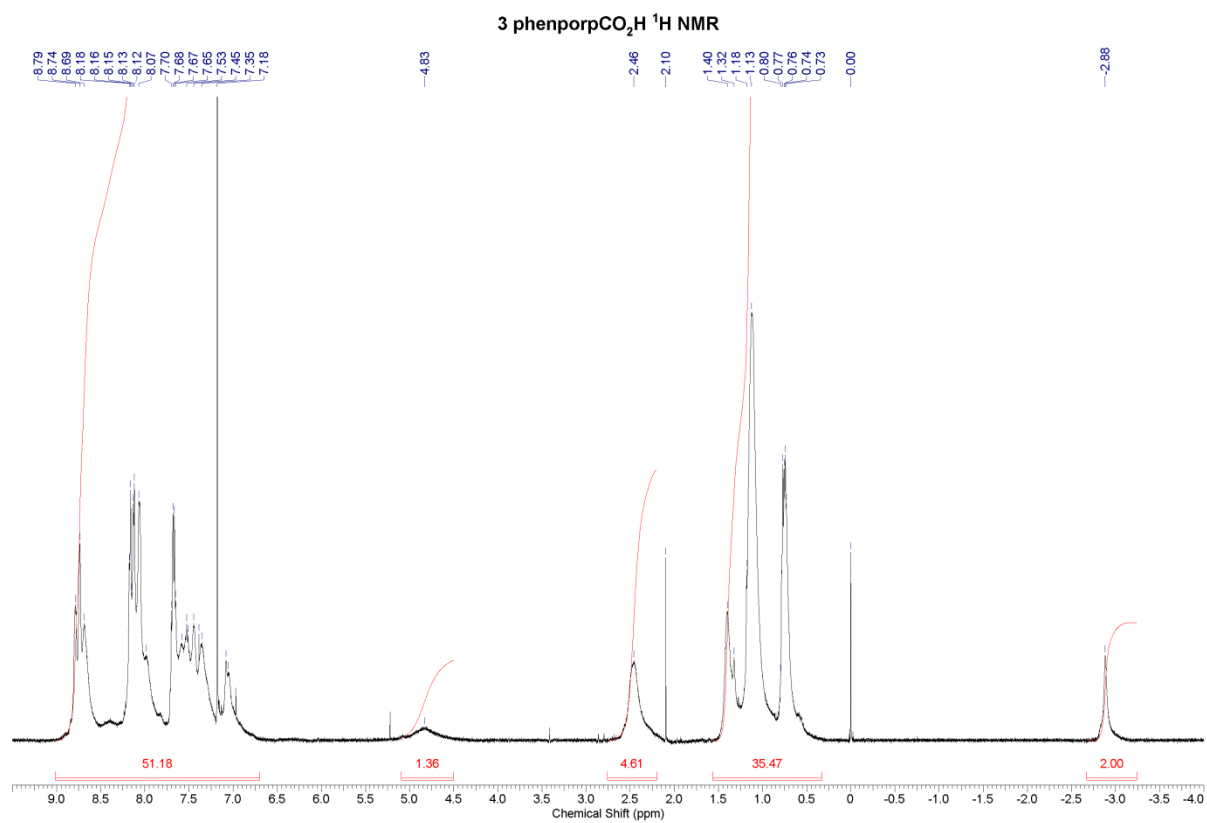
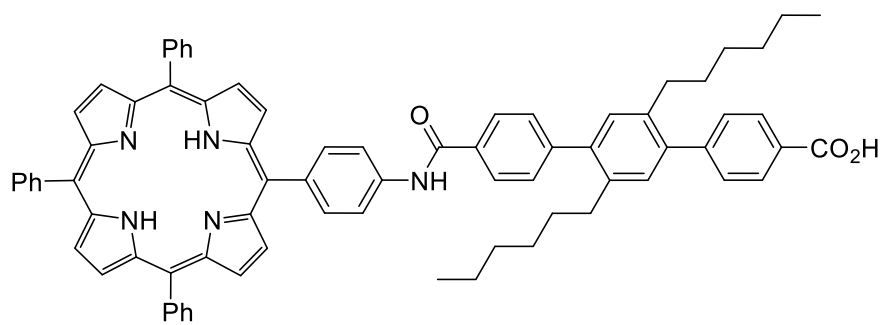


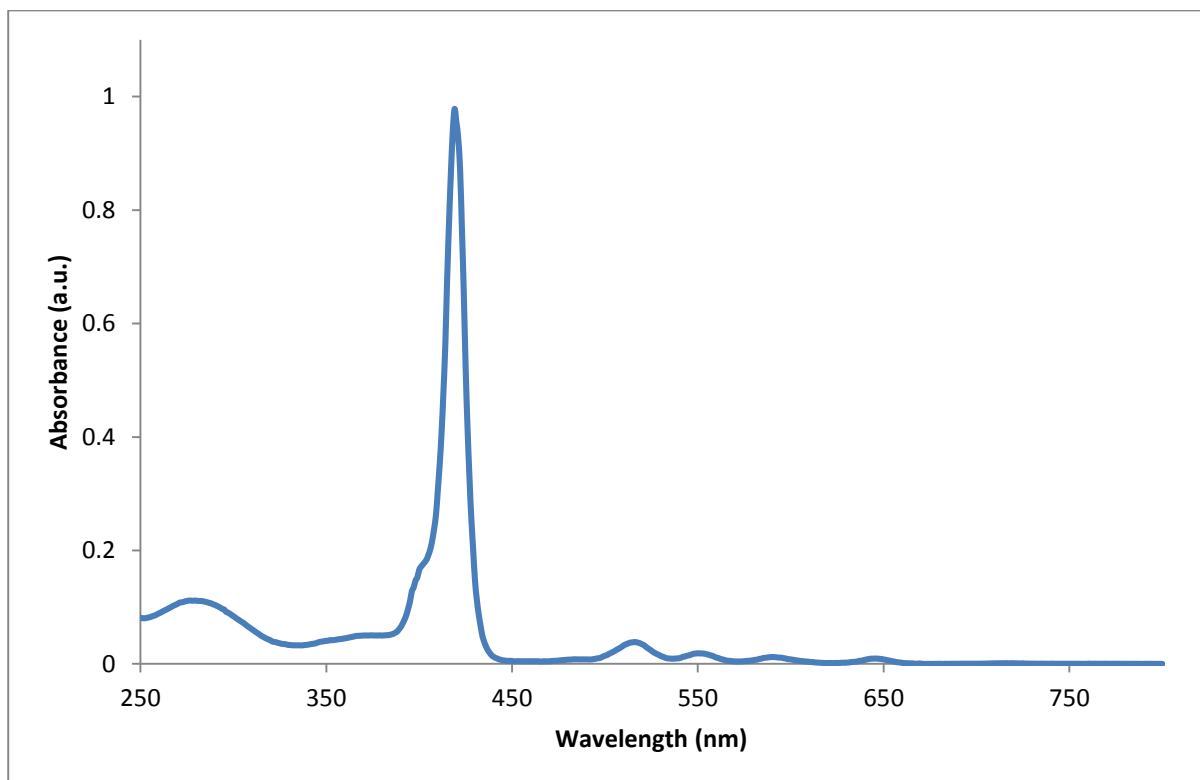
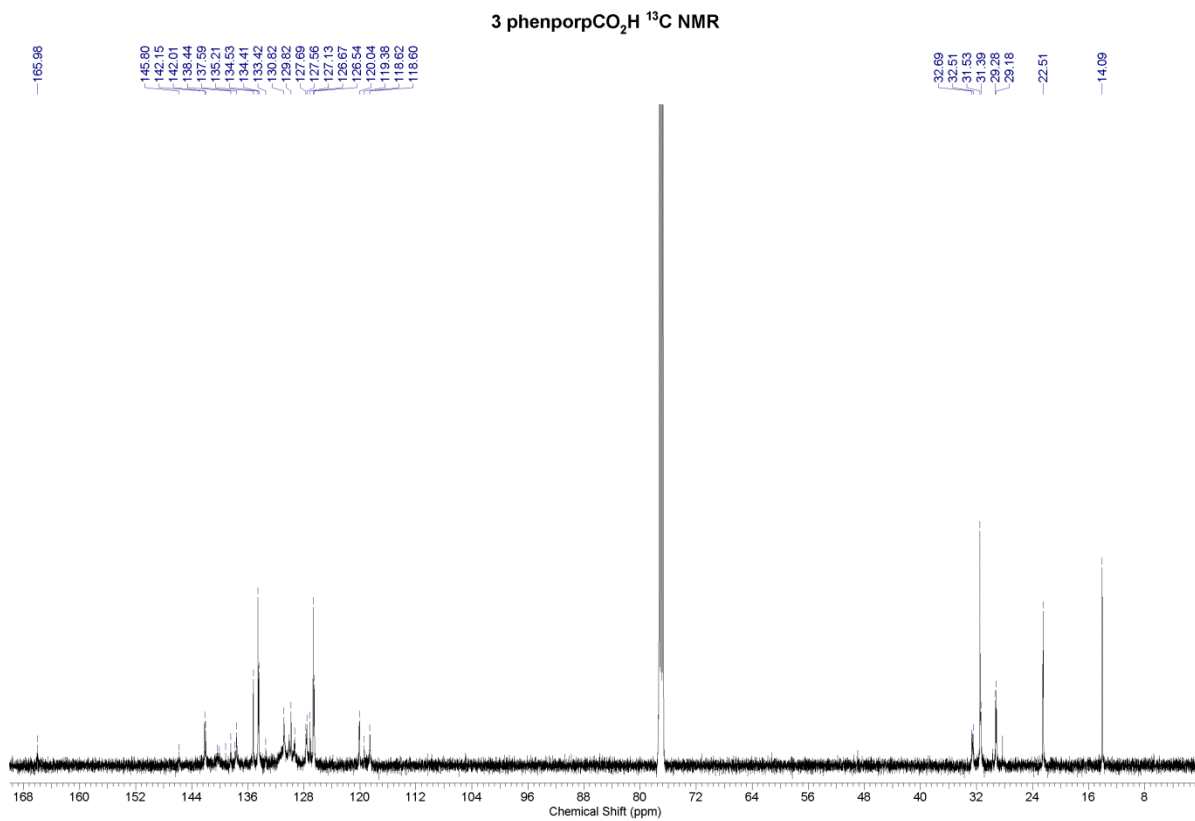
EPR data: Black line - Experimental data, Red line – Simulation (g: [2.0084 2.0065 2.0035] Nucs: 'N' A: [21.3973 21 88.2998] lwpp: [0.1144 0.2000])

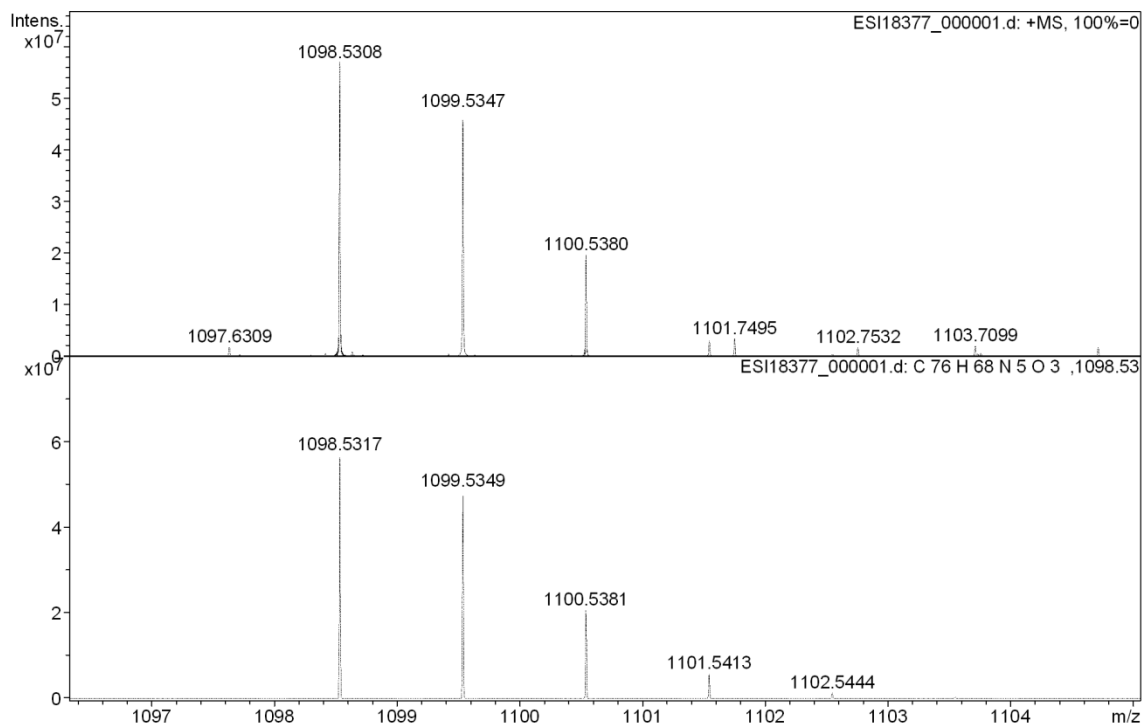


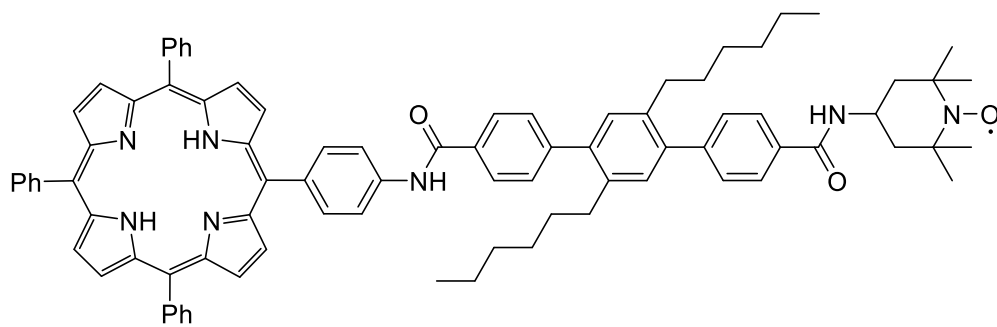




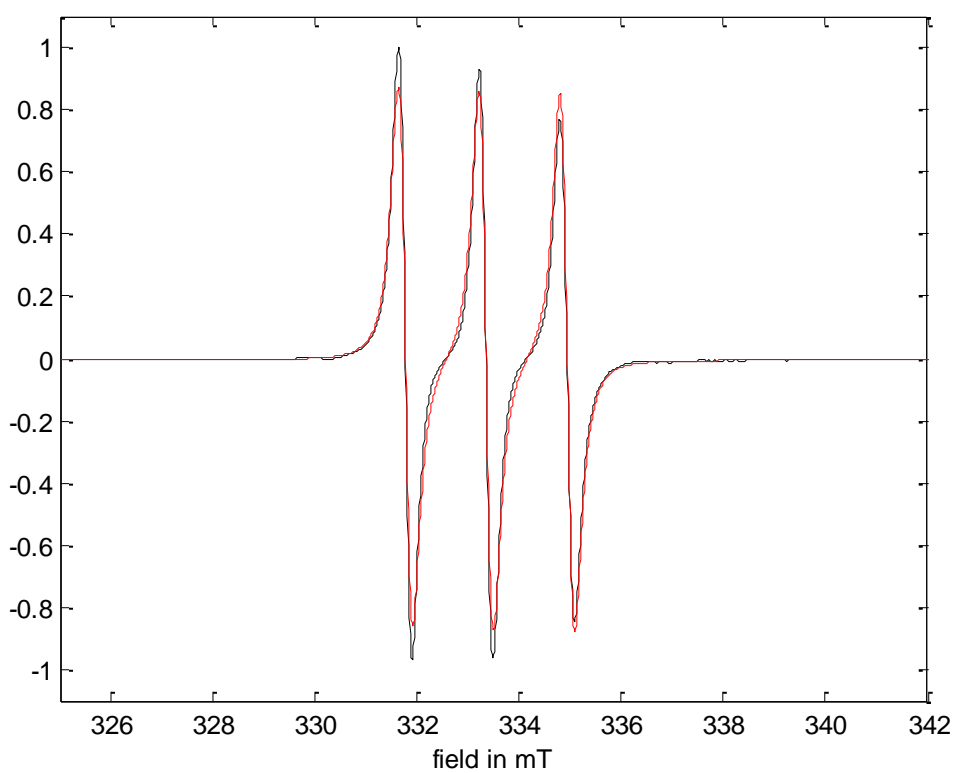


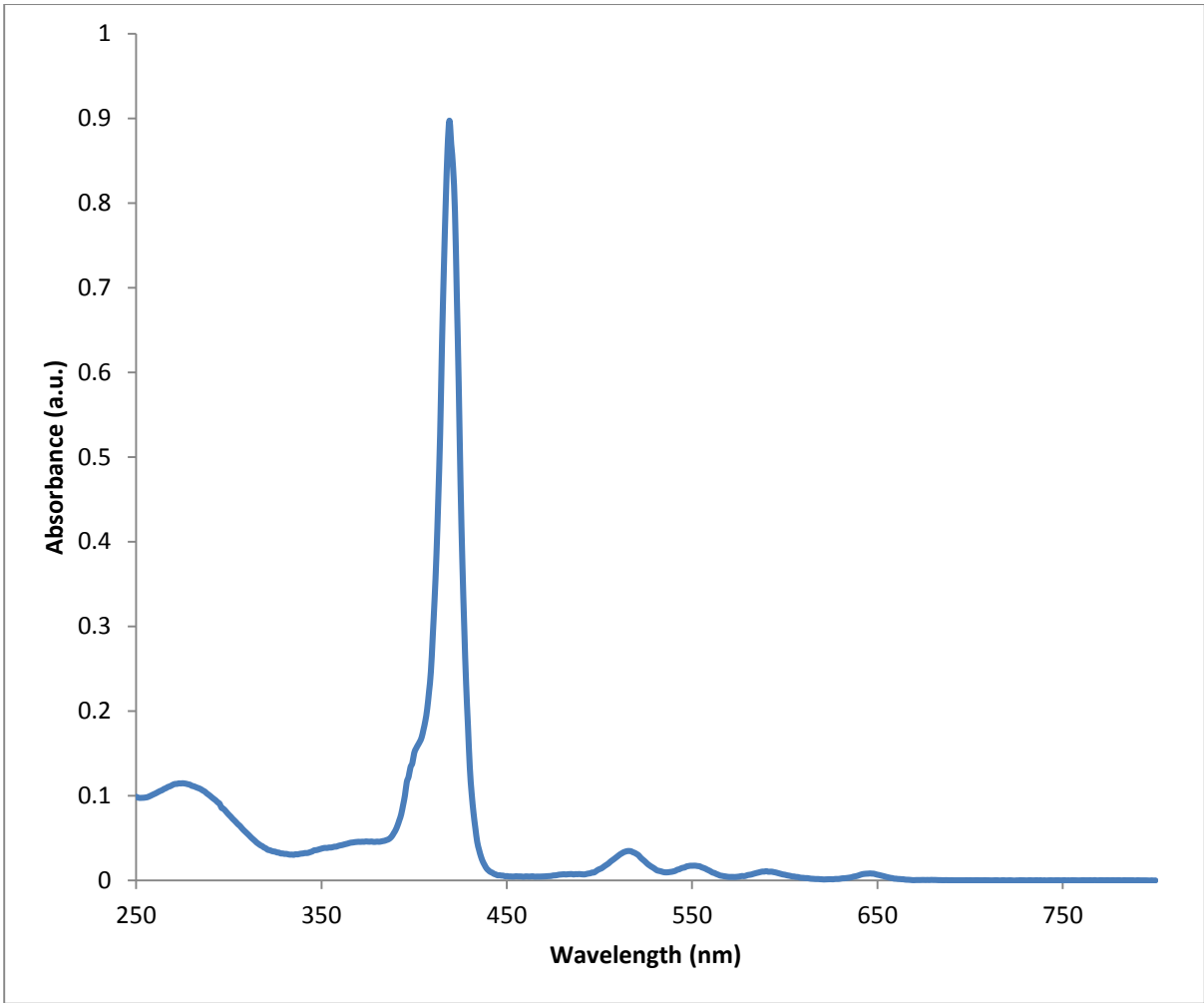


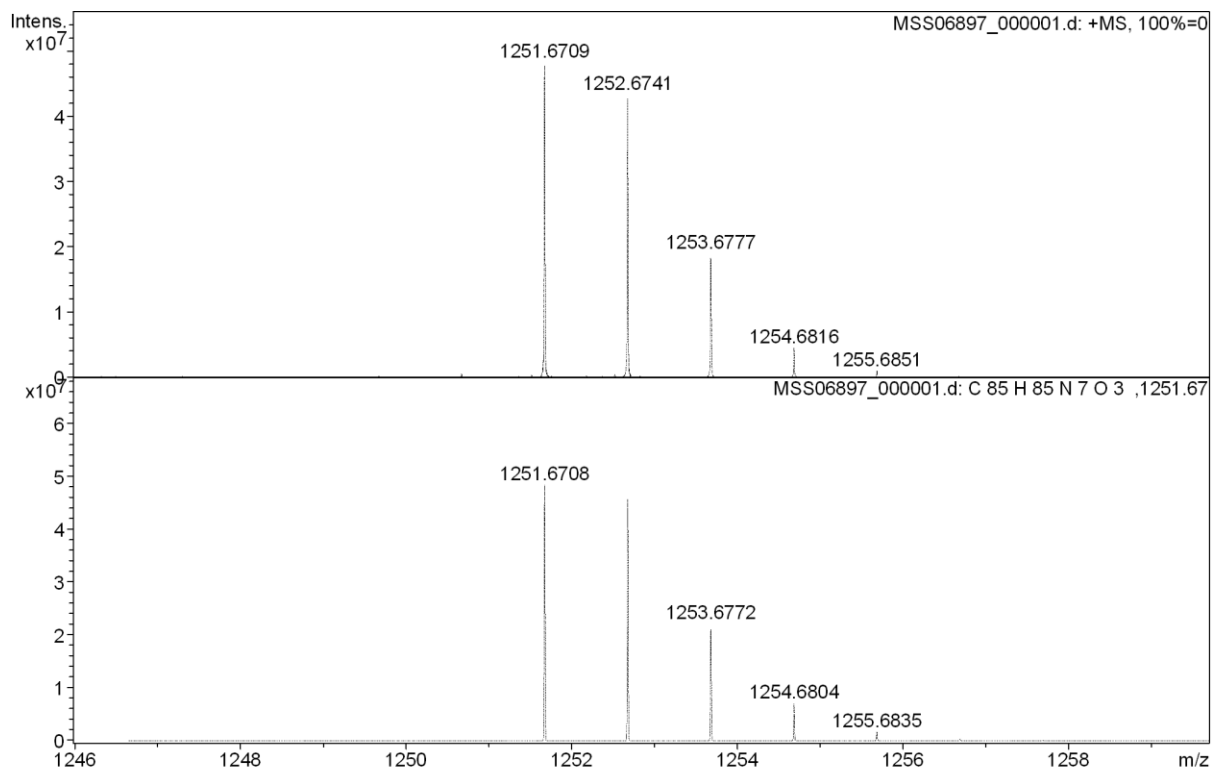


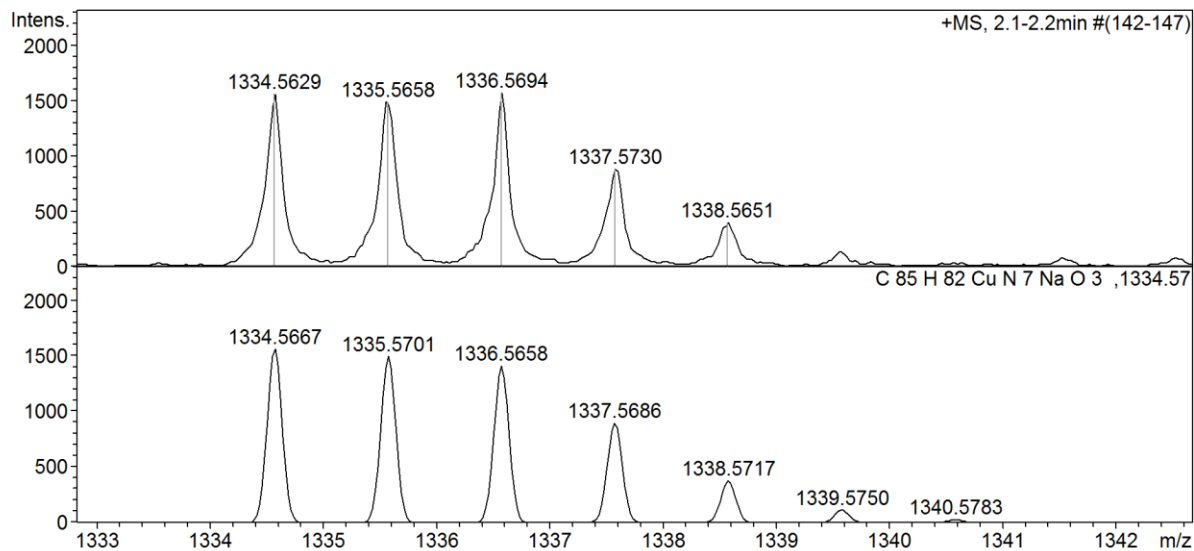


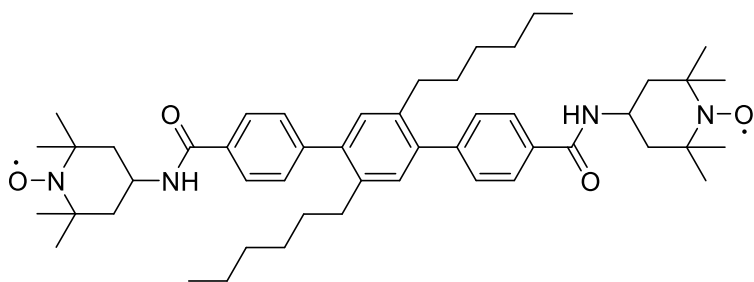
EPR data: Black line - Experimental data, Red line – Simulation (g: [2.0081 2.0058 2.0046] Nucs: 'N' A: [21.0000 22.7274 89.9919] lwpp: [0.1000 0.2406])



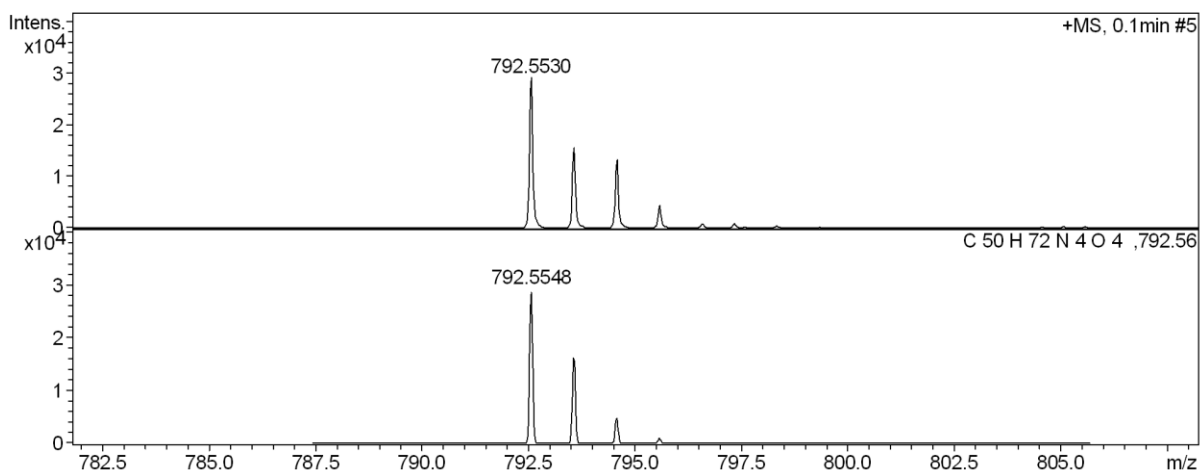
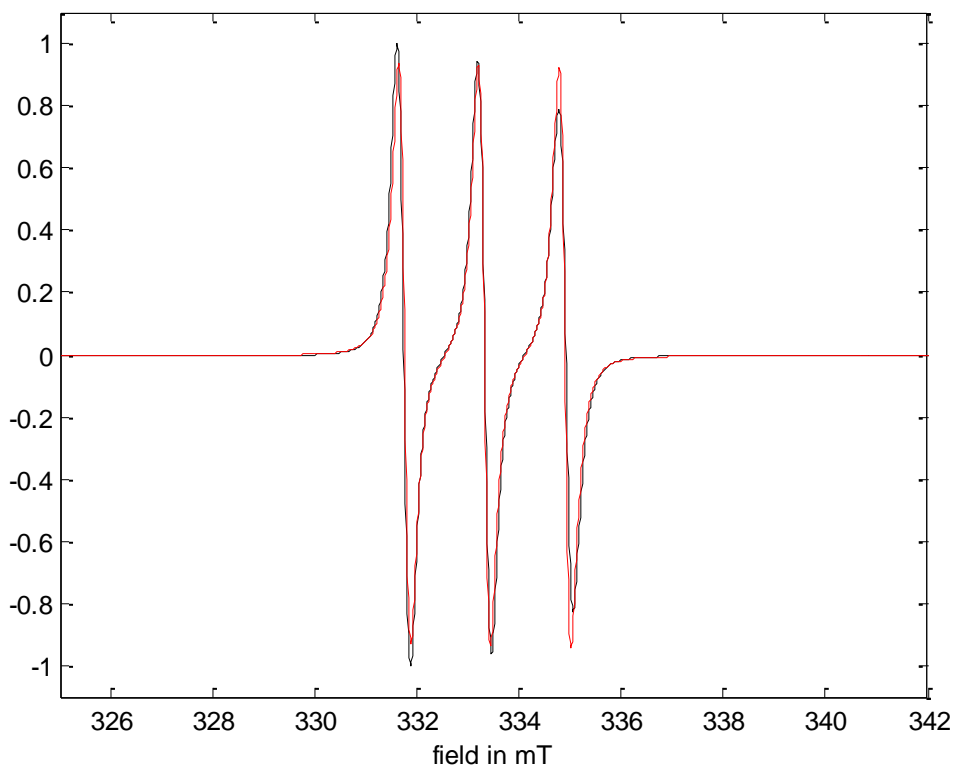








EPR data: Black line - Experimental data, Red line – Simulation (g: [2.0087 2.0063 2.0036] Nucs: 'N' A: [21.9117 21.5106 88.7862] lwpp: [0 0.2235])



References

1. G. Jeschke, V. Chechik, P. Ionita, A. Godt, H. Zimmermann, J. Banham, C. R. Timmel, D. Hilger and H. Jung, *Applied Magnetic Resonance*, 2006, **30**.
2. D. J. Byron, G. W. Gray and R. C. Wilson, *J. Chem. Soc. C*, 1966, 840-845.
3. D. I. Fletcher, C. R. Ganellin, A. Piergentili, P. M. Dunn and D. H. Jenkinson, *Bioorg. Med. Chem.*, 2007, **15**, 5457-5479.
4. M. Rehahn, A. D. Schlueter and W. J. Feast, *Synthesis*, 1988, 386-388.
5. N. Miyaura, K. Yamada and A. Suzuki, *Tetrahedron Letters*, 1979, **20**.
6. N. Miyaura and A. Suzuki, *Chemical Reviews*, 1995, **95**, 2457-2483.
7. M. W. Jones, J. E. Baldwin, A. R. Cowley, J. R. Dilworth, A. Karpov, N. Smiljanic, A. L. Thompson and R. M. Adlington, *Dalton Transactions*, 2012, **41**.
8. R. Luguay, L. Jaquinod, F. R. Fronczek, A. G. H. Vicente and K. M. Smith, *Tetrahedron*, 2004, **60**.
9. A. D. Adler, F. R. Longo, Finarell.Jd, Goldmach.J, J. Assour and Korsakof.L, *Journal of Organic Chemistry*, 1967, **32**, 476.
10. A. Godt, C. Franzen, S. Veit, V. Enkelmann, M. Pannier and G. Jeschke, *Journal of Organic Chemistry*, 2000, **65**, 7575-82.
11. J. Cosier and A. M. Glazer, *Journal of Applied Crystallography*, 1986, **19**, 105-107.
12. Z. Otwinowski and W. Minor, *Macromolecular Crystallography, Pt A*, 1997, **276**, 307-326.
13. A. Altomare, G. Cascarano, C. Giacovazzo and A. Guagliardi, *Journal of Applied Crystallography*, 1994, **27**, 1045-1050.
14. D. Watkin, R. Cooper and C. K. Prout, *Zeitschrift Fur Kristallographie*, 2002, **217**, 429-430.
15. W. J. Kruper, Jr., T. A. Chamberlin and M. Kochanny, *J. Org. Chem.*, 1989, **54**, 2753-2756.
16. M. Rehahn, A. D. Schluter and W. J. Feast, *Synthesis-Stuttgart*, 1988, 386-388.
17. K. Tamao, K. Sumitani and M. Kumada, *Journal of the American Chemical Society*, 1972, **94**, 4374-&.
18. 1. SCM. Amsterdam Density Functional (ADF). <http://www.scm.com/> at <<http://www.scm.com/>>